



HAL
open science

Random tensors and the Sachdev-Ye-Kitaev model

Romain Pascalie

► **To cite this version:**

Romain Pascalie. Random tensors and the Sachdev-Ye-Kitaev model. Mathematical Physics [math-ph]. Université de Bordeaux; Westfälische Wilhelms-Universität (Münster, Allemagne), 2020. English. NNT : 2020BORD0099 . tel-02972655

HAL Id: tel-02972655

<https://theses.hal.science/tel-02972655>

Submitted on 20 Oct 2020

HAL is a multi-disciplinary open access archive for the deposit and dissemination of scientific research documents, whether they are published or not. The documents may come from teaching and research institutions in France or abroad, or from public or private research centers.

L'archive ouverte pluridisciplinaire **HAL**, est destinée au dépôt et à la diffusion de documents scientifiques de niveau recherche, publiés ou non, émanant des établissements d'enseignement et de recherche français ou étrangers, des laboratoires publics ou privés.

THÈSE EN COTUTELLE PRÉSENTÉE
POUR OBTENIR LE GRADE DE
DOCTEUR DE
L'UNIVERSITÉ DE BORDEAUX
ET DE L'UNIVERSITÉ DE MÜNSTER

ÉCOLE DOCTORALE MATHÉMATIQUES ET INFORMATIQUE
SPÉCIALITÉ : MATHÉMATIQUES PURES
DÉPARTEMENT DE MATHÉMATIQUES ET INFORMATIQUE
SPÉCIALITÉ : SCIENCES NATURELLES

Par Romain PASCALIE

Random tensors and the Sachdev-Ye-Kitaev model

Sous la direction de Adrian TANASA
et de Raimar WULKENHAAR

Soutenue le 10 Septembre 2020

Membres du jury:

M. PATRAS Frédéric	Professeur	Université Côte d'Azur	President
M. FERRARI Frank	Professeur	Université Libre de Bruxelles	Rapporteur
M. GURAU Razvan	Chargé de recherche	École Polytechnique	Rapporteur
M. MUKHERJEE Chiranjib	Junior Professor	WWU Münster	Rapporteur
Mme. EICHHORN Astrid	Associate Professor	University of Southern Denmark	Examinatrice
M. MALE Camille	Chargé de recherche	Université de Bordeaux	Examineur
M. TANASA Adrian	Professeur	Université de Bordeaux	Directeur
M. WULKENHAAR Raimar	Professeur	WWU Münster	Directeur

Titre : Tenseurs aléatoires et modèle de Sachdev-Ye-Kitaev

Résumé : Dans cette thèse nous traitons de différents aspects des tenseurs aléatoires. Dans la première partie de la thèse, nous étudions la formulation des tenseurs aléatoires en termes de théorie quantique des champs nommée théorie de champs tensoriels (TFT). En particulier nous déterminons les équations de Schwinger-Dyson pour une TFT de tenseurs de rang arbitraire, munie d'un terme d'interaction quartique melonique $U(N)$ -invariant. Les fonctions de corrélations sont classifiées par des graphes de bords et nous utilisons l'identité de Ward-Takashi pour déterminer le système complet d'équations de Schwinger-Dyson, exactes et analytiques, vérifiées par les fonctions de corrélations avec un graphe de bord connexe.

Nous analysons ensuite la limite de grand N des équations de Schwinger-Dyson à rang 3 et trouvons les facteurs appropriés en puissance de N des différents termes de l'action. Cela nous permet de résoudre les équations de Schwinger-Dyson pour la fonction à 2-points d'une TFT avec seulement une interaction quartique melonique, dont la solution est basée sur la fonction W de Lambert, en utilisant une expansion perturbative et la resommation de Lagrange-Bürmann. Les fonctions de corrélation à plus haut nombre de points s'obtiennent récursivement.

Dans la deuxième partie de la thèse, nous nous intéressons au modèle de Sachdev-Ye-Kitaev (SYK) qui est très similaire aux modèles de tenseurs. Il s'agit d'un modèle composé de N fermions qui interagissent q à la fois et dont le couplage est un tenseur moyenné selon une distribution Gaussienne. Nous étudions les effets du moyennage des couplages aléatoires selon une distribution non-Gaussienne dans une version complexe du modèle SYK. En utilisant une équation de type Polchinski et l'universalité de tenseurs aléatoires Gaussiens, nous montrons que le moyennage selon une distribution non-Gaussienne correspond à l'ordre dominant en N à un moyennage Gaussien avec une variance modifiée. Nous déterminons ensuite la forme de l'action effective à tout ordre et réalisons un calcul explicite de la modification de la variance dans le cas d'une perturbation quartique.

Dans la troisième partie de la thèse, nous étudions une application des tenseurs aléatoires à l'étude des systèmes non-linéaires résonants. Nous nous focalisons sur un modèle typique, similaire au modèle SYK bosonique, dont le couplage tensoriel entre les modes est moyenné selon une distribution Gaussienne, ainsi que les conditions initiales. Dans la limite où la configuration initiale possède un grand nombre de modes excités, nous calculons la variance de normes de Sobolev qui caractérisent la représentativité du modèle moyenné pour cette classe de systèmes résonants.

Mots-clés : Tenseurs aléatoires, non-perturbatif, modèle SYK, systèmes résonants.

Title : Random tensors and the Sachdev-Ye-Kitaev model

Abstrac : This thesis treats different aspects of random tensors. In the first part of the thesis, we study the formulation of random tensors as a quantum field theory called tensor field theory (TFT). In particular we derive the Schwinger-Dyson equations for a tensor field theory with an $U(N)$ -invariant melonic quartic interactions, at any tensor rank. The correlation functions are classified by boundary graphs and we use the Ward-Takahashi identity to derive the complete tower of exact, analytic Schwinger-Dyson equations for correlation functions with connected boundary graph.

We then analyse the large N limit of the Schwinger-Dyson equations for rank 3 tensors.

We find the appropriate scalings in powers of N for the various terms present in the action. This enable us to solve the closed Schwinger-Dyson equation for the 2-point function of a TFT with only one quartic melonic interaction, in terms of Lambert's W -function, using a perturbative expansion and Lagrange-Bürmann resummation. Higher-point functions are then obtained recursively.

In the second part of the thesis, we study the Sachdev-Ye-Kitaev (SYK) model which is closely related to tensor models. The SYK model is a quantum mechanical model of N fermions who interact q at a time and whose coupling constant is a tensor average over a Gaussian distribution. We study the effect of non-Gaussian average over the random couplings in a complex version of the SYK model. Using a Polchinski-like equation and random tensor Gaussian universality, we show that the effect of this non-Gaussian averaging leads to a modification of the variance of the Gaussian distribution of couplings at leading order in N . We then derive the form of the effective action to all orders and perform an explicit computation of the modification of the variance in the case of a quartic perturbation.

In the third part of the thesis, we analyse an application of random tensors to non-linear resonant system. Focusing on a typical model similar to the SYK model but with bosons instead of fermions, we perform a Gaussian averaging both for the tensor coupling between modes and for the initial conditions. In the limit when the initial configuration has many modes excited, we compute the variance of the Sobolev norms to characterise how representative the averaged model is of this class of resonant systems.

Keywords : Random tensors, non-perturbative, SYK model, resonant systems.

Zusammenfassung : Die Doktorarbeit behandelt verschiedene Aspekte von Zufallstensoren. Wir studieren zunächst ihre quantenfeldtheoretische Formulierung, die Tensorfeldtheorie (TFT) genannt wird. Wir leiten Schwinger-Dyson-Gleichungen für eine Tensorfeldtheorie mit $U(N)$ -invarianter melonischer quartischer Wechselwirkung her, für beliebigen Rang der Tensoren. Die Korrelationsfunktionen werden durch Randgraphen klassifiziert. Wir setzen die Ward-Takahashi-Identität ein, um den vollständigen Turm exakter analytischer Schwinger-Dyson-Gleichungen für Korrelationsfunktionen mit zusammenhängendem Randgraphen zu gewinnen.

Anschließend analysieren wir für Rang-3-Tensoren das Grenzverhalten der Schwinger-Dyson-Gleichungen für großes N . Wir bestimmen geeignete Exponenten von N in den Vorfaktoren der Wechselwirkungsterme. Dadurch können wir die geschlossene Schwinger-Dyson-Gleichung für die 2-Punktfunktion einer Tensorfeldtheorie mit nur einer der melonischen quartischen Wechselwirkung, im Limes großer N , exakt lösen. Wir verwenden Störungstheorie und Lagrange-Bürmann-Resummierung, um das Ergebnis durch die Lambertsche W -Funktion auszudrücken. Höhere Korrelationsfunktionen werden rekursiv erhalten.

Das Sachdev-Ye-Kitaev-Modell (SYK-Modell) steht in enger Beziehung zu Tensormodellen. Es ist ein Modell für N Fermionen, von denen jeweils q miteinander wechselwirken. Die entsprechenden tensoriellen Kopplungen werden gemäß einer Gauß-Verteilung gemittelt. Wir studieren in einer komplexifizierten Variante des SYK-Modells den Einfluss einer nicht-Gaussischen Mittelung über die zufälligen Kopplungen. Unter Verwendung einer auf Polchinski zurückgehenden Methode und der Universalität des Gauß-Prozesses zeigen wir, dass, in führender N -Ordnung, die nicht-Gaußsche Mittelung die Varianz der

Verteilung der Kopplungen modifiziert. Wir leiten die Form der effektiven Wirkung zu allen Ordnungen her. Für eine quartische Störung berechnen wir explizit die Modifikation der Varianz.

Schließlich studieren wir eine Anwendung von Modellen von Zufallstensoren auf nicht-lineare Resonanzsysteme. Wir betrachten ein Modell ähnlich zum SYK-Modell, jedoch mit Bosonen. Für dieses führen wir die Gaußsche Mittelung sowohl über die Tensorkopplung zwischen den Moden als auch über die Anfangswerte durch. Im Grenzfall, in dem die Anfangskonfiguration viele angeregte Moden hat, berechnen wir die Varianz der Sobolev-Normen. Dadurch charakterisieren wir, wie repräsentativ das gemittelte Modell innerhalb der Klasse der Resonanzsysteme ist.

Unités de recherche

LaBRI, UMR CNRS 5800
351, cours de la Libération
F-33405 Talence cedex
France

Mathematisches Institut
Fachbereich Mathematik und Informatik
der Universität Münster
Einsteinstrasse 62
48149 Münster
Deutschland

Acknowledgements

The task of writing acknowledgements is daunting because of two opposing reasons. The first one is the impossible wish to acknowledge every one where thanks is due without forgetting someone. The second is the need to keep this section sufficiently short not to exceed the length of the manuscript itself. I will therefore try to keep it short and apologise in advance if I inadvertently forget someone.

I would like to thank first my two supervisors Adrian Tanasa and Raimar Wulkenhaar for their guidance and the many opportunities they gave me to learn from and be part of the research community. In particular the possibility of doing a cotutelle PhD between France and Germany, which was a very insightful experience.

I am grateful to the members of the jury for their participation in the defense. In particular I would like to thank Chiranjib Mukherjee, Frank Ferrari and Razvan Gurau for accepting the task of refereeing this manuscript. Moreover I would like to thank Frank and Razvan for their advice in many discussions throughout my PhD and especially their help for my search on getting a post-doctoral position. I wish to thank Camille Malle also for his support in my thesis monitoring committee in the last three years. And I want to thank to Astrid Eichhorn for accepting to be a part member of the jury and to Frédéric Patras for presiding the jury.

I wish to thank all the members of the "extended tensor family" for the many discussions and shared moments in numerous occasions throughout the world. To name a few, thanks to Thomas, who co-supervised my internship with Adrian before my PhD, for his help and for consistently teaching me new things throughout the thesis. I am grateful to Vincent for his mentoring and advice. I want to thank Dario and Razvan for many helpful discussions. I wish to thank Reiko for great shared moments and discussions. I also would like to thank other members of the tensor community with whom I hope to interact even more in the future, thanks to Joseph, Valentin, Fabien, Sylvain, Luca, Guillaume, Sabine, Vasily, Ariane, Johannes L. and Nicolas who started his PhD at the same time as me and with whom I regularly met in many places in the last three years.

One of the main advantage of a cotutelle PhD is the fact of belonging to two labs which enables you to meet twice as many people, the drawback being you can only spend half of the time with them.

I want to thank Vincent L., Matteo and Stéphane for many interesting discussions in Bordeaux and in particular Matteo and Stéphane for our collaborations. My time in Bordeaux was also made much more pleasant thanks to Théo K., Henri, Théo P., Thomas, Antonin, Thobias, Alexandre and Dimitri for the many entertaining conversations on a wide range of topics.

During my time in Münster, I had many enlightening conversation on physics and mathematics for which I would like to thank Alex S., Johannes T., Carlos, Jins (also for

his crash-courses on Dutch politics) and of course Alex H. with whom I shared an office and who was always a big help.

I could never thank enough my parents for their relentless support and help. I also wish to thank my friend from the ENS time, the prépa years and before whom I would like to see more often. And of course thanks to Öykü for her support and making this last couple of years much more fulfilling.

Contents

Introduction (French version)	9
Introduction	14
1 Schwinger-Dyson equations in melonic tensor field theories	18
1.1 Introduction	18
1.2 Boundary graph expansions	20
1.2.1 Complex tensors and coloured graphs	20
1.2.2 Boundary graphs	24
1.2.3 Graph-generated functionals	27
1.3 The Schwinger-Dyson equation tower in arbitrary rank	31
1.4 Schwinger-Dyson equations for rank-3 theories	36
1.4.1 Four-point function SDEs for the φ_3^4 -theory	40
1.4.2 The Schwinger-Dyson equation for $G_{K_c(3,3)}^{(6)}$	41
1.4.3 The Schwinger-Dyson equation for $G_{Q_a}^{(6)}$	44
1.4.4 The Schwinger-Dyson equation for $G_{\mathcal{E}_a}^{(6)}$	45
1.5 A simple quartic model	47
1.6 Conclusions and perspectives	52
2 Large N limit and solution of a melonic quartic model	54
2.1 Introduction	54
2.2 The model and the tools	55
2.3 Constraints on the scalings in N	58
2.3.1 2-point function SDE	58
2.3.2 $2k$ -point function SDE for connected boundary graphs	60
2.4 The 4-point function SDE with disconnected boundary graph	63
2.5 The SDE in the large N limit	67
2.5.1 2- and 4-point functions	67
2.5.2 Higher-point functions	69
2.6 Perturbative expansion and a simpler model	71
2.6.1 Model with the 3 quartic melonic interactions	71
2.6.2 Model with 1 quartic melonic interaction	72
2.7 Resummation and solution	73
2.8 Higher-point functions	75
2.9 Conclusions and perspectives	76

3	Non-Gaussian disorder average in the Sachdev-Ye-Kitaev model	78
3.1	Introduction	78
3.2	A complex SYK model with non-Gaussian disorder	79
3.3	Gaussian universality	82
3.4	Effective action	84
3.5	A quartic perturbation computation	85
3.5.1	The quartic perturbed model	85
3.5.2	Hubbard-Stratonovich transformation for the disorder	86
3.5.3	First order correction of the effective action	88
3.6	Gross-Rosenhaus SYK model with non-Gaussian disorder	90
3.7	Conclusions and perspectives	94
4	On the variance of Sobolev norms in resonant systems	96
4.1	Resonant systems	96
4.1.1	The model	96
4.1.2	Tree expansion	100
4.1.3	Averaged Sobolev norms	104
4.1.4	Explicit computations at order t^2	106
4.2	Variance of the Sobolev norm at order t^4	110
4.2.1	Melonic diagrams	112
4.2.2	Ladder diagrams	113
4.3	Perspectives	118
	Appendices	121
A	Proof of Lemma 1.4.1	121
B	Rank-four and five melonic quartic theories	126
B.1	Four-coloured graphs and melonic quartic rank-4 theories	126
B.2	Two-point equation for rank-4 theories	129
B.3	Four-point equation for $G_{\mathcal{V}_i}^{(4)}$ in rank-4 theories	131
B.4	Four-point equation for $G_{\mathcal{N}_{ij}}^{(4)}$ in rank-4 theories	132
B.5	Rank-five melonic quartic theory	133
C	Perturbative expansion	134
D	Recurrence relations	142
E	Schwinger-Dyson equations for the intermediate field	146
E.1	Complex SYK	146
E.2	Gross-Rosenhaus SYK generalization	149
F	Explicit computation of the variance at order t^4	151
F.1	Melonic diagrams	151
F.2	Ladder diagrams	152
	Bibliography	157

Introduction (French version)

Cette thèse traite de différents aspects de la théorie des tenseurs aléatoires. Nous étudions leur formulation en tant que théorie quantique des champs appelée théorie de champs tensoriels (TFT). Nous examinons certains aspects de leurs liens avec le modèle de Sachdev-Ye-Kitaev (SYK), et avec les systèmes résonants pour étudier les propriétés typiques d'équations d'évolutions non-linéaires aléatoires.

Des matrices aux tenseurs

L'étude des matrices aléatoires est un champ de recherche majeur en probabilité et en physique mathématique. Les matrices aléatoires ont été introduites pour la première fois en physique mathématique par Wigner [1] pour étudier le noyaux d'atomes lourds et ont depuis été appliquée dans de nombreux domaines de la physique théorique. En particulier, les matrices aléatoires ont été étudiées de façon approfondie pour leur lien avec la gravitation quantique en $2D$, voir l'article de revue [2].

Un des principaux résultat des modèles de matrices fût la découverte de leurs développement en $1/N$ par 't Hooft [3]. Le développement en graphes de Feynman des modèles de matrices est constitué de graphes à rubans qui peuvent être vues comme la discretisation d'une surface de Riemann. A grand N , les modèles de matrices sont dominés par les graphes planaires qui correspondent à la sphère et le développement en $1/N$ est indexé par le genre des surfaces de Riemann duales aux graphes. Par la suite, les modèles de matrices ont été complètement résolus grâce à l'utilisation de la récursion topologique qui fût introduite pour la première fois dans [4] (voir aussi le livre [5]).

En outre, les modèles de matrices apparaissent dans l'étude des théories de champs sur un espace-temps non-commutatif. Ces modèles comportent généralement un mélange UV/IR des divergences qui peut être résolu par l'addition d'un terme d'oscillateur harmonique, comme dans le modèle de Grosse-Wulkenhaar [6] qui peut être exprimé comme un modèle quartique de matrices avec une matrice externe dans le terme cinétique. Une autre manière de résoudre le problème du mélange UV/IR est d'ajouter à l'action dans l'espace des moments, un terme en $1/p^2$ invariant par translation [7].

Dans le but d'étudier la gravitation quantique en dimension supérieure, les modèles de tenseurs sont une généralisation naturelle de modèles de matrices. Ils ont été introduits pour la première fois dans les années 90 dans [8], [9], [10], avec l'idée que de manière similaire aux graphes à rubans, les graphes de tenseurs sont duaux aux discrétisation d'espaces de dimensions supérieures. Cependant le développement des modèles de tenseurs fût entravé par le manque de limite grand N .

Après presque vingt ans, le développement à grand N des tenseurs aléatoires a été

établi pour la première fois dans [11] puis étendue dans [12], pour un type de modèle spécifique appelé modèle de tenseurs colorés. De nombreux développements ont suivi notamment un théorème d’universalité pour les tenseurs aléatoires [13], une version invariante sous $U(N)^D$ des modèles de tenseurs aléatoires (où D est le rang des tenseurs), appelée incolore, a été introduite [14], les modèles de tenseurs multi-orientables invariants sous $U(N)^{D-1} \times O(N)$ furent introduits dans [15], une théorie des champs de tenseur renormalisable a été étudiée dans [16] et un modèle de tenseur aléatoire invariant sous $O(N)^D$ a été proposé dans [17]. Voir aussi l’article de revue [18].

Dans cette thèse nous considérons un modèle de tenseur invariant sous $U(N)^D$ dont le terme cinétique est modifié par l’introduction d’un opérateur de type Laplacien (cet opérateur est un Laplacien discret dans l’espace de Fourier des indices de tenseur). Ce type de modèle de tenseur a été utilisé à l’origine pour implémenter des techniques de renormalisation dans les modèles de tenseurs dans [16] (voir aussi l’article de revue [19] ou la thèse [20] ainsi que les références incluses) et a été aussi étudié comme une TFT de type SYK [21]. Récemment, le groupe de renormalisation fonctionnelle a été utilisé dans [22] pour rechercher l’existence éventuelle d’une limite continue universelle dans les modèles de tenseurs, voir aussi l’article de revue [23]. Cette approche est étroitement liée à l’équation de Polchinski pour les TFT [24]. Notre approche fournit un outil non-perturbatif complémentaire à ces deux approches. De plus, notre étude généralise les techniques utilisées dans le contexte des modèles de matrices [6].

Le modèle de Sachdev-Ye-Kitaev

Le modèle de Sachdev-Ye-Kitaev (SYK) est une version simplifiée du modèle de Sachdev-Ye [25], et a été introduit par Kitaev lors de deux conférences au KITP [26] en tant que modèle jouet pour l’holographie, exactement résoluble. L’holographie réfère à la correspondance précise entre une théorie de gravitation quantique dans un espace-temps asymptotiquement Anti-de-Sitter (AdS) en dimensions $d+1$ (appelé le bulk) et une théorie conforme des champs (CFT) sur le bord de dimension d . Le modèle SYK est un modèle de mécanique quantique constitué de N fermions de Majorana avec des interactions aléatoires impliquant q de ces fermions à la fois. Le couplage est un tenseur de rang q tiré d’une distribution aléatoire Gaussienne.

Le modèle SYK a gagné beaucoup d’intérêt grâce à trois propriétés remarquables [27, 28]:

- Calculable à grand N : dans cette limite les graphes de Feynman peuvent être sommés et les fonctions de corrélations calculées à fort couplage..
- Maximisant le chaos : le chaos quantique est quantifié par un exposant de Lyapunov défini par la fonction à quatre points ”out-of-time order”. L’exposant de Lyapunov d’un trou noir dans la théorie de la gravité d’Einstein est maximal, tout comme celui du modèle SYK.
- Symmétrie conforme émergente : la fonction à deux points a une symmétrie conforme émergente dans la limite IR. Cette symmétrie est spontanément et explicitement brisée par le mode qui maximise le chaos.

Le modèle SYK a été étudié intensivement et de nombreux progrès ont été établis dans la perspective de résoudre complètement le modèle. Entre autres, les fonctions de corrélations à plus grand nombre de point ont été déterminées dans le secteur conforme du modèle

[29, 30], les fonctions à 2-points et 4-points ont été calculées dans la limite de grand q , non seulement dans la limite IR mais à toutes énergies [31, 32]. De plus, dans une version à double échelle du modèle SYK, la fonction à 4-point a été obtenue à toutes énergies en utilisant uniquement des méthodes combinatoires.

De nombreuses généralisations du modèles SYK ont été introduites. Notamment une version ajoutant des saveurs aux fermions [33], une version complètement de symétrie conforme [34], un modèle constitué de fermions complexes [35], une version supersymétrique [36] et de dimension supérieure [37]. Pour une introduction au modèle SYK, voir les articles de revue [38, 39].

En particulier, Witten reformula le modèle SYK en tant que modèle de tenseurs, notant que dans les deux cas, la limite large N est dominée par les mêmes graphes meloniques [40]. Cela a renouvelé l'intérêt pour les modèles de tenseurs et leurs analogues de type SYK, parfois appelés CFT meloniques, voir le cours [41] et l'article de revue [42].

Des version réelles et complexes de modèle de tenseurs décolorés de type SYK ainsi qu'un modèle bosonique ont été introduits pour la première fois dans [43]. Un modèle SYK tensoriel supersymétrique a été proposé dans [44]. Une variante matrice-tenseur a été étudiée impliquant un nouveau type de limite grand N [45, 46]. Les graphes de Feynman au premier ordre sous-dominant dans la limite grand N ont été déterminés par des méthodes combinatoires, pour le modèle SYK originel et la version tensorielle [47]. Un analogue de l'action effective a été obtenu pour les modèles de tenseurs en tant qu'action effective $2PI$ [48]. Des modèles composés de tenseurs de symétries variées ont été considérés [49, 50]. La renormalisation des CFT meloniques a été étudiée pour des interactions quartique [51] ainsi que sextique [52, 53].

Systèmes résonants

La théorie des matrices aléatoires a été appliquée pour la première fois à l'étude des équations d'évolutions linéaires aléatoires par May dans [54], avec pour but de déterminer si de grands systèmes écologiques aléatoires peuvent être stables et d'étudier leur transition vers l'instabilité. Un exemple simple d'équation d'évolution linéaire aléatoire est une équation différentielle dont les coefficients sont des matrices aléatoires. Une telle évolution est stable si et seulement si toutes les valeurs propres des matrices aléatoires ont une partie réelle négative. Cependant, la probabilité de cet événement tend vers zéro avec la taille du système, ainsi ce type d'évolution linéaire aléatoire n'est presque jamais stable. La compréhension des comportements génériques des évolutions aléatoires à grand nombre de variables requiert d'aller au-delà du régime linéaire.

Les évolutions non-linéaires sont bien plus difficiles à analyser, puisque leurs coefficients sont des tenseurs au lieu de matrices. Ces équations d'évolutions émergent dans différents contextes de la physique théorique où une interaction non-linéaire est faible et pour des systèmes possédant un spectre d'énergies hautement résonant (la différence entre deux niveaux d'énergie doit être un entier, ce qui se traduit par une condition de résonance). Par exemple, de telles équations d'évolutions apparaissent dans l'étude de la stabilité gravitationnelle de dynamique faiblement non-linéaire dans un espace-temps AdS, voir l'article de revue [55]. Ces équations émergent aussi dans l'étude des dynamiques des condensats de Bose-Einstein avec une faible interaction de contact dans un piège harmonique isotrope [56], et voir [57] pour des études numériques comparant les

deux modèles mentionnés.

Une version quantique de ce type de modèle [58], sans la condition de résonance est très similaire aux ensembles de matrices Gaussiennes intégrés (voir le livre [59]). De plus, en remplaçant les opérateurs bosoniques par leurs analogues fermioniques, les coefficients des tenseurs aléatoires de l'équation d'évolution correspondent à l'interaction aléatoire du modèle SYK.

Une version classique de ce type de systèmes résonants a été étudiée dans [60]. En utilisant des techniques des tenseurs aléatoires, les auteurs ont montré que les graphes meloniques dominent la théorie de perturbation dans la limite où de nombreux modes sont initialement excités. De plus en restreignant la série de perturbation à l'approximation melonique correspondante, les excitations initiales se propagent vers d'autres modes au moins pendant un intervalle de temps fini comme lors d'une cascade turbulente.

Plan de la thèse

Le Chapitre 1 traite de dérivation des équations de Schwinger-Dyson d'une théorie de champs tensoriels avec une interaction melonique quartique invariante sous $U(N)$, à tout rang des tenseurs. Les fonctions de corrélations sont classifiées par des graphes de bords et nous utilisons l'identité de Ward-Takahashi pour calculer le système complet d'équations de Schwinger-Dyson analytiques pour les fonctions de corrélations à graphe de bords connexe. Nous les écrivons explicitement à rang 3, ainsi qu'à rang 4 et 5 dans l'Annexe B.

Dans le Chapitre 2, nous analysons la limite de grand N des équations de Schwinger-Dyson pour un modèle de tenseurs de rang 3. Pour obtenir une limite de grand N bien définie, des facteurs appropriés en puissance de N sont explicitement déterminés pour les différents termes présents dans l'action. Une vérification perturbative de notre résultat, jusqu'au second ordre dans la constante de couplage, est présentée dans l'Annexe C. Nous résolvons ensuite l'équation de Schwinger-Dyson fermée pour la fonction à 2-point d'une théorie de champ de tenseurs avec une seule interaction quartique melonique, en termes de la fonction W de Lambert, en utilisant un développement perturbatif et un théorème de Lagrange-Bürmann. Les fonctions de corrélations à plus grand nombre de points sont ensuite obtenues récursivement.

Dans le Chapitre 3 nous étudions les effets d'un moyennage non-Gaussien des couplages aléatoires dans une version complexe du modèle SYK. En utilisant une équation de type Polchinski et l'universalité Gaussienne des tenseurs aléatoires, nous montrons qu'à l'ordre dominant en N le moyennage non-Gaussien agit comme une distribution Gaussienne avec une variance modifiée. Nous déterminons ensuite la forme de l'action effective à tout ordre. Un calcul explicite de la modification de la variance dans le cas d'une perturbation quartique est effectué pour le modèle SYK complexe ainsi que pour la généralisation du modèle SYK proposé par Gross et Rosenhaus dans [33].

Le Chapitre 4 est un travail en cours dans le prolongement de [60]. Nous étudions une application des modèles de tenseurs aléatoires aux équations d'évolutions non-linéaires à nombreuses variables. Nous nous concentrons sur un hamiltonien typique dont les équations de mouvement ont la forme d'une approximation de faible non-linéarité à un système non-linéaire résonant possédant des perturbations linéarisées avec un spectre de fréquences hautement résonant. Nous effectuons un moyennage Gaussien du couplage

tensoriel entre les modes ainsi que des conditions initiales. Dans la limites où de nombreux modes sont initialement excités, nous calculons la variance des normes de Sobolev qui caractérisent en moyenne, à quel point les résultats de [60] sont représentatifs pour cette classe de systèmes résonants.

Introduction

This thesis treats different aspects of the theory of random tensors. We study their formulation as a quantum field theory called tensor field theory (TFT). We investigate some aspect of their link with the Sachdev-Ye-Kitaev (SYK) model and with resonant systems, to study typical properties of non-linear random flows.

From matrices to tensors

The study of random matrices is a prominent field of probabilities and mathematical physics. It was first introduced in mathematical physics by Wigner [1] to study the nuclei of heavy atoms and has since then been applied to many areas of theoretical physics. In particular, random matrices were intensively studied for their link with $2D$ quantum gravity, see the review [2].

One of the most crucial development of matrix models was the discovery of their $1/N$ expansion by 't Hooft [3]. The Feynman graph expansion of matrix models is made of ribbon graphs which can be viewed as a discretisation of a Riemann surface. At large N , matrix models are dominated by planar diagrams which correspond to the sphere and the $1/N$ expansion is indexed by the genus of the dual Riemann surfaces. Later matrix models have been fully solved with the use of topological recursion first introduced in [4] (see also the book [5]).

Furthermore matrix models arise from the study of quantum field theory on non-commutative space-time. These models are usually plagued by an UV/IR mixing of the divergences which can be solved by the addition of an harmonic oscillator term, leading to the Grosse-Wulkenhaar model [6] which can be expressed as a quartic matrix model with an external matrix in the kinetic term. Another known solution for curing the UV/IR mixing is the addition of a translation-invariant $1/p^2$ term in the momentum space action [7].

With the aim of studying higher dimensional quantum gravity, tensor models are a natural generalisation of matrix models. They were first introduced in the 90's in [8], [9], [10], with the idea that similarly to ribbon graphs, tensor graphs are dual to discretisation of higher-dimensional spaces. However the developments of tensor model was impaired by the lack of a large N limit.

Almost twenty years later, the large N expansion of random tensor was first exhibited in [11] and then extended in [12], for a specific type of model called coloured tensor models. Many developments followed among which an universality theorem for random tensors [13], an $U(N)^D$ -invariant version of random tensor models (where D is the tensor rank), called uncolored, was introduced [14], an $U(N)^{D-1} \times O(N)$ -invariant tensor model,

called multi-orientable, was introduced in [15], a renormalisable tensor field theory was studied in [16] and an $O(N)^D$ -invariant random tensor model was proposed in [17]. See also the review [18].

In this thesis we consider a $U(N)^D$ -invariant tensor model whose kinetic part is modified to include a Laplacian-like operator (this operator is a discrete Laplacian in the Fourier transformed space of the tensor index space). This type of tensor model has originally been used to implement renormalisation techniques for tensor models in [16] (see also the review [19] or the thesis [20] and references within) and has also been studied as an SYK-like TFT [21]. Recently, the functional renormalisation group has been used in [22] to investigate the existence of a universal continuum limit in tensor models, see also the review [23]. This is also closely related to the Polchinski's equation for TFT [24]. Our approach provides a complementary non-perturbative tool to these two approaches. Moreover, our study generalises the techniques used in the context of matrix model [6].

The Sachdev-Ye-Kitaev model

The Sachdev-Ye-Kitaev (SYK) model is a simplified version of the Sachdev-Ye model [25], and was introduced by Kitaev during two talks at KITP [26] as an exactly solvable toy model of holography. This refers to the precise correspondence between quantum gravity in asymptotically Anti-de Sitter (AdS) space-time in $d + 1$ dimensions (called the bulk) with a Conformal Field Theory (CFT) on the d -dimensional boundary. The SYK model is a quantum-mechanical model with N Majorana fermions with random interactions involving q of these fermions at a time. The coupling is a rank q tensor drawn from a random Gaussian distribution. The SYK model has gained a lot of interest because it has three remarkable properties [27, 28]:

- Solvable at large N : in this limit one can sum all Feynman graphs and compute the correlation functions at strong coupling.
- Maximally chaotic: Quantum chaos is quantified by the Lyapunov exponent defined by the out-of-time order four-point function. The Lyapunov exponent of a black hole in Einstein gravity and of the SYK model both saturates the maximal allowed bound.
- Emergent conformal symmetry: the two point function has an emergent conformal symmetry in the IR limit. This symmetry is spontaneously and explicitly broken by the mode saturating the chaos bound.

The SYK model was extensively studied and numerous progress have been made toward fully solving the model. Among which, the higher point functions were determined in the conformal sector of the model [29, 30], the 2-point and 4-point functions were found in the large q limit not only in the IR but at all energies [31, 32] and in a double scaled version of the SYK model the 4-point function was computed at all energy using only combinatorial methods.

Many generalisation of the SYK model were introduced and studied. Adding flavors to the fermions [33], considering a fully conformal version of the model [34], a model with complex fermions [35], supersymmetric [36] or higher dimensional version of the model [37]. For an introduction to the SYK model, see the reviews [38, 39].

In particular, Witten reformulated the SYK model into a tensor model, pointing out that both large N limits are dominated by the same melonic graphs [40]. This lead to

a renewed interest in tensor models and their SYK-like variant, sometime called melonic CFTs, see the lecture [41] and the review [42].

Real and complex uncoloured SYK-like tensor model as well as a bosonic version were first introduced in [43]. A supersymmetric tensorial SYK model was proposed in [44]. Matrix-tensor variant was studied involving a new type of large N limit [45, 46]. Combinatorial methods were used to determine the Feynman graphs at next to leading order in N for both a standard and tensorial version of the SYK model [47]. An analogue of the effective action was obtained for tensor models as a $2PI$ effective action [48]. Models composed of tensors with various symmetries were studied [49, 50]. The renormalisation of melonic CFT was studied for quartic interactions [51] as well as sextic interactions [52, 53].

Resonant systems

Random matrix theory was first applied to study random linear flows by May in [54] to answer the question if large random ecological system could be expected to be stable and how they transition to instability. A simple example of a random linear flow is a differential equation whose coefficients are random matrices. Such a flow is stable if and only if all the eigenvalues of the random matrix have negative real part. However, the probability that this happens tends toward zero with the size of the system, hence this type of random linear flow is almost never stable. Understanding the generic behaviour of random flows in many variables requires to go beyond the linear regime.

Non-linear flows are much more difficult to analyse, as their coefficients are tensors instead of matrices. They arise in many different contexts of theoretical physics where a non-linear interaction is taken to be weak and with a highly resonant energy spectrum (differences between any two energies are integers which translates into a resonance condition). For example it emerges in the study of gravitational stability of weakly non-linear dynamics in AdS space-time, see the review [55], and in the study of the dynamics of Bose-Einstein condensate with weak contact interaction in an isotropic harmonic trap [56], and see [57] for numerical studies comparing the two models.

The quantum version of this type of model [58], without the resonance condition is very similar to bosonic Gaussian embedded ensembles (see the book [59]). Moreover, by replacing the bosonic operators by their fermionic analogue, the random tensors coefficient of the flow equation correspond to the random interaction of the SYK model.

A classical version of resonant systems has been studied in [60]. By applying the techniques from random tensors the authors showed that melonic graphs dominates perturbation theory in the limit where the initial configuration has many modes excited. Moreover restricting the perturbation series to the corresponding melonic approximation, the initial excitation spreads over more modes at least during a finite time interval as in a turbulence cascade.

Outline of the thesis

Chapter 1 treats the derivation of Schwinger-Dyson equations for a tensor field theory with an $U(N)$ -invariant melonic quartic interactions, at any rank of the tensors. The

correlation function are classified by boundary graphs and we use the Ward-Takahashi identity to derive the complete tower of exact, analytic Schwinger-Dyson equations for correlation functions with connected boundary graphs. We write them explicitly for ranks 3 and for rank 4 and 5 in Appendix B.

In Chapter 2, we analyse the large N limit of the Schwinger-Dyson equations for rank 3 tensor models. In order to have a well-defined large N limit, appropriate scalings in powers of N for the various terms present in the action are explicitly found. A perturbative check of our results is done, up to second order in the coupling constant, in Appendix C. We then solve the closed Schwinger-Dyson equation for the 2-point function of a tensor field theory with only one quartic melonic interaction, in terms of Lambert's W -function, using a perturbative expansion and Lagrange-Bürmann resummation. Higher-point functions are then obtained recursively.

In Chapter 3 we study the effect of non-Gaussian average over the random couplings in a complex version of the SYK model. Using a Polchinski-like equation and random tensor Gaussian universality, we show that the effect of this non-Gaussian averaging leads to a modification of the variance of the Gaussian distribution of couplings at leading order in N . We then derive the form of the effective action to all orders. An explicit computation of the modification of the variance in the case of a quartic perturbation is performed for both the complex SYK model mentioned above and the Gross-Rosenhaus SYK generalisation proposed in [33].

Chapter 4 is a work in progress and a follow up to [60]. We study an application of random tensor models to non-linear random flows in many variables. Focusing on a typical Hamiltonian whose equations of motion have the form of the weakly non-linear approximation to a non-linear resonant system whose linearised perturbations possess highly resonant spectra of frequencies. We perform Gaussian averaging both for the tensor coupling between modes and for the initial conditions. In the limit where the initial configuration has many modes excited, we compute the variance of the Sobolev norms to characterise how much, on average, the results of [60] are representative of this class of resonant systems.

Chapter 1

Schwinger-Dyson equations in melonic tensor field theories

This chapter is an edited version of [61] written in collaboration with C.I. Pérez-Sánchez and R. Wulkenhaar, where the major contribution was made by C.I. Pérez-Sánchez.

1.1 Introduction

All the new results we mentioned in the introduction enliven the physics of random tensors. Yet, the quantum theory of these objects itself deserves a more thorough mathematical scrutiny, and, in this vein, the present chapter is a study of the correlation functions of complex tensor field theories (TFT)¹, already begun in [62], and of the equations they obey (see [63] as well). Unlike usual tensor models, tensor field theories studied here have a non-trivial kinetic term. The models we are studying are related to *uncoloured tensor models* [14], terminology which we do not use here. Rather, since the tensor fields retain some colouring in their indices, which is a byproduct of an independent $U(N)$ -symmetry for each tensor index, we call our models *$U(N)$ -invariant tensor field theories*. For each symmetry, the partition function $Z[J, \bar{J}]$ of a complex TFT satisfies a full version [62] of the Ward-Takahashi identity [64], which is not trivial because the kinetic term in the action breaks the $U(N)$ -symmetry. It has been anticipated [62] that this constraint would allow to derive an equation for each correlation function of complex TFT, and the aim of this chapter is to obtain those for arbitrary rank.

These are the analytic Schwinger-Dyson equations (SDE). Their derivation is independent from existent SDE for tensor models (e.g. those obtained by Gurău [65] or Krajewski and Toriumi [66]), which, crucially, differ from our SDE in that those SDE reported before are algebraic. That is to say, one can see the partition function of a complex tensor model, $Z(\{\lambda_\alpha\}_\alpha)$, as a function of all (possible) coupling constants $\{\lambda_\alpha\}_\alpha$. Whilst [65, 66] derive recursions for (numerical) expectation values $\log Z(\{\lambda_\alpha\}_\alpha)/\partial\lambda_\gamma$, the framework we offer here, on the other hand, allows to derive equations for functional derivatives of $\log Z[J, \bar{J}]$ with respect to the sources J and \bar{J} , thus leading to integro-differential SDE in a quantum field theory context.

The connected correlation $2k$ -point function of rank- D tensor field theories are usually

¹Not to be confused with melonic CFT where tensor fields live on a space-time such as in [48].

defined by

$$G^{(2k)}(\mathbf{x}_1, \dots, \mathbf{x}_k; \mathbf{y}_1, \dots, \mathbf{y}_k) = \left(\prod_{i=1}^k \frac{\delta}{\delta J_{\mathbf{x}_i}} \frac{\delta}{\delta \bar{J}_{\mathbf{y}_i}} \right) \log(Z[J, \bar{J}]) \Big|_{J=\bar{J}=0} \quad (\mathbf{x}_i, \mathbf{y}_i \in \mathbb{Z}^D). \quad (1.1.1)$$

For complex TFT, this definition is redundant, when not equivocal (e.g. $G^{(2)}(\mathbf{x}; \mathbf{y})$ identically vanishes outside the diagonal $\mathbf{x} = \mathbf{y}$). In [62], it was proposed to split each function $G^{(2k)}$ in sectors $G_{\mathcal{B}}^{(2k)}$ that encompass all Feynman graphs indexed by so-called boundary graphs \mathcal{B} (see Sec. 1.2). Here $2k$ denotes the number of vertices of \mathcal{B} and this integer coincides with the number of external legs of the graphs summed in $G_{\mathcal{B}}^{(2k)}$.

There are two reasons to classify correlation functions by boundary graphs. First, by using these correlation functions one gains a clear geometric interpretation in terms of bordisms. Feynman diagrams in complex TFTs are coloured graphs, and these represent graph-encoded triangulations of PL-manifolds. The momentum flux between external legs of an open graph \mathcal{G} determines its so-called boundary, $\mathcal{B} = \partial\mathcal{G}$. Boundary graphs are important because they also triangulate a manifold, and this manifold coincides with the boundary, in the usual sense, of the manifold that the original graph triangulates [18]. Furthermore, by fixing a boundary graph \mathcal{B} , one can sum all connected Feynman graphs that contribute to $G_{\mathcal{B}}^{(2k)}$, and these are interpreted as bordisms whose boundary is triangulated by \mathcal{B} ; for instance, the connected components, \ominus and \boxtimes of (the graph indexing) $G_{|\ominus|, \boxtimes}^{(8)}$ triangulate a sphere and a torus, respectively, and (connected Feynman) graphs contributing to this correlation function are triangulations of bordisms $\mathbb{S}^2 \rightarrow \mathbb{T}^2$ that are compatible with their boundary being ‘triangulated by’ $\ominus \sqcup \boxtimes$.

Secondly, one must do the splitting of the correlations in boundary graphs, otherwise the momenta of the sources interfere with one another. The correlation functions that we propose here need only half the arguments of the functions from definition (1.1.1). For $k = 1, 2, 3, 4$, the connected $2k$ -correlation functions indexed by connected *boundary* graphs are:

$$G_{\ominus}^{(2)}, \quad (1.1.2a)$$

$$G_{1\boxed{1}}^{(4)}, G_{2\boxed{2}}^{(4)}, G_{3\boxed{3}}^{(4)}, \quad (1.1.2b)$$

$$G_{\boxtimes}^{(6)}, G_{\boxplus}^{(6)}, G_{\boxminus}^{(6)}, G_{\boxdot}^{(6)}, G_{\boxed{23}}^{(6)}, G_{\boxed{13}}^{(6)}, G_{\boxed{12}}^{(6)}, \quad (1.1.2c)$$

$$G_{j\boxed{33}i}^{(8)}, G_{\boxed{11}i}^{(8)}, G_{\boxed{11}i}^{(8)}, G_{\boxed{11}i}^{(8)}, G_{\boxed{11}i}^{(8)}, G_{\boxed{11}i}^{(8)}, G_{\boxed{11}i}^{(8)}, G_{\boxed{11}i}^{(8)}, \text{ and } \mathfrak{S}_3\text{-orbits thereof.} \quad (1.1.2d)$$

Moreover, functions such as $G_{|\ominus|\boxed{11}}^{(6)}$ and $G_{|\ominus|\boxtimes}^{(8)}$, indexed by disconnected graphs, need to be considered. None of these graphs is a Feynman graph: in fact we will not deal with them here², since we proceed non-perturbatively.

To these two reasons, we add as motivation the success that this treatment gave for matrix models [6]. There, by splitting in boundary components, the matricial Ward identity was exploited and combined with the Schwinger Dyson equations. This allowed to

²Except Feynman diagram examples appearing in Sec. 1.2.1.

derive an integral equation for the quartic matrix models and, in the planar sector, solve for all correlation functions in terms of the two point function [6] via algebraic recursions. Here, we import these techniques to the complex TFT setting.

In this chapter we derive the full tower of equations that correspond to connected boundary graphs. We also obtain the 2-point and some higher-point Schwinger-Dyson equations (SDE) in an explicit form rank-3 and rank-4 theories. Section 1.2 recalls the setting of complex tensor models in a condensed fashion, and the expansion of the free energy in boundary graphs. The Ward-Takahashi Identity (WTI) [62] for complex TFT, which we recall in Section 1.2.3, is a fundamental auxiliary and bases on this boundary graph expansion. There, we also introduce language to deal with the proper derivation of the full SDE-tower in Section 1.3. We continue with the derivation of the SDE-equations for quartic rank-3 theories (Sec. 1.4) and rank-4 theories in the appendix B (moreover, rank-5 are shortly addressed in B.5).

In order to derive the SDE for a certain $2k$ -point function it is necessary to know, also to order $2k$ in the sources, the form of certain generating functional (for rank 3, Lemma 1.4.1, with proof located in Appendix A) which appears in the Ward-Identity. This requires knowledge of the free energy to order $2(k + 1)$ (in the sources), which in turn needs information about all the graphs with this number of vertices and their coloured automorphism groups. In Appendix B we find the SDE for rank-4 theories with melonic quartic vertices. Explicitly, only the two-point functions and 4-point functions are obtained, since the graph theory in four colours is much more complicated. Section 1.5 before some concluding remarks, presents a model that has simpler SDEs and looks solvable, since, as shown there, it posses a very similar expansion in boundary graphs. It is a tensor field theory that can be used to study the random geometry of 3-spheres.

1.2 Boundary graph expansions

This section rapidly introduces the notation in graph theory and recapitulates previous results that are relevant in our present study. There are few examples in Fig. 1.1 that are intended as support to rapidly grasp the next definitions. Also the rather panoramic Table 1.1 organizes the concepts introduced below.

1.2.1 Complex tensors and coloured graphs

Let N be a (large) integer, thought of as an energy scale, and consider D distinguished representations, $(\mathcal{H}_1, \rho_1), \dots, (\mathcal{H}_D, \rho_D)$ of $U(N)$. A complex tensor field theory is concerned with the quantum theory of tensor fields $\varphi, \bar{\varphi} : \mathcal{H}_1 \otimes \mathcal{H}_2 \otimes \dots \otimes \mathcal{H}_D \rightarrow \mathbb{C}$ whose components transform under said D representations as

$$\begin{aligned} \varphi_{x_1 \dots x_D} &\mapsto \varphi'_{x_1 \dots x_D} = \sum_{y_a} [\rho_a(W_a)]_{x_a y_a} \varphi_{x_1 \dots y_a \dots x_D}, \\ \bar{\varphi}_{x_1 \dots x_D} &\mapsto \bar{\varphi}'_{x_1 \dots x_D} = \sum_{y_a} [\overline{\rho_a(W_a)}]_{x_a y_a} \bar{\varphi}_{x_1 \dots y_a \dots x_D}, \end{aligned}$$

for all $W_a \in U(N)$ and being each x_a and y_a in suitable index-sets $I_a \subset \mathbb{Z}$, for each integer (or *colour*) $a = 1, \dots, D$. Usually one sets $\mathcal{H}_a = \mathbb{C}^N$ or $\mathcal{H}_a = \ell^2[-n, n]$ for suitable

$n = n(N)$, and $\rho_a = \text{id}_{\mathcal{H}_a}$ for each colour a . However, at the same time, one insists that the representations are distinguished, so that indices are anchored to a spot assigned by its colour. Thus, the indices of the tensors have no symmetries (e.g. $\varphi_{ijk} = \varphi_{ikj}$ is forbidden) and only indices of the same colour can be contracted.

A particular tensor model is specified by two additional data: a finite subset of interaction vertices given by real monomials in φ and $\bar{\varphi}$ that are $U(N)$ -invariant under the chosen D representations; the second data is a quadratic form

$$S_0(\varphi, \bar{\varphi}) = \text{Tr}_2(\bar{\varphi}, E\varphi) = \sum_{\mathbf{x}} \bar{\varphi}_{\mathbf{x}} E_{\mathbf{x}} \varphi_{\mathbf{x}}, \quad \text{for certain function } E : I_1 \times \dots \times I_D \rightarrow \mathbb{R}^+,$$

determining the kinetic term S_0 in the classical action. Sums are (implicitly) over the finite lattice $I_1 \times \dots \times I_D \subset \mathbb{Z}^D$. These I_a sets depend usually on a cutoff scale related to N and we will assume, also implicitly, that throughout they are all \mathbb{Z} , keeping in mind that one needs to regularize.

In order to characterize the interaction vertices, one uses vertex-bipartite regularly edge- D -coloured graphs, or, in the sequel, just ‘ D -coloured graphs’. A graph \mathcal{G} being *vertex-bipartite* means that its vertex-set $\mathcal{G}^{(0)}$ splits into two disjoint sets $\mathcal{G}^{(0)} = \mathcal{G}_w^{(0)} \sqcup \mathcal{G}_b^{(0)}$. The set $\mathcal{G}_w^{(0)}$ (resp. $\mathcal{G}_b^{(0)}$) consists of *white* (resp. *black*) vertices. The set of edges, denoted by $\mathcal{G}^{(1)}$ is split as $\mathcal{G}^{(1)} = \sqcup_a \mathcal{G}_a^{(1)}$ into D disjoint sets $\mathcal{G}_a^{(1)}$ of a -coloured edges, $a = 1, \dots, D$. Given any edge e , the white and black vertices e is attached at, are denoted by $s(e) \in \mathcal{G}_w^{(0)}$ and $t(e) \in \mathcal{G}_b^{(0)}$, respectively. This defines the maps $s, t : \mathcal{G}^{(1)} \rightarrow \mathcal{G}^{(0)}$. Regularity of the colouring means that, for each $v \in \mathcal{G}_w^{(0)}$ and each $w \in \mathcal{G}_b^{(0)}$, both preimages $s^{-1}(v)$ and $t^{-1}(w)$ consist precisely of D edges of different colours. By regularity, the number of white and black vertices is the same and is equal to $k(\mathcal{G}) := \#\mathcal{G}^{(0)}/2$. The set of (closed) D -coloured graphs is denoted by $\text{Grph}_D^{\text{cl}}$.

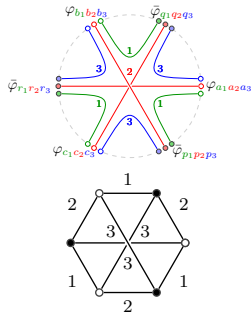
The only way to obtain monomials in the fields φ and $\bar{\varphi}$ that are also invariants, is contracting each coordinate index $\varphi_{\dots x_c \dots}$ by a delta $\delta_{x_c y_c}$ with the coordinate $\bar{\varphi}_{\dots y_c \dots}$ of the respective colour of the field $\bar{\varphi}$. The imposed $U(N)$ -invariance requires then $D \cdot k(\mathcal{G})$ such coloured deltas. One thus associates to each occurrence of φ a white vertex v and to each occurrence of $\bar{\varphi}$ a black vertex w . For each colour c , to each $\delta_{x_c y_c}$ contracting $\varphi_{\dots x_c \dots}$ and $\bar{\varphi}_{\dots y_c \dots}$ one draws a c -coloured edge which starts at v , $v = s(e)$, and ends at w , $w = t(e)$. Thus, any invariant monomial $\text{Tr}_{\mathcal{B}}$ is fully determined by a coloured graph \mathcal{B} , and vice versa. For instance, the trace $\sum_{\mathbf{a}, \mathbf{b}, \mathbf{c}, \mathbf{p}, \mathbf{q}, \mathbf{r}} (\bar{\varphi}_{r_1 r_2 r_3} \bar{\varphi}_{q_1 q_2 q_3} \bar{\varphi}_{p_1 p_2 p_3}) \cdot (\delta_{a_1 p_1} \delta_{a_2 r_2} \delta_{a_3 q_3} \delta_{b_1 q_1} \delta_{b_2 p_2} \delta_{b_3 r_3} \delta_{c_1 r_1} \delta_{c_2 q_2} \delta_{c_3 p_3}) \cdot (\varphi_{a_1 a_2 a_3} \varphi_{b_1 b_2 b_3} \varphi_{c_1 c_2 c_3})$ is depicted in 1.1a.

Any model is then given by an interaction potential $V(\varphi, \bar{\varphi}) = \sum_{\mathcal{B} \in \Lambda} \lambda_{\mathcal{B}} \text{Tr}_{\mathcal{B}}(\varphi, \bar{\varphi})$, for Λ a finite subset of $\text{Grph}_D^{\text{cl}}$. For a fixed model $S = S_0 + V$, one can write down the corresponding partition function:

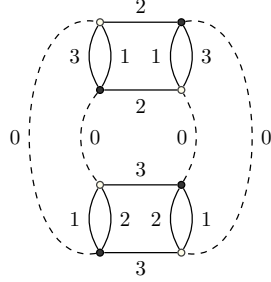
$$Z[J, \bar{J}] = Z_0 \int \mathcal{D}[\varphi, \bar{\varphi}] e^{\text{Tr}_2(\bar{J}, \varphi) + \text{Tr}_2(\bar{\varphi}, J) - N^{D-1} S[\varphi, \bar{\varphi}]}, \quad \mathcal{D}[\varphi, \bar{\varphi}] := \prod_{\mathbf{x} \in \mathbb{Z}^D} N^{D-1} \frac{d\varphi_{\mathbf{x}} d\bar{\varphi}_{\mathbf{x}}}{2\pi i}. \quad (1.2.1)$$

Here $S_0 = \text{Tr}_2(\bar{\varphi}, \varphi)$ is the only quadratic invariant, namely \bigcirc . Later on, at the level of propagator, we will allow this invariance to be broken (see Sec. 1.2).

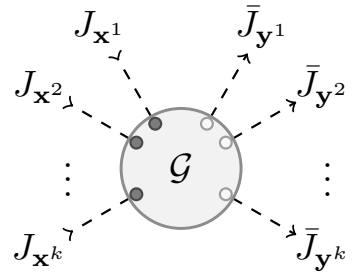
Using Wick’s theorem one evaluates the contributions to the generating functional. Wick’s contractions (*propagators*) are assigned a new colour, 0, which one commonly



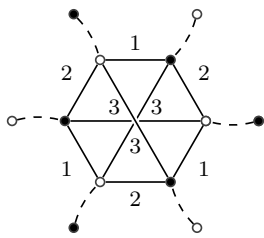
(a) Example of the relation between traces and monomials. This graph is denoted by $K_c(3, 3)$



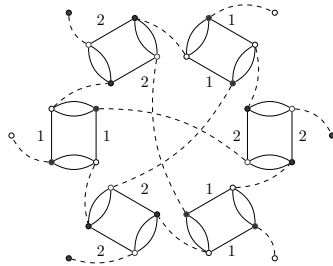
(b) This graph is in $\text{Feyn}_3^v(\varphi^4)$, i.e. it is a vacuum Feynman graph of the φ_3^4 -model, $V(\varphi, \bar{\varphi}) = \lambda(1\text{[1]}_1 + 2\text{[2]}_2 + 3\text{[3]}_3)$



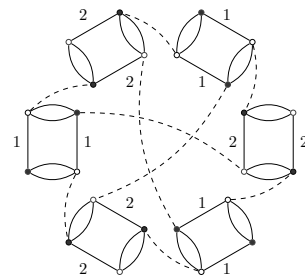
(c) Anatomy of a Feynman graph and how it determines boundary graph \mathcal{B} , which induces the map $\mathcal{B}_* : (\mathbf{x}^1, \dots, \mathbf{x}^k) \mapsto (\mathbf{y}^1, \dots, \mathbf{y}^k)$



(d) Open graph with boundary $K_c(3, 3)$ (in fact it is the cone of $K_c(3, 3)$) but is not in $\text{Feyn}_3(\varphi^4)$



(e) This graph \mathcal{R} is an open graph in $\text{Feyn}_3(\varphi^4) \subset \text{Grph}_{3+1}^{(6)} \subset \text{Grph}_{3+1}$ with $\partial\mathcal{R} = K_c(3, 3)$ (see explanation in 1.1f)



(f) The amputation of \mathcal{R} . If one erases the 0-coloured (or dashed) edges, one gets connected components in $\{1\text{[1]}_1, 2\text{[2]}_2, 3\text{[3]}_3\}$

Figure 1.1: Graph terminology of Sec. 1.2.1 and concerning examples

MAP OF THE GRAPH THEORY OF AN ARBITRARY RANK- D MODEL $V(\varphi, \bar{\varphi})$						
Number of colours	Closed			Open		
	Connected	Disconnected		Connected	Disconnected	
D	<ul style="list-style-type: none"> • Observables • Traces \mathcal{B}, $\text{Tr}_{\mathcal{B}}$ in $V = \sum_{\mathcal{B}} \lambda_{\mathcal{B}} \text{Tr}_{\mathcal{B}}(\varphi, \bar{\varphi})$ • boundaries $\partial\mathcal{G}$ 	<ul style="list-style-type: none"> • generic boundary graph in $\partial(\text{Feyn}_D(V))$ 		\emptyset	\emptyset	
Notation \rightarrow	$\text{Grph}_D^{\text{cl}}$	$\Xi_D^{\text{cl}} = \text{Grph}_D^{\text{ll,cl}} \setminus \text{Grph}_D^{\text{cl}}$		Grph_D	Ξ_D	
$D+1$	vacuum Feynman diagrams, whose set we denote by $\text{Feyn}_D^{\text{v}}(V)$	disconnected \emptyset (no contribution), for taking the logarithm of $Z[J, \bar{J}]$ gets rid of them		the generic Feynman graphs of the model, $\text{Feyn}_D(V)$	\emptyset	
Notation \rightarrow	$\text{Grph}_{D+1}^{\text{cl}}$	$\Xi_{D+1}^{\text{cl}} = \text{Grph}_{D+1}^{\text{ll,cl}} \setminus \text{Grph}_{D+1}^{\text{cl}}$		Grph_{D+1}	Ξ_{D+1}	

Table 1.1: Terminology of Sec. 1.2, and why both graphs in D and $D+1$ number of colours appear in a rank- D models, and which their respective roles are. Here ‘disconnected’ strictly means ‘not connected’. The notation \emptyset stands for ‘no contributions to/no role in the rank- D theory’.

draws as dashed line. For (complex) matrix models ($D = 2$), this 0 colour would be the ribbon line propagator, thus, for tensors, this colour 0 substitutes a cumbersome notation of D parallel lines. It is easy to see that Feynman vacuum graphs of rank- D complex tensors are vertex-bipartite regularly edge- $(D+1)$ -coloured graphs, now the colours being the integers from 0 to D . Vacuum graphs can be connected or disconnected. The set of strictly disconnected graphs is denoted by Ξ_{D+1}^{cl} and $\text{Grph}_{D+1}^{\text{ll,cl}}$ denotes the set of possibly disconnected graphs. We assume that any Feynman graph is connected and get rid of *Feynman* graphs in Ξ_{D+1}^{cl} by working with the free energy, $W[J, \bar{J}] = \log(Z[J, \bar{J}])$, rather than with the partition function.

Since we are mainly interested in the *connected* correlation functions we have to consider *open* Feynman graphs, i.e. graphs with n external legs, each of which is attached to a tensorial source, J or \bar{J} , that obeys the same transformation rules of the field φ or $\bar{\varphi}$, respectively. The external legs are exceptional edges of valence-1 white (for the source J) or black (for \bar{J}) vertices. All external legs’ edges have colour 0. Clearly, because of bipartiteness, this number has to be even, $n = 2k$. We denote by $\text{Grph}_{D+1}^{(2k)}$ the set of Feynman diagrams with $2k$ external legs and further set

$$\text{Grph}_{D+1} = \bigcup_{k=1}^{\infty} \text{Grph}_{D+1}^{(2k)} \cup \text{Grph}_{D+1}^{\text{cl}}$$

generically for open or closed $(D+1)$ -coloured graphs.

Importantly, not every graph in Grph_{D+1} is a Feynman graph. The set of Feynman graphs of a model $V(\varphi, \bar{\varphi}) = \sum_{\mathcal{B} \in \Lambda} \lambda_{\mathcal{B}} \text{Tr}_{\mathcal{B}}(\varphi, \bar{\varphi})$ is denoted by $\text{Feyn}_D(V(\varphi, \bar{\varphi}))$ or $\text{Feyn}_D(V)$. This set consists of the graphs in Grph_{D+1} that satisfy the following condition: after amputating all external legs and removing all the 0-coloured edges, the remaining graph has connected components in the set of interaction-vertices $\Lambda \subset \text{Grph}_D^{\text{cl}}$ (see Figs. 1.1e, 1.1f).

1.2.2 Boundary graphs

There is a boundary map $\partial : \text{Grph}_{D+1} \rightarrow \text{Grph}_D^{\text{II,cl}}$, which for all $\mathcal{G} \in \text{Grph}_{D+1}$ is given by

$$\begin{aligned} (\partial\mathcal{G})^{(0)} &:= \{\text{external legs of } \mathcal{G}\}, \\ (\partial\mathcal{G})_a^{(1)} &:= \{(0a)\text{-bicoloured paths between external legs in } \mathcal{G}\}. \end{aligned}$$

The vertex set inherits the bipartiteness from \mathcal{G} , to wit a vertex in $(\partial\mathcal{G})^{(0)}$ is *black* if it corresponds from an external line attached to a white vertex, and *white* if it is attached to a black vertex in \mathcal{G} . The edge set is regularly D -coloured $(\partial\mathcal{G})^{(1)} = \cup_a (\partial\mathcal{G})_a^{(1)}$.

For a fixed model $V(\varphi, \bar{\varphi})$, the image of the restriction $\partial_V := \partial|_{\text{Feyn}_D(V)}$ of ∂ to $\text{Feyn}_D(V)$ is deemed *boundary sector*, and this set is, of course, model dependent. A graph in the boundary sector is a *boundary graph*. For melonic quartic theories, as a matter of fact [62], this boundary map is surjective, so all (possibly disconnected) D -coloured graphs are boundaries. Thus, all the correlation functions we propose have non-trivial contributions. Incidentally, this means that quartic coloured random tensor models are able to ponder probabilities of triangulation of all bordisms, provided they exist, as in dimension d ($d = D - 1 = 2, 3$) as classical objects (oriented manifolds); in presence of obstructions, there are pseudo-manifolds yielding those bordisms.

Given a closed coloured graph \mathcal{B} , $\text{Aut}_c(\mathcal{B})$ denotes the set of its *coloured automorphisms*. These are graph maps $\mathcal{B} \rightarrow \mathcal{B}$ that preserve adjacency, the bipartiteness of $\mathcal{B}^{(0)}$ and also its edge-colouring. Each automorphism of \mathcal{B} arises from a lifting of an element π of $\text{Sym}(\mathcal{B}_w^{(0)}) = \mathfrak{S}_{k(\mathcal{B})}$ to a unique map $\hat{\pi} : \mathcal{B} \rightarrow \mathcal{B}$, determined by the preservation of said structure. Figures 1.2 and 1.3 show all the automorphism groups for graphs having up to 8 vertices in $D = 3$ and up to 6 vertices for $D = 4$, respectively.

We shall assume that both the white vertex-set $\mathcal{B}_w^{(0)} = (v^1, \dots, v^{k(\mathcal{B})})$ as well as the black vertex-set $\mathcal{B}_b^{(0)} = (w^1, \dots, w^{k(\mathcal{B})})$ of a boundary graph \mathcal{B} are given an ordering. Then $e_a^{v^\mu}$, the edge of colour a attached to a white vertex $v \in \mathcal{B}_w^{(0)}$, i.e. $s(e_a^{v^\mu}) = v^\mu$, is denoted by e_a^μ .

Let \mathcal{B} be a boundary graph and $k = k(\mathcal{B})$. Then \mathcal{B} induces a map³ $\mathcal{B}_* : M_{D \times k}(\mathbb{Z}) \rightarrow M_{D \times k}(\mathbb{Z})$ by $\mathbf{X} = (\mathbf{x}^1, \dots, \mathbf{x}^k) \mapsto \mathcal{B}_*(\mathbf{X}) = (\mathbf{y}^1, \dots, \mathbf{y}^k)$, where $y_a^\alpha = x_a^\nu$ (for $\alpha = 1, \dots, k$) if and only if there exists an a -coloured edge starting at v^α and ending at w^ν . Regularity of the colouring and bipartiteness of the vertex set ensure that there is exactly one such edge, thus rendering \mathcal{B}_* well-defined. This map \mathcal{B}_* is deduced by momentum transmission inside any graph \mathcal{G} for with $\partial\mathcal{G} = \mathcal{B}$ by following the $a0$ -coloured paths in \mathcal{G} between its external vertices. One further associates to \mathcal{B} and \mathbf{X} a cycle of sources

$$\mathbb{J}(\mathcal{B})(\mathbf{X}) = J_{\mathbf{x}^1} \cdots J_{\mathbf{x}^k} \bar{J}_{\mathbf{y}^1} \cdots \bar{J}_{\mathbf{y}^k}, \quad \text{where } \mathcal{B}_*(\mathbf{X}) = (\mathbf{y}^1, \dots, \mathbf{y}^k), \quad (1.2.2)$$

which is evidently independent of the ordering given to $\mathcal{B}_w^{(0)}$ and $\mathcal{B}_b^{(0)}$. According to [62], the free energy $W[J, \bar{J}] = \log(Z[J, \bar{J}])$ can be expanded in these cycles indexed by all the boundary graphs of a given model:

$$W[J, \bar{J}] = \sum_{l=1}^{\infty} \sum_{\substack{\mathcal{B} \in \text{im } \partial_V \\ k(\mathcal{B})=l}} \frac{1}{|\text{Aut}_c(\mathcal{B})|} G_{\mathcal{B}}^{(2l)} \star \mathbb{J}(\mathcal{B}) \quad (1.2.3)$$

³The use of matrices $M_{D \times k}(\mathbb{Z})$, instead of plainly \mathbb{Z}^{kD} , merely eases the definition of $\mathcal{F}_{D,k}$ below. No matrix multiplication is so far needed.

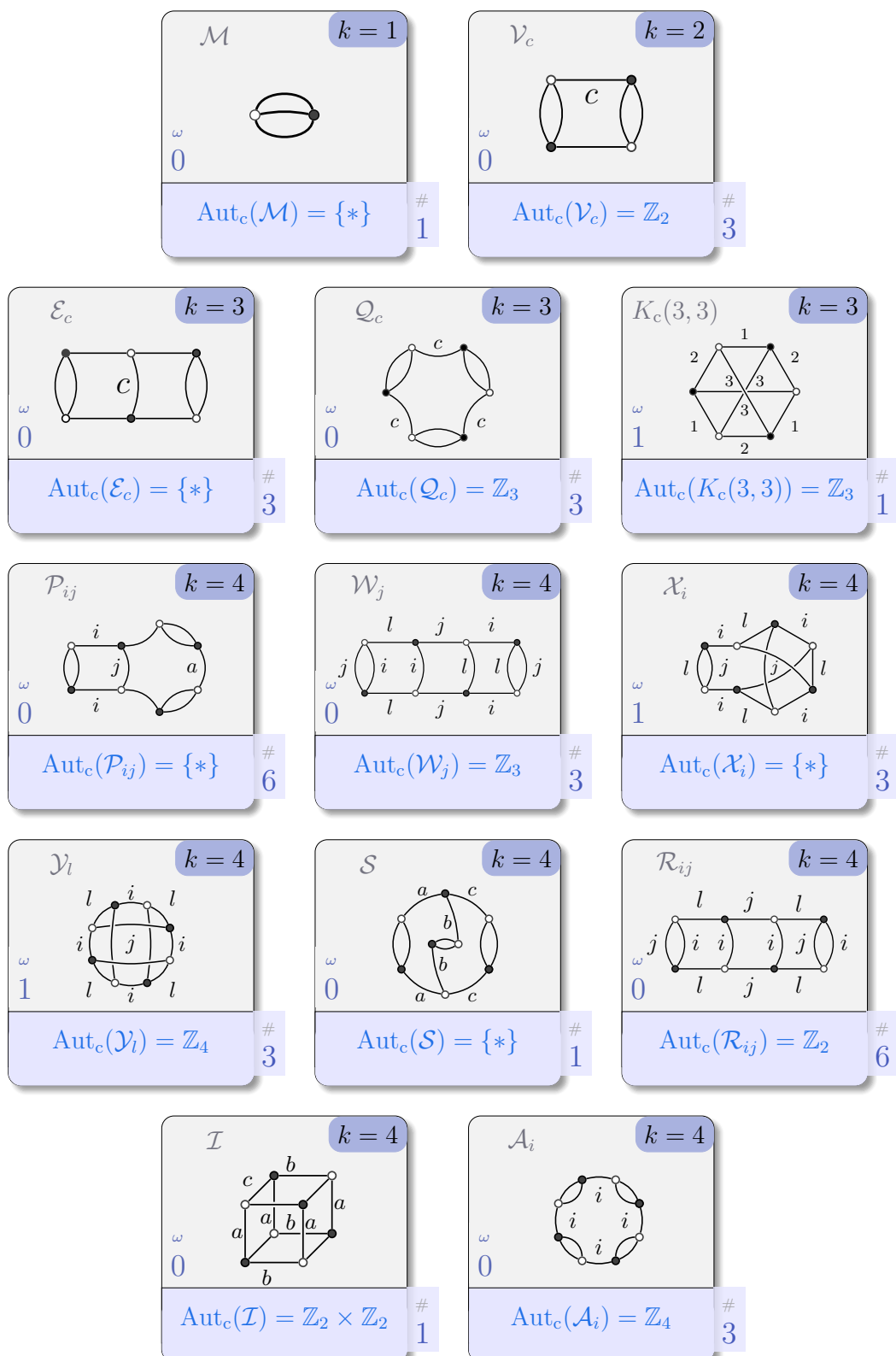


Figure 1.2: Enumeration of 3-coloured graphs with 2, 4, 6 and 8 vertices and their Gurău-degree ω and coloured automorphism group.

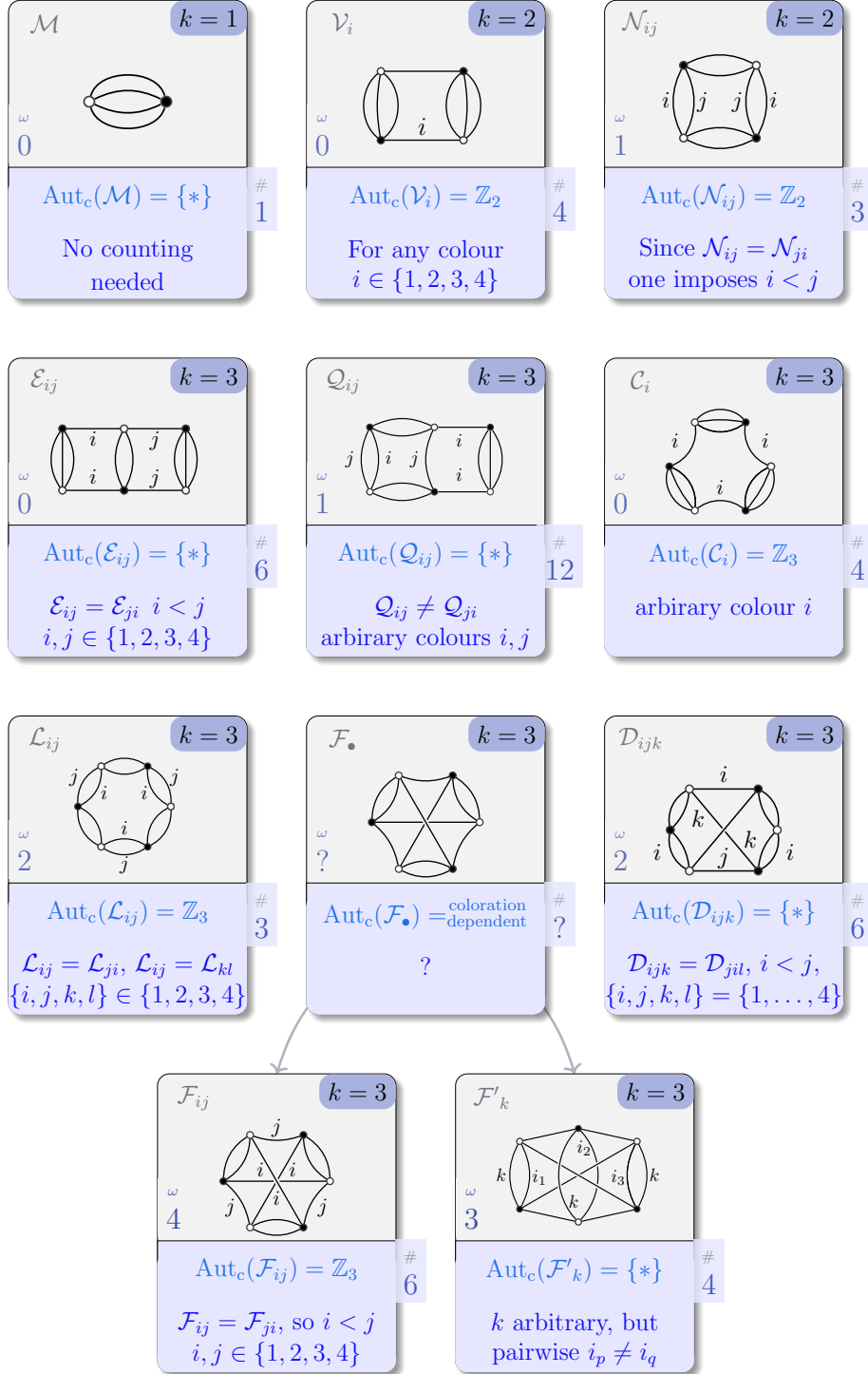


Figure 1.3: This table shows the rank-4 graphs until 6 vertices. As before, # is the number of graphs that are obtained by the action of \mathfrak{S}_4 in the edge-colouring and ω is Gurău's degree of the graph in question. For graphs with $k = 4$ see [49, Fig. 8] (there, only those marked with a B are bipartite). The graphs displayed there are neither given a colouration nor classified by \mathfrak{S}_4 -orbits, though (Klebanov and Tarnopolsky treat them as vacuum Feynman graphs; here our graphs are boundaries and we need to count them and their Aut_c -groups).

where \star is a pairing between a function $f : M_{D \times k(\mathcal{B})} \rightarrow \mathbb{C}$ and a boundary graph $\mathcal{B} \in \text{im } \partial_V \subset \text{Grph}_D^{\text{II,cl}}$ given by $f \star \mathbb{J}(\mathcal{B}) = \sum_{\mathbf{X} \in M_{D \times k(\mathcal{B})}(\mathbb{Z})} f(\mathbf{X}) \cdot \mathbb{J}(\mathcal{B})(\mathbf{X})$. To read off the correlation functions $G_{\mathcal{B}}^{(2l)}$ from eq. (1.2.3), one takes graph derivatives, introduced in [62] and recapitulated in the next section.

1.2.3 Graph-generated functionals

We also recall some results from [62]. Let

$$\mathcal{F}_{D,k} := \{(\mathbf{y}^1, \dots, \mathbf{y}^k) \in M_{D \times k}(\mathbb{Z}) \mid y_c^\alpha \neq y_c^\nu \text{ for all } c = 1, \dots, D \text{ and } \alpha, \nu = 1, \dots, k, \alpha \neq \nu\}.$$

Thus $\mathcal{F}_{D,k}$ is the set of matrices $M_{D \times k}(\mathbb{Z})$ having all different entries on any fixed row. We define the graph derivative of any functional $X[J, \bar{J}]$ with respect to \mathcal{B} at $\mathbf{X} \in \mathcal{F}_{D,k}$ as

$$\frac{\partial X[J, \bar{J}]}{\partial \mathcal{B}(\mathbf{X})} := \frac{\delta^{2k(\mathcal{B})} X[J, \bar{J}]}{\delta(\mathbb{J}(\mathcal{B}))(\mathbf{X})} \Big|_{J=0=\bar{J}} = \prod_{\alpha=1}^k \frac{\delta}{\delta J_{\mathbf{x}^\alpha}} \frac{\delta}{\delta \bar{J}_{\mathbf{y}^\alpha}} X[J, \bar{J}] \Big|_{J=0=\bar{J}}.$$

Let $(\mathbf{y}^1, \dots, \mathbf{y}^l) \in M_{D \times l}(\mathbb{Z})$. For closed, coloured graphs $\mathcal{Q}, \mathcal{C} \in \text{Grph}_D^{\text{cl}}$ one has [62]:

$$\frac{\partial \mathcal{Q}(\mathbf{y}^1, \dots, \mathbf{y}^l)}{\partial \mathcal{C}(\mathbf{x}^1, \dots, \mathbf{x}^k)} = \left\{ \begin{array}{ll} \sum_{\hat{\sigma} \in \text{Aut}_c(\mathcal{C})} \delta_{lk} \cdot \delta_{\mathbf{x}^1, \mathbf{x}^2, \dots, \mathbf{x}^k}^{\mathbf{y}^{\sigma(1)}, \dots, \mathbf{y}^{\sigma(k)}} & \text{if } \mathcal{C} \cong \mathcal{Q} \\ 0 & \text{otherwise} \end{array} \right\} = \sum_{\sigma \in \mathfrak{S}_k} \delta_{\mathbf{x}^1, \mathbf{x}^2, \dots, \mathbf{x}^k}^{\mathbf{y}^{\sigma(1)}, \dots, \mathbf{y}^{\sigma(k)}} \delta(\mathcal{Q}, \mathcal{C}) \quad (1.2.4)$$

where $\delta(\mathcal{Q}, \mathcal{C}) = 1$ if the graphs \mathcal{Q} and \mathcal{C} are isomorphic, and 0 otherwise. We consider functionals generated by a given family of closed D -coloured (non-isomorphic) graphs, $\Upsilon \subset \text{Grph}_D^{\text{II,cl}}$. That means that if

$$X[J, \bar{J}] = \sum_{\mathcal{C} \in \Upsilon} \mathfrak{l}_{\mathcal{C}} \star \mathbb{J}(\mathcal{C}), \quad \text{for } \mathfrak{l}_{\mathcal{C}} : (\mathbb{Z}^D)^{\times k(\mathcal{C})} \rightarrow \mathbb{C}, \quad \mathcal{C} \in \Upsilon, \quad (1.2.5)$$

is known, we want to know the graph derivatives of $X[J, \bar{J}]$ with respect to connected graphs. Here $k(\mathcal{C})$ denotes the number $\#(\mathcal{C}_w^{(0)})$ of white (or black) vertices of \mathcal{C} .

Proposition 1.2.1. *Let X be as in eq. (1.2.5). Then, for all $\mathcal{C} \in \Upsilon \cap \text{Grph}_D^{\text{cl}}$, the functions $\mathfrak{l}_{\mathcal{C}}$ satisfy*

$$\frac{\partial X[J, \bar{J}]}{\partial \mathcal{C}(\mathbf{X})} = \sum_{\hat{\sigma} \in \text{Aut}_c(\mathcal{C})} (\hat{\sigma}^* \mathfrak{l}_{\mathcal{C}})(\mathbf{X}), \text{ where } (\hat{\sigma}^* \mathfrak{l}_{\mathcal{C}})(\mathbf{x}^1, \dots, \mathbf{x}^{k(\mathcal{C})}) := \mathfrak{l}_{\mathcal{C}}(\mathbf{x}^{\hat{\sigma}^{-1}(1)}, \dots, \mathbf{x}^{\hat{\sigma}^{-1}(k(\mathcal{C}))}),$$

for all $\mathbf{X} = (\mathbf{x}^1, \dots, \mathbf{x}^{k(\mathcal{C})}) \in \mathcal{F}_{D, k(\mathcal{C})}$.

Proof. From formula (1.2.4), one has

$$\begin{aligned} \frac{\partial X[J, \bar{J}]}{\partial \mathcal{C}(\mathbf{X})} &= \frac{\partial}{\partial \mathcal{C}(\mathbf{X})} \sum_{\mathcal{Q} \in \Upsilon} \mathfrak{l}_{\mathcal{Q}} \star \mathbb{J}(\mathcal{Q}) = \sum_{\mathcal{Q} \in \Upsilon} \sum_{\mathbf{Y} \in (\mathbb{Z}^D)^k} \mathfrak{l}_{\mathcal{Q}}(\mathbf{Y}) \frac{\partial \mathcal{Q}(\mathbf{Y})}{\partial \mathcal{C}(\mathbf{X})} \\ &= \sum_{\mathcal{Q} \in \Upsilon} \sum_{\mathbf{Y} \in (\mathbb{Z}^D)^{\times k(\mathcal{Q})}} \mathfrak{l}_{\mathcal{Q}}(\mathbf{Y}) \sum_{\sigma \in \mathfrak{S}_{k(\mathcal{Q})}} \delta(\mathcal{Q}, \mathcal{C}) \prod_{i=1}^{k(\mathcal{Q})} \delta(\mathbf{y}^{\sigma(i)}, \mathbf{x}^i) \end{aligned}$$

$$\begin{aligned}
&= \sum_{\mathcal{Q} \in \Upsilon} \sum_{\mathbf{Y} \in (\mathbb{Z}^D)^{\times k(\mathcal{C})}} \iota_{\mathcal{Q}}(\mathbf{Y}) \sum_{\sigma \in \mathfrak{S}_{k(\mathcal{Q})}} \delta(\mathcal{Q}, \mathcal{C}) \prod_{i=1}^{k(\mathcal{Q})} \delta(\mathbf{y}^i, \mathbf{x}^{\sigma^{-1}(i)}) \\
&= \sum_{\mathcal{Q} \in \Upsilon} \sum_{\sigma \in \mathfrak{S}_{k(\mathcal{Q})}} \iota_{\mathcal{C}}(\mathbf{x}^{\sigma^{-1}(1)}, \dots, \mathbf{x}^{\sigma^{-1}(k)}) \delta(\mathcal{Q}, \mathcal{C}).
\end{aligned}$$

Since Υ consists only of graphs that are not isomorphic, the sum over \mathcal{Q} yields, because of the delta $\delta(\mathcal{Q}, \mathcal{C})$, only one term. Hence, the last expression is precisely the sum over automorphisms of \mathcal{C} . \square

As a consequence of this, one can recover the correlation functions via

$$G_{\mathcal{B}}^{(2k(\mathcal{B}))}(\mathbf{X}) = \frac{\partial W[J, \bar{J}]}{\partial \mathcal{B}(\mathbf{X})}.$$

Notice that $\mathbf{X} = (\mathbf{x}^1, \dots, \mathbf{x}^k) \in \mathcal{F}_{D,k}$ if and only if $\mathcal{B}_*(\mathbf{X}) \in \mathcal{F}_{D,k}$. Since $W[J, \bar{J}]$ is real-valued, one has the relation

$$\overline{G_{\mathcal{B}}^{(2k(\mathcal{B}))}}(\mathbf{X}) = \prod_{\alpha=1}^k \frac{\delta}{\delta \bar{J}_{\mathbf{x}^\alpha}} \frac{\delta}{\delta J_{\mathbf{y}^\alpha}} \overline{W[J, \bar{J}]} \Big|_{J=0=\bar{J}} = G_{\bar{\mathcal{B}}}^{(2k(\mathcal{B}))}(\mathcal{B}_*(\mathbf{X})) \quad (\mathbf{X} \in \mathcal{F}_{D,k(\mathcal{B})}), \quad (1.2.6)$$

where $\bar{\mathcal{B}}$ is essentially the graph \mathcal{B} after inverting vertex-colouration, $\bar{\mathcal{B}}_{\mathbf{w}}^{(0)} = \mathcal{B}_{\mathbf{b}}^{(0)}$ and $\bar{\mathcal{B}}_{\mathbf{b}}^{(0)} = \mathcal{B}_{\mathbf{w}}^{(0)}$, but otherwise with the same adjacency and edge-colouration.

We now explain how this graph derivatives are relevant in the WTI. The WTI is rather a set of equations, one for each colour $a = 1, 2, \dots, D$, in which a new generating functional of the form

$$Y_{s_a}^{(a)}[J, \bar{J}] = \sum_{\mathcal{C} \in \Omega_V} \mathfrak{f}_{\mathcal{C}, s_a}^{(a)} \star \mathfrak{J}(\mathcal{C}) \quad (s_a \in I_a \subset \mathbb{Z}) \quad (1.2.7)$$

appears. Here, $\partial_V : \text{Feyn}_D(V) \rightarrow \text{Grph}_D^{\text{II,cl}}$ denotes the boundary map in terms of which we describe the graph family Ω_V as follows: If e_a^v is the a -coloured edge at the white vertex $v \in \mathcal{B}_{\mathbf{w}}^{(0)}$, then the graph $\mathcal{B} \ominus e_a^v$ denotes the graph that is obtained by the next steps: first, remove the two end-vertices, $v = s(e_a^v)$ and $t(e_a^v)$, of e_a^v ; then, remove all their common edges $I(e_a^v) := s^{-1}(s(e_a^v)) \cap t^{-1}(t(e_a^v))$; finally, glue colour-wise the broken edges, i.e. the each broken edge of the set $s^{-1}(v) \setminus I(e_a^v)$ with the respective broken edge in $t^{-1}(t(e_a^v)) \setminus I(e_a^v)$. Then Ω is defined by

$$\Omega_V := \{\mathcal{B} \ominus e_a^v \mid \mathcal{B} \in \text{im } \partial_V, v \in \mathcal{B}_{\mathbf{w}}^{(0)}\}.$$

Definition 1.2.2. Let a be a colour, $F : (\mathbb{Z}^D)^k \rightarrow \mathbb{C}$ a function and $\mathcal{B} \in \text{Grph}_D^{\text{II,cl}}$. For any integer r , $1 \leq r \leq k(\mathcal{B})$, we define the function $\Delta_{s_a, r}^{\mathcal{B}} F : (\mathbb{Z}^D)^{k-1} \rightarrow \mathbb{C}$ by

$$(\Delta_{s_a, r}^{\mathcal{B}} F)(\mathbf{Y}) = \sum_{q_h} F(\mathbf{y}^1, \dots, \mathbf{y}^{r-1}, \mathbf{z}^r(s_a, \mathbf{q}, \mathbf{Y}), \mathbf{y}^r, \dots, \mathbf{y}^{k-1}),$$

for each $\mathbf{Y} = (\mathbf{y}^1, \dots, \mathbf{y}^{k-1}) \in (\mathbb{Z}^D)^{k-1}$, where the sum is over a dummy variable q_h for each element of the set $h \in I(e_a^r) \setminus \{a\}$. Before specifying $\mathbf{z}^r(s_a, \mathbf{q}, \mathbf{Y})$, we stress that this sum can be empty, in which case

$$(\Delta_{s_a, r}^{\mathcal{B}} F)(\mathbf{Y}) = F(\mathbf{y}^1, \dots, \mathbf{y}^{r-1}, \mathbf{z}^r(s_a, \mathbf{Y}), \mathbf{y}^r, \dots, \mathbf{y}^k).$$



(a) Locally, edge and vertex labelling in \mathcal{B} before forming $\mathcal{B} \ominus e_a^r$

(b) Locally $\mathcal{B} \ominus e_a^r$

Figure 1.4: Some notation concerning the definition of $\Delta_{s_a, r}^{\mathcal{B}}$.

The momentum $\mathbf{z}^r \in \mathbb{Z}^D$ has entries defined by:

$$z_i^r(s_a, \mathbf{q}, \mathbf{Y}) = \begin{cases} s_a & \text{if } i = a, \\ q_i & \text{if } i \in I(e_a^r) \setminus \{a\}, \\ y_i^{\kappa(r,i,a)} & \text{if } i \in \text{colours of } A_{t(e_a^r)} = \{1, \dots, D\} \setminus I(e_a^r), \end{cases}$$

where $\mathbf{y}^{\kappa(r,i,a)}$ ($1 \leq \kappa(r,i,a) < k$) is the white vertex $\mathcal{B} \ominus e_a^r$ defined by

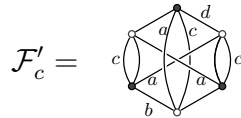
$$\kappa(r,i,a) = \begin{cases} \xi(r,i,a) & \text{if } \xi(r,i,a) < r, \\ \xi(r,i,a) - 1 & \text{if } \xi(r,i,a) > r. \end{cases} \quad (1.2.8)$$

(see also Fig. 1.4). This definition depends on the labeling of the vertices. However, the pairing $\langle\langle G_{\mathcal{B}}^{(2k)}, \mathcal{B} \rangle\rangle_{s_a}$ defined as follows does not, for it is a sum over graphs after removal of *all* a -coloured edges:

$$\langle\langle G_{\mathcal{B}}^{(2k)}, \mathcal{B} \rangle\rangle_{s_a} := \sum_{r=1}^k \left(\Delta_{s_a, r}^{\mathcal{B}} G_{\mathcal{B}}^{(2k)} \right) \star \mathbb{J}(\mathcal{B} \ominus e_a^r). \quad (1.2.9)$$

Remark 1.2.3. Unless otherwise stated, we set the convention of ordering the white-vertex-set $\mathcal{B}_w^{(0)}$ in appearance from left to right.

Example 1.2.4. Let $\{a, b, c, d\} = \{1, 2, 3, 4\}$ and



(see also Fig. 1.2). For a fixed colour a and $s_a \in I_a \subset \mathbb{Z}$, we obtain $\langle\langle G_{\mathcal{F}'_c}^{(2k)}, \mathcal{F}'_c \rangle\rangle_{s_a}$. According to remark 1.2.3, the first white vertex is the left upper left white vertex, the second is the lowermost, the third is the upper right. This orders the a -coloured edges $\{e_a^1, e_a^2, e_a^3\}$. Explicitly,

$$\mathcal{F}'_c = \text{graph with 6 vertices and 10 edges} , \text{ thus, } \mathcal{F}'_c \ominus e_a^1 = \mathcal{F}'_c \ominus e_a^3 = \text{graph with 4 vertices and 4 edges} , \quad \mathcal{F}'_c \ominus e_a^2 = \text{graph with 4 vertices and 4 edges}$$

hence

$$\langle\langle G_{\mathcal{F}'_c}^{(6)}, \mathcal{F}'_c \rangle\rangle_{s_a} = \Delta_{s_a, 1} G_{\mathcal{F}'_c}^{(6)} \star \mathbb{J}(\text{graph with 4 vertices and 4 edges}) + \Delta_{s_a, 2} G_{\mathcal{F}'_c}^{(6)} \star \mathbb{J}(\text{graph with 4 vertices and 4 edges}) + \Delta_{s_a, 3} G_{\mathcal{F}'_c}^{(6)} \star \mathbb{J}(\text{graph with 4 vertices and 4 edges})$$

which, in turn, equals

$$\begin{aligned}
& \sum_{\mathbf{y}, \mathbf{z}} \left\{ \Delta_{s_a, 1} G_{\mathcal{F}'_c}^{(6)}(\mathbf{y}, \mathbf{z}) \mathbb{J} \left(\begin{array}{c} a \\ \text{---} \\ \text{---} \\ \text{---} \\ c \\ \text{---} \\ \text{---} \\ a \end{array} \right) (\mathbf{y}, \mathbf{z}) + \Delta_{s_a, 2} G_{\mathcal{F}'_c}^{(6)}(\mathbf{y}, \mathbf{z}) \mathbb{J} \left(\begin{array}{c} \text{---} \\ a \end{array} \right) (\mathbf{y}, \mathbf{z}) \right. \\
& \quad \left. + \Delta_{s_a, 3} G_{\mathcal{F}'_c}^{(6)}(\mathbf{y}, \mathbf{z}) \mathbb{J} \left(\begin{array}{c} a \\ \text{---} \\ \text{---} \\ \text{---} \\ c \\ \text{---} \\ \text{---} \\ a \end{array} \right) (\mathbf{y}, \mathbf{z}) \right\} \\
& = \sum_{\mathbf{y}, \mathbf{z}} \left\{ G_{\mathcal{F}'_c}^{(6)}(s_a, z_b, z_c, y_d, \mathbf{y}, \mathbf{z}) \bar{J}_{y_a z_b y_c z_d} \bar{J}_{z_a y_b z_c y_d} J_{\mathbf{y}} J_{\mathbf{z}} + \left(\sum_{q_c} G_{\mathcal{F}'_c}^{(6)}(\mathbf{y}, s_a, y_b, q_c, z_d, \mathbf{z}) \right. \right. \\
& \quad \left. \left. \times \bar{J}_{y_a z_b z_c z_d} \bar{J}_{z_a y_b y_c y_d} J_{\mathbf{y}} J_{\mathbf{z}} \right) + G_{\mathcal{F}'_c}^{(6)}(\mathbf{y}, \mathbf{z}, s_a, z_b, y_c, y_d) \bar{J}_{y_a z_b y_c z_d} \bar{J}_{z_a y_b z_c y_d} J_{\mathbf{y}} J_{\mathbf{z}} \right\}.
\end{aligned}$$

We assume all the entries of momenta in \mathbb{Z}^4 are ordered by colour, e.g. $(z_1 y_4 z_3 y_2)$ really means $(z_1 y_2 z_3 y_4)$.

We now recall the full Ward-Takahashi Identity, proven in [62].

Theorem 1.2.5. *Consider a rank- D tensor model, $S = S_0 + V$, with a kinetic form $\text{Tr}_2(\bar{\varphi}, E\varphi)$ such that the difference of propagators $E_{p_1 \dots p_{a-1} m_a p_{a+1} \dots p_D} - E_{p_1 \dots p_{a-1} n_a p_{a+1} \dots p_D} = E(m_a, n_a)$ is independent of the momenta $\mathbf{p}_a = (p_1, \dots, \hat{p}_a, \dots, p_D)$. Then that model has a partition function $Z[J, \bar{J}]$ that satisfies*

$$\begin{aligned}
& \sum_{\mathbf{p}_a} \frac{\delta^2 Z[J, \bar{J}]}{\delta J_{p_1 \dots p_{a-1} m_a p_{a+1} \dots p_D} \delta \bar{J}_{p_1 \dots p_{a-1} n_a p_{a+1} \dots p_D}} - (\delta_{m_a n_a} Y_{m_a}^{(a)}[J, \bar{J}]) \cdot Z[J, \bar{J}] \quad (1.2.10) \\
& = \sum_{\mathbf{p}_a} \frac{1}{E_{p_1 \dots m_a \dots p_D} - E_{p_1 \dots n_a \dots p_D}} \left(\bar{J}_{p_1 \dots m_a \dots p_D} \frac{\delta}{\delta \bar{J}_{p_1 \dots n_a \dots p_D}} - J_{p_1 \dots n_a \dots p_D} \frac{\delta}{\delta J_{p_1 \dots m_a \dots p_D}} \right) Z[J, \bar{J}]
\end{aligned}$$

where

$$Y_{m_a}^{(a)}[J, \bar{J}] := \sum_{l=1}^{\infty} \sum_{\substack{\mathcal{B} \in \text{im } \partial_V \\ k(\mathcal{B})=l}} \langle\langle G_{\mathcal{B}}^{(2l)}, \mathcal{B} \rangle\rangle_{m_a}. \quad (1.2.11)$$

There is a subtlety regarding the ordering of the vertices. We associate an ordering of the white vertices of a graph \mathcal{B} in $G_{\mathcal{B}}^{(2k)}$. The k arguments (in \mathbb{Z}^D) of this function match this vertex-ordering. But the edge-removal sometimes will yield a graph which should be reoriented. To illustrate this, for $D = 3$, consider for instance the next graph \mathcal{S} . The edge contraction yields, for any $i = 1, 2, 3$, the following:

$$\text{If } \mathcal{S} = \begin{array}{c} a \quad c \\ \text{---} \\ \text{---} \\ \text{---} \\ b \\ \text{---} \\ \text{---} \\ a \quad c \end{array} \text{ then } \mathcal{S} \ominus e_i^1 = \begin{array}{c} a \quad c \\ \text{---} \\ \text{---} \\ \text{---} \\ b \\ \text{---} \\ \text{---} \\ a \quad c \end{array} \ominus e_i^1 = \begin{array}{c} c \\ \text{---} \\ \text{---} \\ \text{---} \\ b \\ \text{---} \\ \text{---} \\ a \end{array} \quad (1.2.12)$$

As a graph, $\mathcal{S} \ominus e_i^1$ is just $\begin{array}{c} b \quad c \\ \text{---} \\ \text{---} \\ \text{---} \\ a \end{array}$, but when one considers $f \star \mathbb{J}(\mathcal{S} \ominus e_i^1)$, for some function $f : (\mathbb{Z}^3)^{\times 3} \rightarrow \mathbb{C}$, the order of the vertices does matter:

$$f \star \mathbb{J} \left(\begin{array}{c} c \\ \text{---} \\ \text{---} \\ \text{---} \\ b \\ \text{---} \\ \text{---} \\ a \end{array} \right) = ((12)^* f) \star \mathbb{J} \left(\begin{array}{c} b \quad c \\ \text{---} \\ \text{---} \\ \text{---} \\ a \end{array} \right)$$

In going from the graph 1.2.12 to $\overset{b}{\circ} \overset{c}{\circ}$, one permuted the first and second white vertices. Accordingly, one ‘corrects’ f and replaces it by $(12)^*(f)$. Notice that the cycle $(12) \in \mathfrak{S}_3$ does not lift to a coloured automorphism. If this was the case, we could just as well ignore the correction.

The next definition is needed in order to describe some terms appearing in the SDEs.

Definition 1.2.6. Let $\mathcal{B} \in \text{Grph}_D^{\text{cl}}$ and let v, w be vertices of the same colour (either both black $v, w \in \mathcal{B}_b^{(0)}$ or both white $v, w \in \mathcal{B}_w^{(0)}$). We define the graph $\varsigma_a(\mathcal{B}; v, w)$ as the coloured graph obtained from \mathcal{B} by swapping the a -coloured edges at v and w . Usually, vertices in boundary graphs are indexed by numbered momenta $v = \mathbf{x}^\alpha, w = \mathbf{x}^\gamma \in \mathbb{Z}^D$, in which case we write $\varsigma_a(\mathcal{B}; \mathbf{x}^\alpha, \mathbf{x}^\gamma)$ or just $\varsigma_a(\mathcal{B}; \alpha, \gamma)$. These graphs are, generally, disconnected.

Example 1.2.7. For any colour $a = 1, 2, 3$, one has $\varsigma_a(\overset{b}{\circ} \overset{c}{\circ}; u, v) = \overset{b}{\circ} \overset{c}{\circ} \overset{a}{\circ} =: \mathcal{E}_a$ for two black (or white) vertices u, v of $\overset{b}{\circ} \overset{c}{\circ}$. If x and y are the leftmost black vertices of \mathcal{E}_a , then $\varsigma_b(\mathcal{E}_a; x, y) = \overset{b}{\circ} \sqcup \overset{c}{\circ}$.

1.3 The Schwinger-Dyson equation tower in arbitrary rank

We pick the following quartic model $S = S_0 + \mathcal{S}_{\text{int}}$, with interaction vertices $\mathcal{S}_{\text{int}}[\varphi, \bar{\varphi}] = \lambda \sum_{a=1}^D \text{Tr}_{\mathcal{V}_a}(\varphi, \bar{\varphi})$, being each vertex \mathcal{V}_a the melonic vertex of colour a ,

$$\mathcal{V}_a = \begin{array}{c} a \\ \circ \quad \circ \\ \vdots \quad \vdots \\ \circ \quad \circ \\ a \end{array} \quad (1.3.1)$$

Moreover, assume that the propagator obeys that, for each colour a , the following difference

$$E(t_a, s_a) := E_{p_1 \dots t_a \dots p_D} - E_{p_1 \dots s_a \dots p_D}$$

does not depend on p_i , for each $i \neq a$. Such is the case for Tensor Group Field theories, say with group $U(1)$, being the origin of E is the Laplacian operator on $U(1)^D$ after taking Fourier transform, and the tensors the Fourier modes. We call this model the $\varphi_{D,m}^4$ -theory⁴. Here, the subindex ‘m’ denotes melonicity. For specific choices of propagators and renormalizability, see [67] and references therein (additionally [68, 69, 70]).

One observes that, if $\delta(\mathcal{V}_a)(\mathbf{b}, \mathbf{c}, \mathbf{x}, \mathbf{y})$ is the invariant of the trace, that is

$$\text{Tr}_{\mathcal{V}_a}(\varphi, \bar{\varphi}) = \lambda \sum_{\mathbf{b}, \mathbf{c}, \mathbf{x}, \mathbf{y}} \bar{\varphi}_{\mathbf{b}} \bar{\varphi}_{\mathbf{c}} \delta(\mathcal{V}_a)(\mathbf{b}, \mathbf{c}, \mathbf{x}, \mathbf{y}) \varphi_{\mathbf{y}} \varphi_{\mathbf{x}},$$

one gets for $\mathbf{s} = (s_1, \dots, s_D) \in \mathbb{Z}^D$, the following expression:

$$\left(\frac{\partial \mathcal{S}_{\text{int}}(\varphi, \bar{\varphi})}{\partial \bar{\varphi}_{\mathbf{s}}} \right)_{\varphi^b \rightarrow \delta / \delta J^\#} = 2\lambda \left\{ \sum_a \left(\sum_{b_a} \frac{\delta}{\delta \bar{J}_{s_1 \dots s_{a-1} b_a s_{a+1} \dots s_D}} \sum_{\mathbf{b}_a} \frac{\delta}{\delta J_{b_1 \dots b_D}} \frac{\delta}{\delta \bar{J}_{b_1 \dots b_{a-1} s_a b_{a+1} \dots b_D}} \right) \right\}, \quad (1.3.2)$$

⁴For $D = 3$ all quartic invariants are melonic, so we refer to it only as φ_3^4 -theory.

where $\mathbf{b}_{\hat{a}} = (b_1, \dots, \hat{b}_a, \dots, b_D) = (b_1, \dots, b_{a-1}, b_{a+1}, \dots, b_D) \in \mathbb{Z}^{D-1}$ and \sharp can either act trivially on a variable or be complex conjugation, and $\varphi^{\flat} = \bar{\varphi}$ or $\varphi^{\flat} = \varphi$ according to whether $J^{\sharp} = \bar{J}$ or $J^{\sharp} = J$, respectively. The term $(\partial \mathcal{S}_{\text{int}}(\varphi, \bar{\varphi}) / \partial \bar{\varphi}_{\mathbf{s}}) \big|_{\varphi^{\flat} \rightarrow \delta / \delta J^{\sharp}} Z[J, \bar{J}]$ can be computed with aid of the WTI. We depart from the formally integrated form of the partition function

$$Z[J, \bar{J}] \propto \exp(-\mathcal{S}_{\text{int}}(\varphi, \bar{\varphi})) \big|_{\varphi^{\flat} \rightarrow \delta / \delta J^{\sharp}} \exp\left(\sum_{\mathbf{q} \in \mathbb{Z}^D} \bar{J}_{\mathbf{q}} E_{\mathbf{q}}^{-1} J_{\mathbf{q}}\right),$$

where we will ignore a (possibly infinite) constant and write equality and derive its logarithm:

$$\begin{aligned} \frac{\delta W[J, \bar{J}]}{\delta \bar{J}_{\mathbf{s}}} &= \frac{1}{Z[J, \bar{J}]} \exp(-\mathcal{S}_{\text{int}}(\delta / \delta \bar{J}, \delta / \delta J)) J_{\mathbf{s}} E_{\mathbf{s}}^{-1} e^{\sum_{\mathbf{q} \in \mathbb{Z}^D} \bar{J}_{\mathbf{q}} E_{\mathbf{q}}^{-1} J_{\mathbf{q}}} \quad (1.3.3) \\ &= \frac{1}{Z[J, \bar{J}]} \left\{ \frac{1}{E_{\mathbf{s}}} J_{\mathbf{s}} \exp(-\mathcal{S}_{\text{int}}(\delta / \delta \bar{J}, \delta / \delta J)) e^{\sum_{\mathbf{q} \in \mathbb{Z}^D} \bar{J}_{\mathbf{q}} E_{\mathbf{q}}^{-1} J_{\mathbf{q}}} \right. \\ &\quad \left. + \left(\frac{\partial \mathcal{S}_{\text{int}}(\varphi, \bar{\varphi})}{\partial \bar{\varphi}_{\mathbf{s}}} \right) \bigg|_{\varphi^{\flat} \rightarrow \delta / \delta J^{\sharp}} \exp(-\mathcal{S}_{\text{int}}(\varphi, \bar{\varphi})) \big|_{\varphi^{\flat} \rightarrow \delta / \delta J^{\sharp}} e^{\sum_{\mathbf{q} \in \mathbb{Z}^D} \bar{J}_{\mathbf{q}} E_{\mathbf{q}}^{-1} J_{\mathbf{q}}} \right\} \\ &= \frac{1}{E_{\mathbf{s}}} \left\{ J_{\mathbf{s}} - \frac{1}{Z[J, \bar{J}]} \left(\frac{\partial \mathcal{S}_{\text{int}}(\varphi, \bar{\varphi})}{\partial \bar{\varphi}_{\mathbf{s}}} \right) \bigg|_{\varphi^{\flat} \rightarrow \delta / \delta J^{\sharp}} Z[J, \bar{J}] \right\}. \end{aligned}$$

For sake of notation, we introduce the shorthands $\mathbf{b}_{\hat{a}s_a} = (b_1, \dots, b_{a-1}, s_a, b_{a+1}, \dots, b_D)$ and, similarly, $\mathbf{s}_{\hat{a}b_a} = (s_1, \dots, s_{a-1}, b_a, s_{a+1}, \dots, s_D)$, for any $a = 1, \dots, D$. By applying the colour- a -WTI to the rightmost double derivative term appearing in (1.3.2), the following:

$$\begin{aligned} \left(\frac{\partial \mathcal{S}_{\text{int}}(\varphi, \bar{\varphi})}{\partial \bar{\varphi}_{\mathbf{s}}} \right) \bigg|_{\varphi^{\flat} \rightarrow \delta / \delta J^{\sharp}} Z[J, \bar{J}] &= 2\lambda \sum_a \left\{ \sum_{b_a} \frac{\delta}{\delta \bar{J}_{\mathbf{s}_{\hat{a}b_a}}} \left(\delta_{s_a b_a} Y_{s_a}^{(a)}[J, \bar{J}] \cdot \right. \quad (1.3.4) \right. \\ &\quad \left. + \sum_{\mathbf{b}_{\hat{a}}} \frac{1}{E(b_a, s_a)} \left(\bar{J}_{\mathbf{b}} \frac{\delta}{\delta \bar{J}_{\mathbf{b}_{\hat{a}s_a}}} - J_{\mathbf{b}_{\hat{a}s_a}} \frac{\delta}{\delta J_{\mathbf{b}}} \right) Z[J, \bar{J}] \right\} \\ &= 2\lambda \sum_a \left\{ \frac{\delta Y_{s_a}^{(a)}[J, \bar{J}]}{\delta \bar{J}_{\mathbf{s}}} \cdot Z[J, \bar{J}] + Y_{s_a}^{(a)}[J, \bar{J}] \cdot \frac{\delta Z[J, \bar{J}]}{\delta \bar{J}_{\mathbf{s}}} \right. \\ &\quad \left. + \sum_{\mathbf{b}} \frac{1}{E(b_a, s_a)} \frac{\delta}{\delta \bar{J}_{\mathbf{s}_{\hat{a}b_a}}} \left(\bar{J}_{\mathbf{b}} \frac{\delta}{\delta \bar{J}_{\mathbf{b}_{\hat{a}s_a}}} - J_{\mathbf{b}_{\hat{a}s_a}} \frac{\delta}{\delta J_{\mathbf{b}}} \right) Z[J, \bar{J}] \right\} \\ &= 2\lambda \sum_a \left\{ \frac{\delta Y_{s_a}^{(a)}[J, \bar{J}]}{\delta \bar{J}_{\mathbf{s}}} \cdot Z[J, \bar{J}] + Y_{s_a}^{(a)}[J, \bar{J}] \cdot \frac{\delta Z[J, \bar{J}]}{\delta \bar{J}_{\mathbf{s}}} \right. \\ &\quad \left. + \sum_{b_a} \frac{1}{E(b_a, s_a)} \frac{\delta Z[J, \bar{J}]}{\delta \bar{J}_{\mathbf{s}}} + \sum_{\mathbf{b}} \frac{\bar{J}_{\mathbf{b}}}{E(b_a, s_a)} \frac{\delta^2 Z[J, \bar{J}]}{\delta \bar{J}_{\mathbf{s}_{\hat{a}b_a}} \delta \bar{J}_{\mathbf{b}_{\hat{a}s_a}}} \right. \\ &\quad \left. - \sum_{\mathbf{b}} \frac{1}{E(b_a, s_a)} J_{\mathbf{b}_{\hat{a}s_a}} \frac{\delta^2 Z[J, \bar{J}]}{\delta \bar{J}_{\mathbf{s}_{\hat{a}b_a}} \delta J_{\mathbf{b}}} \right\} \\ &= 2\lambda \sum_a (A_a(\mathbf{s}) - B_a(\mathbf{s}) + C_a(\mathbf{s}) + D_a(\mathbf{s}) + F_a(\mathbf{s})), \end{aligned}$$

with

$$\begin{aligned}
A_a(\mathbf{s}) &= Y_{s_a}^{(a)}[J, \bar{J}] \cdot \frac{\delta Z[J, \bar{J}]}{\delta \bar{J}_{\mathbf{s}}}, & B_a(\mathbf{s}) &= \sum_{\mathbf{b}} \frac{1}{E(b_a, s_a)} J_{\mathbf{b}_a s_a} \frac{\delta^2 Z[J, \bar{J}]}{\delta \bar{J}_{s_a b_a} \delta J_{\mathbf{b}}}, \\
C_a(\mathbf{s}) &= \sum_{b_a} \frac{1}{E(b_a, s_a)} \frac{\delta Z[J, \bar{J}]}{\delta \bar{J}_{\mathbf{s}}}, & D_a(\mathbf{s}) &= \sum_{\mathbf{b}} \frac{\bar{J}_{\mathbf{b}}}{E(b_a, s_a)} \frac{\delta^2 Z[J, \bar{J}]}{\delta \bar{J}_{s_a b_a} \delta \bar{J}_{\mathbf{b}_a s_a}}, \\
F_a(\mathbf{s}) &= \frac{\delta Y_{s_a}^{(a)}[J, \bar{J}]}{\delta \bar{J}_{\mathbf{s}}} \cdot Z[J, \bar{J}].
\end{aligned}$$

One shall be interested in derivatives of $W[J, \bar{J}]$ of the following form:

$$\left(\prod_{i=1}^k \frac{\delta}{\delta J_{\mathbf{x}_i}} \frac{\delta}{\delta \bar{J}_{\mathbf{y}_i}} \right) W[J, \bar{J}] \Big|_{J=\bar{J}=0}, \quad \mathbf{X} = (\mathbf{x}^1, \dots, \mathbf{x}^k) \in \mathcal{F}_{D,k}, \quad \mathcal{B}_*(\mathbf{X}) = (\mathbf{y}^1, \dots, \mathbf{y}^k), \tag{1.3.5}$$

for $\mathcal{B} \in \text{Grph}_D^{\text{cl}}$, and then use formula (1.3.4) with, say, the vertex $\mathbf{s} = \mathbf{y}^1$. As said in the introduction, deltas of the interaction vertices and the propagators (proportional to deltas) inside each Feynman diagrams render the definition of the $2k$ -multi-point function based on (1.3.5) redundant, if one treats the \mathbf{x} -variables and the \mathbf{y} -variables as independent. In fact, all the \mathbf{y} 's can be expressed in terms of coordinates of $\mathbf{X} = (\mathbf{x}^1, \dots, \mathbf{x}^k)$ of the same colour, the combinatorics of which uniquely determines a so-called boundary graph \mathcal{B} with $2k$ vertices; moreover, non-vanishing terms in the formula above are precisely a *graph derivative of $W[J, \bar{J}]$* with respect to \mathcal{B} at \mathbf{X} .

For the time being, we pick only a *connected* boundary graph \mathcal{B} and we want to know what the rest of the derivatives $\delta/\delta J_{\mathbf{x}^\alpha}, \delta/\delta \bar{J}_{\mathbf{y}^\alpha \{\mathbf{x}^\nu\}_\nu}$, ($\alpha = 2, \dots, D$) do to the expression (1.3.3). By using (1.3.4) with $\mathbf{s} = \mathbf{y}^1$ we analyze the five summands in the (lowermost) RHS:

$$\mathbf{m}_a(\mathbf{X}; \mathbf{s}; \mathcal{B}) := \frac{1}{Z_0} \prod_{\substack{\alpha > 1 \\ \nu=1, \dots, k}} \frac{\delta}{\delta \bar{J}_{\mathbf{y}^\alpha}} \frac{\delta}{\delta J_{\mathbf{x}^\nu}} M_a(\mathbf{s}) \Big|_{J=\bar{J}=0}$$

for

$$(\mathbf{m}, M) \in \{(\mathbf{a}, A), (\mathbf{b}, B), (\mathbf{c}, C), (\mathbf{d}, D), (\mathbf{f}, F)\}.$$

Actually \mathbf{s} is a function of \mathbf{X} —and so is any other \mathbf{y}^α — but the dependence of \mathbf{m}_a on it only shows that \mathbf{s} is the variable respect to which we firstly derived $W[J, \bar{J}]$. Each \mathbf{m}_a depends on the boundary graph \mathcal{B} through $\{\mathbf{y}^\alpha\}_{\alpha=1}^k$ given by (1.2.2). Ignoring the common $(-2\lambda/E_s)$ prefactor:

- $\mathbf{a}_a(\mathbf{X}; \mathbf{s}; \mathcal{B})$ directly yields $Y_{s_a}^{(a)}[0, 0] \cdot G_{\mathcal{B}}^{(2k)}(\mathbf{X})$
- also, derivatives on $C_a(\mathbf{s}), \mathbf{c}_a(\mathbf{X}; \mathbf{s}; \mathcal{B})$, readily give $\sum_{b_a} E(b_a, s_a)^{-1} G_{\mathcal{B}}^{(2k)}(\mathbf{X})$
- the term $\mathbf{f}_a(\mathbf{X}; \mathbf{s}; \mathcal{B})$ is, according to Proposition 1.2.1, $\sum_{\hat{\pi} \in \text{Aut}_c(\mathcal{B})} \pi^* \mathbf{f}_{\mathcal{B}}^{(a)}(\mathbf{X})$

The remaining two terms, \mathbf{b}_a and \mathbf{d}_a , need a more detailed inspection, though:

$$\mathcal{O}(\bar{J}) + \prod_{\substack{\alpha > 1 \\ \nu=1, \dots, k}} \frac{\delta}{\delta \bar{J}_{\mathbf{y}^\alpha}} \frac{\delta}{\delta J_{\mathbf{x}^\nu}} D_a(\mathbf{s}) = \prod_{\alpha > 1; \nu} \frac{\delta}{\delta \bar{J}_{\mathbf{y}^\alpha}} \frac{\delta}{\delta J_{\mathbf{x}^\nu}} \left[\sum_{\mathbf{b}} \frac{1}{E(b_a, s_a)} \bar{J}_{\mathbf{b}} \frac{\delta^2 Z[J, \bar{J}]}{\delta \bar{J}_{s_a b_a} \delta \bar{J}_{\mathbf{b}_a s_a}} \right]$$

$$\begin{aligned}
&= \sum_{\rho=2}^k \prod_{\substack{\alpha>1(\alpha\neq\rho) \\ \nu=1,\dots,k}} \frac{\delta}{\delta \bar{J}_{\mathbf{y}^\alpha}} \frac{\delta}{\delta J_{\mathbf{x}^\nu}} \left[\sum_{\mathbf{b}} \frac{\delta_{\mathbf{y}^\rho}^{\mathbf{b}}}{E(b_a, s_a)} \frac{\delta^2 Z[J, \bar{J}]}{\delta \bar{J}_{\mathbf{s}_a b_a} \delta \bar{J}_{\mathbf{b}_a s_a}} \right] \\
&= \sum_{\rho=2}^k \prod_{\substack{\alpha:(1\neq\alpha\neq\rho) \\ \nu=1,\dots,k}} \frac{\delta}{\delta \bar{J}_{\mathbf{y}^\alpha}} \frac{\delta}{\delta J_{\mathbf{x}^\nu}} \left[\frac{1}{E(y_a^\rho, s_a)} \frac{\delta^2 Z[J, \bar{J}]}{\delta \bar{J}_{\mathbf{s}_a y_a^\rho} \delta \bar{J}_{\mathbf{y}_a^\rho s_a}} \right].
\end{aligned} \tag{1.3.6}$$

As for the derivatives on $B_a(\mathbf{s})$,

$$\begin{aligned}
\mathcal{O}(J) + \prod_{\substack{\alpha>1 \\ \nu=1,\dots,k}} \frac{\delta}{\delta \bar{J}_{\mathbf{y}^\alpha}} \frac{\delta}{\delta J_{\mathbf{x}^\nu}} B_a(\mathbf{s}) &= \prod_{\alpha>1;\nu} \frac{\delta}{\delta \bar{J}_{\mathbf{y}^\alpha}} \frac{\delta}{\delta J_{\mathbf{x}^\nu}} \left[\sum_{\mathbf{b}} \frac{1}{E(b_a, s_a)} J_{\mathbf{b}_a s_a} \frac{\delta^2 Z[J, \bar{J}]}{\delta \bar{J}_{\mathbf{s}_a b_a} \delta J_{\mathbf{b}}} \right] \\
&= \sum_{\beta=1}^k \prod_{\alpha>1;\nu\neq\beta} \frac{\delta}{\delta \bar{J}_{\mathbf{y}^\alpha}} \frac{\delta}{\delta J_{\mathbf{x}^\nu}} \left[\sum_{\mathbf{b}} \frac{1}{E(b_a, s_a)} \delta_{x_a^\beta}^{s_a} \delta_{\mathbf{x}_a^\beta}^{\mathbf{b}_a} \frac{\delta^2 Z[J, \bar{J}]}{\delta \bar{J}_{\mathbf{s}_a b_a} \delta J_{\mathbf{b}}} \right] \\
&= \sum_{\beta=1}^k \prod_{\alpha>1;\nu\neq\beta} \frac{\delta}{\delta \bar{J}_{\mathbf{y}^\alpha}} \frac{\delta}{\delta J_{\mathbf{x}^\nu}} \left[\sum_{b_a} \frac{1}{E(b_a, s_a)} \delta_{x_a^\beta}^{s_a} \frac{\delta^2 Z[J, \bar{J}]}{\delta \bar{J}_{\mathbf{s}_a b_a} \delta J_{\mathbf{x}_a^\beta b_a}} \right] \\
&= \prod_{\alpha>1;\nu\neq\gamma} \frac{\delta}{\delta \bar{J}_{\mathbf{y}^\alpha}} \frac{\delta}{\delta J_{\mathbf{x}^\nu}} \left[\sum_{b_a} \frac{1}{E(b_a, x_a^\gamma)} \frac{\delta^2 Z[J, \bar{J}]}{\delta \bar{J}_{\mathbf{s}_a b_a} \delta J_{\mathbf{x}_a^\gamma b_a}} \right].
\end{aligned} \tag{1.3.7}$$

For the last equality, one uses the fact that \mathcal{B} is regular. Thus, there exists precisely one white vertex \mathbf{x}^γ , $\gamma = \gamma(a)$, such that $x_a^\gamma = s_a$. In turn, this means that $\delta_{x_a^\beta}^{s_a} = \delta_{x_a^\beta}^{s_a} \delta_\beta^\gamma$.

- as evident in eq. (1.3.6), the derivatives on the D_a -term give, after setting the sources to zero, all the (coloured) graphs obtained from \mathcal{B} by a swapping of the following form (only a -colour and only the four implied vertices visible):

$$\begin{array}{ccc}
\begin{array}{l} \mathbf{s} = s_a \mathbf{s}_a \\ = x_a^\gamma \mathbf{s}_a \\ \bullet \\ \curvearrowright \\ a \\ \circ \\ \mathbf{x}^\gamma = (x_a^\gamma \mathbf{x}_a^\gamma) \end{array} & \begin{array}{l} \mathbf{y}^\rho = (y_a^\rho \mathbf{y}_a^\rho) \\ = (x_a^{\kappa(\rho)} \mathbf{y}_a^\rho) \\ \bullet \\ \curvearrowright \\ a \\ \circ \\ \mathbf{x}^{\kappa(\rho)} \end{array} & \rightarrow & \begin{array}{l} (x_a^{\kappa(\rho)} \mathbf{s}_a) \quad (x_a^\gamma \mathbf{y}_a^\rho) = (s_a \mathbf{y}_a^\rho) \\ \bullet \quad \bullet \\ \curvearrowright \quad \curvearrowright \\ a \quad a \\ \circ \quad \circ \\ \mathbf{x}^\gamma \quad \mathbf{x}^{\kappa(\rho)} \end{array}
\end{array} \tag{1.3.8}$$

for ρ running over the black vertices which are not $\bar{J}_s = \bar{J}_{\mathbf{y}^1}$. Hence the contribution of this term is

$$\sum_{\rho>1} \frac{1}{E(y_a^\rho, s_a)} Z_0^{-1} \frac{\partial Z[J, \bar{J}]}{\partial \varsigma_a(\mathcal{B}; 1, \rho)(\mathbf{X})} \text{ for } \rho = 2, \dots, k.$$

Since $\mathbf{y}^1 = \mathbf{s}$, we also write $\varsigma_a(\mathcal{B}; \mathbf{y}^1, \mathbf{y}^\rho) = \varsigma_a(\mathcal{B}; 1, \rho)$ for this new indexing graph ($\rho > 1$).

- concerning the derivatives of B_a above in eq. (1.3.7), the only surviving term is $\delta^2 Z[J, \bar{J}] / \delta \bar{J}_{\mathbf{s}_a b_a} \delta J_{\mathbf{x}_a^\gamma b_a}$, and is selected by $\delta_{x_a^\beta}^{s_a}$, which is just, after taking into account

the rest of the derivatives, the graph derivative $\partial Z/\partial \mathcal{B}(\mathbf{X})|_{x_a^\gamma \rightarrow b_a}$, with the single coordinate x_a^γ being substituted by (the running) b_a . If \mathcal{B} is connected (as we assumed), after setting the sources to zero, this accounts for the *firstline* in the next term:

$$\begin{aligned} \mathfrak{b}_a(\mathbf{X}; \mathbf{s}; \mathcal{B}) &= \sum_{b_a} \frac{1}{E(b_a, x_a^\gamma)} G_{\mathcal{B}}^{(2k)}(\mathbf{x}^1, \dots, \mathbf{x}^{\gamma-1}, (x_1^\gamma, \dots, x_{a-1}^\gamma, b_a, x_{a+1}^\gamma, \dots, x_D^\gamma), \mathbf{x}^{\gamma+1}, \dots, \mathbf{x}^k) \\ &\quad + \sum_{\rho > 1} \frac{1}{E(x_a^{\kappa(\rho)}, x_a^\gamma)} \frac{\partial Z[J, \bar{J}]}{\partial \varsigma_a(\mathcal{B}; 1, \rho)}(\mathbf{x}^1, \dots, (x_1^\gamma, \dots, x_{a-1}^\gamma, x_a^{\kappa(\rho)}, x_{a+1}^\gamma, \dots, x_D^\gamma), \dots, \mathbf{x}^k). \end{aligned} \quad (1.3.9)$$

The second line is found by noticing that one also gets a contribution from the graph derivative $\partial Z[J, \bar{J}]/\partial \varsigma_a(\mathcal{B}; 1, \rho)$ if this is evaluated at $\mathbf{X}|_{x_a^\gamma \rightarrow x_a^{\kappa(\rho)}}$, where $\kappa(\rho)$ is determined by (1.3.8) (i.e. $x_a^{\kappa(\rho)} = y_a^\rho$). From eqs. (1.3.4) one has

$$\begin{aligned} \frac{\partial W[J, \bar{J}]}{\partial \mathcal{B}(\mathbf{X})} &= \prod_{\substack{\alpha > 1 \\ \nu=1, \dots, k}} \frac{\delta}{\delta \bar{J}_{\mathbf{y}^\alpha}} \frac{\delta}{\delta J_{\mathbf{x}^\nu}} \left(\frac{-2\lambda E_{\mathbf{s}}^{-1}}{Z[J, \bar{J}]} \sum_a (A_a(\mathbf{s}) + C_a(\mathbf{s}) + D_a(\mathbf{s}) + F_a(\mathbf{s}) - B_a(\mathbf{s})) \right) \Big|_{\substack{\bar{J}=0 \\ J=0}} \\ &= \frac{(-2\lambda)}{E_{\mathbf{s}}} \sum_a (\mathfrak{a}_a(\mathbf{X}; \mathbf{s}; \mathcal{B}) + \mathfrak{c}_a(\mathbf{X}; \mathbf{s}; \mathcal{B}) + \mathfrak{d}_a(\mathbf{X}; \mathbf{s}; \mathcal{B}) + \mathfrak{f}_a(\mathbf{X}; \mathbf{s}; \mathcal{B}) - \mathfrak{b}_a(\mathbf{X}; \mathbf{s}; \mathcal{B})), \end{aligned}$$

where each summand is now known. Because $Y_{s_a}^{(a)}[0, 0] = \Delta_{s_a, 1} G_{\mathcal{B}}^{(2)}$ we have proven:

Theorem 1.3.1 (Schwinger-Dyson equations). *Let $D \geq 3$ and let \mathcal{B} be a connected boundary graph of the quartic melonic model, $\mathcal{B} \in \text{Feyn}_D(\varphi_{m,D}^4) = \text{Grph}_D^{\text{II,cl}}$. Let $2k$ denote the number of vertices of \mathcal{B} . Pick a \bar{J} -external line, that is, $\bar{J}_{\mathbf{y}^\alpha}$, for $1 \leq \alpha \leq k$, where $\mathcal{B}_*(\mathbf{X}) = (\mathbf{y}^1, \dots, \mathbf{y}^\alpha, \dots, \mathbf{y}^k)$ for $\mathbf{X} \in \mathcal{F}_{k(\mathcal{B}), D}$, and set $\mathbf{s} = \mathbf{y}^\alpha$ for sake of notation. The $(2k)$ -point Schwinger-Dyson equation corresponding to \mathcal{B} is*

$$\begin{aligned} &\left(1 + \frac{2\lambda}{E_{\mathbf{s}}} \sum_{a=1}^D \sum_{\mathbf{q}_{\hat{a}}} G_{\mathcal{B}}^{(2)}(s_a, \mathbf{q}_{\hat{a}}) \right) G_{\mathcal{B}}^{(2k)}(\mathbf{X}) \\ &= \frac{\delta_{1,k}}{E_{\mathbf{s}}} + \frac{(-2\lambda)}{E_{\mathbf{s}}} \sum_{a=1}^D \left\{ \sum_{\hat{\sigma} \in \text{Aut}_c(\mathcal{B})} \sigma^* \mathfrak{f}_{\mathcal{B}, s_a}^{(a)}(\mathbf{X}) \right. \\ &\quad \left. + \sum_{\rho \neq \alpha} \frac{Z_0^{-1}}{E(y_a^\rho, s_a)} \left[\frac{\partial Z[J, J]}{\partial \varsigma_a(\mathcal{B}; \alpha, \rho)}(\mathbf{X}) - \frac{\partial Z[J, J]}{\partial \varsigma_a(\mathcal{B}; \alpha, \rho)}(\mathbf{X}|_{s_a \rightarrow y_a^\rho}) \right] \right. \\ &\quad \left. - \sum_{b_a} \frac{1}{E(s_a, b_a)} [G_{\mathcal{B}}^{(2k)}(\mathbf{X}) - G_{\mathcal{B}}^{(2k)}(\mathbf{X}|_{s_a \rightarrow b_a})] \right\} \end{aligned} \quad (1.3.10)$$

for all $\mathbf{X} \in \mathcal{F}_{D, k(\mathcal{B})}$. Notice that $s_a = x_a^\gamma$ for certain γ , $\mathbf{X} = (\mathbf{x}^1, \dots, \mathbf{x}^\gamma, \dots, \mathbf{x}^k)$, and in this sense $\mathbf{X}|_{s_a \rightarrow b_a}$ means the replacement in \mathbf{X} of x_a^γ by the summed index b_a (see eq. (1.3.9), with a similar situation for $\mathbf{X}|_{s_a \rightarrow y_a^\rho}$). Here $(s_a, \mathbf{q}_{\hat{a}})$ is abuse of notation for $(q_1, q_2, \dots, q_{a-1}, s_a, q_{a+1}, \dots, q_D)$. Also recall that $E(u_a, v_a) = E_{u_a \mathbf{q}_{\hat{a}}} - E_{v_a \mathbf{q}_{\hat{a}}}$.

Proof. The 2-point equation has the same structure, but the propagator is added (accounting for the delta $\delta_{1,k}$ term. This equation has been proven in [62]. For the higher-point functions, the proof of this theorem (with $\alpha = 1$) precedes the statement. We remark that, since $\mathbf{X} \in \mathcal{F}_{k(\mathcal{B}),D}$, the denominators of the form $E(y_a^\rho, s_a)$ are well defined. In the limit $b_a \rightarrow s_a$, $E(s_a, b_a)$ becomes singular, but also the numerator, and a derivative term arises. \square

A graphical interpretation of this theorem shall be given in a future work; therein, in particular, the perturbative expansion of this equation will be addressed in simple cases.

We will ease the notation $\mathfrak{f}_{\mathcal{B},s_a}^{(a)} = \mathfrak{f}_{\mathcal{B}}^{(a)}$, when no risk of confusion arises, keeping in mind the dependence of this function on s_a . Notice that if the graph $\varsigma_a(\mathcal{B}; 1, \rho)$ is connected, then the respective derivative on $Z[J, \bar{J}]$ is just

$$\frac{1}{Z_0} \frac{\partial Z[J, \bar{J}]}{\partial \varsigma_a(\mathcal{B}; 1, \rho)}(\mathbf{X}) = G_{\varsigma_a(\mathcal{B}; 1, \rho)}^{(2k)}(\mathbf{X});$$

otherwise, the RHS of this expression contains, on top of $G_{\varsigma_a(\mathcal{B}; 1, \rho)}^{(2k)}$, also a product of correlation functions indexed by the connected components of $\varsigma_a(\mathcal{B}; 1, \rho)$ with a number of points which add up to $2k$ (see Sec. 1.4.1). Observe that the equation still depends at this stage on the choice of the vertex \bar{J}_s , with respect to which we first derived. Thus, one has k independent SDE for $G_{\mathcal{B}}^{(2k)}$, when \mathcal{B} has no symmetries.

1.4 Schwinger-Dyson equations for rank-3 theories

According to [62], the boundary sector $\text{im } \partial$ of the φ_3^4 -theory is all of $\partial(\text{Feyn}_3(\varphi^4)) = \text{Grph}_3^{\text{II,cl}}$. Therefore $W[J, \bar{J}] = \log Z[J, \bar{J}]$ can be expanded in boundary graphs as:

$$\begin{aligned} W_{D=3}[J, \bar{J}] &= G_{\ominus}^{(2)} \star \mathbb{J}(\ominus) + \frac{1}{2!} G_{|\ominus| \ominus |}^{(4)} \star \mathbb{J}(\ominus \sqcup^2) + \frac{1}{2} \sum_c G_{c \square c}^{(4)} \star \mathbb{J}(\square^c) + \frac{1}{3} \sum_c G_{\text{triangle}}^{(6)} \star \\ &\mathbb{J}(\text{triangle}^c) + \frac{1}{3} G_{\text{tetra}}^{(6)} \star \mathbb{J}(\text{tetra}) + \sum_i G_{\square \square}^{(6)} \star \mathbb{J}(\square \square) + \frac{1}{3!} G_{|\ominus| \ominus | \ominus |}^{(6)} \star \mathbb{J}(\ominus \sqcup^3) + \frac{1}{2} \sum_c G_{|\ominus| \ominus | c \square c |}^{(6)} \star \\ &\mathbb{J}(\ominus \sqcup \square^c) + \frac{1}{2! \cdot 2^2} \sum_c G_{|c \square c | c \square c |}^{(8)} \star \mathbb{J}(\square^c \sqcup \square^c) + \frac{1}{2^2} \sum_{c < i} G_{|c \square c | i \square i |}^{(8)} \star \mathbb{J}(\square^c \sqcup \square^i) + \\ &\frac{1}{4!} G_{|\ominus| \ominus | \ominus | \ominus |}^{(8)} \star \mathbb{J}(\ominus \sqcup^4) + \frac{1}{2 \cdot 2!} \sum_c G_{|\ominus| \ominus | \ominus | c \square c |}^{(8)} \star \mathbb{J}(\ominus \sqcup \ominus \sqcup \square^c) + \frac{1}{3} G_{|\ominus| \text{triangle}}^{(8)} \star \\ &\mathbb{J}(\ominus \sqcup \text{triangle}) + \frac{1}{3} \sum_c G_{|\ominus| \text{triangle}^c}^{(8)} \star \mathbb{J}(\ominus \sqcup \text{triangle}^c) + \sum_i G_{|\ominus| \square \square}^{(8)} \star \mathbb{J}(\ominus \sqcup \square \square) + \sum_{j; l < i} G_{\square \square \square}^{(8)} \star \\ &\mathbb{J}(j \begin{array}{c} l \quad j \quad i \\ \text{---} \text{---} \text{---} \\ l \quad j \quad i \end{array} j) + \sum_{j \neq i} G_{j \begin{array}{c} \square \square \square \\ \text{---} \text{---} \text{---} \\ i \end{array} i}^{(8)} \star \mathbb{J}(j \begin{array}{c} l \quad j \quad l \\ \text{---} \text{---} \text{---} \\ l \quad j \quad l \end{array} i) + \frac{1}{4} \sum_j G_{\text{cube}}^{(8)} \star \mathbb{J}(\text{cube}^j) + \sum_{j \neq i} G_{\text{cube}^j}^{(8)} \star \\ &\mathbb{J}(\text{cube}^j) + \sum_i G_{\text{cube}^i}^{(8)} \star \mathbb{J}(\text{cube}^i) + \sum_{l \neq i \neq j} G_{\text{cube}^i}^{(8)} \star \mathbb{J}(\text{cube}^i) + G_{\text{cube}^i}^{(8)} \star \mathbb{J}(\text{cube}^i) + \\ &G_{\text{cube}^i}^{(8)} \star \mathbb{J}(\text{cube}^i) + \mathcal{O}(10). \end{aligned}$$

The WTI will be used for each colour $a = 1, 2, 3$, and it will be convenient to single out a in this last expression. From here on⁵ $b = b(a) = \min(\{1, 2, 3\} \setminus \{a\})$ and $c = c(a) = \max(\{1, 2, 3\} \setminus \{a\})$:

$$\begin{aligned}
W_{D=3}[J, \bar{J}] = & G_{\ominus}^{(2)} \star \mathbb{J}(\ominus) + \frac{1}{2!} G_{|\ominus|\ominus}^{(4)} \star \mathbb{J}(\ominus \sqcup \ominus) + \frac{1}{2} G_{a\bar{a}}^{(4)} \star \mathbb{J}(\overline{a}) + \frac{1}{2} \sum_{i \neq a} G_{i\bar{i}}^{(4)} \star \mathbb{J}(\overline{i}) \\
& + \frac{1}{3} G_a^{(6)} \star \mathbb{J}(\overline{a}) + \frac{1}{3} \sum_{i \neq a} G_i^{(6)} \star \mathbb{J}(\overline{i}) + \frac{1}{3!} G_{|\ominus|\ominus|\ominus}^{(6)} \star \mathbb{J}(\ominus \sqcup \ominus \sqcup \ominus) \\
& + \frac{1}{3} G_{\triangle}^{(6)} \star \mathbb{J}(\triangle) + G_{\overline{bc}}^{(6)} \star \mathbb{J}(\overline{a}) + G_{\overline{ac}}^{(6)} \star \mathbb{J}(\overline{b}) + G_{\overline{ab}}^{(6)} \star \mathbb{J}(\overline{c}) \\
& + \frac{1}{2} G_{|\ominus|\overline{a}}^{(6)} \star \mathbb{J}(\ominus \sqcup \overline{a}) + \frac{1}{2} \sum_{i \neq a} G_{|\ominus|\overline{i}}^{(6)} \star \mathbb{J}(\ominus \sqcup \overline{i}) \\
& + \frac{1}{2! \cdot 2^2} G_{|\overline{a}|\overline{a}}^{(8)} \star \mathbb{J}(\overline{a} \sqcup \overline{a}) + \frac{1}{2! \cdot 2^2} \sum_{i \neq a} G_{|\overline{i}|\overline{i}}^{(8)} \star \mathbb{J}(\overline{i} \sqcup \overline{i}) \\
& + \frac{1}{2^2} \sum_{i \neq a} G_{|\overline{i}|\overline{a}}^{(8)} \star \mathbb{J}(\overline{i} \sqcup \overline{a}) + \frac{1}{2^2} G_{|\overline{b}|\overline{c}}^{(8)} \star \mathbb{J}(\overline{b} \sqcup \overline{c}) \\
& + \frac{1}{3} G_{|\ominus|\triangle}^{(8)} \star \mathbb{J}(\ominus \sqcup \triangle) + \frac{1}{3} \sum_{i \neq a} G_{|\ominus|\overline{i}}^{(8)} \star \mathbb{J}(\ominus \sqcup \overline{i}) \\
& + \frac{1}{3} G_{|\ominus|\overline{a}}^{(8)} \star \mathbb{J}(\ominus \sqcup \overline{a}) + \sum_{i \neq a} G_{|\ominus|\overline{a}\overline{i}}^{(8)} \star \mathbb{J}(\ominus \sqcup \overline{a}\overline{i}) \\
& + G_{|\ominus|\overline{bc}}^{(8)} \star \mathbb{J}(\ominus \sqcup \overline{a}) + \frac{1}{2 \cdot 2!} \sum_{i \neq a} G_{|\ominus|\ominus|\overline{i}}^{(8)} \star \mathbb{J}(\ominus \sqcup \ominus \sqcup \overline{i}) \\
& + \frac{1}{2 \cdot 2!} G_{|\ominus|\ominus|\overline{a}}^{(8)} \star \mathbb{J}(\ominus \sqcup \ominus \sqcup \overline{a}) + \frac{1}{4!} G_{|\ominus|\ominus|\ominus|\ominus}^{(8)} \star \mathbb{J}(\ominus \sqcup \ominus \sqcup \ominus \sqcup \ominus) \\
& + G_{\overline{bc}}^{(8)} \star \mathbb{J}(a \overline{c} \overline{c} \overline{b} \overline{b} a) + G_{\overline{ab}}^{(8)} \star \mathbb{J}(b \overline{c} \overline{b} \overline{a} \overline{c} \overline{c} \overline{b} a) \\
& + G_{\overline{ac}}^{(8)} \star \mathbb{J}(c \overline{b} \overline{b} \overline{a} \overline{a} c) + \frac{1}{2} \sum_{\substack{i=b,c \\ (a \neq j \neq i)}} G_{\overline{a}\overline{a}\overline{i}}^{(8)} \star \mathbb{J}(j \overline{a} \overline{i} \overline{i} \overline{i} \overline{j} \overline{a} i) \\
& + \frac{1}{2} \sum_{i=b,c} G_{\overline{a}\overline{a}\overline{a}\overline{i}}^{(8)} \star \mathbb{J}(i \overline{a} \overline{a} \overline{a} \overline{i} \overline{a} a) + \frac{1}{2} \sum_{i=b,c} G_{\overline{a}\overline{a}\overline{a}\overline{a}\overline{i}}^{(8)} \star \mathbb{J}(a \overline{a} \overline{a} \overline{a} \overline{a} \overline{i} a i) \\
& + \frac{1}{4} \sum_{j \neq a} G_{\overline{a}\overline{a}\overline{a}\overline{a}\overline{j}}^{(8)} \star \mathbb{J}(\overline{a} \overline{a} \overline{a} \overline{a} \overline{j}) + \frac{1}{4} G_{\overline{a}\overline{a}\overline{a}\overline{a}}^{(8)} \star \mathbb{J}(\overline{a} \overline{a} \overline{a} \overline{a}) + \sum_{i \neq a} G_{\overline{a}\overline{a}\overline{a}\overline{i}}^{(8)} \star \mathbb{J}(\overline{a} \overline{a} \overline{a} \overline{i})
\end{aligned}$$

⁵Beware this is only a notation for rank-3 theories; for rank 4 another notation shall be used

$$\begin{aligned}
& + \sum_{i \neq a} G_{\text{diagram}}^{(8)} \star \mathbb{J} \left(\text{diagram} \right) + \sum_{i \neq a \neq j} G_{\text{diagram}}^{(8)} \star \mathbb{J} \left(\text{diagram} \right) + \sum_{i \neq a} G_{\text{diagram}}^{(8)} \star \mathbb{J} \left(\text{diagram} \right) \\
& + \sum_{i \neq a} G_{\text{diagram}}^{(8)} \star \mathbb{J} \left(\text{diagram} \right) + G_{\text{diagram}}^{(8)} \star \mathbb{J} \left(\text{diagram} \right) + \frac{1}{4} G_{\text{diagram}}^{(8)} \star \mathbb{J} \left[\text{diagram} \right] \\
& + \frac{1}{4} \sum_{i \neq j} G_{\text{diagram}}^{(8)} \star \mathbb{J} \left(\text{diagram} \right) + \frac{1}{4} G_{\text{diagram}}^{(8)} \star \mathbb{J} \left(\text{diagram} \right) + \mathcal{O}(10)
\end{aligned}$$

In [62], the term $Y_{s_a}^{(a)}[J, \bar{J}]$ for the φ_3^4 -theory to $\mathcal{O}(4)$ has been found. This expansion is enough for deriving any of the 4-point SDEs. However, since we want the explicit 6-point SDEs, we need to compute $Y_{s_a}^{(a)}[J, \bar{J}]$ to $\mathcal{O}(6)$ in the sources, i.e. consider the free energy to order $\mathcal{O}(J^4, \bar{J}^4)$, to be precise.

Lemma 1.4.1. *To order-6, $Y_{s_a}^{(a)}[J, \bar{J}]$ is given by:*

$$\begin{aligned}
& Y_{s_a}^{(a)}[J, \bar{J}] \\
& = \sum_{q_b, q_c} G_{\ominus}^{(2)}(s_a, q_b, q_c) + \frac{1}{2} \sum_{r=1}^2 (\Delta_{s_a, r} G_{|\ominus| \ominus| \ominus|}^{(4)} + \Delta_{s_a, r} G_{|\square_1|}^{(4)} + \Delta_{s_a, r} G_{|\square_2|}^{(4)} + \Delta_{s_a, r} G_{|\square_3|}^{(4)}) \star \mathbb{J}(\ominus) \\
& + \left(\frac{1}{3} \sum_{r=1}^3 (\Delta_{s_a, r} G_{\text{diagram}}^{(6)} + \Delta_{s_a, r} G_{\text{diagram}}^{(6)}) + \Delta_{s_a, 3} G_{\text{diagram}}^{(6)} + \Delta_{s_a, 3} G_{\text{diagram}}^{(6)} + \frac{1}{2} \Delta_{s_a, 1} G_{|\ominus| \ominus| \ominus|}^{(6)} \right) \star \mathbb{J}(\text{diagram}) \\
& + \left(\frac{1}{3} \sum_{r=1}^3 \Delta_{s_a, r} G_{\text{diagram}}^{(6)} + \Delta_{s_a, 3} G_{\text{diagram}}^{(6)} + \sum_{r=1}^2 \Delta_{s_a, r} G_{\text{diagram}}^{(6)} + \frac{1}{2} \Delta_{s_a, 1} G_{|\ominus| \ominus| \ominus|}^{(6)} \right) \star \mathbb{J}(\text{diagram}) \\
& + \left(\frac{1}{3} \sum_{r=1}^3 \Delta_{s_a, r} G_{\text{diagram}}^{(6)} + \Delta_{s_a, 2} G_{\text{diagram}}^{(6)} + \sum_{r=1}^2 \Delta_{s_a, r} G_{\text{diagram}}^{(6)} + \frac{1}{2} \Delta_{s_a, 1} G_{|\ominus| \ominus| \ominus|}^{(6)} \right) \star \mathbb{J}(\text{diagram}) \\
& + \left(\frac{1}{3!} \sum_{r=1}^3 \Delta_{s_a, r} G_{|\ominus| \ominus| \ominus| \ominus|}^{(6)} + \Delta_{s_a, 2} G_{\text{diagram}}^{(6)} + \sum_{r=2,3} \sum_{i=1}^3 \Delta_{s_a, r} G_{|\ominus| \ominus| \ominus|}^{(6)} \right) \star \mathbb{J}(\ominus \sqcup \ominus) \\
& + \left\{ \frac{1}{4} \sum_{p=3,4} (\Delta_{s_a, p} G_{|\ominus| \ominus| \ominus| \ominus|}^{(8)} + \Delta_{s_a, p} G_{|\ominus| \ominus| \ominus| \ominus|}^{(8)}) \right. \\
& + \left. \frac{1}{4!} \sum_{u=1}^4 (\Delta_{s_a, u} G_{|\ominus| \ominus| \ominus| \ominus| \ominus|}^{(8)} + \Delta_{s_a, 3} G_{|\ominus| \text{diagram}}^{(8)}) \right\} \star \mathbb{J}(\ominus \sqcup \ominus \sqcup \ominus) \\
& + \left\{ \frac{1}{8} \left(\sum_{r=1,2} \Delta_{s_a, r} G_{|\text{diagram}| \text{diagram}}^{(8)} + \sum_{r=3,4} (123)^* (\Delta_{s_a, r} G_{|\text{diagram}| \text{diagram}}^{(8)}) \right) + \frac{1}{4} \sum_{i \neq a} \left(\sum_{r=1,2} \Delta_{s_a, r} G_{|\text{diagram}| \text{diagram}}^{(8)} \right) \right. \\
& + \frac{1}{3} \sum_{q=2,3,4} \Delta_{s_a, q} G_{|\ominus| \text{diagram}}^{(8)} + \frac{1}{3} \sum_{q=2,3,4} \Delta_{s_a, q} G_{|\ominus| \text{diagram}}^{(8)} + \Delta_{s_a, 4} G_{|\ominus| \text{diagram}}^{(8)} + \Delta_{s_a, 4} G_{|\ominus| \text{diagram}}^{(8)} \\
& + \left. \frac{1}{4} \sum_{r=1,2} \Delta_{s_a, r} G_{|\ominus| \ominus| \ominus| \text{diagram}}^{(8)} + \Delta_{s_a, 2} G_{\text{diagram}}^{(8)} + (123)^* (\Delta_{s_a, 3} G_{\text{diagram}}^{(8)}) \right\} \star \mathbb{J}(\ominus \sqcup \text{diagram})
\end{aligned}$$

$$\begin{aligned}
& + \left\{ \frac{1}{8} \left(\sum_{r=1,2} \Delta_{s_a,r} G_{|\overline{ab}| \overline{bc}|}^{(8)} + \sum_{r=3,4} (123)^* \Delta_{s_a,r} G_{|\overline{ab}| \overline{bc}|}^{(8)} \right) + \frac{1}{4} \sum_{p=3,4} (123)^* \Delta_{s_a,p} G_{|\overline{ab}| \overline{ca}|}^{(8)} \right. \\
& + \frac{1}{4} \sum_{p=3,4} (123)^* \Delta_{s_a,p} G_{|\overline{ab}| \overline{ca}|}^{(8)} + \sum_{h=2,3} \Delta_{s_a,h} G_{|\ominus| \overline{ab}|}^{(8)} + \Delta_{s_a,4} G_{|\ominus| \overline{bc}|}^{(8)} + \frac{1}{4} \sum_{r=1,2} \Delta_{s_a,r} G_{|\ominus| \overline{bc}|}^{(8)} \\
& + \frac{1}{2} \left(\Delta_{s_a,2} G_{c \overline{ab} \overline{ca}}^{(8)} + (123)^* \left(\Delta_{s_a,3} G_{c \overline{ab} \overline{ca}}^{(8)} \right) \right) + \Delta_{s_a,2} G_{\overline{ab} \overline{ca}}^{(8)} \left. \right\} \star \mathbb{J}(\ominus \sqcup \overline{ab}) \\
& + \left\{ \frac{1}{8} \left(\sum_{r=1,2} \Delta_{s_a,r} G_{|\overline{bc}| \overline{ca}|}^{(8)} + \sum_{r=3,4} (123)^* \Delta_{s_a,r} G_{|\overline{bc}| \overline{ca}|}^{(8)} + \frac{1}{4} \sum_{p=3,4} (123)^* \Delta_{s_a,p} G_{|\overline{bc}| \overline{ca}|}^{(8)} \right) \right. \\
& + \frac{1}{4} \left(\sum_{r=1,2} \Delta_{s_a,r} G_{|\overline{bc}| \overline{ca}|}^{(8)} \right) + \sum_{h=2,3} \Delta_{s_a,h} G_{|\ominus| \overline{ac}|}^{(8)} + \Delta_{s_a,2} G_{|\ominus| \overline{bc}|}^{(8)} + \frac{1}{4} \sum_{r=1,2} \Delta_{s_a,r} G_{|\ominus| \overline{bc}|}^{(8)} \\
& + \frac{1}{2} \left(\Delta_{s_a,2} G_{b \overline{ca} \overline{ab}}^{(8)} + (123)^* \left(\Delta_{s_a,3} G_{b \overline{ca} \overline{ab}}^{(8)} \right) \right) + \Delta_{s_a,2} G_{\overline{ca} \overline{ab}}^{(8)} \left. \right\} \star \mathbb{J}(\ominus \sqcup \overline{ca}) \\
& + \left\{ \frac{1}{3} \Delta_{s_a,1} G_{|\ominus| \overline{ab}|}^{(8)} + \Delta_{s_a,1} G_{a \overline{bc}|}^{(8)} + \Delta_{s_a,1} G_{a \overline{cb}|}^{(8)} \right. \\
& \quad + \sum_{p=3,4} \Delta_{s_a,p} G_{i \overline{ab}|}^{(8)} + \frac{1}{4} \sum_{u=1}^4 \Delta_{s_a,u} G_{\overline{ab}|}^{(8)} \left. \right\} \star \mathbb{J}(\overline{ab}) \\
& + \left\{ \frac{1}{3} \Delta_{s_a,1} G_{|\ominus| \overline{ca}|}^{(8)} + \Delta_{s_a,1} G_{\overline{ca}|}^{(8)} + \Delta_{s_a,1} G_{\overline{cb}|}^{(8)} + \right. \\
& \quad + \frac{1}{4} \sum_{r=1}^4 \Delta_{s_a,r} G_{\overline{ca}|}^{(8)} + \sum_{r=1,2} \Delta_{s_a,r} G_{\overline{cb}|}^{(8)} \left. \right\} \star \mathbb{J}(\overline{ca}) \\
& + \left\{ \frac{1}{3} \Delta_{s_a,1} G_{|\ominus| \overline{cb}|}^{(8)} + \frac{1}{2} \sum_{h=2,3} \Delta_{s_a,h} G_{a \overline{cb} \overline{ca}}^{(8)} \right. \\
& \quad + \frac{1}{4} \sum_{r=1}^4 \Delta_{s_a,r} G_{\overline{cb}|}^{(8)} + \Delta_{s_a,1} G_{\overline{cb}|}^{(8)} + \sum_{r=1,2} \Delta_{s_a,r} G_{\overline{cb}|}^{(8)} \left. \right\} \star \mathbb{J}(\overline{cb}) \\
& + \left\{ \frac{1}{3} \Delta_{s_a,1} G_{|\ominus| \overline{ca}|}^{(8)} + \frac{1}{2} \sum_{h=2,3} \Delta_{s_a,h} G_{a \overline{ca} \overline{ab}}^{(8)} \right. \\
& \quad + \frac{1}{4} \sum_{r=1}^4 \Delta_{s_a,r} G_{\overline{ca}|}^{(8)} + \Delta_{s_a,1} G_{\overline{ca}|}^{(8)} + \sum_{r=1,2} \Delta_{s_a,r} G_{\overline{ca}|}^{(8)} \left. \right\} \star \mathbb{J}(\overline{ca}) \\
& + \left\{ \Delta_{s_a,1} G_{|\ominus| \overline{bc}|}^{(8)} + \sum_{h=2,3} \Delta_{s_a,h} G_{\overline{bc} \overline{ca}}^{(8)} + (13)^* \left(\Delta_{s_a,3} G_{\overline{bc} \overline{ca}}^{(8)} \right) + (13)^* \left(\Delta_{s_a,4} G_{\overline{bc} \overline{ca}}^{(8)} \right) \right. \\
& + \sum_{p=3,4} \left(\Delta_{s_a,p} G_{\overline{ca} \overline{ab}}^{(8)} + (13)^* \Delta_{s_a,p} G_{\overline{ca} \overline{ab}}^{(8)} \right) + (13)^* \left(\Delta_{s_a,1} G_{\overline{ca} \overline{ab}}^{(8)} \right) + (13)^* \left(\Delta_{s_a,2} G_{\overline{ca} \overline{ab}}^{(8)} \right) \\
& + \frac{1}{2} \left(\Delta_{s_a,1} G_{b \overline{ca} \overline{ab}}^{(8)} + (13)^* \left(\Delta_{s_a,1} G_{c \overline{ca} \overline{ab}}^{(8)} \right) + (13)^* \left(\Delta_{s_a,4} G_{b \overline{ca} \overline{ab}}^{(8)} \right) + \Delta_{s_a,4} G_{c \overline{ca} \overline{ab}}^{(8)} \right) \\
& + \sum_{r=1,2} (13)^* \left(\Delta_{s_a,r} G_{\overline{ca} \overline{ab}}^{(8)} \right) + \frac{1}{4} \left((123)^* \Delta_{s_a,1} G_{\overline{ca} \overline{ab}}^{(8)} + \Delta_{s_a,2} G_{\overline{ca} \overline{ab}}^{(8)} \right. \\
& \quad \left. + (13)^* \Delta_{s_a,3} G_{\overline{ca} \overline{ab}}^{(8)} + (123)^* \Delta_{s_a,4} G_{\overline{ca} \overline{ab}}^{(8)} \right) \left. \right\} \star \mathbb{J}(\overline{ca})
\end{aligned}$$

$$\begin{aligned}
& + \left\{ \Delta_{s_a,1} G_{|\ominus| \begin{array}{|c|} \hline a \\ \hline \end{array}}^{(8)} + \Delta_{s_a,1} G_{\begin{array}{|c|} \hline (b) \\ \hline \end{array}}^{(8)} + \Delta_{s_a,4} G_{\begin{array}{|c|} \hline (a) \\ \hline \end{array}}^{(8)} + \frac{1}{2} \left(\sum_{r=1,2} (13)^* (\Delta_{s_a,r} G_{\begin{array}{|c|} \hline (a) \\ \hline \end{array}}^{(8)}) \right) \right. \\
& + \sum_{p=3,4} \Delta_{s_a,p} G_{\begin{array}{|c|} \hline (a) \\ \hline \end{array}}^{(8)} + \Delta_{s_a,1} G_{\begin{array}{|c|} \hline (a) \\ \hline \end{array}}^{(8)} + (13)^* \Delta_{s_a,4} G_{\begin{array}{|c|} \hline (a) \\ \hline \end{array}}^{(8)} \left. \right) + \sum_{p=3,4} \Delta_{s_a,p} G_{\begin{array}{|c|} \hline (a) \\ \hline \end{array}}^{(8)} \\
& + \sum_{q=2,3,4} (13)^* \Delta_{s_a,q} G_{\begin{array}{|c|} \hline (a) \\ \hline \end{array}}^{(8)} + (13)^* \Delta_{s_a,q} G_{\begin{array}{|c|} \hline (a) \\ \hline \end{array}}^{(8)} + \Delta_{s_a,3} G_{\begin{array}{|c|} \hline (a) \\ \hline \end{array}}^{(8)} \\
& + \frac{1}{4} (\Delta_{s_a,1} G_{\begin{array}{|c|} \hline (a) \\ \hline \end{array}}^{(8)} + (123)^* \Delta_{s_a,2} G_{\begin{array}{|c|} \hline (a) \\ \hline \end{array}}^{(8)} + (23)^* \Delta_{s_a,3} G_{\begin{array}{|c|} \hline (a) \\ \hline \end{array}}^{(8)} + (13)^* \Delta_{s_a,4} G_{\begin{array}{|c|} \hline (a) \\ \hline \end{array}}^{(8)}) \} \star \mathbb{J} \left(\begin{array}{|c|} \hline (a) \\ \hline \end{array} \right) \\
& + \left\{ \Delta_{s_a,1} G_{|\ominus| \begin{array}{|c|} \hline a \\ \hline \end{array}}^{(8)} + (13)^* (\Delta_{s_a,4} G_{\begin{array}{|c|} \hline (a) \\ \hline \end{array}}^{(8)}) + (13)^* (\Delta_{s_a,1} G_{\begin{array}{|c|} \hline (a) \\ \hline \end{array}}^{(8)}) \right. \\
& + \frac{1}{2} \left(\sum_{r=1,2} (13)^* (\Delta_{s_a,r} G_{\begin{array}{|c|} \hline (a) \\ \hline \end{array}}^{(8)}) \right) + \sum_{p=3,4} \Delta_{s_a,p} G_{\begin{array}{|c|} \hline (a) \\ \hline \end{array}}^{(8)} + \Delta_{s_a,1} G_{\begin{array}{|c|} \hline (a) \\ \hline \end{array}}^{(8)} \\
& + (13)^* \Delta_{s_a,4} G_{\begin{array}{|c|} \hline (a) \\ \hline \end{array}}^{(8)} \left. \right) + \sum_{p=3,4} \Delta_{s_a,p} G_{\begin{array}{|c|} \hline (a) \\ \hline \end{array}}^{(8)} + \sum_{q=2,3,4} (13)^* \Delta_{s_a,q} G_{\begin{array}{|c|} \hline (a) \\ \hline \end{array}}^{(8)} \\
& + \sum_{q=2,3,4} (13)^* \Delta_{s_a,q} G_{\begin{array}{|c|} \hline (a) \\ \hline \end{array}}^{(8)} + \sum_{p=3,4} (13)^* (\Delta_{s_a,p} G_{\begin{array}{|c|} \hline (a) \\ \hline \end{array}}^{(8)}) \\
& + \frac{1}{4} (\Delta_{s_a,1} G_{\begin{array}{|c|} \hline (a) \\ \hline \end{array}}^{(8)} + (123)^* \Delta_{s_a,2} G_{\begin{array}{|c|} \hline (a) \\ \hline \end{array}}^{(8)} + (23)^* \Delta_{s_a,3} G_{\begin{array}{|c|} \hline (a) \\ \hline \end{array}}^{(8)} + (13)^* \Delta_{s_a,4} G_{\begin{array}{|c|} \hline (a) \\ \hline \end{array}}^{(8)}) \} \star \mathbb{J} \left(\begin{array}{|c|} \hline (a) \\ \hline \end{array} \right).
\end{aligned}$$

Proof. See Appendix A. □

Since the 2-point equation was already derived in [62], we immediately proceed with the higher-point functions. Nevertheless, a detail derivation of the 2-point is done in Chapter 2 in order to study its large N limit.

1.4.1 Four-point function SDEs for the φ_3^4 -theory

We can use the colour symmetry in order to write down the equations for $G_{2\begin{array}{|c|} \hline 2 \\ \hline \end{array}}^{(4)}$ and $G_{3\begin{array}{|c|} \hline 3 \\ \hline \end{array}}^{(4)}$ from that for $G_{1\begin{array}{|c|} \hline 1 \\ \hline \end{array}}^{(4)}$, which we now compute. We will obtain, as stated by the theorem of previous section, the SDE for $G_{1\begin{array}{|c|} \hline 1 \\ \hline \end{array}}^{(4)}$.

We need first, to compute the functions $f_{1\begin{array}{|c|} \hline 1 \\ \hline \end{array}}^{(a)}$ for each colour a . To this end, Lemma 1.4.1 is used:

$$\begin{aligned}
f_{1\begin{array}{|c|} \hline 1 \\ \hline \end{array}}^{(1)} &= \frac{1}{3} \sum_{r=1}^3 (\Delta_{x_1,r} G_{\begin{array}{|c|} \hline (1) \\ \hline \end{array}}^{(6)}) + \frac{1}{3} \sum_{r=1}^3 (\Delta_{x_1,r} G_{\begin{array}{|c|} \hline (1) \\ \hline \end{array}}^{(6)}) + (\Delta_{x_1,3} G_{\begin{array}{|c|} \hline (1) \\ \hline \end{array}}^{(6)} + \Delta_{x_1,3} G_{\begin{array}{|c|} \hline (1) \\ \hline \end{array}}^{(6)}) + \Delta_{x_1,1} G_{|\ominus| 1\begin{array}{|c|} \hline 1 \\ \hline \end{array}}^{(6)}), \\
f_{1\begin{array}{|c|} \hline 1 \\ \hline \end{array}}^{(2)} &= \frac{1}{3} \sum_{r=1}^3 (\Delta_{y_2,r} G_{\begin{array}{|c|} \hline (2) \\ \hline \end{array}}^{(6)}) + \Delta_{y_2,3} G_{\begin{array}{|c|} \hline (2) \\ \hline \end{array}}^{(6)} + \sum_{r=1}^2 (\Delta_{y_2,r} G_{\begin{array}{|c|} \hline (2) \\ \hline \end{array}}^{(6)}) + \frac{1}{2} (\Delta_{y_2,1} G_{|\ominus| 1\begin{array}{|c|} \hline 1 \\ \hline \end{array}}^{(6)}), \\
f_{1\begin{array}{|c|} \hline 1 \\ \hline \end{array}}^{(3)} &= \frac{1}{3} \sum_{r=1}^3 (\Delta_{y_3,r} G_{\begin{array}{|c|} \hline (3) \\ \hline \end{array}}^{(6)}) + \Delta_{y_2,3} G_{\begin{array}{|c|} \hline (3) \\ \hline \end{array}}^{(6)} + \sum_{r=1}^2 (\Delta_{y_3,r} G_{\begin{array}{|c|} \hline (3) \\ \hline \end{array}}^{(6)}) + \frac{1}{2} (\Delta_{y_3,1} G_{|\ominus| 1\begin{array}{|c|} \hline 1 \\ \hline \end{array}}^{(6)}).
\end{aligned}$$

Also notice that

$$\varsigma_1(1\begin{array}{|c|} \hline 1 \\ \hline \end{array}; 1, 2) = \ominus \sqcup \ominus, \quad \varsigma_2(1\begin{array}{|c|} \hline 1 \\ \hline \end{array}; 1, 2) = 3\begin{array}{|c|} \hline 3 \\ \hline \end{array}, \quad \varsigma_3(1\begin{array}{|c|} \hline 1 \\ \hline \end{array}; 1, 2) = 2\begin{array}{|c|} \hline 2 \\ \hline \end{array}.$$

The derivatives with respect to these, evaluated in $\mathbf{X} = (\mathbf{x}, \mathbf{y})$ are then

$$G_{\ominus}^{(2)}(\mathbf{x}) \cdot G_{\ominus}^{(2)}(\mathbf{y}) + G_{|\ominus| \ominus}^{(4)}(\mathbf{x}, \mathbf{y}), \quad G_{3\overline{\square}_3}^{(4)}(\mathbf{x}, \mathbf{y}), \quad \text{and } G_{2\overline{\square}_2}^{(4)}(\mathbf{x}, \mathbf{y}).$$

respectively. Letting $\mathbf{s} = (x_1, y_2, y_3)$ and $\mathbf{t} = (y_1, x_2, x_3)$ and using Theorem 1.3.1, one obtains

$$\begin{aligned} & \left(1 + \frac{2\lambda}{E_{\mathbf{s}}} \sum_a \sum_{\mathbf{q}_{\hat{a}}} G_{\ominus}^{(2)}(s_a, \mathbf{q}_{\hat{a}})\right) \cdot G_{1\overline{\square}_1}^{(4)}(\mathbf{x}, \mathbf{y}) \\ &= \frac{(-2\lambda)}{E_{\mathbf{s}}} \sum_{a=1}^3 \left\{ \sum_{\hat{\sigma} \in \text{Aut}_c(1\overline{\square}_1)} \sigma^* \mathfrak{f}_{1\overline{\square}_1}^{(a)}(\mathbf{X}) \right. \\ & \quad + \sum_{\rho > 1} \frac{Z_0^{-1}}{E(y_a^\rho, s_a)} \frac{\partial Z[J, J]}{\partial \varsigma_a(1\overline{\square}_1; 1, \rho)}(\mathbf{X}) - \sum_{\rho > 1} \frac{Z_0^{-1}}{E(y_a^\rho, s_a)} \frac{\partial Z[J, J]}{\partial \varsigma_a(1\overline{\square}_1; 1, \rho)}(\mathbf{X}|_{s_a \rightarrow y_a^\rho}) \\ & \quad \left. - \sum_{b_a} \frac{1}{E(s_a, b_a)} [G_{1\overline{\square}_1}^{(4)}(\mathbf{X}) - G_{1\overline{\square}_1}^{(4)}(\mathbf{X}|_{s_a \rightarrow b_a})] \right\} \\ &= \frac{(-2\lambda)}{E_{x_1 y_2 y_3}} \left\{ (\delta_{\mathbf{u}}^{\mathbf{x}} \delta_{\mathbf{v}}^{\mathbf{y}} + \delta_{\mathbf{u}}^{\mathbf{y}} \delta_{\mathbf{v}}^{\mathbf{x}}) \cdot \left(\frac{1}{3} \sum_{r=1}^3 (\Delta_{x_1, r} G_{\overline{\square}_3}^{(6)}) + \frac{1}{3} \sum_{r=1}^3 (\Delta_{x_1, r} G_{\overline{\square}_2}^{(6)}) \right) \right. \\ & \quad + (\Delta_{x_1, 3} G_{\overline{\square}_{13}}^{(6)} + \Delta_{x_1, 3} G_{\overline{\square}_{12}}^{(6)}) + \Delta_{x_1, 1} G_{|\ominus| 1\overline{\square}_1}^{(6)} \\ & \quad + \frac{1}{3} \sum_{r=1}^3 (\Delta_{y_2, r} G_{\overline{\square}_3}^{(6)}) + \Delta_{y_2, 3} G_{\overline{\square}_{13}}^{(6)} + \sum_{r=1}^2 (\Delta_{y_2, r} G_{\overline{\square}_{12}}^{(6)}) + \frac{1}{2} (\Delta_{y_2, 1} G_{|\ominus| 1\overline{\square}_1}^{(6)}) \\ & \quad + \frac{1}{3} \sum_{r=1}^3 (\Delta_{y_3, r} G_{\overline{\square}_3}^{(6)}) + \Delta_{y_3, 3} G_{\overline{\square}_{12}}^{(6)} + \sum_{r=1}^2 (\Delta_{y_3, r} G_{\overline{\square}_{13}}^{(6)}) + \frac{1}{2} (\Delta_{y_3, 1} G_{|\ominus| 1\overline{\square}_1}^{(6)}) (\mathbf{u}, \mathbf{v}) \\ & \quad + \frac{1}{E(y_1, x_1)} [(G_{\ominus}^{(2)}(\mathbf{x}) - G_{\ominus}^{(2)}(y_1, x_2, x_3)) \cdot G_{\ominus}^{(2)}(\mathbf{y}) \\ & \quad \quad \quad + G_{|\ominus| \ominus}^{(4)}(\mathbf{x}, \mathbf{y}) - G_{|\ominus| \ominus}^{(4)}(y_1, x_2, x_3, \mathbf{y})] \\ & \quad + \frac{G_{3\overline{\square}_3}^{(4)}(\mathbf{x}, \mathbf{y}) - G_{3\overline{\square}_3}^{(4)}(\mathbf{x}, y_1, x_2, y_3)}{E(x_2, y_2)} + \frac{G_{2\overline{\square}_2}^{(4)}(\mathbf{x}, \mathbf{y}) - G_{2\overline{\square}_2}^{(4)}(\mathbf{x}, y_1, y_2, x_3)}{E(x_3, y_3)} \\ & \quad - \sum_{b_1} \frac{1}{E(x_1, b_1)} (G_{1\overline{\square}_1}^{(4)}(\mathbf{x}, \mathbf{y}) - G_{1\overline{\square}_1}^{(4)}(b_1, x_2, x_3, \mathbf{y})) \\ & \quad - \sum_{b_2} \frac{1}{E(y_2, b_2)} (G_{1\overline{\square}_1}^{(4)}(\mathbf{x}, \mathbf{y}) - G_{1\overline{\square}_1}^{(4)}(\mathbf{x}, y_1, b_2, y_3)) \\ & \quad \left. - \sum_{b_3} \frac{1}{E(y_3, b_3)} (G_{1\overline{\square}_1}^{(4)}(\mathbf{x}, \mathbf{y}) - G_{1\overline{\square}_1}^{(4)}(\mathbf{x}, y_1, y_2, b_3)) \right\} \end{aligned} \tag{1.4.2}$$

1.4.2 The Schwinger-Dyson equation for $G_{\overline{\square}_3}^{(6)}$

We now derive the whole set of six-point function equations for the φ_3^4 -theory. They hold for any model whose boundary sector is the whole of $\text{Grph}_3^{\text{II, cl}}$. From Prop. 1.4.1, one can

read off the $f_B^{(a)}$ functions.

For the boundary graph \heartsuit , one has, for each colour $a = 1, 2, 3$,

$$f_{\heartsuit}^{(a)} = \frac{1}{3} \Delta_{s_a, 1} G_{|\ominus| |\heartsuit|}^{(8)} + \Delta_{s_a, 1} G_{a \begin{smallmatrix} \heartsuit \\ b \end{smallmatrix}}^{(8)} + \Delta_{s_a, 1} G_{a \begin{smallmatrix} \heartsuit \\ c \end{smallmatrix}}^{(8)} + \sum_{p=3,4} \Delta_{s_a, p} G_{i \begin{smallmatrix} \heartsuit \\ a \end{smallmatrix}}^{(8)} + \frac{1}{4} \sum_{u=1}^4 \Delta_{s_a, u} G_{\begin{smallmatrix} \heartsuit \\ i \end{smallmatrix}}^{(8)}.$$

Departing from Theorem 1.3.1, this last very expression allows now for an explicit derivation of the equation for $G_{\heartsuit}^{(6)}$. Namely, for $\mathbf{X} = (\mathbf{x}^1, \mathbf{x}^2, \mathbf{x}^3) = (\mathbf{x}, \mathbf{y}, \mathbf{z})$, and choosing $\mathbf{s} = (x_1, y_2, z_3)$,

$$\begin{aligned} & \left(1 + \frac{2\lambda}{E_{x_1 y_2 z_3}} \sum_{a=1}^3 \sum_{\mathbf{q}\hat{a}} G_{\ominus}^{(2)}(s_a, \mathbf{q}\hat{a}) \right) G_{\heartsuit}^{(6)}(\mathbf{X}) \\ &= \frac{(-2\lambda)}{E_{x_1 y_2 z_3}} \sum_{a=1}^3 \left\{ \sum_{\hat{\sigma} \in \text{Aut}_c(\heartsuit)} \sigma^* f_{\heartsuit}^{(a)}(\mathbf{X}) + \sum_{\rho > 1} \frac{Z_0^{-1}}{E(y_a^\rho, s_a)} \left[\frac{\partial Z[J, J]}{\partial \varsigma_a(\heartsuit; 1, \rho)}(\mathbf{X}) - \frac{\partial Z[J, J]}{\partial \varsigma_a(\heartsuit; 1, \rho)}(\mathbf{X}|_{x_a \rightarrow s_a}) \right] \right. \\ & \quad \left. - \sum_{b_a} \frac{1}{E(s_a, b_a)} [G_{\heartsuit}^{(6)}(\mathbf{X}) - G_{\heartsuit}^{(6)}(\mathbf{X}|_{s_a \rightarrow b_a})] \right\} \end{aligned} \quad (1.4.3)$$

One finds:

$$\begin{aligned} & \sum_{a=1}^3 \sum_{\rho > 1} \frac{Z_0^{-1}}{E(y_a^\rho, s_a)} \frac{\partial Z[J, J]}{\partial \varsigma_a(\heartsuit; 1, \rho)}(\mathbf{X}) \\ &= \left(\frac{1}{E(y_1, x_1)} (23)^* G_{\begin{smallmatrix} \heartsuit \\ 23 \end{smallmatrix}}^{(6)} + \frac{1}{E(z_1, x_1)} (13)^* G_{\begin{smallmatrix} \heartsuit \\ 23 \end{smallmatrix}}^{(6)} + \frac{1}{E(z_2, y_2)} (123)^* G_{\begin{smallmatrix} \heartsuit \\ 13 \end{smallmatrix}}^{(6)} \right. \\ & \quad \left. + \frac{1}{E(x_2, y_2)} (132)^* G_{\begin{smallmatrix} \heartsuit \\ 13 \end{smallmatrix}}^{(6)} + \frac{1}{E(x_3, z_3)} (13)^* G_{\begin{smallmatrix} \heartsuit \\ 12 \end{smallmatrix}}^{(6)} + \frac{1}{E(y_3, z_3)} (123)^* G_{\begin{smallmatrix} \heartsuit \\ 12 \end{smallmatrix}}^{(6)} \right) (\mathbf{X}), \end{aligned}$$

where we recall that for a function of three arguments and $\sigma \in \mathfrak{S}_3$, $\sigma^* f$ is given by Prop. 1.2.1.

The meaning of the $f_{\heartsuit}^{(a)}$ summed over colours a and over the automorphism group is

$$\begin{aligned} & \sum_a \sum_{\hat{\pi} \in \mathbb{Z}_3} \pi^* \left\{ \frac{1}{3} G_{|\ominus| |\heartsuit|}^{(8)} + \Delta_{s_a, 1} G_{a \begin{smallmatrix} \heartsuit \\ b \end{smallmatrix}}^{(8)} + \Delta_{s_a, 1} G_{a \begin{smallmatrix} \heartsuit \\ c \end{smallmatrix}}^{(8)} \right. \\ & \quad \left. + \sum_{p=3,4} \Delta_{s_a, p} G_{i \begin{smallmatrix} \heartsuit \\ a \end{smallmatrix}}^{(8)} + \frac{1}{4} \sum_{u=1}^4 \Delta_{s_a, u} G_{\begin{smallmatrix} \heartsuit \\ i \end{smallmatrix}}^{(8)} \right\} \\ &= \sum_{\hat{\pi} \in \mathbb{Z}_3} \pi^* \left\{ \frac{1}{3} \sum_a \Delta_{s_a, 1} G_{|\ominus| |\heartsuit|}^{(8)} + (\Delta_{x_1, 1} G_{1 \begin{smallmatrix} \heartsuit \\ 2 \end{smallmatrix}}^{(8)} + \Delta_{x_1, 1} G_{2 \begin{smallmatrix} \heartsuit \\ 3 \end{smallmatrix}}^{(8)} + \Delta_{y_2, 1} G_{3 \begin{smallmatrix} \heartsuit \\ 1 \end{smallmatrix}}^{(8)} + \Delta_{y_2, 1} G_{2 \begin{smallmatrix} \heartsuit \\ 3 \end{smallmatrix}}^{(8)} \right. \\ & \quad + \Delta_{z_3, 1} G_{1 \begin{smallmatrix} \heartsuit \\ 2 \end{smallmatrix}}^{(8)} + \Delta_{z_3, 1} G_{2 \begin{smallmatrix} \heartsuit \\ 3 \end{smallmatrix}}^{(8)} + \sum_{p=3,4} \Delta_{x_1, p} G_{3 \begin{smallmatrix} \heartsuit \\ 1 \end{smallmatrix}}^{(8)} + \Delta_{y_2, p} G_{1 \begin{smallmatrix} \heartsuit \\ 2 \end{smallmatrix}}^{(8)} + \Delta_{z_3, p} G_{2 \begin{smallmatrix} \heartsuit \\ 3 \end{smallmatrix}}^{(8)}) \\ & \quad \left. + \frac{1}{4} \sum_{u=1}^4 (\Delta_{x_1, u} G_{\begin{smallmatrix} \heartsuit \\ 3 \end{smallmatrix}}^{(8)} + \Delta_{y_2, u} G_{\begin{smallmatrix} \heartsuit \\ 1 \end{smallmatrix}}^{(8)} + \Delta_{z_3, u} G_{\begin{smallmatrix} \heartsuit \\ 2 \end{smallmatrix}}^{(8)}) \right\} \end{aligned}$$

where \mathbb{Z}_3 is generated rotation of \otimes by $2\pi/3$, that is $\hat{\pi}$ is the liftings of the identity, of (123) and (132) in \mathfrak{S}_3 . Finally, the difference-term is

$$\begin{aligned} \sum_a \sum_{b_a} \frac{1}{E(s_a, b_a)} [G_{\otimes}^{(6)}(\mathbf{X}) - G_{\otimes}^{(6)}(\mathbf{X}|_{s_a \rightarrow b_a})] &= \sum_{b_1} \frac{1}{E(x_1, b_1)} [G_{\otimes}^{(6)}(\mathbf{X}) - G_{\otimes}^{(6)}(b_1, x_2, x_3; \mathbf{y}; \mathbf{z})] \\ &+ \sum_{b_2} \frac{1}{E(y_2, b_2)} [G_{\otimes}^{(6)}(\mathbf{X}) - G_{\otimes}^{(6)}(\mathbf{x}; y_1, b_2, y_3; \mathbf{z})] \\ &+ \sum_{b_3} \frac{1}{E(z_3, b_3)} [G_{\otimes}^{(6)}(\mathbf{X}) - G_{\otimes}^{(6)}(\mathbf{x}; \mathbf{y}; z_1, z_2, b_3)] \end{aligned}$$

Explicitly,

$$\begin{aligned} & - \left(\frac{E_{x_1 y_2 z_3}}{2\lambda} + \sum_{m,n} [G_{\ominus}^{(2)}(x_1, m, n) + G_{\ominus}^{(2)}(m, y_2, n) + G_{\ominus}^{(2)}(m, n, z_3)] \right) \cdot G_{\otimes}^{(6)}(\mathbf{X}) \\ &= \left(\frac{1}{E(y_1, x_1)} [G_{\begin{smallmatrix} \square \\ \square \\ \square \end{smallmatrix}}^{(6)}(\mathbf{x}, \mathbf{z}, \mathbf{y}) - G_{\begin{smallmatrix} \square \\ \square \\ \square \end{smallmatrix}}^{(6)}(y_1, x_2, x_3, \mathbf{z}, \mathbf{y})] \right. \\ &+ \frac{1}{E(z_1, x_1)} [G_{\begin{smallmatrix} \square \\ \square \\ \square \end{smallmatrix}}^{(6)}(\mathbf{z}, \mathbf{y}, \mathbf{x}) - G_{\begin{smallmatrix} \square \\ \square \\ \square \end{smallmatrix}}^{(6)}(\mathbf{z}, \mathbf{y}, z_1, x_2, x_3)] \\ &+ \frac{1}{E(z_2, y_2)} [G_{\begin{smallmatrix} \square \\ \square \\ \square \end{smallmatrix}}^{(6)}(\mathbf{z}, \mathbf{x}, \mathbf{y}) - G_{\begin{smallmatrix} \square \\ \square \\ \square \end{smallmatrix}}^{(6)}(\mathbf{z}, \mathbf{x}, y_1, z_2, y_3)] \\ &+ \frac{1}{E(x_2, y_2)} [G_{\begin{smallmatrix} \square \\ \square \\ \square \end{smallmatrix}}^{(6)}(\mathbf{y}, \mathbf{z}, \mathbf{x}) - G_{\begin{smallmatrix} \square \\ \square \\ \square \end{smallmatrix}}^{(6)}(y_1, x_2, y_3, \mathbf{z}, \mathbf{x})] \\ &+ \frac{1}{E(x_3, z_3)} [G_{\begin{smallmatrix} \square \\ \square \\ \square \end{smallmatrix}}^{(6)}(\mathbf{z}, \mathbf{y}, \mathbf{x}) - G_{\begin{smallmatrix} \square \\ \square \\ \square \end{smallmatrix}}^{(6)}(z_1, z_2, x_3, \mathbf{y}, \mathbf{x})] \\ &+ \left. \frac{1}{E(y_3, z_3)} [G_{\begin{smallmatrix} \square \\ \square \\ \square \end{smallmatrix}}^{(6)}(\mathbf{y}, \mathbf{x}, \mathbf{z}) - G_{\begin{smallmatrix} \square \\ \square \\ \square \end{smallmatrix}}^{(6)}(\mathbf{y}, \mathbf{x}, z_1, z_2, y_3)] \right) \tag{1.4.4} \\ &+ \sum_{\hat{\pi} \in \mathbb{Z}_3} \pi^* \left[\frac{1}{3} \sum_a \Delta_{s_a, 1} G_{|\ominus| \otimes}^{(8)} \right] \tag{1.4.5} \\ &+ (\Delta_{x_1, 1} G_{\begin{smallmatrix} \square \\ \square \\ \square \end{smallmatrix}}^{(8)} + \Delta_{x_1, 1} G_{\begin{smallmatrix} \square \\ \square \\ \square \end{smallmatrix}}^{(8)} + \Delta_{y_2, 1} G_{\begin{smallmatrix} \square \\ \square \\ \square \end{smallmatrix}}^{(8)} + \Delta_{y_2, 1} G_{\begin{smallmatrix} \square \\ \square \\ \square \end{smallmatrix}}^{(8)} + \Delta_{z_3, 1} G_{\begin{smallmatrix} \square \\ \square \\ \square \end{smallmatrix}}^{(8)} + \Delta_{z_3, 1} G_{\begin{smallmatrix} \square \\ \square \\ \square \end{smallmatrix}}^{(8)} \\ &+ \sum_{p=3,4} \Delta_{x_1, p} G_{\begin{smallmatrix} \square \\ \square \\ \square \end{smallmatrix}}^{(8)} + \Delta_{y_2, p} G_{\begin{smallmatrix} \square \\ \square \\ \square \end{smallmatrix}}^{(8)} + \Delta_{z_3, p} G_{\begin{smallmatrix} \square \\ \square \\ \square \end{smallmatrix}}^{(8)} + \frac{1}{4} \sum_{u=1}^4 (\Delta_{x_1, u} G_{\begin{smallmatrix} \square \\ \square \\ \square \end{smallmatrix}}^{(8)} \\ &+ \Delta_{y_2, u} G_{\begin{smallmatrix} \square \\ \square \\ \square \end{smallmatrix}}^{(8)} + \Delta_{z_3, u} G_{\begin{smallmatrix} \square \\ \square \\ \square \end{smallmatrix}}^{(8)}) \Big] (\mathbf{X}) - \sum_{b_1} \frac{1}{E(x_1, b_1)} [G_{\otimes}^{(6)}(\mathbf{X}) - G_{\otimes}^{(6)}(b_1, x_2, x_3; \mathbf{y}; \mathbf{z})] \\ &- \sum_{b_2} \frac{1}{E(y_2, b_2)} [G_{\otimes}^{(6)}(\mathbf{X}) - G_{\otimes}^{(6)}(\mathbf{x}; y_1, b_2, y_3; \mathbf{z})] \\ &- \sum_{b_3} \frac{1}{E(z_3, b_3)} [G_{\otimes}^{(6)}(\mathbf{X}) - G_{\otimes}^{(6)}(\mathbf{x}; \mathbf{y}; z_1, z_2, b_3)]. \end{aligned}$$

1.4.3 The Schwinger-Dyson equation for $G_{\text{a}}^{(6)}$

First, we compute \mathfrak{b}_a -terms for \mathcal{Q}_a , one by one are:

$$\frac{1}{Z_0} \frac{\partial Z[J, J]}{\partial \varsigma_1(\text{a}; 1, 2)} = G_{1\text{a}}^{(4)}(\mathbf{x}, \mathbf{z}) \cdot G_{\ominus}^{(2)}(\mathbf{y}) + (12)^* G_{|\ominus|\text{a}}^{(6)}(\mathbf{X}), \quad (1.4.6a)$$

$$\frac{1}{Z_0} \frac{\partial Z[J, J]}{\partial \varsigma_1(\text{a}; 1, 3)} = G_{1\text{a}}^{(4)}(\mathbf{y}, \mathbf{z}) \cdot G_{\ominus}^{(2)}(\mathbf{x}) + G_{|\ominus|\text{a}}^{(6)}(\mathbf{X}), \quad (1.4.6b)$$

$$\frac{1}{Z_0} \frac{\partial Z[J, J]}{\partial \varsigma_2(\text{a}; 1, 2)} = (23)^* G_{\text{a}}^{(6)}(\mathbf{X}), \quad \frac{1}{Z_0} \frac{\partial Z[J, J]}{\partial \varsigma_2(\text{a}; 1, 2)} = (13)^* G_{\text{a}}^{(6)}(\mathbf{X}), \quad (1.4.6c,d)$$

$$\frac{1}{Z_0} \frac{\partial Z[J, J]}{\partial \varsigma_3(\text{a}; 1, 3)} = (23)^* G_{\text{a}}^{(6)}(\mathbf{X}), \quad \frac{1}{Z_0} \frac{\partial Z[J, J]}{\partial \varsigma_3(\text{a}; 1, 3)} = (13)^* G_{\text{a}}^{(6)}(\mathbf{X}). \quad (1.4.6e,f)$$

We stepwise collect the $\mathfrak{f}_{\text{a}}^{(a)}$ -terms from the expansion in Prop. 1.4.1:

$$\mathfrak{f}_{\text{a}}^{(1)} \text{ is the coefficient of } \mathbb{J}(\text{a}) \text{ in } Y_{x_1}^{(1)}[J, \bar{J}] \text{ with } a = 1, b = 2, c = 2, \quad (1.4.7)$$

$$\mathfrak{f}_{\text{a}}^{(2)} \text{ is the coefficient of } \mathbb{J}(\text{a}) \text{ in } Y_{y_2}^{(2)}[J, \bar{J}] \text{ with } a = 2, b = 1, c = 3, \text{ and} \quad (1.4.8)$$

$$\mathfrak{f}_{\text{a}}^{(3)} \text{ is the coefficient of } \mathbb{J}(\text{a}) \text{ in } Y_{y_3}^{(3)}[J, \bar{J}] \text{ with } a = 3, b = 1, c = 2, \quad (1.4.9)$$

namely

$$\mathfrak{f}_{\text{a}}^{(1)} = \frac{1}{3} \Delta_{x_1,1} G_{|\ominus|\text{a}}^{(8)} + \Delta_{x_1,1} G_{\text{a}}^{(8)} + \Delta_{x_1,1} G_{\text{a}}^{(8)} + \frac{1}{4} \sum_{r=1}^4 \Delta_{x_1,r} G_{\text{a}}^{(8)} + \sum_{r=1,2} \Delta_{x_1,r} G_{\text{a}}^{(8)},$$

$$\mathfrak{f}_{\text{a}}^{(2)} = \frac{1}{3} \Delta_{y_2,1} G_{|\ominus|\text{a}}^{(8)} + \frac{1}{2} \sum_{h=2,3} \Delta_{y_2,h} G_{\text{a}}^{(8)} + \frac{1}{4} \sum_{r=1}^4 \Delta_{y_2,r} G_{\text{a}}^{(8)} + \Delta_{y_2,1} G_{\text{a}}^{(8)} + \sum_{r=1,2} \Delta_{y_2,r} G_{\text{a}}^{(8)},$$

$$\mathfrak{f}_{\text{a}}^{(3)} = \frac{1}{3} \Delta_{y_3,1} G_{|\ominus|\text{a}}^{(8)} + \frac{1}{2} \sum_{h=2,3} \Delta_{y_3,h} G_{\text{a}}^{(8)} + \frac{1}{4} \sum_{r=1}^4 \Delta_{y_3,r} G_{\text{a}}^{(8)} + \Delta_{y_3,1} G_{\text{a}}^{(8)} + \sum_{r=1,2} \Delta_{y_3,r} G_{\text{a}}^{(8)}.$$

Explicitly,

$$\begin{aligned} & - \left(\frac{E_{x_1 y_2 y_3}}{2\lambda} + \sum_{m,n} [G_{\ominus}^{(2)}(x_1, m, n) + G_{\ominus}^{(2)}(m, y_2, n) + G_{\ominus}^{(2)}(m, n, y_3)] \right) \cdot G_{\text{a}}^{(6)}(\mathbf{X}) \\ & = \frac{1}{E(y_1, x_1)} [G_{1\text{a}}^{(4)}(\mathbf{x}, \mathbf{z}) - G_{1\text{a}}^{(4)}(y_1, x_2, x_3, \mathbf{z})] \cdot G_{\ominus}^{(2)}(\mathbf{y}) \end{aligned}$$

$$\begin{aligned}
& + \frac{1}{E(z_1, x_1)} [G_{\ominus}^{(2)}(\mathbf{x}) - G_{\ominus}^{(2)}(z_1, x_2, x_3)] \cdot G_{\square_1}^{(4)}(\mathbf{y}, \mathbf{z}) \\
& + \frac{1}{E(y_1, x_1)} [G_{|\ominus|\square_1|}^{(6)}(\mathbf{y}, \mathbf{x}, \mathbf{z}) - G_{|\ominus|\square_1|}^{(6)}(\mathbf{y}, y_1, x_2, x_3, \mathbf{z})] \\
& + \frac{1}{E(z_1, x_1)} [G_{|\ominus|\square_1|}^{(6)}(\mathbf{x}, \mathbf{y}, \mathbf{z}) - G_{|\ominus|\square_1|}^{(6)}(z_1, x_2, x_3, \mathbf{y}, \mathbf{z})] \\
& + \frac{1}{E(z_2, y_2)} [G_{\square_{13}}^{(6)}(\mathbf{x}, \mathbf{z}, \mathbf{y}) - G_{\square_{13}}^{(6)}(\mathbf{x}, \mathbf{z}, y_1, z_2, y_3)] \\
& + \frac{1}{E(x_2, y_2)} [G_{\square_{13}}^{(6)}(\mathbf{z}, \mathbf{y}, \mathbf{x}) - G_{\square_{13}}^{(6)}(\mathbf{z}, y_1, x_2, y_3, \mathbf{x})] \\
& + \frac{1}{E(z_3, y_3)} [G_{\square_{12}}^{(6)}(\mathbf{x}, \mathbf{z}, \mathbf{y}) - G_{\square_{12}}^{(6)}(\mathbf{x}, \mathbf{z}, y_1, y_2, z_3)] \\
& + \frac{1}{E(x_3, y_3)} [G_{\square_{12}}^{(6)}(\mathbf{z}, \mathbf{y}, \mathbf{x}) - G_{\square_{12}}^{(6)}(\mathbf{z}, y_1, y_2, x_3, \mathbf{x})] \\
& + \sum_{\hat{\pi} \in \mathbb{Z}_3} \pi^* \left[\frac{1}{3} \Delta_{x_1,1} G_{|\ominus|\square_1|}^{(8)} + \Delta_{x_1,1} G_{\square_3}^{(8)} + \Delta_{x_1,1} G_{\square_2}^{(8)} \right. \\
& + \frac{1}{4} \sum_{r=1}^4 \Delta_{x_1,r} G_{\square_1}^{(8)} + \sum_{r=1,2} \Delta_{x_1,r} G_{\square_3}^{(8)} + \frac{1}{3} \Delta_{y_2,1} G_{|\ominus|\square_1|}^{(8)} + \frac{1}{2} \sum_{h=2,3} \Delta_{y_2,h} G_{\square_{2(33)3}^{(8)}} \\
& + \frac{1}{4} \sum_{r=1}^4 \Delta_{y_2,r} G_{\square_1}^{(8)} + \Delta_{y_2,1} G_{\square_3}^{(8)} + \sum_{r=1,2} \Delta_{y_2,r} G_{\square_2}^{(8)} + \frac{1}{3} \Delta_{y_3,1} G_{|\ominus|\square_1|}^{(8)} \\
& \left. + \frac{1}{2} \sum_{h=2,3} \Delta_{y_3,h} G_{\square_{3(22)2}^{(8)}} + \frac{1}{4} \sum_{r=1}^4 \Delta_{y_3,r} G_{\square_1}^{(8)} + \Delta_{y_3,1} G_{\square_2}^{(8)} + \sum_{r=1,2} \Delta_{y_3,r} G_{\square_3}^{(8)} \right] (\mathbf{X}) \\
& - \sum_{b_1} \frac{1}{E(x_1, b_1)} [G_{\square_1}^{(6)}(\mathbf{X}) - G_{\square_1}^{(6)}(b_1, x_2, x_3; \mathbf{y}; \mathbf{z})] \\
& - \sum_{b_2} \frac{1}{E(y_2, b_2)} [G_{\square_1}^{(6)}(\mathbf{X}) - G_{\square_1}^{(6)}(\mathbf{x}; y_1, b_2, y_3; \mathbf{z})] \\
& - \sum_{b_3} \frac{1}{E(y_3, b_3)} [G_{\square_1}^{(6)}(\mathbf{X}) - G_{\square_1}^{(6)}(\mathbf{x}; y_1, y_2, b_3; \mathbf{z})].
\end{aligned} \tag{1.4.10}$$

1.4.4 The Schwinger-Dyson equation for $G_{\square_1}^{(6)}$

Concerning the correlation function $G_{\square_1}^{(6)}$, the terms with swapping black vertices are

$$G_{\square_1}^{(6)}, G_{\square_2}^{(6)}, G_{|\ominus|\square_1|}^{(6)}, G_{\ominus}^{(2)} \cdot G_{\square_3}^{(4)}, (132)^* G_{\square_{12}}^{(6)}, G_{\square_{13}}^{(6)}, (12)^* G_{\square_{13}}^{(6)}, \tag{1.4.11}$$

which need to be divided by differences of propagators. We now find the rest of the terms. Since $\text{Aut}_c(\square_{23})$ is trivial, the contribution of the \square_{23} -derivative on $\sum_a Y_{s_a}^{(a)}[J, \bar{J}]$ is given by the sum $\sum_a \mathfrak{f}_{\square_{23}}^{(a)}$ where, for each colour a :

$$\mathfrak{f}_{\square_{23}}^{(1)} = \Delta_{x_1,1} G_{|\ominus|\square_{23}|}^{(8)} + \sum_{h=2,3} \Delta_{x_1,h} G_{\square_{(2)13}}^{(8)} + (13)^*(\Delta_{x_1,3} G_{\square_{(3)21}}^{(8)}) + (13)^*(\Delta_{x_1,4} G_{\square_{(3)21}}^{(8)})$$

$$\begin{aligned}
& + \sum_{p=3,4} (\Delta_{x_1,p} G_{\frac{1}{2} \begin{smallmatrix} 1 \\ 2 \end{smallmatrix}}^{(8)} + (13)^* \Delta_{x_1,p} G_{\frac{1}{3} \begin{smallmatrix} 1 \\ 3 \end{smallmatrix}}^{(8)}) + (13)^* (\Delta_{x_1,1} G_{\frac{1}{1} \begin{smallmatrix} 1 \\ 2 \\ 2 \end{smallmatrix}}^{(8)}) + (13)^* (\Delta_{x_1,2} G_{\frac{1}{1} \begin{smallmatrix} 1 \\ 3 \\ 2 \end{smallmatrix}}^{(8)}) \\
& + \frac{1}{2} (\Delta_{x_1,1} G_{\frac{2}{2} \begin{smallmatrix} 1 \\ 1 \\ 1 \\ 2 \end{smallmatrix}}^{(8)} + (13)^* (\Delta_{x_1,1} G_{\frac{3}{3} \begin{smallmatrix} 1 \\ 1 \\ 1 \\ 3 \end{smallmatrix}}^{(8)}) + (13)^* (\Delta_{x_1,4} G_{\frac{3}{3} \begin{smallmatrix} 1 \\ 1 \\ 1 \\ 3 \end{smallmatrix}}^{(8)}) + \Delta_{x_1,4} G_{\frac{3}{3} \begin{smallmatrix} 1 \\ 1 \\ 1 \\ 3 \end{smallmatrix}}^{(8)}) \\
& + \sum_{r=1,2} (13)^* (\Delta_{x_1,r} G_{\frac{1}{3} \begin{smallmatrix} 1 \\ 3 \end{smallmatrix}}^{(8)}) + \frac{1}{4} ((23)^* \Delta_{x_1,1} G_{\frac{1}{2} \begin{smallmatrix} 1 \\ 2 \\ 3 \end{smallmatrix}}^{(8)} + \Delta_{x_1,2} G_{\frac{1}{2} \begin{smallmatrix} 1 \\ 2 \\ 3 \end{smallmatrix}}^{(8)} + (13)^* \Delta_{x_1,3} G_{\frac{1}{2} \begin{smallmatrix} 1 \\ 2 \\ 3 \end{smallmatrix}}^{(8)} \\
& \hspace{15em} + (123)^* \Delta_{x_1,4} G_{\frac{1}{2} \begin{smallmatrix} 1 \\ 2 \\ 3 \end{smallmatrix}}^{(8)}) \\
\mathfrak{f}_{\frac{2}{1} \begin{smallmatrix} 2 \\ 3 \end{smallmatrix}}^{(2)} & = \Delta_{y_2,1} G_{\frac{1}{1} \begin{smallmatrix} 2 \\ 3 \end{smallmatrix}}^{(8)} + \Delta_{y_2,1} G_{\frac{1}{1} \begin{smallmatrix} 1 \\ 3 \\ 2 \end{smallmatrix}}^{(8)} + \Delta_{y_2,4} G_{\frac{1}{1} \begin{smallmatrix} 1 \\ 3 \\ 2 \end{smallmatrix}}^{(8)} + \frac{1}{2} (\sum_{r=1,2} (13)^* (\Delta_{y_2,r} G_{\frac{3}{3} \begin{smallmatrix} 1 \\ 1 \\ 1 \\ 3 \end{smallmatrix}}^{(8)}) \\
& + \sum_{p=3,4} \Delta_{y_2,p} G_{\frac{3}{3} \begin{smallmatrix} 1 \\ 1 \\ 1 \\ 3 \end{smallmatrix}}^{(8)} + \Delta_{y_2,1} G_{\frac{2}{2} \begin{smallmatrix} 1 \\ 1 \\ 1 \\ 2 \end{smallmatrix}}^{(8)} + (13)^* \Delta_{y_2,4} G_{\frac{2}{2} \begin{smallmatrix} 1 \\ 1 \\ 1 \\ 2 \end{smallmatrix}}^{(8)}) \\
& + \sum_{p=3,4} \Delta_{y_2,p} G_{\frac{1}{2} \begin{smallmatrix} 1 \\ 2 \\ 3 \end{smallmatrix}}^{(8)} + \sum_{q=2,3,4} (13)^* \Delta_{y_2,q} G_{\frac{1}{2} \begin{smallmatrix} 1 \\ 2 \\ 3 \end{smallmatrix}}^{(8)} + (13)^* \Delta_{y_2,q} G_{\frac{2}{3} \begin{smallmatrix} 1 \\ 2 \\ 3 \end{smallmatrix}}^{(8)} \\
& + \Delta_{y_2,3} G_{\frac{1}{3} \begin{smallmatrix} 1 \\ 3 \end{smallmatrix}}^{(8)} + \frac{1}{4} (\Delta_{y_2,1} G_{\frac{1}{2} \begin{smallmatrix} 1 \\ 2 \\ 3 \end{smallmatrix}}^{(8)} + (123)^* \Delta_{y_2,2} G_{\frac{1}{2} \begin{smallmatrix} 1 \\ 2 \\ 3 \end{smallmatrix}}^{(8)} + (23)^* \Delta_{y_2,3} G_{\frac{1}{2} \begin{smallmatrix} 1 \\ 2 \\ 3 \end{smallmatrix}}^{(8)} + (13)^* \Delta_{y_2,4} G_{\frac{1}{2} \begin{smallmatrix} 1 \\ 2 \\ 3 \end{smallmatrix}}^{(8)}) \\
\mathfrak{f}_{\frac{3}{1} \begin{smallmatrix} 3 \\ 2 \end{smallmatrix}}^{(3)} & = (13)^* \Delta_{x_3,1} G_{\frac{1}{1} \begin{smallmatrix} 2 \\ 3 \end{smallmatrix}}^{(8)} + \Delta_{x_3,1} G_{\frac{1}{1} \begin{smallmatrix} 1 \\ 3 \\ 2 \end{smallmatrix}}^{(8)} + \Delta_{x_3,4} G_{\frac{1}{1} \begin{smallmatrix} 1 \\ 3 \\ 2 \end{smallmatrix}}^{(8)} + \frac{1}{2} (\sum_{r=1,2} (13)^* (\Delta_{x_3,r} G_{\frac{2}{2} \begin{smallmatrix} 1 \\ 1 \\ 1 \\ 2 \end{smallmatrix}}^{(8)}) \\
& + \sum_{p=3,4} \Delta_{x_3,p} G_{\frac{2}{2} \begin{smallmatrix} 1 \\ 1 \\ 1 \\ 2 \end{smallmatrix}}^{(8)} + \Delta_{x_3,1} G_{\frac{3}{3} \begin{smallmatrix} 1 \\ 1 \\ 1 \\ 3 \end{smallmatrix}}^{(8)} + (13)^* \Delta_{x_3,4} G_{\frac{3}{3} \begin{smallmatrix} 1 \\ 1 \\ 1 \\ 3 \end{smallmatrix}}^{(8)}) + \sum_{p=3,4} \Delta_{x_3,p} G_{\frac{1}{3} \begin{smallmatrix} 1 \\ 3 \end{smallmatrix}}^{(8)} \\
& + \sum_{q=2,3,4} (13)^* \Delta_{x_3,q} G_{\frac{1}{2} \begin{smallmatrix} 1 \\ 2 \\ 3 \end{smallmatrix}}^{(8)} + (13)^* \Delta_{x_3,q} G_{\frac{1}{2} \begin{smallmatrix} 1 \\ 2 \\ 3 \end{smallmatrix}}^{(8)} + \Delta_{x_3,3} G_{\frac{1}{3} \begin{smallmatrix} 1 \\ 3 \end{smallmatrix}}^{(8)} \\
& + \frac{1}{4} (\Delta_{x_3,1} G_{\frac{1}{2} \begin{smallmatrix} 1 \\ 2 \\ 3 \end{smallmatrix}}^{(8)} + (123)^* \Delta_{x_3,2} G_{\frac{1}{2} \begin{smallmatrix} 1 \\ 2 \\ 3 \end{smallmatrix}}^{(8)} + (23)^* \Delta_{x_3,3} G_{\frac{1}{2} \begin{smallmatrix} 1 \\ 2 \\ 3 \end{smallmatrix}}^{(8)} + (13)^* \Delta_{x_3,4} G_{\frac{1}{2} \begin{smallmatrix} 1 \\ 2 \\ 3 \end{smallmatrix}}^{(8)})
\end{aligned}$$

Here $\mathbf{s} = (x_1, y_2, x_3)$. Therefore, the explicit equation is

$$- \left(\frac{E_{x_1 y_2 x_3}}{2\lambda} + \sum_{m,n} [G_{\ominus}^{(2)}(x_1, m, n) + G_{\ominus}^{(2)}(m, y_2, n) + G_{\ominus}^{(2)}(m, n, x_3)] \right) \cdot G_{\frac{1}{2} \begin{smallmatrix} 1 \\ 3 \end{smallmatrix}}^{(6)}(\mathbf{X}) \tag{1.4.12}$$

$$\begin{aligned}
& = \frac{1}{E(y_1, x_1)} [G_{\frac{1}{2} \begin{smallmatrix} 1 \\ 3 \end{smallmatrix}}^{(6)}(\mathbf{x}, \mathbf{y}, \mathbf{z}) - G_{\frac{1}{2} \begin{smallmatrix} 1 \\ 3 \end{smallmatrix}}^{(6)}(y_1, x_2, x_3, \mathbf{y}, \mathbf{z})] \\
& + \frac{1}{E(z_1, x_1)} [G_{\frac{1}{2} \begin{smallmatrix} 1 \\ 3 \end{smallmatrix}}^{(6)}(\mathbf{x}, \mathbf{y}, \mathbf{z}) - G_{\frac{1}{2} \begin{smallmatrix} 1 \\ 3 \end{smallmatrix}}^{(6)}(z_1, x_2, x_3, \mathbf{y}, \mathbf{z})] \\
& + \frac{1}{E(x_2, y_2)} [G_{\frac{1}{1} \begin{smallmatrix} 1 \\ 3 \end{smallmatrix}}^{(6)}(\mathbf{x}, \mathbf{y}, \mathbf{z}) - G_{\frac{1}{1} \begin{smallmatrix} 1 \\ 3 \end{smallmatrix}}^{(6)}(\mathbf{x}, y_1, x_2, y_3, \mathbf{z})] \\
& + \frac{1}{E(z_2, y_2)} [G_{\frac{1}{1} \begin{smallmatrix} 1 \\ 3 \end{smallmatrix}}^{(6)}(\mathbf{y}, \mathbf{z}, \mathbf{x}) - G_{\frac{1}{1} \begin{smallmatrix} 1 \\ 3 \end{smallmatrix}}^{(6)}(y_1, z_2, y_3, \mathbf{z}, \mathbf{x})] \\
& + \frac{1}{E(z_3, x_3)} [G_{\frac{1}{1} \begin{smallmatrix} 1 \\ 3 \end{smallmatrix}}^{(6)}(\mathbf{x}, \mathbf{y}, \mathbf{z}) - G_{\frac{1}{1} \begin{smallmatrix} 1 \\ 3 \end{smallmatrix}}^{(6)}(x_1, x_2, z_3, \mathbf{y}, \mathbf{z})] \\
& + \frac{1}{E(y_3, x_3)} [G_{\frac{1}{1} \begin{smallmatrix} 1 \\ 3 \end{smallmatrix}}^{(6)}(\mathbf{y}, \mathbf{x}, \mathbf{z}) - G_{\frac{1}{1} \begin{smallmatrix} 1 \\ 3 \end{smallmatrix}}^{(6)}(\mathbf{y}, x_1, x_2, y_3, \mathbf{z})]
\end{aligned}$$

$$\begin{aligned}
& + \frac{1}{E(x_2, y_2)} \left(G_{\overline{3} \overline{2} \overline{3}}^{(4)}(\mathbf{y}, \mathbf{z}) - G_{\overline{3} \overline{2} \overline{3}}^{(4)}(y_1, x_2, y_3, \mathbf{z}) \right) \cdot G_{\ominus}^{(2)}(\mathbf{x}) \\
& + \left\{ \Delta_{x_1,1} G_{\overline{1} \overline{2} \overline{3}}^{(8)} + \sum_{h=2,3} \Delta_{x_1,h} G_{\overline{2} \overline{1} \overline{3}}^{(8)} + (13)^* (\Delta_{x_1,3} G_{\overline{3} \overline{2} \overline{1}}^{(8)}) + (13)^* (\Delta_{x_1,4} G_{\overline{3} \overline{2} \overline{1}}^{(8)}) \right. \\
& + \sum_{p=3,4} (\Delta_{x_1,p} G_{\overline{2} \overline{1} \overline{3}}^{(8)} + (13)^* \Delta_{x_1,p} G_{\overline{1} \overline{2} \overline{3}}^{(8)}) + (13)^* (\Delta_{x_1,1} G_{\overline{1} \overline{2} \overline{3}}^{(8)}) + (13)^* (\Delta_{x_1,2} G_{\overline{1} \overline{2} \overline{3}}^{(8)}) \\
& + \frac{1}{2} (\Delta_{x_1,1} G_{\overline{2} \overline{1} \overline{1} \overline{2} \overline{3}}^{(8)} + (13)^* (\Delta_{x_1,1} G_{\overline{3} \overline{1} \overline{1} \overline{3}}^{(8)}) + (13)^* (\Delta_{x_1,4} G_{\overline{3} \overline{1} \overline{1} \overline{3}}^{(8)}) + \Delta_{x_1,4} G_{\overline{3} \overline{1} \overline{1} \overline{3}}^{(8)}) \\
& + \sum_{r=1,2} (13)^* (\Delta_{x_1,r} G_{\overline{1} \overline{3}}^{(8)}) + \Delta_{y_2,1} G_{\overline{1} \overline{2} \overline{3}}^{(8)} + \Delta_{y_2,1} G_{\overline{1} \overline{1} \overline{2} \overline{3}}^{(8)} + \Delta_{y_2,4} G_{\overline{1} \overline{1} \overline{2} \overline{3}}^{(8)} \\
& + \frac{1}{4} ((23)^* \Delta_{x_1,1} G_{\overline{1} \overline{2} \overline{3}}^{(8)} + \Delta_{x_1,2} G_{\overline{1} \overline{2} \overline{3}}^{(8)} + (13)^* \Delta_{x_1,3} G_{\overline{1} \overline{2} \overline{3}}^{(8)} + (123)^* \Delta_{x_1,4} G_{\overline{1} \overline{2} \overline{3}}^{(8)}) \\
& + \frac{1}{2} (\sum_{r=1,2} (13)^* (\Delta_{y_2,r} G_{\overline{3} \overline{1} \overline{1} \overline{3}}^{(8)}) + \sum_{p=3,4} \Delta_{y_2,p} G_{\overline{3} \overline{1} \overline{1} \overline{3}}^{(8)} + \Delta_{y_2,1} G_{\overline{2} \overline{1} \overline{1} \overline{2} \overline{3}}^{(8)} \\
& + (13)^* \Delta_{y_2,4} G_{\overline{2} \overline{1} \overline{1} \overline{2} \overline{3}}^{(8)}) + \sum_{p=3,4} \Delta_{y_2,p} G_{\overline{2} \overline{1} \overline{3}}^{(8)} + \sum_{q=2,3,4} (13)^* \Delta_{y_2,q} G_{\overline{1} \overline{1} \overline{3}}^{(8)} + (13)^* \Delta_{y_2,q} G_{\overline{2} \overline{1} \overline{3}}^{(8)} \\
& + \Delta_{y_2,3} G_{\overline{1} \overline{3}}^{(8)} + \frac{1}{4} (\Delta_{y_2,1} G_{\overline{2} \overline{1}}^{(8)} + (123)^* \Delta_{y_2,2} G_{\overline{2} \overline{1}}^{(8)} + (23)^* \Delta_{y_2,3} G_{\overline{2} \overline{1}}^{(8)} + (13)^* \Delta_{y_2,4} G_{\overline{2} \overline{1}}^{(8)}) \\
& + (13)^* \left[(13)^* \Delta_{x_3,1} G_{\overline{1} \overline{2} \overline{3}}^{(8)} + \Delta_{x_3,1} G_{\overline{1} \overline{1} \overline{2} \overline{3}}^{(8)} + \Delta_{x_3,4} G_{\overline{1} \overline{1} \overline{2} \overline{3}}^{(8)} + \frac{1}{2} (\sum_{r=1,2} (13)^* (\Delta_{x_3,r} G_{\overline{2} \overline{1} \overline{1} \overline{2} \overline{3}}^{(8)})) \right. \\
& + \sum_{p=3,4} \Delta_{x_3,p} G_{\overline{2} \overline{1} \overline{1} \overline{2} \overline{3}}^{(8)} + \Delta_{x_3,1} G_{\overline{3} \overline{1} \overline{1} \overline{3}}^{(8)} + (13)^* \Delta_{x_3,4} G_{\overline{3} \overline{1} \overline{1} \overline{3}}^{(8)} \\
& + \sum_{p=3,4} \Delta_{x_3,p} G_{\overline{1} \overline{2} \overline{3}}^{(8)} + \sum_{q=2,3,4} (13)^* \Delta_{x_3,q} G_{\overline{1} \overline{2} \overline{3}}^{(8)} + (13)^* \Delta_{x_3,q} G_{\overline{1} \overline{1} \overline{2} \overline{3}}^{(8)} + \Delta_{x_3,3} G_{\overline{1} \overline{3}}^{(8)} \\
& \left. + \frac{1}{4} (\Delta_{x_3,1} G_{\overline{1} \overline{2} \overline{3}}^{(8)} + (123)^* \Delta_{x_3,2} G_{\overline{1} \overline{2} \overline{3}}^{(8)} + (23)^* \Delta_{x_3,3} G_{\overline{1} \overline{2} \overline{3}}^{(8)} + (13)^* \Delta_{x_3,4} G_{\overline{1} \overline{2} \overline{3}}^{(8)}) \right\} (\mathbf{X}) \\
& - \sum_{b_1} \frac{1}{E(x_1, b_1)} [G_{\overline{2} \overline{3}}^{(6)}(\mathbf{X}) - G_{\overline{2} \overline{3}}^{(6)}(b_1, x_2, x_3; \mathbf{y}; \mathbf{z})] \\
& - \sum_{b_2} \frac{1}{E(y_2, b_2)} [G_{\overline{2} \overline{3}}^{(6)}(\mathbf{X}) - G_{\overline{2} \overline{3}}^{(6)}(\mathbf{x}; y_1, b_2, y_3; \mathbf{z})] \\
& - \sum_{b_3} \frac{1}{E(x_3, b_3)} [G_{\overline{2} \overline{3}}^{(6)}(\mathbf{X}) - G_{\overline{2} \overline{3}}^{(6)}(x_1, x_2, b_3; \mathbf{y}; \mathbf{z})].
\end{aligned}$$

1.5 A simple quartic model

In order to obtain a simpler set of SDE, we consider a model which has less correlation functions. Its probability theory is expected to ponder only geometries with spherical boundaries. Nevertheless, it is interesting because its equations are particularly simple. We consider the rank-3 tensor field theory with action $S[\varphi, \bar{\varphi}] = S_0[\varphi, \bar{\varphi}] + \mathcal{S}_{\text{int}}[\varphi, \bar{\varphi}]$ where

$$S_0[\varphi, \bar{\varphi}] = \text{Tr}_2(\bar{\varphi}, E\varphi) = \sum_{\mathbf{x} \in \mathbb{Z}^3} \bar{\varphi}_{\mathbf{x}}(m^2 + |\mathbf{x}|^2)\varphi_{\mathbf{x}} \quad \text{and} \quad \mathcal{S}_{\text{int}}[\varphi, \bar{\varphi}] = \lambda \cdot 1_{\square_1}. \quad (1.5.1)$$

Here $|\mathbf{x}|^2 = x_1^2 + x_2^2 + x_3^2$, $\mathbf{x} = (x_1, x_2, x_3) \in \mathbb{Z}^3$. In particular all the bordisms that this theory triangulates are null-bordisms and bordisms between spheres. Notice that the boundary graphs are all graphs having the following property: two edges are connected by a 2-coloured edge, if and only if they are connected by a 3-coloured edge. We denote by Θ ($\Theta \subset \text{Grph}_3$) the set of *connected* graphs with this property. Thus

$$\text{Feyn}_3(1_{\square_1}) = \{\mathcal{B} \in \text{Grph}_3^{\text{II}} : \mathcal{B} \text{ has connected components in } \Theta\},$$

being

$$\Theta = \left\{ \bigcirc, 1_{\square_1}, \begin{array}{c} \text{---} \\ | \\ \text{---} \end{array}, \begin{array}{c} \text{---} \\ | \\ \text{---} \\ | \\ \text{---} \end{array}, \begin{array}{c} \text{---} \\ | \\ \text{---} \\ | \\ \text{---} \\ | \\ \text{---} \end{array}, \dots \right\}.$$

Let \mathcal{X}_{2k} be the graph in Θ with $2k$ vertices. That is to say, the set of (connected) correlation functions with connected boundary is precisely indexed by Θ and we set $G^{(2k)} := G_{\mathcal{X}_{2k}}^{(2k)}$, i.e.

$$G^{(2)} = G_{\bigcirc}^{(2)}, \quad G^{(4)} = G_{1_{\square_1}}^{(4)}, \quad G^{(6)} = G_{\begin{array}{c} \text{---} \\ | \\ \text{---} \end{array}}^{(6)}, \quad G^{(8)} = G_{\begin{array}{c} \text{---} \\ | \\ \text{---} \\ | \\ \text{---} \end{array}}^{(8)}, \quad G^{(10)} = G_{\begin{array}{c} \text{---} \\ | \\ \text{---} \\ | \\ \text{---} \\ | \\ \text{---} \end{array}}^{(10)}.$$

Any $(2k)$ -point function with disconnected components can be labeled by integer partitions (n_1, \dots, n_ℓ) such that

$$\mathcal{B} = \mathcal{X}_2^{n_1} \sqcup \mathcal{X}_4^{n_1} \sqcup \dots \sqcup \mathcal{X}_{2\ell}^{n_\ell}, \quad (1.5.2)$$

being ℓ the maximum number of vertices that a connected component of \mathcal{B} has. These numbers n_i satisfy

$$k = \sum_{i=1}^{\ell} i \cdot n_i \quad \text{and} \quad B = \sum_{i=1}^{\ell} n_i, \quad (1.5.3)$$

where B is the number of connected components of \mathcal{B} . Then, the free energy boils down to the expression

$$W[J, \bar{J}] = \sum_{l=1}^{\infty} \sum'_{\substack{\mathcal{B} \in \partial(\text{Feyn}_3(1_{\square_1})) \\ k(\mathcal{B})=l}} G_{\mathcal{B}}^{(2l)} \star \mathbb{J}(\mathcal{B}), \quad (1.5.4)$$

where the prime in the sum means that it is performed with the restrictions (1.5.3). More concretely, writing any graph \mathcal{B} as in eq. (1.5.2), one can rephrase the sum rather over ℓ , the largest number of black (or white) vertices found in a connected component of \mathcal{B} . This modification readily yields

$$W[J, \bar{J}] = \sum_{\ell=1}^{\infty} \left(\prod_{j=1}^{\ell} \frac{1}{j^{n_j} \cdot n_j!} \right) G_{|\mathcal{X}_2^{\sqcup n_1}| \dots |\mathcal{X}_{2i}^{\sqcup n_i}| \dots |\mathcal{X}_{2\ell}^{\sqcup n_\ell}|}^{(2\ell)} \star \mathbb{J}(\mathcal{X}_2^{n_1} \sqcup \mathcal{X}_4^{n_1} \sqcup \dots \sqcup \mathcal{X}_{2\ell}^{n_\ell}).$$

To obtain the last line one observes that $\text{Aut}_c(\mathcal{X}_{2k}) = \langle \text{rotation by } 2\pi/k \rangle = \mathbb{Z}_k$, and $|\text{Aut}_c(\mathcal{B})| = n_1! \dots n_\ell! \cdot |\text{Aut}_c(\mathcal{X}_{2_2})|^{n_1} \dots |\text{Aut}_c(\mathcal{X}_{2_\ell})|^{n_\ell}$. It should be noticed that this form has already been found in the free energy expansion of (real) matrix models, here with twice the number of sources of each monomial with respect to that [6, Sec. 2.3]. It is also noteworthy that the Grosse-Wulkenhar model ($\varphi_4^{\star 4}$ self-dual theory) [6] was shown to be solvable by using matrix techniques. Here we have shown that the $1\boxed{1}$ -model obeys the very same expansion of the free energy and that the number of $(2k)$ -point functions of both theories is the same for any k .

The growth, as function of the number of vertices, of the number of correlation functions of this model is milder than that of the models with full boundary sector. We further simplify the notation and set $\mathfrak{f}_{2k,s_1} = \mathfrak{f}_{\mathcal{X}_{2k},s_1}^{(1)}$. With this notation, the Schwinger-Dyson equations in Section 1.3 can be derived for the connected boundary graphs of the $1\boxed{1}$ -model.

Proposition 1.5.1 (Schwinger-Dyson equations for the $1\boxed{1}$ -model). *Let \mathcal{B} be a connected boundary graph of the quartic model with $2k$ vertices ($k \geq 1$), $\mathcal{B} \in \text{Feyn}_3(1\boxed{1})$. Let $\mathbf{s} = \mathbf{y}^1$, where $(\mathcal{X}_{2k})_*(\mathbf{X}) = (\mathbf{y}^1, \dots, \mathbf{y}^k)$ for any $\mathbf{X} \in \mathcal{F}_{3,k}$. The $(2k)$ -point Schwinger-Dyson equation corresponding to \mathcal{B} is*

$$\begin{aligned} & \left(1 + \frac{2\lambda}{m^2 + |\mathbf{s}|^2} \sum_{q,p \in \mathbb{Z}} G^{(2)}(s_1, q, p) \right) \cdot G^{(2k)}(\mathbf{X}) \\ &= \frac{2\lambda}{m^2 + |\mathbf{s}|^2} \left\{ \frac{\delta_{1,k}}{2\lambda} - \sum_{\hat{\sigma} \in \mathbb{Z}_k} \sigma^* \mathfrak{f}_{2k,s_1}(\mathbf{X}) \right. \\ & \quad - \sum_{\rho > 1} \frac{Z_0^{-1}}{[(y_1^\rho)^2 - s_1^2]} \cdot \left[\frac{\partial Z[J, J]}{\partial \varsigma_1(\mathcal{X}_{2k}; 1, \rho)}(\mathbf{X}) - \frac{\partial Z[J, J]}{\partial \varsigma_1(\mathcal{X}_{2k}; 1, \rho)}(\mathbf{X}|_{s_1 \rightarrow y_1^\rho}) \right] \\ & \quad \left. + \sum_{q \in \mathbb{Z}} \frac{1}{s_1^2 - q^2} [G^{(2k)}(\mathbf{X}) - G^{(2k)}(\mathbf{X}|_{s_1 \rightarrow q})] \right\}. \end{aligned} \tag{1.5.5}$$

Proof. For $k > 1$, it is immediate by setting $D = 3$ and by cutting the sums over the number of colours to only $a = 1$, since one does no longer have the vertices $2\boxed{2}$ and $3\boxed{3}$ in the action. After using $\text{Aut}_c(\mathcal{X}_{2k}) = \mathbb{Z}_k$, and after inserting the form of the difference of propagators, as given by (1.5.1), the result follows. If $k = 1$, one additionally obtains the pure propagator term (the $\delta_{1,k}$ -term) that would be otherwise annihilated by fourth or higher derivatives. For $k = 1$, the sum over ρ is empty (thus equal to zero). \square

One can still work out the functions \mathfrak{f}_{2k} and give the correlation functions implied in the $\varsigma_1(\mathcal{X}_{2k}; 1, \rho)$ -derivatives in eq. (1.5.5). Notice that the expansion of the term $Y_{s_1}^{(1)}[J, \bar{J}]$ is

$$Y_{s_1}^{(1)}[J, \bar{J}] = \sum_{k=0}^{\infty} \mathfrak{f}_{2k,s_1} \star \mathbb{J}(\mathcal{X}_{2k}) + \sum_{\mathcal{C} \text{ disconnected}} \mathfrak{f}_{\mathcal{C},s_1}^{(1)} \star \mathbb{J}(\mathcal{C}) \tag{1.5.6}$$

In order to determine \mathfrak{f}_{2k,s_1} we find the graphs \mathcal{B} such that $\mathcal{B} \ominus e_1^r = \mathcal{X}_{2k}$ for certain (say, the r -th) vertex of \mathcal{B} . The restrictions (1.5.3) with $B \geq 2$ and the connectedness of \mathcal{B} after edge-removal imply that either

$$n_1 = n_k = 1 \quad \text{and} \quad n_i = 0, \quad \text{if } i \neq 1, k,$$

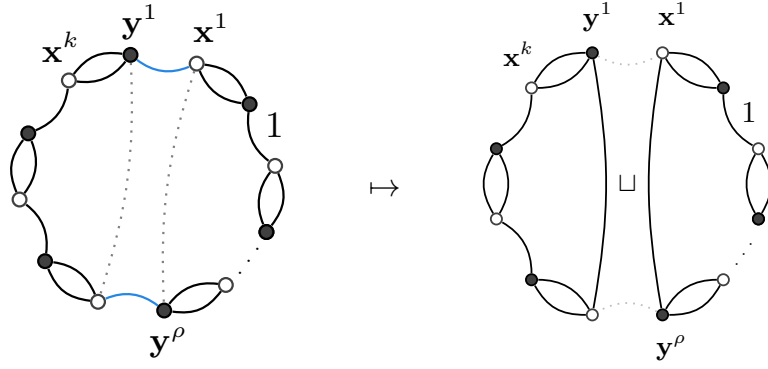


Figure 1.5: Shows the splitting of \mathcal{X}_{2k} into the two components of $\varsigma_1(\mathcal{X}_{2k}; 1, \rho)$, $\rho > 0$

or

$$n_{k+1} = 1 \quad \text{and} \quad n_i = 0 \quad \text{if } i \neq k+1.$$

That is to say, any such \mathcal{B} has $2(k+1)$ vertices and, concretely, they might only be either $\ominus \sqcup \mathcal{X}_{2k}$ or \mathcal{X}_{2k+2} , when $k \geq 2$. Adding the obvious case when $k = 1$, one has:

$$\mathfrak{f}_{2, s_1} = \frac{1}{2} \sum_{r=1}^2 (\Delta_{s_1, r} G_{|\ominus| \ominus|}^{(4)} + \Delta_{s_1, r} G^{(4)}) \quad (1.5.7a)$$

$$\mathfrak{f}_{2k, s_1} = \frac{1}{k} \Delta_{s_1, 1} G_{|\ominus| \mathcal{X}_{2k}|}^{(2k+2)} + \frac{1}{k+1} \sum_{r=1}^k \Delta_{s_1, r} G^{(2k+2)}, \quad \text{for } k \geq 2. \quad (1.5.7b)$$

Notice that $\varsigma_1(\mathcal{X}_{2k}; 1, \rho) = \mathcal{X}_{2\rho-2} \sqcup \mathcal{X}_{2k-2\rho+2}$, whence (see Fig. 1.5)

$$\begin{aligned} \frac{1}{Z_0} \frac{\partial Z[J, J]}{\partial \varsigma_1(\mathcal{X}_{2k}; 1, \rho)(\mathbf{X})} &= G^{(2\rho-2)}(\mathbf{x}^1, \dots, \mathbf{x}^{\rho-1}) \cdot G^{(2k-2\rho+2)}(\mathbf{x}^\rho, \dots, \mathbf{x}^k) \\ &\quad + G_{|\mathcal{X}_{2(\rho-1)}| \mathcal{X}_{2k-2(\rho-1)}|}^{(2k)}(\mathbf{X}). \end{aligned} \quad (1.5.8)$$

Using the last four equations one can prove

Corollary 1.5.2. *The exact 2-point equation for the $1\overline{\square}1$ -model is given, for any $\mathbf{x} = (x_1, x_2, x_3) \in \mathbb{Z}^3$, by*

$$\begin{aligned} &\left(1 + \frac{2\lambda}{m^2 + |\mathbf{x}|^2} \sum_{q, p \in \mathbb{Z}} G^{(2)}(x_1, q, p) \right) \cdot G^{(2)}(\mathbf{x}) \\ &= \frac{1}{m^2 + |\mathbf{x}|^2} + \frac{(-2\lambda)}{m^2 + |\mathbf{x}|^2} \left\{ \sum_{p, q \in \mathbb{Z}} G_{|\ominus| \ominus|}^{(4)}(x_1, q, p, \mathbf{x}) + G^{(4)}(\mathbf{x}, \mathbf{x}) \right. \\ &\quad \left. - \sum_{q \in \mathbb{Z}} \frac{1}{x_1^2 - q^2} [G^{(2)}(x_1, x_2, x_3) - G^{(2)}(q, x_2, x_3)] \right\}. \end{aligned} \quad (1.5.9)$$

For $k \geq 2$, the multi-point equation for $G^{(2k)}$, the single correlation function of connected boundary graph, is given by

$$\begin{aligned}
& \left(1 + \frac{2\lambda}{m^2 + |\mathbf{s}|^2} \sum_{q,p \in \mathbb{Z}} G^{(2)}(x_1^1, q, p) \right) \cdot G^{(2k)}(\mathbf{x}^1, \dots, \mathbf{x}^k) \\
&= \frac{(-2\lambda)}{m^2 + |\mathbf{s}|^2} \left\{ \sum_{l=1}^k \left[\frac{1}{k} \sum_{p,q \in \mathbb{Z}} G_{|\ominus|\mathcal{X}_{2k}|}^{(2k+2)}(x_1^1, q, p; \mathbf{x}^{1+l}, \dots, \mathbf{x}^{k+l}) \right. \right. \\
&\quad \left. \left. + \frac{1}{k+1} \sum_{r=1}^k G^{(2k+2)}(\mathbf{x}^{1+l}, \mathbf{x}^{2+l}, \dots, \mathbf{x}^{r+l-1}, x_1^1, x_2^{r+l-1}, x_2^{r+l-1}, \mathbf{x}^{r+l}, \dots, \mathbf{x}^{k+l}) \right] \right. \\
&\quad \left. + \sum_{\rho=2}^k \left[\frac{G^{(2\rho-2)}(\mathbf{x}^1, \dots, \mathbf{x}^{\rho-1}) - G^{(2\rho-2)}(x_1^\rho, x_2^1, x_3^1, \dots, \mathbf{x}^{\rho-1})}{[(x_1^\rho)^2 - (x_1^1)^2]} \cdot G^{(2k-2\rho+2)}(\mathbf{x}^\rho, \dots, \mathbf{x}^k) \right. \right. \\
&\quad \left. \left. + \frac{G_{|\mathcal{X}_{2(\rho-1)}|\mathcal{X}_{2k-2(\rho-1)}|}^{(2k)}(\mathbf{X}) - G_{|\mathcal{X}_{2(\rho-1)}|\mathcal{X}_{2k-2(\rho-1)}|}^{(2k)}(x_1^\rho, x_2^1, x_3^1, \mathbf{x}^2, \dots, \mathbf{x}^k)}{[(x_1^\rho)^2 - (x_1^1)^2]} \right] \right. \\
&\quad \left. - \sum_{q \in \mathbb{Z}} \frac{G^{(2k)}(x_1^1, x_2^1, x_3^1, \mathbf{x}^2, \dots, \mathbf{x}^k) - G^{(2k)}(q, x_2^1, x_3^1, \mathbf{x}^2, \dots, \mathbf{x}^k)}{(x_1^1)^2 - q^2} \right\}. \tag{1.5.10}
\end{aligned}$$

for $\mathbf{X} = (\mathbf{x}^1, \dots, \mathbf{x}^k) \in \mathcal{F}_{3,k}$, $\mathbf{s} := (x_1^1, x_2^r, x_3^r)$, and $\mathbf{x}^i = (x_1^i, x_2^i, x_3^i)$ for all $i \in \{1, \dots, k\}$. Moreover $\mathbf{x}^j = \mathbf{x}^i \pmod k$, for and $j \in \mathbb{N}$ with $i \in \{1, \dots, k\}$.

It is pertinent to stress that $\mathbf{s} = \mathbf{y}^1$ is a ‘chosen’ black vertex, and this equation holds for any other choice $\mathbf{s} = \mathbf{y}^i$, $i \neq 1$, $(\mathcal{X}_{2k})_*(\mathbf{X}) = (\mathbf{y}^1, \dots, \mathbf{y}^k)$, after the pertinent changes (e.g. the sum over ρ excludes not 1 but i).

Proof. One uses the equations (1.5.7) and (1.5.8), the triviality of the automorphisms group $\text{Aut}_c(\ominus)$, and the invariance of $G_{|\ominus|\ominus|}^{(4)}$ and $G^{(4)}$:

$$G_{|\ominus|\ominus|}^{(4)}(\mathbf{z}, \mathbf{y}) = G_{|\ominus|\ominus|}^{(4)}(\mathbf{y}, \mathbf{z}) \quad \text{and} \quad G^{(4)}(\mathbf{z}, \mathbf{y}) = G^{(4)}(\mathbf{y}, \mathbf{z}).$$

This is enough to obtain the 2-point equation. For $k \geq 2$, on top of using (1.5.7) and (1.5.8) one explicitly writes the action of $\sigma \in \mathbb{Z}_k$. This is rotation by $2\pi l/k$, $1 \leq l \leq k$, so

$$\sigma^* f(\mathbf{X}) = f(\mathbf{x}^{\sigma^{-1}(1)}, \dots, \mathbf{x}^{\sigma^{-1}(k)}) = f(\mathbf{x}^{1+l}, \dots, \mathbf{x}^{k+l})$$

where $\mathbf{x}^j = \mathbf{x}^i \pmod k$, for $i \in \{1, \dots, k\}$ and $j \in \mathbb{N}$ and f any (appropriate) function. \square

Remark 1.5.3. An analysis on the divergence degree as function of Gurău’s degree, and the boundary components was done in [68, 16] for group field theories. It turns out that graphs with a disconnected boundary are suppressed and therefore any graph contributing to $G_{|\ominus|\ominus|}^{(4)}$ is expected to be suppressed at least by N^{-1} , with respect to those summed in $G^{(4)}$. Nevertheless these correlation functions with disconnected boundary can back react as do their analogous in matrix models in the topological recursion [5]. Also, by results of matrix theory [6], we could expect that the term $G^{(4)}(\mathbf{x}, \mathbf{x})$ would be analogously

suppressed. Hence, conjecturally, for the $1\overline{\square}_1$ -model, the leading order $G_{\text{mel}}^{(2)}$ of the two-point function (1.5.9) would satisfy the closed equation

$$\begin{aligned} & \left(m^2 + |\mathbf{x}|^2 + 2\lambda \sum_{q,p \in \mathbb{Z}} G_{\text{mel}}^{(2)}(x_1, q, p) \right) \cdot G_{\text{mel}}^{(2)}(\mathbf{x}) \\ &= 1 + 2\lambda \sum_{q \in \mathbb{Z}} \frac{1}{x_1^2 - q^2} [G_{\text{mel}}^{(2)}(x_1, x_2, x_3) - G_{\text{mel}}^{(2)}(q, x_2, x_3)]. \end{aligned} \quad (1.5.11)$$

and by the same token, one could truncate the equation for the $2k$ -point function (1.5.10) to the following one, where the equally suppressed terms \mathbf{f}_{2k,s_1} also are neglected:

$$\begin{aligned} & \left(1 + \frac{2\lambda}{m^2 + |\mathbf{s}|^2} \sum_{q,p \in \mathbb{Z}} G_{\text{mel}}^{(2)}(x_1, q, p) \right) \cdot G_{\text{mel}}^{(2k)}(\mathbf{x}^1, \dots, \mathbf{x}^k) \\ &= \frac{(-2\lambda)}{m^2 + |\mathbf{s}|^2} \left[\sum_{\rho=2}^k \frac{G_{\text{mel}}^{(2\rho-2)}(\mathbf{x}^1, \dots, \mathbf{x}^{\rho-1}) - G_{\text{mel}}^{(2\rho-2)}(x_1^\rho, x_2^1, x_3^1, \mathbf{x}^2, \dots, \mathbf{x}^{\rho-1})}{[(x_1^\rho)^2 - (x_1^1)^2]} \cdot G_{\text{mel}}^{(2k-2\rho+2)}(\mathbf{x}^\rho, \dots, \mathbf{x}^k) \right. \\ & \quad \left. - \sum_{q \in \mathbb{Z}} \frac{G_{\text{mel}}^{(2k)}(x_1, x_2^1, x_3^1, \mathbf{x}^2, \dots, \mathbf{x}^k) - G_{\text{mel}}^{(2k)}(q, x_2^1, x_3^1, \mathbf{x}^2, \dots, \mathbf{x}^k)}{(x_1^1)^2 - q^2} \right]. \end{aligned} \quad (1.5.12)$$

These relations corresponds to the planar limit in matrix models [6]. As we will see in Chapter 2 the term last term on the RHS of the two previous equation will also be suppressed. Nevertheless already at this point, it is very encouraging to see that after determining $G_{\text{mel}}^{(2)}$, the ‘melonc 2k-point SDE’ (1.5.12) for any $k > 1$ could be entirely expressed in terms of already known functions $G_{\text{mel}}^{(2)}, G_{\text{mel}}^{(4)}, \dots, G_{\text{mel}}^{(2k-2)}$ and constitutes an equation only for $G_{\text{mel}}^{(2k)}$, which would decouple the tower. We will further explore this point in Chapter 2.

1.6 Conclusions and perspectives

We studied the correlation functions of complex tensor field theories and, mainly, presented a collection of generating functionals that allowed us to derive the exact Schwinger-Dyson equations for complex TFTs of rank 3 (and in Appendix B, rank 4 and 5 theories). The next step is to define a large N limit in the hope that the tower of equation decouples and we obtain a closed equation for the 2-point function similarly to what has been done in [6] for matrix models. That result would provide insight on the solvability of the $1\overline{\square}_1$ -model. Both problems are addressed in the Chapter 2.

Another natural extension of this work is to study if TFTs satisfy topological recursion. It is unclear that such a recursion can be understood directly from the study of the SDE. However for regular tensor models with quartic melonic interactions, topological recursion was studied in [71]. Using a Hubbard-Stratonovich transformation to rewrite the tensor model as a multi-matrix model with multi-trace interactions, the authors were able to write the loop equations for the matrix model. In the particular case of tensor model with a rank of the form $d = 4\delta + 2$, they showed that the model satisfies blobbed topological recursion [72, 73]. Moreover, they proposed a method to recover tensor model observables from the matrix model ones, computed in the recursion.

Hence in order to study the topological recursion for TFT, following the lines of [71] seems to be a better approach. Nevertheless one needs to be careful while taking into account the effect of the discrete Laplacian particular to TFT after the Hubbard-Stratonovich transformation. Furthermore, the study at rank 3 is already not complete for regular tensor models, then a realistic first step should be to determine the spectral curve of the multi-matrix model associated to the TFT, as well as the loop equations. At this stage, it would be insightful to compare the form of the loop equations in the matrix model to the SDE of the TFT, using the map between the two set of observables.

It would also be interesting to extend the graph calculus developed in [62] (further elaborated in this chapter and [74]) to the recently introduced 2PI formalism of tensor models [48]. In particular, the tensor-models-compatible connected sum defined in [75] imply that the 2PI functional of rank-3 models is the generating functional of prime 3-manifolds.

Chapter 2

Large N limit and solution of a melonic quartic model

This chapter is an edited version of [76] written in collaboration with C.I. Pérez-Sánchez, A. Tanasa and R. Wulkenhaar, and of [77].

2.1 Introduction

In this chapter, we study in detail the large N limit of the SDE obtained in the previous chapter. We thus find appropriate scalings in powers of N for the various terms present in the action of a rank-3 model. Moreover, we analyse in detail a case where the boundary graph is disconnected.

Let us mention here that in [24], scaling dimensions for interactions in Abelian tensorial group field theories with a closure constraint have been obtained. However, the mathematical physics techniques used in [24] (namely general formulations of exact renormalisation group equations and loop equations for tensor models and tensorial group field theories) are different from the techniques used here.

We would like to note that the WTI has been already successfully used to study the SDE in the context of matrix models of non-commutative quantum field theory - see [78] and [6]. In particular, the closed SDE 2-point function for the non-commutative and 2 dimensional $\lambda\varphi^4$ has been solved in [79] using and resumming a perturbative expansion. The building block of this solution is the Lambert- W function.

The chapter is organised as follows. In the following section we give the action of the tensor model we work with, and we recall tensor model tools used in the sequel, such as the boundary graph expansion of the free energy and the WTI. In particular we simplify some notations introduced in Chapter 1 and recall explicit results that we will use in this chapter. Section 2.3 is dedicated to the analysis of the scalings in powers of N of the various terms present in the action. Having a well-defined large N limit of the SDE imposes a series of constraints on these scalings. Section 2.4 treats in detail the case of the 4-point function with disconnected boundary graph. In section 2.5 we find appropriate scalings in order to have a coherent large N limit of the SDE. Section 2.6 consists of the analysis of the perturbative expansion of the 2-point function which leads us to consider the model with one quartic melonic interaction. We perform the resummation of the perturbative expansion, in order to obtain the non-perturbative solution of the SDE in

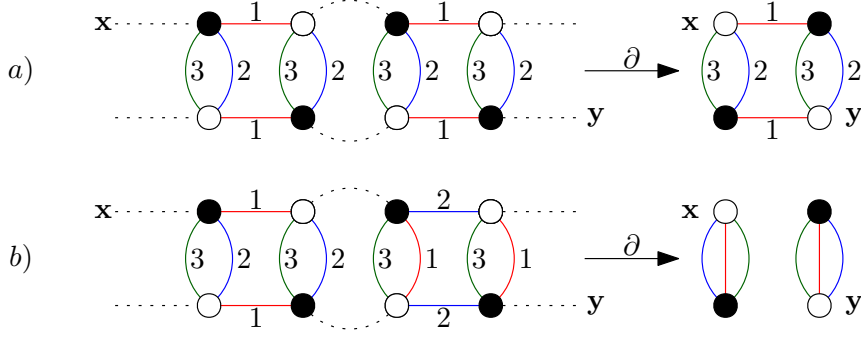


Figure 2.1: Two connected Feynman graphs and the associated boundary graphs in the tensor field theory (2.2.1) for $D = 3$. In figure a) the boundary graph is connected and in fig. b) the boundary graph is disconnected.

section 2.7. Then we discuss shortly the higher-point functions in section 2.8 before giving some concluding remarks in section 2.9. In Appendix C a perturbative expansion check of the SDE and the large N limit is performed up to second order. In Appendix D we obtain recurrence relations on the number appearing in the perturbative expansion of the 2-point function which translate into formulas involving Stirling numbers.

2.2 The model and the tools

In this chapter we focus on the following complex rank-3 bosonic tensor field theory with an action of the form

$$\begin{aligned} \mathcal{S}[\varphi, \bar{\varphi}] &= \mathcal{S}_0[\varphi, \bar{\varphi}] + \mathcal{S}_{\text{int}}[\varphi, \bar{\varphi}] \\ &= \sum_{\mathbf{x}} \bar{\varphi}^{\mathbf{x}} (1 + |\mathbf{x}|^2) \varphi^{\mathbf{x}} + \lambda \sum_{c=1}^3 \sum_{\mathbf{a}, \mathbf{b}} \varphi^{\mathbf{b}} \bar{\varphi}^{\mathbf{b} \varepsilon^{\mathbf{a} c}} \bar{\varphi}^{\mathbf{a} \varepsilon^{\mathbf{b} c}} \varphi^{\mathbf{a}}, \end{aligned} \quad (2.2.1)$$

with $\mathbf{x} = (x_1, \dots, x_3) \in \{\frac{1}{N}, \frac{2}{N}, \dots, 1\}^D$ and $|\mathbf{x}|^2 = \sum_{i=1}^3 x_i^2$. The interaction terms in the action are the three $U(N)^3$ -invariant pillow interaction as in Chapter 1 and we fix a specific kinetic term as in section 1.5.

In order to define the large N limit, we consider the following generating functional of the model

$$Z[J, \bar{J}] = \int \mathcal{D}\varphi \mathcal{D}\bar{\varphi} \exp \left(-N^\gamma \mathcal{S}[\varphi, \bar{\varphi}] + N^\beta \sum_{\mathbf{x}} (\bar{J}_{\mathbf{x}} \varphi^{\mathbf{x}} + J_{\mathbf{x}} \bar{\varphi}^{\mathbf{x}}) \right). \quad (2.2.2)$$

Note that we have introduced here the scaling β and γ , for the action and the source terms. Let us also introduce the scaling δ for the coupling constant $\lambda = N^\delta \lambda$. These scalings will be determined in the sequel, using the SDE.

We would like to remind the reader that even though the Feynman graph of the theory are connected, the associated boundary graphs can be disconnected (see figure 2.1). The connected $2k$ -point functions are split into sectors indexed by a boundary

Correlation functions and graph names				
Order (i.e. # vertices)	Explicit notation	Simplified notation	Graph	Graph name
2-pt function	$G_{\ominus}^{(2)}$	$G^{(2)}$		m
4-pt functions	$G_{a\boxed{a}}^{(4)}$	$G_a^{(4)}$		V_a
	$G_{\ominus \ominus}^{(4)}$	$G_m^{(4)}$		m m
6-pt functions	$G_{\text{hex}}^{(6)}$	$G_a^{(6)}$		Q_a
	$G_{\text{tri}}^{(6)}$	$G_K^{(6)}$		K
	$G_{\text{rect}}^{(6)}$	$G_{a;bc}^{(6)}$		$F_{a;bc}$
	$G_{\ominus a\boxed{a}}^{(6)}$	$G_{m a}^{(6)}$		m V_a
	$G_{\ominus \ominus \ominus}^{(6)}$	$G_m^{(6)}$		m m m

Table 2.1: The adopted notation for the correlation functions in the tensor field theory (2.2.1) for $D = 3$. In this table a is any colour and b and c are chosen such that $\{a, b, c\} = \{1, 2, 3\}$.

graph \mathcal{B} (see Table 2.1 where the notations used in this chapter have been simplified compare to Chapter 1), and taken to be

$$G_{\mathcal{B}}^{(2k)}(\mathbf{X}) = \frac{N^{-\alpha(\mathcal{B})}}{Z_0} \frac{\delta}{\delta \mathbb{J}(\mathcal{B})(\mathbf{X})} Z[J, \bar{J}] \Big|_{J=\bar{J}=0} = \frac{N^{-\alpha(\mathcal{B})}}{Z_0} \prod_{i=1}^k \left(\frac{\delta}{\delta \bar{J}_{\mathbf{p}^i}} \frac{\delta}{\delta J_{\mathbf{x}^i}} \right) Z[J, \bar{J}] \Big|_{J=\bar{J}=0}, \quad (2.2.3)$$

where $\mathbf{X} = (\mathbf{x}^1, \dots, \mathbf{x}^k) \in \{\frac{1}{N}, \frac{2}{N}, \dots, 1\}^{Dk}$ so that for all $c \in \{1, \dots, D\}$ and $(i, j) \in \{1, \dots, k\}^2$, $x_c^i \neq x_c^j$, and $Z_0 = Z[0, 0]$.

We introduced the scalings $\alpha(\mathcal{B})$ for each boundary graph \mathcal{B} , note that they do not depend on the choice of colouring of the respective graph \mathcal{B} . For example, $\alpha(V_1) = \alpha(V_2) = \alpha(V_3)$. These scalings also appear in the boundary graphs expansion of the free energy:

$$W[J, \bar{J}] = \sum_{k=1}^{\infty} \sum_{\substack{\mathcal{B} \in \partial \mathcal{S}_{\text{int}} \\ V(\mathcal{B})=2k}} \sum_{\mathbf{X}} \frac{N^{\alpha(\mathcal{B})}}{|\text{Aut}(\mathcal{B})|} G_{\mathcal{B}}^{(2k)}(\mathbf{X}) \cdot \mathbb{J}(\mathcal{B})(\mathbf{X}). \quad (2.2.4)$$

Moreover the scalings β and γ appear in the WTI:

$$\sum_{\mathbf{q}_a} \frac{\delta Z[J, \bar{J}]}{\delta J_{\mathbf{q}_a m_a} \delta \bar{J}_{\mathbf{q}_a n_a}} - \delta_{m_a n_a} Y_{m_a}^{(a)}[J, \bar{J}] \cdot Z[J, \bar{J}] = \frac{N^{3\beta-2\gamma}}{m_a^2 n_a^2} \sum_{\mathbf{q}_a} \left(\bar{J}_{\mathbf{q}_a m_a} \frac{\delta}{\delta J_{\mathbf{q}_a n_a}} - J_{\mathbf{q}_a n_a} \frac{\delta}{\delta J_{\mathbf{q}_a m_a}} \right) Z[J, \bar{J}], \quad (2.2.5)$$

and the Y-term is given by

$$Y_{m_a}^{(a)}[J, \bar{J}] = \sum_{\mathbf{q}_a} \frac{\delta^2 W[J, \bar{J}]}{\delta J_{\mathbf{q}_a m_a} \delta \bar{J}_{\mathbf{q}_a m_a}}$$

$$= \sum_{\mathcal{B} \in \partial \mathcal{S}_{\text{int}}} \sum_{\mathbf{X}} \mathfrak{f}_{\mathcal{B}, m_a}^{(a)}(\mathbf{X}) \cdot \mathbb{J}(\mathcal{B})(\mathbf{X}), \quad (2.2.6)$$

where $\mathfrak{f}_{\mathcal{B}, m_a}^{(a)}(\mathbf{X})$ is the function-coefficient of $\mathbb{J}(\mathcal{B})(\mathbf{X})$ in the graph expansion of the Y-term. The $\mathfrak{f}_{\mathcal{B}, m_a}^{(a)}$ -functions can be computed using a graph algorithm detailed in Chapter 1. Moreover, for a graph \mathcal{B} with $2k$ vertices, we recall that

$$\begin{aligned} \mathfrak{f}_a(\mathbf{X}; m_a; \mathcal{B}) &= \frac{\delta^{2k}}{\delta \mathbb{J}(\mathcal{B})(\mathbf{X})} Y_{m_a}^{(a)}[J, \bar{J}] \Big|_{J=\bar{J}=0} \\ &= \sum_{\hat{\pi} \in \text{Aut}(\mathcal{B})} (\pi^* \mathfrak{f}_{\mathcal{B}, m_a}^{(a)})(\mathbf{X}), \end{aligned} \quad (2.2.7)$$

where $(\pi^* f)(\mathbf{x}^1, \dots, \mathbf{x}^k) = f(\mathbf{x}^{\pi^{-1}(1)}, \dots, \mathbf{x}^{\pi^{-1}(k)})$, π is the restriction of the automorphism $\hat{\pi}$ to the white vertices of \mathcal{B} , and the equality between the first and second line was obtained in the proposition 1.2.1. In particular, for the pillow graphs V_a , equation (2.2.7) states that

$$\begin{aligned} \mathfrak{f}_a(\mathbf{x}, \mathbf{y}; m_a; V_a) &= \sum_{\hat{\pi} \in \mathbb{Z}_2} (\pi^* \mathfrak{f}_{V_a, m_a}^{(a)})(\mathbf{x}, \mathbf{y}) \\ &= \mathfrak{f}_{V_a, m_a}^{(a)}(\mathbf{x}, \mathbf{y}) + \mathfrak{f}_{V_a, m_a}^{(a)}(\mathbf{y}, \mathbf{x}). \end{aligned} \quad (2.2.8)$$

Here we are only interested in the explicit coefficients of the graph expansion of the Y-term up to order four in the sources, in the rank 3 tensor field theory (2.2.1). In the following equations, $\{a, b, c\} = \{1, 2, 3\}$, an automatic reordering of the entries by ascending sub-index is implied, and we omit the powers in N associated to each Green's function. One thus has:

$$\mathfrak{f}_{\mathfrak{m}, s_a}^{(a)}(\mathbf{x}) = G_a^{(4)}(\mathbf{x}, s_a, x_b, x_c) + \sum_{c \neq a} \sum_{q_b} G_c^{(4)}(\mathbf{x}, s_a, q_b, x_c) + \sum_{q_b, q_c} G_{\mathfrak{m}}^{(4)}(\mathbf{x}, s_a, q_b, q_c), \quad (2.2.9a)$$

$$\begin{aligned} \mathfrak{f}_{V_a, s_a}^{(a)}(\mathbf{x}, \mathbf{y}) &= \frac{1}{3} \left(G_a^{(6)}(s_a, x_b, x_c, \mathbf{x}, \mathbf{y}) + \text{cyclic perm.} \right) + \frac{1}{2} \sum_{q_b, q_c} G_{\mathfrak{m}|a}^{(6)}(s_a, q_b, q_c, \mathbf{x}, \mathbf{y}) \\ &+ \frac{1}{3} \left(G_K^{(6)}(s_a, x_b, y_c, \mathbf{x}, \mathbf{y}) + \text{cyclic perm.} \right) + \sum_{q_b} G_{b;ac}^{(6)}(\mathbf{x}, \mathbf{y}, s_a, q_b, y_c) \\ &+ \sum_{q_c} G_{c;ab}^{(6)}(\mathbf{x}, \mathbf{y}, s_a, q_c, y_b), \end{aligned} \quad (2.2.9b)$$

$$\begin{aligned} \mathfrak{f}_{V_b, s_a}^{(a)}(\mathbf{x}, \mathbf{y}) &= \frac{1}{3} \left(\sum_{q_b} G_b^{(6)}(s_a, q_b, y_c, \mathbf{x}, \mathbf{y}) + \text{cyclic perm.} \right) + G_{c;ab}^{(6)}(s_a, y_b, x_c, \mathbf{x}, \mathbf{y}) \\ &+ G_{c;ab}^{(6)}(\mathbf{x}, s_a, x_b, x_c, \mathbf{y}) + \sum_{q_b} G_{a;bc}^{(6)}(\mathbf{x}, \mathbf{y}, s_a, q_b, y_c) + \frac{1}{2} \sum_{q_b, q_c} G_{\mathfrak{m}|b}^{(6)}(s_a, q_b, q_c, \mathbf{x}, \mathbf{y}), \end{aligned} \quad (2.2.9c)$$

$$\begin{aligned} \mathfrak{f}_{V_c, s_a}^{(a)}(\mathbf{x}, \mathbf{y}) &= \frac{1}{3} \left(\sum_{q_c} G_c^{(6)}(s_a, y_b, q_c, \mathbf{x}, \mathbf{y}) + \text{cyclic perm.} \right) + G_{c;ab}^{(6)}(s_a, y_b, x_c, \mathbf{x}, \mathbf{y}) \\ &+ G_{c;ab}^{(6)}(\mathbf{x}, s_a, x_b, x_c, \mathbf{y}) + \sum_{q_c} G_{a;bc}^{(6)}(\mathbf{x}, s_a, x_b, q_c, \mathbf{y}) + \frac{1}{2} \sum_{q_b, q_c} G_{\mathfrak{m}|c}^{(6)}(s_a, q_b, q_c, \mathbf{x}, \mathbf{y}), \end{aligned} \quad (2.2.9d)$$

$$\begin{aligned}
\mathfrak{f}_{\mathbf{m}|\mathbf{m},s_a}^{(a)}(\mathbf{x}, \mathbf{y}) &= \left(\sum_{q_b, q_c} G_{\mathbf{m}}^{(6)}(s_a, q_b, q_c, \mathbf{x}, \mathbf{y}) + \text{cyclic perm.} \right) + G_{a;bc}^{(6)}(\mathbf{x}, s_a, x_b, y_c, \mathbf{y}) \\
&+ G_{\mathbf{m}|a}^{(6)}(\mathbf{x}, s_a, y_b, y_c, \mathbf{y}) + \sum_{q_c} G_{\mathbf{m}|b}^{(6)}(\mathbf{x}, s_a, y_b, q_c, \mathbf{y}) + \sum_{q_b} G_{\mathbf{m}|c}^{(6)}(\mathbf{x}, s_a, q_b, y_c, \mathbf{y}) \\
&+ \sum_{q_c} G_{\mathbf{m}|b}^{(6)}(\mathbf{x}, \mathbf{y}, s_a, y_b, q_c) + \sum_{q_b} G_{\mathbf{m}|c}^{(6)}(\mathbf{x}, \mathbf{y}, s_a, q_b, y_c) + G_{\mathbf{m}|a}^{(6)}(\mathbf{x}, \mathbf{y}, s_a, y_b, y_c). \quad (2.2.9e)
\end{aligned}$$

One should keep in mind that s_a is an external data. Also notice that the super-index a breaks the symmetry between the colours. These equations follow from the expansion of the Y-term in the lemma 1.4.1. Here ‘cyclic perm.’ means the cyclic permutation in the 3-tuples, e.g. ‘ $F(s_a, x_b, x_c, \mathbf{x}, \mathbf{y}) + \text{cyclic perm.}$ ’ abbreviates $F(s_a, x_b, x_c, \mathbf{x}, \mathbf{y}) + F(\mathbf{y}, s_a, x_b, x_c, \mathbf{x}) + F(\mathbf{x}, \mathbf{y}, s_a, x_b, x_c)$.

2.3 Constraints on the scalings in N

2.3.1 2-point function SDE

In this subsection, we start with the explicit definition of the 2-point function, and using the WTI to obtain SDE, we finally get a set of inequalities between the scaling coefficients α , β , γ and δ .

The 2-point function explicitly writes

$$\begin{aligned}
G^{(2)}(\mathbf{x}) &= \frac{N^{-\alpha} \delta^2 Z[J, \bar{J}]}{Z_0 \delta \bar{J}_{\mathbf{x}} \delta J_{\mathbf{x}}} \Big|_{J=\bar{J}=0} \quad (2.3.1) \\
&= \frac{N^{-\alpha} \delta^2}{Z_0 \delta J_{\mathbf{x}} \delta \bar{J}_{\mathbf{x}}} \exp \left(-N^\gamma \mathcal{S}_{\text{int}} \left[\frac{1}{N^{2\beta-\gamma}} \frac{\delta}{\delta J}, \frac{1}{N^{2\beta-\gamma}} \frac{\delta}{\delta \bar{J}} \right] \right) \exp \left(N^{2\beta-\gamma} \sum_{\mathbf{x}} \frac{J_{\mathbf{x}} \bar{J}_{\mathbf{x}}}{1 + |\mathbf{x}|^2} \right) \Big|_{J=\bar{J}=0} \\
&= \frac{N^{2\beta-\gamma-\alpha} \delta}{Z_0 \delta J_{\mathbf{x}}} \exp \left(-N^\gamma \mathcal{S}_{\text{int}}^\partial \right) \frac{J_{\mathbf{x}}}{1 + |\mathbf{x}|^2} \exp \left(N^{2\beta-\gamma} \sum_{\mathbf{x}} \frac{J_{\mathbf{x}} \bar{J}_{\mathbf{x}}}{1 + |\mathbf{x}|^2} \right) \Big|_{J=\bar{J}=0} \\
&= \frac{N^{2\beta-\gamma-\alpha}}{1 + |\mathbf{x}|^2} + \frac{N^{2\beta-\gamma-\alpha}}{Z_0} \exp \left(-N^\gamma \mathcal{S}_{\text{int}}^\partial \right) \frac{J_{\mathbf{x}}}{1 + |\mathbf{x}|^2} \frac{\delta}{\delta J_{\mathbf{x}}} \exp \left(N^{2\beta-\gamma} \sum_{\mathbf{x}} \frac{J_{\mathbf{x}} \bar{J}_{\mathbf{x}}}{1 + |\mathbf{x}|^2} \right) \Big|_{J=\bar{J}=0} \\
&= \frac{N^{2\beta-\gamma-\alpha}}{1 + |\mathbf{x}|^2} - \frac{N^{2\beta-\gamma-\alpha}}{Z_0} \frac{N^\gamma}{1 + |\mathbf{x}|^2} \left(\bar{\varphi}^{\mathbf{x}} \frac{\partial \mathcal{S}_{\text{int}}}{\partial \bar{\varphi}^{\mathbf{x}}} \right) \left[\frac{1}{N^{2\beta-\gamma}} \frac{\delta}{\delta J}, \frac{1}{N^{2\beta-\gamma}} \frac{\delta}{\delta \bar{J}} \right] Z[J, \bar{J}] \Big|_{J=\bar{J}=0},
\end{aligned}$$

where we note $F^\partial = F \left[\frac{1}{N^{2\beta-\gamma}} \frac{\delta}{\delta J}, \frac{1}{N^{2\beta-\gamma}} \frac{\delta}{\delta \bar{J}} \right]$. In order for the free propagator to be dominant in the large N limit, we must fix:

$$\alpha = 2\beta - \gamma. \quad (2.3.2)$$

To simplify the equations, we consider first the contribution of the pillow interaction V_1 and we then add the analogous contributions coming from the contributions of the pillow interactions V_2 and V_3 . One has:

$$N^\gamma \left(\bar{\varphi}^{\mathbf{x}} \frac{\partial \mathcal{S}_{\text{int}}}{\partial \bar{\varphi}^{\mathbf{x}}} \right)^\partial = 2\lambda \frac{N^{5\gamma+\delta}}{N^{8\beta}} \sum_{\mathbf{a}} \frac{\delta}{\delta J_{x_1 x_2 x_3}} \frac{\delta}{\delta \bar{J}_{a_1 x_2 x_3}} \frac{\delta}{\delta J_{a_1 a_2 a_3}} \frac{\delta}{\delta \bar{J}_{x_1 a_2 a_3}}. \quad (2.3.3)$$

Using the WTI for the two rightmost derivatives in the expression (2.3.3) enables us to write:

$$N^\gamma \left(\bar{\varphi}^{\mathbf{x}} \frac{\partial \mathcal{S}_{\text{int}}}{\partial \bar{\varphi}^{\mathbf{x}}} \right)^\partial Z[J, \bar{J}] \Big|_{J=\bar{J}=0} = \frac{2\lambda N^{5\gamma+\delta}}{N^{8\beta}} \frac{\delta}{\delta J_{\mathbf{x}}} \sum_{a_1} \frac{\delta}{\delta \bar{J}_{a_1 x_2 x_3}} \left\{ (\delta_{x_1 a_1} Y_{a_1}^{(1)}[J, \bar{J}]) \cdot Z[J, \bar{J}] \right. \\ \left. + \sum_{a_2, a_3} \frac{N^{3\beta-2\gamma}}{a_1^2 - x_1^2} \left(\bar{J}_{a_1 a_2 a_3} \frac{\delta}{\delta \bar{J}_{x_1 a_2 a_3}} - J_{x_1 a_2 a_3} \frac{\delta}{\delta J_{a_1 a_2 a_3}} \right) Z[J, \bar{J}] \right\} \Big|_{J=\bar{J}=0}. \quad (2.3.4)$$

Acting with the two remaining derivatives in (2.3.3) on the second term on the RHS of (2.3.4), and using (2.3.2), we get:

$$\frac{2\lambda}{N} \sum_{a_1} \frac{N^{2\gamma+\delta+1-3\beta}}{a_1^2 - x_1^2} (G^{(2)}(\mathbf{x}) - G^{(2)}(a_1, x_2, x_3)). \quad (2.3.5)$$

For this term to give a well defined large N limit we need the following relation:

$$3\beta \geq 2\gamma + \delta + 1. \quad (2.3.6)$$

Note that if the inequality (2.3.6) is taken to be an equality, then the term (2.3.5) is a leading order term in the large N limit.

Acting with the remaining derivative on the factor $Z[J, \bar{J}]$ of the first term of the RHS of (2.3.4) gives:

$$\frac{2\lambda}{N^{6\beta-4\gamma-\delta}} \delta_{x_1 a_1} Y_{a_1}^{(1)}[0, 0] G^{(2)}(\mathbf{x}) = \frac{2\lambda N^{3\gamma+2+\delta-4\beta}}{N^2} \sum_{a_2, a_3} G^{(2)}(x_1, a_2, a_3) G^{(2)}(\mathbf{x}). \quad (2.3.7)$$

This term implies a new inequality on the exponents:

$$4\beta \geq 3\gamma + \delta + 2. \quad (2.3.8)$$

Acting now with these remaining derivatives on the factor $Y_{a_1}^{(1)}[J, \bar{J}]$ of the first term of the RHS of (2.3.4) gives:

$$\delta_{x_1 a_1} \frac{\delta Y_{a_1}^{(1)}[J, \bar{J}]}{\delta J_{\mathbf{x}} \delta \bar{J}_{a_1 x_2 x_3}} \Big|_{J=\bar{J}=0} = N^{\alpha(V_1)} G_1^{(4)}(\mathbf{x}, \mathbf{x}) + \frac{N^{\alpha(\text{m|m})+2}}{N^2} \sum_{a_2, a_3} G_{\text{m}}^{(4)}(\mathbf{x}, x_1, a_2, a_3). \quad (2.3.9)$$

Putting these terms together, we obtain the SDE for the 2-point function:

$$G^{(2)}(\mathbf{x}) = \frac{1}{1 + |\mathbf{x}|^2} - \frac{2\lambda}{1 + |\mathbf{x}|^2} \left(\frac{N^{3\gamma+2+\delta-4\beta}}{N^2} \sum_{a_2, a_3} G^{(2)}(p_1, a_2, a_3) G^{(2)}(\mathbf{x}) + \frac{N^{\alpha(V_1)}}{N^{8\beta-5\gamma-\delta}} G_1^{(4)}(\mathbf{x}, \mathbf{x}) \right. \\ \left. + \frac{N^{\alpha(\text{m|m})+2}}{N^{8\beta-5\gamma-\delta}} \frac{1}{N^2} \sum_{a_2, a_3} G_{\text{m}}^{(4)}(x_1, a_2, a_3, \mathbf{x}) + \frac{1}{N} \sum_{a_1} \frac{N^{2\gamma+\delta+1-3\beta}}{x_1^2 - a_1^2} (G^{(2)}(a_1, x_2, x_3) - G^{(2)}(\mathbf{x})) \right). \quad (2.3.10)$$

For the 4-point function to be sub-leading in the large N limit taken in (2.3.10) above, we need to impose the following two inequalities on the exponents:

$$\alpha(V_1) < 8\beta - 5\gamma - \delta, \quad (2.3.11)$$

$$\alpha(\text{m|m}) < 8\beta - 5\gamma - \delta - 2. \quad (2.3.12)$$

As announced above, we now add the contributions coming from the 2^{nd} and 3^{rd} pillow interaction terms, V_2 and V_3 , of the action. We then get:

$$\begin{aligned}
G^{(2)}(\mathbf{x}) &= \frac{1}{1 + |\mathbf{x}|^2} - \frac{2\lambda}{1 + |\mathbf{x}|^2} \sum_{a=1}^3 \left(\frac{N^{3\gamma+2+\delta-4\beta}}{N^2} \sum_{\mathbf{q}_{\hat{a}}} G^{(2)}(\mathbf{q}_{\hat{a}}x_a) G^{(2)}(\mathbf{x}) + \frac{N^{\alpha(V_1)}}{N^{8\beta-5\gamma-\delta}} G_a^{(4)}(\mathbf{x}, \mathbf{x}) \right. \\
&+ \frac{N^{\alpha(m|m)+2}}{N^{8\beta-5\gamma-\delta}} \frac{1}{N^2} \sum_{\mathbf{q}_{\hat{a}}} G_m^{(4)}(\mathbf{q}_{\hat{a}}x_a, \mathbf{x}) + \frac{1}{N} \sum_{q_a} \frac{N^{2\gamma+\delta+1-3\beta}}{x_a^2 - q_a^2} (G^{(2)}(\mathbf{x}_{\hat{a}}q_a) - G^{(2)}(\mathbf{x})) \\
&\left. + \frac{N^{\alpha(V_1)+1}}{N^{8\beta-5\gamma-\delta}} \frac{1}{N} \sum_{c \neq a} \sum_{q_b} G_c^{(4)}(\mathbf{x}, \mathbf{x}_b q_b) \right), \tag{2.3.13}
\end{aligned}$$

where in the last term $b \neq c$ and $b \neq a$. This last term leads to a stronger condition than (2.3.11):

$$\alpha(V_1) < 8\beta - 5\gamma - \delta - 1. \tag{2.3.14}$$

Moreover for $a_1 \neq x_1$ and using (2.3.2), the WTI implies

$$\begin{aligned}
N^{5\beta-3\gamma} \frac{G^{(2)}(a_1, x_2, x_3) - G^{(2)}(\mathbf{x})}{x_1^2 - a_1^2} &= N^{4\beta-2\gamma} G^{(2)}(a_1, x_2, x_3) G^{(2)}(\mathbf{x}) + \frac{N^{\alpha(V_1)+2}}{N^2} \sum_{a_2, a_3} G_1^{(4)}(\mathbf{a}, \mathbf{x}) \\
&+ \frac{N^{\alpha(V_1)+1}}{N} \left(\sum_{a_3} G_2^{(4)}(\mathbf{x}, a_1, x_2, a_3) + \sum_{a_2} G_3^{(4)}(\mathbf{x}, a_1, a_2, x_3) \right). \tag{2.3.15}
\end{aligned}$$

This identity rewrites as

$$\begin{aligned}
\frac{G^{(2)}(a_1, x_2, x_3) - G^{(2)}(\mathbf{x})}{x_1^2 - a_1^2} &= \frac{1}{N^{\beta-\gamma}} G^{(2)}(a_1, x_2, x_3) G^{(2)}(\mathbf{x}) + \frac{N^{\alpha(V_1)+2}}{N^{5\beta-3\gamma}} \frac{1}{N^2} \sum_{a_2, a_3} G_1^{(4)}(\mathbf{a}, \mathbf{x}) \\
&+ \frac{N^{\alpha(V_1)+1}}{N^{5\beta-3\gamma}} \left(\frac{1}{N} \sum_{a_3} G_2^{(4)}(\mathbf{x}, a_1, x_2, a_3) + \frac{1}{N} \sum_{a_2} G_3^{(4)}(\mathbf{x}, a_1, a_2, x_3) \right), \tag{2.3.16}
\end{aligned}$$

which implies the following two inequalities:

$$\beta \geq \gamma, \tag{2.3.17}$$

$$\alpha(V_1) \leq 5\beta - 3\gamma - 2. \tag{2.3.18}$$

2.3.2 $2k$ -point function SDE for connected boundary graphs

In this subsection we start with the definition of the $2k$ -point function, and as above, we use WTI to obtain the SDE. This finally leads to a new inequality between the scaling coefficients.

From now on we consider altogether the contributions coming from the three pillow interactions V_1 , V_2 and V_3 . Let us start from the definition of a $2k$ -point function with a connected boundary graph given in (2.2.3). As in Chapter 1, in order to obtain the SDE,

we first consider the term:

$$\begin{aligned} \frac{\delta W[J, \bar{J}]}{\delta \bar{J}_{\mathbf{s}}} &= \frac{N^{2\beta-\gamma}}{Z[J, \bar{J}]} \exp(-N\gamma \mathcal{S}_{\text{int}}^{\partial}) \frac{J_{\mathbf{s}}}{1+|\mathbf{s}|^2} \exp\left(N^{2\beta-\gamma} \sum_{\mathbf{a}} \frac{\bar{J}_{\mathbf{a}} J_{\mathbf{a}}}{1+|\mathbf{a}|^2}\right) \\ &= N^{2\beta-\gamma} \frac{J_{\mathbf{s}}}{1+|\mathbf{s}|^2} - \frac{1}{1+|\mathbf{s}|^2} \frac{N^{2\beta}}{Z[J, \bar{J}]} \left(\frac{\delta \mathcal{S}_{\text{int}}}{\delta \bar{\varphi}^{\mathbf{s}}}\right)^{\partial} Z[J, \bar{J}]. \end{aligned} \quad (2.3.19)$$

Note that here \mathbf{s} is an unspecified vector of indices. The WTI enables us to write:

$$\begin{aligned} N^{2\beta} \left(\frac{\delta \mathcal{S}_{\text{int}}}{\delta \bar{\varphi}^{\mathbf{s}}}\right)^{\partial} Z[J, \bar{J}] &= \frac{2\lambda N^{4\gamma+\delta}}{N^{6\beta}} \sum_{a=1}^3 \sum_{b_a} \frac{\delta}{\delta \bar{J}_{\mathbf{s}_a b_a}} \sum_{\mathbf{b}_a} \frac{\delta}{\delta J_{\mathbf{b}}} \frac{\delta}{\delta \bar{J}_{\mathbf{b}_a s_a}} Z[J, \bar{J}] \\ &= \frac{2\lambda N^{4\gamma+\delta}}{N^{6\beta}} \sum_{a=1}^3 \left(\frac{\delta \left(Y_{s_a}^{(a)}[J, \bar{J}] \cdot Z[J, \bar{J}]\right)}{\delta \bar{J}_{\mathbf{s}}} + \sum_{b_a} \frac{N^{3\beta-2\gamma} \delta Z[J, \bar{J}]}{b_a^2 - s_a^2} \frac{\delta}{\delta \bar{J}_{\mathbf{s}}} \right. \\ &\quad \left. - N^{3\beta-2\gamma} \sum_{\mathbf{b}} \frac{J_{\mathbf{b}_a s_a}}{b_a^2 - s_a^2} \frac{\delta^2 Z[J, \bar{J}]}{\delta \bar{J}_{\mathbf{s}_a b_a} \delta J_{\mathbf{b}}} + N^{3\beta-2\gamma} \sum_{\mathbf{b}} \frac{\bar{J}_{\mathbf{b}}}{b_a^2 - s_a^2} \frac{\delta^2 Z[J, \bar{J}]}{\delta \bar{J}_{\mathbf{s}_a b_a} \delta \bar{J}_{\mathbf{b}_a s_a}} \right). \end{aligned} \quad (2.3.20)$$

For $\mathbf{s} = \mathbf{p}^1$, recalling that

$$Y_{p_a^1}^{(a)}[0, 0] = N^{\alpha} \sum_{\mathbf{q}_a} G^{(2)}(\mathbf{q}_a p_a^1), \quad (2.3.21)$$

we apply the remaining $2k - 1$ derivatives of (2.2.3) to (2.3.20). This leads to the SDE for a $2k$ -point function with a connected boundary graph:

$$\begin{aligned} G_{\mathcal{B}}^{(2k)}(\mathbf{X}) &= -\frac{2\lambda}{1+|\mathbf{p}^1|^2} \sum_a \left\{ \frac{N^{3\gamma+2+\delta-4\beta}}{N^2} \sum_{\mathbf{q}_a} G^{(2)}(\mathbf{q}_a p_a^1) G_{\mathcal{B}}^{(2k)}(\mathbf{X}) + \frac{N^{4\gamma+\delta-6\beta}}{N^{\alpha(\mathcal{B})}} f_a(\mathbf{X}; p_a^1; \mathcal{B}) \right. \\ &\quad + \frac{1}{N} \sum_{b_a} \frac{N^{2\gamma+\delta+1-3\beta}}{b_a^2 - (x_a^\gamma)^2} \left(G_{\mathcal{B}}^{(2k)}(\mathbf{X}) - G_{\mathcal{B}}^{(2k)}(\mathbf{X}|_{x_a^\gamma \rightarrow b_a}) \right) \\ &\quad \left. + \frac{N^{2\gamma+\delta-3\beta}}{N^{\alpha(\mathcal{B})}} \sum_{\rho=2}^k \frac{1}{(p_a^\rho)^2 - (p_a^1)^2} \frac{1}{Z_0} \left[\frac{\partial Z[J, \bar{J}]}{\partial \zeta_a(\mathcal{B}; 1, \rho)}(\mathbf{X}) - \frac{\partial Z[J, \bar{J}]}{\partial \zeta_a(\mathcal{B}; 1, \rho)}(\mathbf{X}|_{x_a^\gamma \rightarrow p_a^\rho}) \right] \right\}, \end{aligned} \quad (2.3.22)$$

where \mathbf{x}^γ corresponds to the only white vertex such that $x_a^\gamma = s_a$ and $\zeta_a(\mathcal{B}; 1, \rho)$ is the graph obtained by swapping the a -coloured lines between \mathbf{p}^1 and \mathbf{p}^ρ in a graph \mathcal{B} (see figure 2.2). Similarly to \mathbf{x}^γ , we note $\mathbf{x}^{\kappa(\rho)}$ the only white vertex such that $x_a^{\kappa(\rho)} = p_a^\rho$. An explicit example of this operation is given in figure 2.3. Starting from the pillow graph V_1 , swapping edges of colour 2 and resp. 3 gives the graphs V_3 and resp. V_2 ; however swapping edges of colour 1 gives the disconnected graph $m|m$.

The first term of the RHS of (2.3.22) gives a well defined large N limit if (2.3.8) is satisfied. The terms of the second line of (2.3.22) require (2.3.6). The terms contributing to $f_a(\mathbf{X}; p_a^1; \mathcal{B})$ for $V(\mathcal{B}) = 2k$ are $2(k+1)$ -point functions with at most two sums on dummy variables. Hence to get a well defined large N limit we need:

$$\alpha(\mathcal{B}) \geq \alpha(\mathcal{B}') + 2 + 4\gamma + \delta - 6\beta, \quad (2.3.23)$$

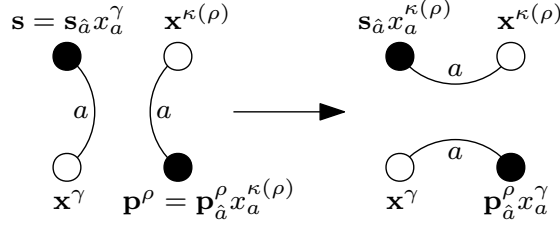


Figure 2.2: Swapping of two a -coloured edges.

with $V(\mathcal{B}') = 2k + 2$. If the inequality is strict, the $2(k + 1)$ -point function terms in the SDE for the $2k$ -point function are sub-leading and the tower of SDE decouples at leading order.

For the 4-point function and for $\mathbf{s} = (x_1, y_2, y_3)$, the general equation (2.3.22) gives

$$\begin{aligned}
G_1^{(4)}(\mathbf{x}, \mathbf{y}) = & -\frac{2\lambda}{1 + |\mathbf{s}|^2} \left\{ \frac{N^{4\gamma + \delta - 6\beta}}{N^{\alpha(V_1)}} \sum_{a=1}^3 \mathfrak{f}_a(\mathbf{x}, \mathbf{y}; s_a; V_a) \right. \\
& + \frac{N^{3\gamma + 2 + \delta - 4\beta}}{N^2} \sum_{a=1}^3 \sum_{\mathbf{q}_{\hat{a}}} G^{(2)}(\mathbf{q}_{\hat{a}} s_a) G_1^{(4)}(\mathbf{x}, \mathbf{y}) \\
& + \frac{1}{N} \sum_{b_1} \frac{N^{2\gamma + \delta + 1 - 3\beta}}{b_1^2 - x_1^2} \left(G_1^{(4)}(\mathbf{x}, \mathbf{y}) - G_1^{(4)}(b_1, x_2, x_3, \mathbf{y}) \right) \\
& + \frac{N^{2\gamma + \delta - 3\beta}}{y_2^2 - x_2^2} \left(G_3^{(4)}(\mathbf{x}, y_1, x_2, y_3) - G_3^{(4)}(\mathbf{x}, \mathbf{y}) \right) \\
& + \frac{1}{N} \sum_{b_2} \frac{N^{2\gamma + \delta + 1 - 3\beta}}{b_2^2 - y_2^2} \left(G_1^{(4)}(\mathbf{x}, \mathbf{y}) - G_1^{(4)}(\mathbf{x}, y_1, b_2, y_3) \right) \\
& + \frac{N^{2\gamma + \delta - 3\beta}}{y_3^2 - x_3^2} \left(G_2^{(4)}(\mathbf{x}, y_1, y_2, x_3) - G_2^{(4)}(\mathbf{x}, \mathbf{y}) \right) \\
& + \frac{1}{N} \sum_{b_3} \frac{N^{2\gamma + \delta + 1 - 3\beta}}{b_3^2 - y_3^2} \left(G_1^{(4)}(\mathbf{x}, \mathbf{y}) - G_1^{(4)}(\mathbf{x}, y_1, y_2, b_3) \right) \\
& + \frac{N^{2\gamma + \delta - 3\beta}}{y_1^2 - x_1^2} \frac{N^{2\alpha}}{N^{\alpha(V_1)}} G^{(2)}(\mathbf{y}) \left(G^{(2)}(\mathbf{x}) - G^{(2)}(y_1, x_2, x_3) \right) \\
& \left. + \frac{N^{2\gamma + \delta - 3\beta}}{y_1^2 - x_1^2} \frac{N^{\alpha(m|m)}}{N^{\alpha(V_1)}} \left(G_m^{(4)}(\mathbf{x}, \mathbf{y}) - G_m^{(4)}(x_1, x_2, x_3, \mathbf{y}) \right) \right\}. \tag{2.3.24}
\end{aligned}$$

Using (2.3.2), the eighth term in (2.3.24) leads to

$$\alpha(V_1) \geq \beta + \delta, \tag{2.3.25}$$

The last term of (2.3.24) leads to

$$\alpha(V_1) \geq \alpha(m|m) + 2\gamma + \delta - 3\beta. \tag{2.3.26}$$

Moreover the fourth and sixth terms imply

$$3\beta \geq 2\gamma + \delta, \tag{2.3.27}$$

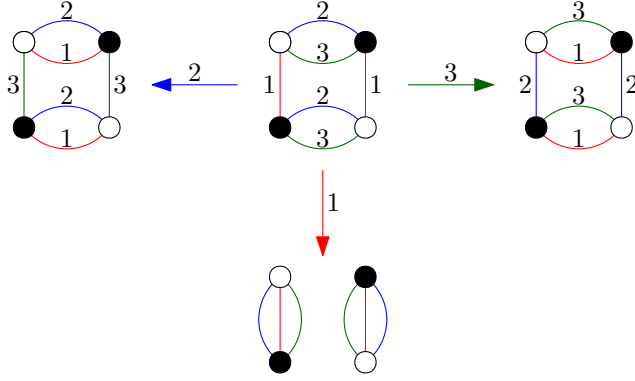


Figure 2.3: Swapping of the three different colours edges, starting from the pillow graph V_1 .

which must be a strict inequality to be consistent with (2.3.6). Hence these two terms are sub-leading in the large N limit.

Remark. The colour- a edge swapping ζ_a appeared naturally in Chapter 1 while describing the SDE. Leaving the restriction to boundary graphs, in general, when ζ_a is applied to a connected coloured graph (i.e. when it is a unary operation), ζ_a is known as *flip* and this terminology traces back to the theory of graph encoded manifolds (GEM) Flips and *blobs* (in the tensor model context known as *melon insertion*) are two fundamental operations in the sense that coloured graphs representing the same piece-wise manifold might differ only by a finite sequence of flips and blobs. The binary version of $\zeta_a(\mathcal{B}_1 \sqcup \mathcal{B}_2; w, v)$ (when the argument is a two-component graph and the two vertices v and w are in different components) has been explored in [75] and in the tensor model context represents the graph theoretical connected sum¹.

2.4 The 4-point function SDE with disconnected boundary graph

In this section, we apply the same approach for the 4-point function SDE with disconnected boundary graph. This case was not considered in Chapter 1.

The 4-point function with a disconnected boundary graph writes

$$G_m^{(4)}(\mathbf{x}, \mathbf{y}) = \frac{1}{N^{\alpha(m|m)}} \frac{\delta^4 W[J, \bar{J}]}{\delta \bar{J}_y \delta J_y \delta \bar{J}_x \delta J_x} \Big|_{J=\bar{J}=0}, \quad (2.4.1)$$

Let us start from (2.3.19) with $\mathbf{s} = \mathbf{x}$ and where we applied the three remaining derivatives

¹The virtue of this connected sum is being a binary operation on the set of Feynman diagrams of a tensor model \mathcal{S}_{int} , $\zeta_{a=0} : \text{Feyn}(\mathcal{S}_{\text{int}}) \times \text{Feyn}(\mathcal{S}_{\text{int}}) \rightarrow \text{Feyn}(\mathcal{S}_{\text{int}})$ (by preserving the interaction vertices that would be destroyed by the old connected sum of the “crystallisation theory” that consist of the removal of two graph-vertices). This is seen from the fact that propagators are represented by the 0 colour; therefore $\zeta_{a=0}$ only swaps two ends of two propagators inside a Feynman graph, leaving untouched the interaction vertices of the model \mathcal{S}_{int} in question.

$$\frac{\delta^4 \mathbb{W}[J, \bar{J}]}{\delta \bar{J}_y \delta J_y \delta \bar{J}_x \delta J_x} = -\frac{N^{2\beta}}{1 + |\mathbf{x}|^2} \frac{\delta^2}{\delta \bar{J}_y \delta J_y} \left(\frac{1}{Z[J, \bar{J}]} \frac{\delta}{\delta J_x} \left(\frac{\delta \mathcal{S}_{\text{int}}}{\delta \bar{\varphi}^{\mathbf{x}}} \right)^\partial Z[J, \bar{J}] \right). \quad (2.4.2)$$

For a connected boundary graph, all the derivatives give a vanishing contribution when applied to $\frac{1}{Z[J, \bar{J}]}$. For the disconnected boundary graph case we treat here, one has:

$$\begin{aligned} \frac{\delta^4 \mathbb{W}[J, \bar{J}]}{\delta \bar{J}_y \delta J_y \delta \bar{J}_x \delta J_x} &= -\frac{N^{2\beta}}{1 + |\mathbf{x}|^2} \frac{1}{Z[J, \bar{J}]} \frac{\delta^3}{\delta J_x \delta \bar{J}_y \delta J_y} \left(\frac{\delta \mathcal{S}_{\text{int}}}{\delta \bar{\varphi}^{\mathbf{x}}} \right)^\partial Z[J, \bar{J}] \\ &+ \frac{N^{2\beta}}{1 + |\mathbf{x}|^2} \frac{1}{Z^2[J, \bar{J}]} \frac{\delta^2 Z[J, \bar{J}]}{\delta \bar{J}_y \delta J_y} \frac{\delta}{\delta J_x} \left(\frac{\delta \mathcal{S}_{\text{int}}}{\delta \bar{\varphi}^{\mathbf{x}}} \right)^\partial Z[J, \bar{J}]. \end{aligned} \quad (2.4.3)$$

The first line is the same as in the case of a connected boundary graph, the second line is a new type of term. As above, the WTI leads to the first term below:

$$\begin{aligned} \frac{1}{Z_0} \frac{\delta^4 \left(Y_{x_a}^{(a)}[J, \bar{J}] \cdot Z[J, \bar{J}] \right)}{\delta \bar{J}_y \delta J_y \delta \bar{J}_x \delta J_x} \Bigg|_{J=\bar{J}=0} &= N^\alpha \sum_{\mathbf{q}_a} G^{(2)}(\mathbf{q}_a, x_a) \left(N^{\alpha(m|m)} G_m^{(4)}(\mathbf{x}, \mathbf{y}) + N^{2\alpha} G^{(2)}(\mathbf{x}) G^{(2)}(\mathbf{y}) \right) \\ &+ N^\alpha G^{(2)}(\mathbf{x}) \frac{\delta^2 Y_{x_a}^{(a)}[J, \bar{J}]}{\delta \bar{J}_y \delta J_y} \Bigg|_{J=\bar{J}=0} + N^\alpha G^{(2)}(\mathbf{y}) \frac{\delta^2 Y_{x_a}^{(a)}[J, \bar{J}]}{\delta \bar{J}_x \delta J_x} \Bigg|_{J=\bar{J}=0} + \frac{\delta^4 Y_{x_a}^{(a)}[J, \bar{J}]}{\delta(m|m)} \Bigg|_{J=\bar{J}=0}, \end{aligned} \quad (2.4.4)$$

where

$$\frac{\delta^4 Y_{x_a}^{(a)}[J, \bar{J}]}{\delta(m|m)} \Bigg|_{J=\bar{J}=0} = \mathfrak{f}_{m|m, x_a}^{(a)}(\mathbf{x}, \mathbf{y}) + \mathfrak{f}_{m|m, x_a}^{(a)}(\mathbf{y}, \mathbf{x}), \quad (2.4.5)$$

$$\frac{\delta^2 Y_{x_a}^{(a)}[J, \bar{J}]}{\delta \bar{J}_x \delta J_x} \Bigg|_{J=\bar{J}=0} = \mathfrak{f}_{m, x_a}^{(a)}(\mathbf{x}), \quad (2.4.6)$$

$$\frac{\delta^2 Y_{x_a}^{(a)}[J, \bar{J}]}{\delta \bar{J}_y \delta J_y} \Bigg|_{J=\bar{J}=0} = \mathfrak{f}_{m, x_a}^{(a)}(\mathbf{y}). \quad (2.4.7)$$

This term corresponds to the first term in (2.3.20). We also need to compute the contribution from the swapping (the term corresponding to the last term of (2.3.20)). This writes

$$\frac{1}{Z_0} \frac{\partial Z[J, \bar{J}]}{\partial \zeta_a(m|m, 1, 2)(\mathbf{x}, \mathbf{y})} \Bigg|_{J=\bar{J}=0} = N^{\alpha(V_1)} G_a^{(4)}(\mathbf{x}, \mathbf{y}), \quad (2.4.8)$$

Finally, the contribution from the two remaining terms of (2.3.20) writes

$$\begin{aligned} &- N^{3\beta-2\gamma} \sum_{\mathbf{b}} \frac{\delta^3}{\delta \bar{J}_y \delta J_y \delta J_x} \left(\frac{J_{\mathbf{b}_a x_a}}{b_a^2 - x_a^2} \frac{\delta^2 Z[J, \bar{J}]}{\delta \bar{J}_{\mathbf{x}_a b_a} \delta J_{\mathbf{b}}} \right) \Bigg|_{J=\bar{J}=0} = \\ &- \frac{1}{N} \sum_{b_a} \frac{N^{3\beta-2\gamma+1}}{b_a^2 - x_a^2} \left(N^{\alpha(m|m)} G_m^{(4)}(\mathbf{x}_a b_a, \mathbf{y}) + N^{2\alpha} G^{(2)}(\mathbf{x}_a b_a) G^{(2)}(\mathbf{y}) + N^{\alpha(a)} \delta_{y_a}^{b_a} G_a^{(4)}(\mathbf{x}_a y_a, \mathbf{y}) \right), \end{aligned} \quad (2.4.9)$$

$$\begin{aligned}
& \sum_{b_a} \frac{N^{3\beta-2\gamma}}{b_a^2 - x_a^2} \frac{1}{Z_0} \left. \frac{\delta^4 Z[J, \bar{J}]}{\delta \bar{J}_y \delta J_y \delta \bar{J}_{\mathbf{x}_{\hat{a}b_a}} \delta J_{\mathbf{x}}} \right|_{J=\bar{J}=0} \\
&= \frac{1}{N} \sum_{b_a} \frac{N^{3\beta-2\gamma+1}}{b_a^2 - x_a^2} \left(N^{\alpha(m|m)} G_m^{(4)}(\mathbf{x}, \mathbf{y}) + N^{2\alpha} G^{(2)}(\mathbf{x}) G^{(2)}(\mathbf{y}) \right). \tag{2.4.10}
\end{aligned}$$

Let us note here that in (2.4.9), we obtain not only a contribution coming from the disconnected 4-point function, but also a supplementary contribution as a product of 2-point functions. These products of 2-point functions and the term

$$G^{(2)}(\mathbf{y}) \frac{\delta^2 Y_{x_a}^{(a)}[J, \bar{J}]}{\delta \bar{J}_{\mathbf{x}} \delta J_{\mathbf{x}}}, \tag{2.4.11}$$

give rise to disconnected Feynman graphs because the dependence in momenta factorises. They should not appear in a connected Green's function, hence they need to be compensated.

They will be cancelled by the term coming from the second line of (2.4.3). This will give us new relations on the exponents of N . Noting that

$$\frac{\delta}{\delta J_{\mathbf{x}}} \left(\frac{\delta \mathcal{S}_{\text{int}}}{\delta \bar{\varphi}^{\mathbf{x}}} \right)^{\partial} Z[J, \bar{J}] = \left(\bar{\varphi}^{\mathbf{x}} \frac{\partial \mathcal{S}_{\text{int}}}{\partial \bar{\varphi}^{\mathbf{x}}} \right)^{\partial} Z[J, \bar{J}], \tag{2.4.12}$$

we already have computed these terms in the SDE for the 2-point function. Indeed, all the terms proportional to λ in the SDE for the 2-point function are multiplied by

$$-\frac{N^{2\beta-\gamma}}{N^{\alpha(m|m)}} \frac{\delta^2 Z[J, \bar{J}]}{\delta \bar{J}_y \delta J_y} \tag{2.4.13}$$

to obtain the contribution from the second line of (2.4.3) in the SDE for the 4-point function with a disconnected boundary graph. This writes:

$$\begin{aligned}
& \frac{2\lambda}{1 + |\mathbf{x}|^2} \frac{G^{(2)}(\mathbf{y})}{N^{\alpha(m|m)}} \sum_{a=1}^3 \left(\frac{N^{3\gamma+2+\delta-4\beta}}{N^2} \sum_{\mathbf{q}_{\hat{a}}} G^{(2)}(\mathbf{q}_{\hat{a}} x_a) G^{(2)}(\mathbf{x}) + \frac{\mathbf{f}_{\mathbf{m}, x_a}^{(a)}(\mathbf{x})}{N^{8\beta-5\gamma-\delta}} \right. \\
& \left. + \frac{1}{N} \sum_{q_a} \frac{N^{2\gamma+\delta+1-3\beta}}{(x_a)^2 - q_a^2} (G^{(2)}(\mathbf{x}_{\hat{a}} q_a) - G^{(2)}(\mathbf{x})) \right). \tag{2.4.14}
\end{aligned}$$

Collecting all the terms above and again making use of (2.3.2), we get

$$\begin{aligned}
G_m^{(4)}(\mathbf{x}, \mathbf{y}) &= -\frac{2\lambda}{1 + |\mathbf{x}|^2} \sum_{a=1}^3 \left\{ \frac{1}{N^2} \sum_{\mathbf{q}_{\hat{a}}} G^{(2)}(\mathbf{q}_{\hat{a}} x_a) \left(\frac{G_m^{(4)}(\mathbf{x}, \mathbf{y})}{N^{4\beta-3\gamma-\delta-2}} + \frac{N^{\gamma+\delta+2}}{N^{\alpha(m|m)}} G^{(2)}(\mathbf{x}) G^{(2)}(\mathbf{y}) \right) \right. \\
& - \frac{1}{N} \sum_{q_a} \frac{1}{q_a^2 - x_a^2} \left(N^{2\gamma+\delta-3\beta+1} G_m^{(4)}(\mathbf{x}_{\hat{a}} q_a, \mathbf{y}) + \frac{N^{\beta+\delta+1}}{N^{\alpha(m|m)}} G^{(2)}(\mathbf{x}_{\hat{a}} q_a) G^{(2)}(\mathbf{x}) \right) \\
& + \frac{1}{N} \sum_{q_a} \frac{1}{q_a^2 - x_a^2} \left(N^{2\gamma+\delta-3\beta+1} G_m^{(4)}(\mathbf{x}, \mathbf{y}) + \frac{N^{\beta+\delta+1}}{N^{\alpha(m|m)}} G^{(2)}(\mathbf{x}) G^{(2)}(\mathbf{y}) \right) \\
& \left. + \frac{N^{\alpha(V_1)+2\gamma+\delta-3\beta}}{N^{\alpha(m|m)}} \frac{1}{y_a^2 - x_a^2} (G_a^{(4)}(\mathbf{x}, \mathbf{y}) - G_a^{(4)}(\mathbf{x}_{\hat{a}} y_a, \mathbf{x}^2)) + \frac{N^{3\gamma+\delta-4\beta}}{N^{\alpha(m|m)}} G^{(2)}(\mathbf{x}) \mathbf{f}_{\mathbf{m}, x_a}^{(a)}(\mathbf{y}) \right.
\end{aligned}$$

$$\begin{aligned}
& + \frac{N^{4\gamma+\delta-6\beta}}{N^{\alpha(m|m)}} \left(\mathfrak{f}_{m|x_a^1}^{(a)}(\mathbf{x}, \mathbf{y}) + \mathfrak{f}_{m|x_a^1}^{(a)}(\mathbf{y}, \mathbf{x}) \right) + \frac{N^{3\gamma+\delta-4\beta}}{N^{\alpha(m|m)}} G^{(2)}(\mathbf{y}) \mathfrak{f}_{m,x_a}^{(a)}(\mathbf{x}) \\
& - \frac{N^{5\gamma+\delta-8\beta}}{N^{\alpha(m|m)}} G^{(2)}(\mathbf{y}) \mathfrak{f}_{m,x_a}^{(a)}(\mathbf{x}) - \frac{N^{3\gamma+2+\delta-4\beta}}{N^{\alpha(m|m)}} \frac{G^{(2)}(\mathbf{y})}{N^2} \sum_{\mathbf{q}_{\hat{a}}} G^{(2)}(\mathbf{q}_{\hat{a}} x_a) G^{(2)}(\mathbf{x}) \\
& - \left. \frac{N^{2\gamma+\delta+1-3\beta}}{N^{\alpha(m|m)}} \frac{G^{(2)}(\mathbf{y})}{N} \sum_{q_a} \frac{1}{x_a^2 - q_a^2} (G^{(2)}(\mathbf{x}_{\hat{a}} q_a) - G^{(2)}(\mathbf{x})) \right\}. \tag{2.4.15}
\end{aligned}$$

Let us determine the conditions on the exponents for the disconnected term to be cancelled. We have the following three identities:

$$\frac{N^{3\gamma+\delta-4\beta}}{N^{\alpha(m|m)}} G^{(2)}(\mathbf{y}) \mathfrak{f}_{m,x_a}^{(a)}(\mathbf{x}) = \frac{N^{5\gamma+\delta-8\beta}}{N^{\alpha(m|m)}} G^{(2)}(\mathbf{y}) \mathfrak{f}_{m,x_a}^{(a)}(\mathbf{x}), \tag{2.4.16}$$

$$\frac{N^{\gamma+\delta+2}}{N^{\alpha(m|m)}} G^{(2)}(\mathbf{x}) G^{(2)}(\mathbf{y}) = \frac{N^{3\gamma+2+\delta-4\beta}}{N^{\alpha(m|m)}} G^{(2)}(\mathbf{x}) G^{(2)}(\mathbf{y}), \tag{2.4.17}$$

$$\frac{N^{\beta+\delta+1}}{N^{\alpha(m|m)}} G^{(2)}(\mathbf{y}) \frac{G^{(2)}(\mathbf{x}_{\hat{a}} q_a) - G^{(2)}(\mathbf{x})}{x_a^2 - q_a^2} = \frac{N^{2\gamma+\delta+1-3\beta}}{N^{\alpha(m|m)}} G^{(2)}(\mathbf{y}) \frac{G^{(2)}(\mathbf{x}_{\hat{a}} q_a) - G^{(2)}(\mathbf{x})}{x_a^2 - q_a^2}. \tag{2.4.18}$$

Each of these identities leads to the condition:

$$2\beta = \gamma. \tag{2.4.19}$$

The SDE for the 4-point function with a disconnected boundary graph then writes:

$$\begin{aligned}
G_m^{(4)}(\mathbf{x}, \mathbf{y}) & = -\frac{2\lambda}{1 + |\mathbf{x}|^2} \sum_{a=1}^3 \left\{ \frac{1}{N^2} \sum_{\mathbf{q}_{\hat{a}}} G^{(2)}(\mathbf{q}_{\hat{a}} x_a) \left(\frac{G_m^{(4)}(\mathbf{x}, \mathbf{y})}{N^{4\beta-3\gamma-\delta-2}} \right) \right. \\
& + \frac{N^{4\gamma+\delta-6\beta}}{N^{\alpha(m|m)}} \left(\mathfrak{f}_{m|x_a}^{(a)}(\mathbf{x}, \mathbf{y}) + \mathfrak{f}_{m|x_a}^{(a)}(\mathbf{y}, \mathbf{x}) \right) \\
& + \frac{1}{N} \sum_{q_a} \frac{N^{2\gamma+\delta-3\beta+1}}{x_a^2 - q_a^2} (G_m^{(4)}(\mathbf{x}_{\hat{a}} q_a, \mathbf{y}) - G_m^{(4)}(\mathbf{x}, \mathbf{y})) \\
& \left. + \frac{N^{\alpha(V_1)+2\gamma+\delta-3\beta}}{N^{\alpha(m|m)}} \frac{1}{y_a^2 - x_a^2} (G_a^{(4)}(\mathbf{x}, \mathbf{y}) - G_a^{(4)}(\mathbf{x}_{\hat{a}} y_a, \mathbf{y})) + \frac{N^{3\gamma+\delta-4\beta}}{N^{\alpha(m|m)}} G^{(2)}(\mathbf{x}) \mathfrak{f}_{m,x_a}^{(a)}(\mathbf{y}) \right\}. \tag{2.4.20}
\end{aligned}$$

The first term of the RHS requires again (2.3.8); the third term gives again (2.3.6). Then, the fourth term gives the relation:

$$\alpha(m|m) \geq \alpha(V_1) + 2\gamma + \delta - 3\beta. \tag{2.4.21}$$

To obtain relations on the exponents from the last term we need the following expression

$$\begin{aligned}
\mathfrak{f}_{m,x_a}^{(a)}(\mathbf{y}) & = N^{\alpha(V_1)} G_a^{(4)}(\mathbf{y}; x_a, y_b, y_c) + \frac{N^{\alpha(V_1)+1}}{N} \sum_{c \neq a} \sum_{q_b} G_c^{(4)}(\mathbf{y}; x_a, q_b, y_c) \\
& + \frac{N^{\alpha(m|m)+2}}{N^2} \sum_{q_b, q_c} G_m^{(4)}(\mathbf{y}; x_a, q_b, q_c). \tag{2.4.22}
\end{aligned}$$

From the first term of this equation we recover the same relation between $\alpha(m|m)$ and $\alpha(V_1)$ as above, but we also have a stronger condition from the second term. This condition writes:

$$\alpha(m|m) \geq \alpha(V_1) + 2\gamma + \delta - 3\beta + 1, \quad (2.4.23)$$

which becomes an equality if one wants the second order graphs in the perturbation expansion (which are the lowest order graphs) to be leading order. The last term requires again (2.3.8). Finally, the terms in $\mathfrak{f}_{m|m,x_a}^{(a)}$ give the same type of relations as (2.3.23).

As a by-product of this computation we obtained the following result:

Proposition 2.4.1. *The Schwinger-Dyson equation for the 4-point function with disconnected boundary graph $G_m^{(4)}$ is:*

$$\begin{aligned} G_m^{(4)}(\mathbf{x}, \mathbf{y}) = & -\frac{2\lambda}{1+|\mathbf{x}|^2} \sum_{a=1}^3 \left\{ \sum_{\mathbf{q}_{\hat{a}}} G^{(2)}(\mathbf{q}_{\hat{a}}x_a) G_m^{(4)}(\mathbf{x}, \mathbf{y}) + \mathfrak{f}_{m|m,x_a}^{(a)}(\mathbf{x}, \mathbf{y}) + \mathfrak{f}_{m|m,x_a}^{(a)}(\mathbf{y}, \mathbf{x}) \right. \\ & + \sum_{q_a} \frac{1}{x_a^2 - q_a^2} (G_m^{(4)}(\mathbf{x}_{\hat{a}}q_a, \mathbf{y}) - G_m^{(4)}(\mathbf{x}, \mathbf{y})) + \frac{1}{y_a^2 - x_a^2} (G_a^{(4)}(\mathbf{x}, \mathbf{y}) - G_a^{(4)}(\mathbf{x}_{\hat{a}}y_a, \mathbf{y})) \\ & \left. + G^{(2)}(\mathbf{x}) \left(G_a^{(4)}(\mathbf{y}; x_a, y_b, y_c) + \sum_{c \neq a} \sum_{q_b} G_c^{(4)}(\mathbf{y}; x_a, q_b, y_c) + \sum_{q_b, q_c} G_m^{(4)}(\mathbf{y}; x_a, q_b, q_c) \right) \right\}. \end{aligned} \quad (2.4.24)$$

2.5 The SDE in the large N limit

In this section we find appropriate scalings which allow us to obtain a well defined SDE in the large N limit.

2.5.1 2- and 4-point functions

Using (2.3.2) and (2.4.19) one has:

$$\alpha = 0. \quad (2.5.1)$$

In the large N limit, we need the 2-point function SDE to have the following form:

$$G^{(2)}(\mathbf{x}) = \frac{1}{1+|\mathbf{x}|^2} - \frac{2\lambda}{1+|\mathbf{x}|^2} \sum_{a=1}^3 \sum_{\mathbf{q}_{\hat{a}}} G^{(2)}(\mathbf{q}_{\hat{a}}x_a) G^{(2)}(\mathbf{x}). \quad (2.5.2)$$

We need $4\beta = 3\gamma + \delta + 2$. Using (2.3.6), we get:

$$\delta = -2 - 2\beta, \quad (2.5.3)$$

$$\beta > -1. \quad (2.5.4)$$

The relations (2.3.17) and (2.4.19) between β and γ lead to:

$$0 > \beta > \gamma, \text{ or } \beta = \gamma = 0. \quad (2.5.5)$$

From the inequalities (2.3.18) and (2.3.25) on $\alpha(V_1)$, we get:

$$\alpha(V_1) = -2 - \beta. \quad (2.5.6)$$

From now on we chose $\beta = \gamma = 0$. Note that we could chose $0 > \beta > -1$. However, this would change the value of the exponents $\alpha(\mathcal{B})$ but would give the same SDE. Equations (2.5.3) and (2.5.6) thus become:

$$\alpha(V_1) = -2 = \delta. \quad (2.5.7)$$

Assuming that $\alpha(V_1) > \alpha(m|m)$ leads to:

$$-2 > \alpha(m|m) \geq -3, \quad (2.5.8)$$

When choosing

$$\alpha(m|m) = -3. \quad (2.5.9)$$

we have a well defined large N limit. Moreover, we can see that in general we need that $\alpha(\mathcal{B})$ decreases strictly with the number of points of the Green function and the number of connected components of \mathcal{B} . Hence at this point we can conjecture that

$$\alpha(\mathcal{B}) = 3 - B - 2k, \quad (2.5.10)$$

where $2k$ is the number of vertices of \mathcal{B} , B is its number of connected components.

With the scalings above, the SDE for the 2-point function is

$$\begin{aligned} G^{(2)}(\mathbf{x}) &= \frac{1}{1 + |\mathbf{x}|^2} - \frac{2\lambda}{1 + |\mathbf{x}|^2} \sum_{a=1}^3 \left(\frac{1}{N^2} \sum_{\mathbf{q}_a} G^{(2)}(\mathbf{q}_a x_a) G^{(2)}(\mathbf{x}) + \frac{1}{N^4} G_a^{(4)}(\mathbf{x}, \mathbf{x}) \right. \\ &+ \left. \frac{1}{N^5} \sum_{\mathbf{q}_a} G_{m|m}^{(4)}(\mathbf{q}_a x_a, \mathbf{x}) + \frac{1}{N^2} \sum_{q_a} \frac{G^{(2)}(\mathbf{x}_a q_a) - G^{(2)}(\mathbf{x})}{x_a^2 - q_a^2} + \frac{1}{N^4} \sum_{c \neq a} \sum_{q_b} G_c^{(4)}(\mathbf{x}, \mathbf{x}_b q_b) \right), \end{aligned} \quad (2.5.11)$$

where in the last term $b \neq c$ and $b \neq a$. For $N = \frac{\tilde{N}}{\Lambda}$ and using

$$\lim_{\tilde{N} \rightarrow \infty} \frac{\Lambda}{\tilde{N}} \sum_{k=1}^{\tilde{N}} f\left(\frac{k\Lambda}{\tilde{N}}\right) = \int_0^\Lambda dx f(x), \quad (2.5.12)$$

and taking the limit $\Lambda = \infty$ we get the following proposition:

Proposition 2.5.1. *The Schwinger-Dyson equation for the 2-point function in the large N limit is*

$$G^{(2)}(\mathbf{x}) = \left(1 + |\mathbf{x}|^2 + 2\lambda \sum_{c=1}^3 \int_0^\infty d\mathbf{q}_c G^{(2)}(\mathbf{q}_c x_c) \right)^{-1}, \quad (2.5.13)$$

where $d\mathbf{q}_{\hat{c}} = \prod_{d \neq c} dq_d$.

From this we get the SDE for the 4-point functions.

Corollary 2.5.2. *The Schwinger-Dyson equations for the 4-point functions in the large N limit are:*

$$G_a^{(4)}(\mathbf{x}, \mathbf{y}) = -2\lambda G^{(2)}(\mathbf{y}_{\hat{a}} x_a) G^{(2)}(\mathbf{y}) \frac{G^{(2)}(\mathbf{x}) - G^{(2)}(\mathbf{x}_{\hat{a}} y_a)}{y_a^2 - x_a^2}, \quad (2.5.14)$$

$$G_m^{(4)}(\mathbf{x}, \mathbf{y}) = -2\lambda (G^{(2)}(\mathbf{x}))^2 \sum_{a=1}^3 \left\{ \sum_{c \neq a} \int dq_b G_c^{(4)}(x_a, q_b, y_c, \mathbf{y}) + \int d\mathbf{q}_{\hat{a}} G_m^{(4)}(\mathbf{q}_{\hat{a}} x_a, \mathbf{y}) \right\}, \quad (2.5.15)$$

where we used the SDE for the 2-point function to rewrite the SDE for the 4-point functions and where $d\mathbf{q}_{\hat{a}} = dq_b dq_c$ for $a \neq b, c$.

2.5.2 Higher-point functions

Let us now look at the SDE for the higher-point functions with a connected boundary graph in the large N limit, and in particular to the 6-point functions.

From (2.3.22), we get

$$G_{\mathcal{B}}^{(2k)}(\mathbf{X}) = -\frac{2\lambda}{1 + |\mathbf{s}|^2} \sum_{a=1}^3 \left\{ \int d\mathbf{q}_{\hat{a}} G^{(2)}(\mathbf{q}_{\hat{a}} s_a) G_{\mathcal{B}}^{(2k)}(\mathbf{X}) \right. \\ \left. + N^{-\alpha(\mathcal{B})-2} \sum_{\rho=2}^k \frac{1}{(p_a^\rho)^2 - s_a^2} \frac{1}{Z_0} \left[\frac{\partial Z[J, \bar{J}]}{\partial \zeta_a(\mathcal{B}; 1, \rho)}(\mathbf{X}) - \frac{\partial Z[J, \bar{J}]}{\partial \zeta_a(\mathcal{B}; 1, \rho)}(\mathbf{X}|_{x_a^\gamma \rightarrow p_a^\rho}) \right] \right\}. \quad (2.5.16)$$

Let us analyse the large N limit of this equation. The first term in the RHS is always present in the large N limit, but the terms coming from the swappings can be of leading order or be neglected. Indeed, a swapping can add at most one more connected component (see figure 2.3), then the second term of the RHS can give differences of three type of terms: $N^{\alpha(m|\mathcal{B}')} G_{m|\mathcal{B}'}^{(2k)}$, $N^{\alpha(\mathcal{B}')} G^{(2)} G_{\mathcal{B}'}^{(2(k-1))}$ and $N^{\alpha(\mathcal{B}'')} G_{\mathcal{B}''}^{(2k)}$. The first type of term is neglected, since in the large N limit, we took $\alpha(m|\mathcal{B}') = \alpha(\mathcal{B}') - 1$ and $\alpha(\mathcal{B}') = \alpha(\mathcal{B}) + 2$, hence $\alpha(m|\mathcal{B}') - \alpha(\mathcal{B}) - 2 = -1$. However, the second type of term is of leading order since $\alpha(\mathcal{B}') - \alpha(\mathcal{B}) - 2 = 0$. Let us now analyse the last term, which is more involved. From the study of the 4-point functions one could think that $\alpha(\mathcal{B}) = \alpha(\mathcal{B}'')$ for all connected boundary graphs \mathcal{B} and \mathcal{B}'' with $2k$ vertices. Nevertheless, this does not hold. This follows from the analysis of the 6-point functions and in particular of $G_K^{(6)}$. In fact, applying the swapping procedure to K can only give $F_{a;bc}$ for $\{a, b, c\} = \{1, 2, 3\}$, which has six vertices. Hence if we take $\alpha(K) = \alpha(F_{a;bc})$ and from the previous discussion, we get, for $\mathbf{s} = (x_1, y_2, z_3)$, the SDE

$$G_K^{(6)}(\mathbf{x}, \mathbf{y}, \mathbf{z}) = -\frac{2\lambda}{1 + x_1^2 + y_2^2 + z_3^2} \sum_{a=1}^3 \int d\mathbf{q}_{\hat{a}} G^{(2)}(\mathbf{q}_{\hat{a}} s_a) G_K^{(6)}(\mathbf{x}, \mathbf{y}, \mathbf{z}). \quad (2.5.17)$$

However, this equation does not give any information on the 6-point function $G_K^{(6)}$. This implies that we need to define $\alpha(K)$ such that the terms in $G_{a;bc}^{(6)}$ are also of leading order. We thus need to have the following scaling:

$$\alpha(K) = \alpha(F_{a;bc}) - 2. \quad (2.5.18)$$

This gives the following SDE, for $\mathbf{s} = (x_1, y_2, z_3)$ and where we used equation (2.5.13):

$$\begin{aligned}
G_K^{(6)}(\mathbf{x}, \mathbf{y}, \mathbf{z}) = & -2\lambda G^{(2)}(x_1, y_2, z_3) \left\{ \frac{G_{1;23}^{(6)}(\mathbf{x}, \mathbf{z}, \mathbf{y}) - G_{1;23}^{(6)}(y_1, x_2, x_3, \mathbf{z}, \mathbf{y})}{y_1^2 - x_1^2} \right. \\
& + \frac{G_{1;23}^{(6)}(\mathbf{z}, \mathbf{x}, \mathbf{y}) - G_{1;23}^{(6)}(\mathbf{z}, \mathbf{y}, z_1, x_2, x_3)}{z_1^2 - x_1^2} + \frac{G_{2;13}^{(6)}(\mathbf{z}, \mathbf{x}, \mathbf{y}) - G_{2;13}^{(6)}(\mathbf{z}, \mathbf{x}, y_1, z_2, y_3)}{z_2^2 - y_2^2} \\
& + \frac{G_{1;23}^{(6)}(\mathbf{y}, \mathbf{z}, \mathbf{x}) - G_{1;23}^{(6)}(y_1, x_2, y_3, \mathbf{z}, \mathbf{x})}{x_2^2 - y_2^2} + \frac{G_{3;12}^{(6)}(\mathbf{z}, \mathbf{y}, \mathbf{x}) - G_{2;13}^{(6)}(z_1, z_2, x_3, \mathbf{z}, \mathbf{x})}{x_3^2 - z_3^2} \\
& \left. + \frac{G_{3;12}^{(6)}(\mathbf{y}, \mathbf{x}, \mathbf{z}) - G_{1;23}^{(6)}(\mathbf{y}, \mathbf{x}, z_1, z_2, y_3)}{y_3^2 - z_3^2} \right\}. \tag{2.5.19}
\end{aligned}$$

Note that this could be expected because K is the first non-planar graph which appears in our analysis. Moreover, in the large N limit and using (2.5.13), the SDE for the other 6-point functions with connected boundary graphs (see table 2.1) are

$$\begin{aligned}
G_1^{(6)}(\mathbf{x}, \mathbf{y}, \mathbf{z}) = & -2\lambda G^{(2)}(x_1, y_2, y_3) \left\{ G^{(2)}(\mathbf{y}) \frac{G_1^{(4)}(\mathbf{x}, \mathbf{z}) - G_1^{(4)}(y_1, x_2, x_3, \mathbf{z})}{y_1^2 - x_1^2} \right. \\
& \left. + G_1^{(4)}(\mathbf{y}, \mathbf{z}) \frac{G^{(2)}(\mathbf{x}) - G^{(2)}(z_1, x_2, x_3)}{z_1^2 - x_1^2} \right\}, \tag{2.5.20}
\end{aligned}$$

for $\mathbf{s} = (x_1, y_2, y_3)$, and

$$G_{1;23}^{(6)}(\mathbf{x}, \mathbf{y}, \mathbf{z}) = -2\lambda G^{(2)}(x_1, y_2, x_3) G^{(2)}(\mathbf{x}) \frac{G_3^{(4)}(\mathbf{y}, \mathbf{z}) - G_3^{(4)}(y_1, x_2, y_3, \mathbf{z})}{x_2^2 - y_2^2}, \tag{2.5.21}$$

for $\mathbf{s} = (x_1, y_2, x_3)$.

We can see that all these equations are algebraic. For a connected boundary graph of degree zero, the SDE depends only on lower-point functions with a connected boundary graph. However, the K SDE depends only on the other 6-point functions and the 2-point function.

Finally, from the previous discussions, we can conjecture a general formula for the scaling:

Conjecture 2.5.3. *The tensor field theory defined by the action*

$$\mathcal{S}[\varphi, \bar{\varphi}] = \sum_{\mathbf{x}} \bar{\varphi}^{\mathbf{x}} (1 + |\mathbf{x}|^2) \varphi^{\mathbf{x}} + \frac{\lambda}{N^2} \sum_{c=1}^3 \sum_{\mathbf{a}, \mathbf{b}} \varphi^{\mathbf{b}} \bar{\varphi}^{\mathbf{b}_c a_c} \bar{\varphi}^{\mathbf{a}_c b_c} \varphi^{\mathbf{a}}, \tag{2.5.22}$$

and the free energy

$$W[J, \bar{J}] = \sum_{k=1}^{\infty} \sum_{\substack{\mathcal{B} \in \partial_{S_{\text{int}}} \\ V(\mathcal{B})=2k}} \sum_{\mathbf{X}} \frac{N^{\alpha(\mathcal{B})}}{|\text{Aut}(\mathcal{B})|} G_{\mathcal{B}}^{(2k)}(\mathbf{X}) \cdot \mathbb{J}(\mathcal{B})(\mathbf{X}), \tag{2.5.23}$$

has a well defined large N limit with the scalings

$$\alpha(\mathcal{B}) = 3 - B - 2g - 2k, \tag{2.5.24}$$

where $2k$ is the number of vertices of \mathcal{B} , B its number of connected components and g its genus.

Note that, since we deal in this chapter with rank three tensors, for boundary graphs (where one colour is lost) the degree is the genus (see [80] and [81]).

2.6 Perturbative expansion and a simpler model

In this section we will compute the first orders of the perturbative expansion of the 2-point function. We use a Taylor subtraction scheme to renormalise the UV divergences. For simplicity, let us plug in equation (2.5.13), the following expansion of the 2-point function

$$G^{(2)}(\mathbf{x}) = \sum_{n \geq 0} \lambda^n G_n^{(2)}(\mathbf{x}), \quad (2.6.1)$$

in order to obtain a recursive equation for $n \geq 1$, which writes:

$$G_n^{(2)}(\mathbf{x}) = -\frac{2}{1+|\mathbf{x}|^2} \sum_{c=1}^3 \int d\mathbf{q}_{\hat{c}} \sum_{k=0}^{n-1} \left(G_k^{(2)}(\mathbf{q}_{\hat{c}}x_c) - \frac{\delta_{k0}}{1+|\mathbf{q}_{\hat{c}}|^2} \right) G_{n-k-1}^{(2)}(\mathbf{x}), \quad (2.6.2)$$

where $|\mathbf{q}_{\hat{c}}|^2 = \sum_{d \neq c} q_d^2$, the integration on q_c is over $[0, \infty]$, and when $k = 0$ we subtract the first Taylor term to regularise the divergent integration on the free propagator $G_0^{(2)}$.

2.6.1 Model with the 3 quartic melonic interactions

Using the recursive equation (2.6.2), we get

$$G_0^{(2)}(\mathbf{x}) = \frac{1}{1+|\mathbf{x}|^2}, \quad (2.6.3)$$

$$\begin{aligned} G_1^{(2)}(\mathbf{x}) &= -\frac{2}{(1+|\mathbf{x}|^2)^2} \sum_{c=1}^3 \int d\mathbf{q}_{\hat{c}} \left(\frac{1}{1+|\mathbf{q}_{\hat{c}}x_c|^2} - \frac{1}{1+|\mathbf{q}_{\hat{c}}|^2} \right) \\ &= \frac{\pi}{2(1+|\mathbf{x}|^2)^2} \sum_{c=1}^3 \log(x_c^2 + 1), \end{aligned} \quad (2.6.4)$$

$$\begin{aligned} G_2^{(2)}(\mathbf{x}) &= -\frac{2}{1+|\mathbf{x}|^2} \sum_{c=1}^3 \int d\mathbf{q}_{\hat{c}} \left\{ \left(\frac{1}{1+|\mathbf{q}_{\hat{c}}x_c|^2} - \frac{1}{1+|\mathbf{q}_{\hat{c}}|^2} \right) \frac{\pi}{2(1+|\mathbf{x}|^2)^2} \sum_{d=1}^3 \log(x_d^2 + 1) \right. \\ &\quad \left. + \frac{1}{1+|\mathbf{x}|^2} \frac{\pi}{2(1+|\mathbf{q}_{\hat{c}}x_c|^2)^2} \sum_{d=1}^3 \log((\mathbf{q}_{\hat{c}}x_c)_d + 1) \right\}, \end{aligned} \quad (2.6.5)$$

$$\begin{aligned} &= \frac{1}{(1+|\mathbf{x}|^2)^2} \left(\sum_{c=1}^3 \sum_{d=1}^3 \frac{\pi^2 \log(x_c^2 + 1) \log(x_d^2 + 1)}{4(1+|\mathbf{x}|^2)} - \sum_{c=1}^3 \frac{\pi \log(x_c^2 + 1)}{2(x_c^2 + 1)} \right. \\ &\quad \left. - \pi^2 \sum_{c=1}^3 \frac{x_c \log\left(\frac{1}{4}(x_c^2 + 1)\right) + 2 \tan^{-1}(x_c)}{2(x_c^3 + x_c)} \right). \end{aligned} \quad (2.6.6)$$

We can remark that the last term in $G_2^{(2)}(\mathbf{x})$ is the only term not containing powers of logarithms. It comes from the last term of (2.6.5) for $d \neq c$, which graphically corresponds to figure 2.4. This suggests that if we look at a model with only 1 pillow interaction, such graphs cannot exist, and the perturbative expansion should only be made of powers of logarithms.

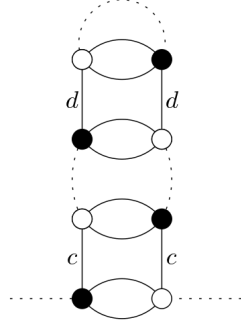


Figure 2.4: The only graphs at 2-loop order, giving contribution other than powers of logarithms for $d \neq c$.

2.6.2 Model with 1 quartic melonic interaction

Indeed, for only the pillow for the colour 1 as an interaction, we get:

$$G^{(2)}(\mathbf{x}) = \frac{1}{1 + |\mathbf{x}|^2} + \frac{\pi\lambda}{2(1 + |\mathbf{x}|^2)^2} \log(x_1^2 + 1) + \frac{(\pi\lambda)^2}{4(1 + |\mathbf{x}|^2)^2} \left(\frac{\log^2(x_1^2 + 1)}{(1 + |\mathbf{x}|^2)} - \frac{\log(x_1^2 + 1)}{(x_1^2 + 1)} \right) + O(\lambda^3). \quad (2.6.7)$$

In this case, we can notice that only two types of integrals appear:

$$\int d\mathbf{q}_1 \left(\frac{1}{1 + |\mathbf{q}_1 x_1|^2} - \frac{1}{1 + |\mathbf{q}_1|^2} \right) = -\frac{\pi}{4} \log(x_1^2 + 1), \quad (2.6.8)$$

$$\int d\mathbf{q}_1 \frac{1}{(1 + |\mathbf{q}_1 x_1|^2)^n} = \frac{\pi(1 + x_1^2)^{1-n}}{4(n-1)} \quad \text{for } n > 1. \quad (2.6.9)$$

Hence, we can compute easily higher orders in the loop expansion², which suggest the following form for all order n in the coupling

$$G_n^{(2)}(\mathbf{x}) = \left(\frac{\pi}{2} \right)^n \left(\frac{\log^n(1 + x_1^2)}{(1 + |\mathbf{x}|^2)^{n+1}} + \frac{(-1)^n}{(1 + x_1^2)^n} \sum_{k=1}^{n-1} (-1)^k \log^k(1 + x_1^2) \sum_{m=1}^k a_{n,k,m} \frac{(1 + x_1^2)^m}{(1 + |\mathbf{x}|^2)^{m+1}} \right), \quad (2.6.10)$$

where we conjecture that the numbers $a_{n,k,m}$ are

$$\begin{aligned} a_{n,k,m} &= \binom{n-1}{m-1} \frac{m!}{k!} |s_{n-m,n-k}| \\ &= (-1)^{k-m} (n-1)! m \frac{s_{n-m,n-k}}{(n-m)! k!}, \end{aligned} \quad (2.6.11)$$

where $s_{n,k}$ are the Stirling numbers of the 1st kind. Using the change of variable $j = n - m$, we have

$$b_{n,k,j} = (-1)^{k+j-n} (n-1)! (n-j) \frac{s_{j,n-k}}{j! k!}. \quad (2.6.12)$$

²We computed the expansion up to order 9 in the coupling using Mathematica.

Noting that $s_{j,n-k} = 0$ if $j < n - k$ and if $k = 0$ or $k = n$, we can write the sum on j from 1 to $n - 1$ and the sum on k from 0 to n . This leads to the following expression:

$$\begin{aligned} G_n^{(2)}(\mathbf{x}) &= \left(\frac{\pi}{2}\right)^n \left(\frac{\log^n(1+x_1^2)}{(1+|\mathbf{x}|^2)^{n+1}} + \frac{(-1)^n}{(1+x_1^2)^n} \sum_{k=1}^{n-1} (-1)^k \log^k(1+x_1^2) \sum_{m=1}^k a_{n,k,m} \frac{(1+x_1^2)^m}{(1+|\mathbf{x}|^2)^{m+1}} \right) \\ &= \left(\frac{\pi}{2}\right)^n \left(\frac{\log^n(1+x_1^2)}{(1+|\mathbf{x}|^2)^{n+1}} + (n-1)! \sum_{k=0}^n \sum_{j=1}^{n-1} \frac{s_{j,n-k}}{j!k!} \frac{(-1)^j(n-j)}{(1+|\mathbf{x}|^2)^{n+1-j}(1+x_1^2)^j} \log^k(1+x_1^2) \right). \end{aligned} \quad (2.6.13)$$

The structure of the perturbative expansion is similar to the one studied in [79]. In the next section, we will sum the expansion following the same method.

2.7 Resummation and solution

In this section we perform the resummation of the perturbative expansion to obtain an explicit expression for the 2-point function. Let us use the formulas

$$(-1)^j s_{j,n-k} = \frac{1}{(n-k)!} \frac{d^{n-k}}{du^{n-k}} \frac{\Gamma(j-u)}{\Gamma(-u)} \Big|_{u=0}, \quad (2.7.1)$$

$$\log^k(1+x_1^2) = \frac{d^k}{du^k} (1+x_1^2)^u \Big|_{u=0}, \quad (2.7.2)$$

to rewrite the second term of the RHS of (2.6.13) as

$$\begin{aligned} &\left(\frac{\pi}{2}\right)^n \sum_{j=1}^{n-1} \frac{n-j}{j!n} \frac{1}{(1+|\mathbf{x}|^2)^{n+1-j}(1+x_1^2)^j} \sum_{k=0}^n \binom{n}{k} \left(\frac{d^{n-k}}{du^{n-k}} \frac{\Gamma(j-u)}{\Gamma(-u)} \right) \left(\frac{d^k}{du^k} (1+x_1^2)^u \right) \Big|_{u=0} \\ &= \left(\frac{\pi}{2}\right)^n \sum_{j=1}^{n-1} \frac{n-j}{j!n} \frac{1}{(1+|\mathbf{x}|^2)^{n+1-j}(1+x_1^2)^j} \frac{d^n}{du^n} \left(\frac{\Gamma(j-u)}{\Gamma(-u)} (1+x_1^2)^u \right) \Big|_{u=0}. \end{aligned} \quad (2.7.3)$$

Then using

$$\begin{aligned} \frac{d^n}{du^n} \left(\frac{\Gamma(j-u)}{\Gamma(-u)} (1+x_1^2)^u \right) &= \frac{d^n}{du^n} \left((-1)^j (1+x_1^2)^j \frac{d^j}{d(x_1^2)^j} (1+x_1^2)^u \right) \Big|_{u=0} \\ &= (-1)^j (1+x_1^2)^j \frac{d^j}{d(x_1^2)^j} \log^n(1+x_1^2), \end{aligned} \quad (2.7.4)$$

and realising that the first term of the rhs of (2.6.13) corresponds to $j = 0$, we have

$$\begin{aligned} G_n^{(2)}(\mathbf{x}) &= \left(\frac{\pi}{2}\right)^n \left(\frac{\log^n(1+x_1^2)}{(1+|\mathbf{x}|^2)^{n+1}} + \sum_{j=1}^{n-1} \frac{n-j}{j!n} \frac{(-1)^j}{(1+|\mathbf{x}|^2)^{n+1-j}} \frac{d^j}{d(x_1^2)^j} \log^n(1+x_1^2) \right) \\ &= \left(\frac{\pi}{2}\right)^n \sum_{j=0}^{n-1} \frac{n-j}{j!n} \frac{(-1)^j}{(1+|\mathbf{x}|^2)^{n+1-j}} \frac{d^j}{d(x_1^2)^j} \log^n(1+x_1^2). \end{aligned} \quad (2.7.5)$$

We then write

$$\frac{1}{(1 + |\mathbf{x}|^2)^{n+1-j}} = \frac{(-1)^{n-j}}{(n-j)!} \frac{d^{n-j}}{d(x_1^2)^{n-j}} \frac{1}{(1 + |\mathbf{x}|^2)}, \quad (2.7.6)$$

to get

$$\begin{aligned} G^{(2)}(\mathbf{x}) &= \frac{1}{1 + |\mathbf{x}|^2} + \sum_{n=1}^{\infty} \left(\frac{\pi}{2}\right)^n \frac{(-1)^n \lambda^n}{n!} \sum_{j=0}^{n-1} \binom{n-1}{j} \frac{d^{n-j}}{d(x_1^2)^{n-j}} \frac{1}{(1 + |\mathbf{x}|^2)} \frac{d^j}{d(x_1^2)^j} \log^n(1 + x_1^2) \\ &= \frac{1}{1 + |\mathbf{x}|^2} - \sum_{n=1}^{\infty} \left(\frac{\pi}{2}\right)^n \frac{\lambda^n}{n!} \frac{d^{n-1}}{d(x_1^2)^{n-1}} \frac{(-\log(1 + x_1^2))^n}{(1 + |\mathbf{x}|^2)^2}. \end{aligned} \quad (2.7.7)$$

To sum this series, we use the Lagrange-Bürmann inversion formula [82], [83].

Theorem 2.7.1 (Lagrange-Bürmann inversion). *Let $\varphi(\omega)$ be a function analytic at $\omega = 0$, such that $\varphi(0) \neq 0$ and $f(\omega) = \frac{\omega}{\varphi(\omega)}$. The inverse function $g(z)$ of $f(\omega)$, defined such that $z = f(g(z))$, is analytic at $z = 0$ and given by*

$$g(z) = \sum_{n=1}^{\infty} \frac{z^n}{n!} \frac{d^{n-1}}{d\omega^{n-1}} \varphi(\omega)^n \Big|_{\omega=0}. \quad (2.7.8)$$

Moreover, for any analytic function $H(z)$ such that $H(0) = 0$,

$$H(g(z)) = \sum_{n=1}^{\infty} \frac{z^n}{n!} \frac{d^{n-1}}{d\omega^{n-1}} \left(H'(\omega) \varphi(\omega)^n \right) \Big|_{\omega=0}. \quad (2.7.9)$$

Hence, for $z = \frac{\pi}{2} \lambda$, $\varphi(\omega) = -\log(1 + \omega + x_1^2)$ and $H(\omega) = \frac{1}{1+\omega+|\mathbf{x}|^2} - \frac{1}{1+|\mathbf{x}|^2}$, equation (2.7.8) gives

$$g(x_1, z) = \sum_{n=1}^{\infty} \frac{z^n}{n!} \frac{d^{n-1}}{d(x_1^2)^{n-1}} (-\log(1 + x_1^2))^n, \quad (2.7.10)$$

such that

$$z = -\frac{g(x_1, z)}{\log(1 + g(x_1, z) + x_1^2)}, \quad (2.7.11)$$

which is solved by

$$g(x_1, z) = zW\left(\frac{1}{z}e^{\frac{1+x_1^2}{z}}\right) - 1 - x_1^2, \quad (2.7.12)$$

where $W(z)$ is the Lambert function defined by $z = W(ze^z)$. Then, using equation (2.7.9), we can write

$$G^{(2)}(\mathbf{x}) = \frac{1}{1 + |\mathbf{x}|^2} - \sum_{n=1}^{\infty} \frac{z^n}{n!} \frac{d^{n-1}}{d(x_1^2)^{n-1}} \frac{(-\log(1 + x_1^2))^n}{(1 + |\mathbf{x}|^2)^2} = \frac{1}{1 + |\mathbf{x}|^2 + g(x_1, z)}. \quad (2.7.13)$$

This result can be integrated:

$$\int d\mathbf{q}_1 \left(G(\mathbf{q}_1 x_1) - \frac{1}{1 + |\mathbf{q}_1|^2} \right) = -\frac{\pi}{4} \log(1 + x_1^2 + g(x_1, z)). \quad (2.7.14)$$

Using (2.5.13) for $c = 1$, we recover (2.7.11).

We have thus proved the following theorem:

Theorem 2.7.2. *The renormalised Schwinger-Dyson equation for the 2-point function*

$$G^{(2)}(\mathbf{x}) = \left(1 + |\mathbf{x}|^2 + 2\lambda \int d\mathbf{q}_1 (G(\mathbf{q}_1 x_1) - \frac{1}{1 + |\mathbf{q}_1|^2})\right)^{-1}, \quad (2.7.15)$$

is solved by

$$G^{(2)}(\mathbf{x}) = \frac{1}{1 + |\mathbf{x}|^2 + g(x_1, \frac{\pi}{2}\lambda)}, \quad (2.7.16)$$

$$g(x_1, z) = zW\left(\frac{1}{z}e^{\frac{1+x_1^2}{z}}\right) - 1 - x_1^2. \quad (2.7.17)$$

In the limit $\lambda \rightarrow 0$, using $W(x) = \log x - \log \log x + o(1)$ we get

$$\lim_{\lambda \rightarrow 0} \frac{\pi\lambda}{2} W\left(\frac{2}{\pi\lambda}e^{\frac{2(1+x_1^2)}{\pi\lambda}}\right) = 1 + x_1^2, \quad (2.7.18)$$

so that

$$\lim_{\lambda \rightarrow 0} G^{(2)}(\mathbf{x}) = \frac{1}{1 + |\mathbf{x}|^2}, \quad (2.7.19)$$

and we recover the free propagator, as expected.

We established our solution for $\lambda > 0$ with $x_1, x_2, x_3 \geq 0$ but it can be analytically extended. The Lambert function has many branches behaving differently on the complex plane [84], the branch assignment of our solution depends on λ . We give a short comment on the holomorphic extension of our solution in $z = \frac{\pi}{2}\lambda$ for a fixed \mathbf{x} , which is heavily based on [79] where all the details are discussed.

One first needs to study the map $z \rightarrow zW\left(\frac{1}{z}e^{\frac{1+x_1^2}{z}}\right)$ to get proposition 15 of [79]. Taking into account a rescaling of $\frac{2}{\pi}$ to translate their results in term of our λ , this map is holomorphic on $\mathbb{C} \setminus \{-\frac{2}{\pi}(1+x_1^2)\frac{\sin\alpha}{\alpha} | \frac{\sin\alpha}{\alpha} e^{\alpha \cot\alpha} \geq \frac{\pi e}{2(1+x_1^2)}, -\pi < \alpha < \pi\}$. Varying x_1 , the common holomorphic domain Ω is at the right of the curve $\mathcal{C} = \{-e^{1-\alpha \cot\alpha + i\alpha} | -\pi < \alpha < \pi\}$ and is not affected by the rescaling. In particular, it contains the disk $|\lambda| < 1$ and the map has a convergent radius ≥ 1 in λ for all $x_1 \geq 0$. In our case, we can have poles if $zW\left(\frac{1}{z}e^{\frac{1+x_1^2}{z}}\right) = -x_2^2 - x_3^2 \mp i\epsilon = -y \mp i\epsilon$ with $y > 0$. This equation can be solved with $\epsilon \rightarrow 0$ by $\lambda_{x_1}^\pm(y)$, a critical line in the z -plane, parametrised by y ($\lambda_a^\pm(\varphi)$ in the notation of [79], Lemma 18) and with a specific branch of the Lambert function. For this branch we would get a pole, however the actual branch assignment in our solution for $\lambda = \lambda_{x_1}^\pm(y)$ is a different branch and the critical line does not cause any singularity. The two-point function is then holomorphic in the domain Ω of the complex plane depicted in figure 1 of [79].

2.8 Higher-point functions

The boundary graphs of the model with 1 quartic melonic interaction have connected components of the form of figure 2.5. The $2k$ -point function SDE with connected boundary graph was derived in the section 1.5, taking the large N limit established in section 2.5, we get

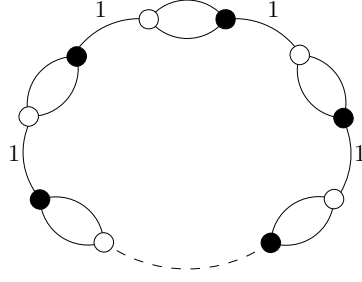


Figure 2.5: General form of the connected components of boundary graphs in the model with 1 quartic melonic interaction.

Corollary 2.8.1. *The Schwinger-Dyson equation for any $2k$ -point function with a connected boundary graph is given by*

$$G^{(2k)}(\mathbf{X}) = 2\lambda G^{(2)}(x_1^1, x_2^2, x_3^2) \times \sum_{\rho=2}^k G^{(2k-2\rho+2)}(\mathbf{x}^\rho, \dots, \mathbf{x}^k) \frac{G^{(2\rho-2)}(\mathbf{x}^1, \dots, \mathbf{x}^{\rho-1}) - G^{(2\rho-2)}(x_1^\rho, x_2^1, x_3^1, \dots, \mathbf{x}^{\rho-1})}{(x_1^1)^2 - (x_1^\rho)^2}. \quad (2.8.1)$$

From the solution (2.7.13) of the 2-point function SDE, we can recursively obtain any higher-point function with a connected boundary graph.

The case of disconnected boundary graph is more involved [74] and no general expression of the SDE in the large N limit have yet been obtained. The simplest equation is the SDE for the 4-point function with disconnected boundary graph, which for only 1 quartic interaction and in the large N limit reduces to

$$G_m^{(4)}(\mathbf{x}, \mathbf{y}) = -2\lambda (G^{(2)}(\mathbf{x}))^2 \int dq_2 dq_3 G_m^{(4)}(x_1, q_2, q_3, \mathbf{y}). \quad (2.8.2)$$

Analysing the perturbative expansion of $G_m^{(4)}$, we see that there is no contribution at order λ^0 , since the Feynman graph which can contribute (made with two free propagator) is disconnected. Moreover in the appendix C, we determined that the first contribution to the perturbative expansion is at order λ^2 and corresponds to graphs built with 2 different pillow interactions, of the form of the Feynman graph of figure 2.1 b). In the present case of the model with only 1 quartic melonic interaction, no such graph exists. Then, by plugging an expansion of the form of (2.6.1) for the 2- and 4-point functions in (2.8.2), we can recursively establish that all order of the perturbative expansion of $G_m^{(4)}$ are null. Hence, at leading order in the large N limit, $G_m^{(4)}$ is completely suppressed.

2.9 Conclusions and perspectives

In this chapter we have used the WTI to study the large N limit of SDE of tensor field theory. This allowed us to obtain explicit values for the scalings of the various terms appearing in the action our model. Then we have solved the 2-point function of a tensor field theory with 1 quartic melonic interaction, with building block the Lambert-W function, using a perturbative expansion and a Lagrange-Bürmann resummation. From this result,

all higher-point functions with connected boundary graph can be obtained recursively. Moreover, we have shown by a perturbative argument that the 4-point function with a disconnected boundary graph is null at leading order in the large N limit.

The first perspectives of this work is the proof of the conjecture (2.5.24) and the study of higher-point functions with disconnected boundary graph. Now one has to prove this conjecture using the SDE for disconnected boundary graph that have been determined in [74]. As in the connected boundary case, the large N limit of these SDE are expected to involve only lower correlation functions and in particular the 2-point function. The fact that the 4-point function with a disconnected boundary graph is null may indicate that at least some of the higher-point functions will also be suppressed at leading order in N .

A second perspective is the study the model with 3 quartic melonic interactions. The perturbative expansion is more involved and other techniques may need to be used.

Chapter 3

Non-Gaussian disorder average in the Sachdev-Ye-Kitaev model

This chapter is based of [85] written in collaboration with T. Krajewski, M. Laudonio and A. Tanasa.

3.1 Introduction

In this chapter, we investigate the behavior of the SYK model with couplings drawn from a non-Gaussian random distribution.

We first work with a version of the SYK model containing q flavors of complex fermions, each of them appearing once in the interaction. This model is very close in the spirit to the coloured tensor model (see the book [86]) and it is a particular case of a complex version of the Gross-Rosenhaus SYK generalisation proposed in [33]. This particular version of the SYK model has already been studied in [87], [88], [89], [47] and [90].

Following the approach proposed in [91] for tensor models and group field theory (see also [92], [66] and [93]), we first use a Polchinski-like flow equation to obtain Gaussian universality. This Gaussian universality result for the coloured tensor model was initially proved in [13]. Let us also mention here that this universality result for coloured tensor models was also exploited in [94], in a condensed matter physics setting, to identify an infinite universality class of infinite-range p -spin glasses with non-Gaussian correlated quenched distributions.

In this chapter we further obtain the effective action for the non-Gaussian averaged complex SYK model studied here. We show that the effect of this non-Gaussian averaging is a modification of the variance of the Gaussian distribution of couplings at leading order in N .

We then choose a specific quartic perturbation (known in the tensor model literature as a pillow or a melonic quartic perturbation, see for example, [61], [76], [17] or [95] or the TASI lectures on large N tensor models [41]) and, using the Hubbard-Stratanovitch (or the intermediate filed representation) for the disorder J , we explicitly compute the first order correction of the effective action and the modification of the Gaussian distribution of the couplings J at leading order in N . We then generalize these explicit calculations for the Gross-Rosenhaus SYK model proposed in [33] (the fermionic fields being this time real) and, as above, we obtain the first order correction of the Gross-Rosenhaus SYK

effective action and the modification of the Gaussian distribution of the couplings J at leading order in N .

For the sake of completeness, let us mention that in [96], the 4-point function of SYK model in a double-scaling limit was computed and the random couplings did not necessarily had to be independent and Gaussian - it was enough for these random couplings to be taken independent random variables, with zero mean and uniformly bounded moments independent of N .

The chapter is organised as follows. In the following section we introduce the complex SYK model we initially work with and we express the non-Gaussian potential as a sum over particular graphs. In section 3.3, the Gaussian universality result is exhibited, using a Polchinski-like equation. Section 3.4 is dedicated to the study of the the effective action for this model. In sections 3.5 and resp. 3.6 we perform our explicit calculations for quartic perturbations for the complex SYK and resp. the (real) Gross-Rosenhaus SYK generalisation. The section 3.7 lists some concluding remarks. For the sake of completeness, we derive the Dyson-Schwinger equations for the intermediate field used in this chapter in Appendix E. This construction follows the lines of [97], and it is done for both the complex SYK and resp. the (real) Gross-Rosenhaus SYK generalisation studied here.

3.2 A complex SYK model with non-Gaussian disorder

We study here a complex SYK model with q complex fermions $\psi_{i_a}^a(t)$, where the label $a = 1, \dots, q$ is the flavor and each fermion carries an index $i_a = 1, \dots, N$. The action writes:

$$S_J(\psi, \bar{\psi}) = \int dt \left(\sum_{a, i_a} \bar{\psi}_{i_a}^a \partial_t \psi_{i_a}^a + i^{\frac{q}{2}} \sum_{i_1, \dots, i_q} \bar{J}_{i_1, \dots, i_q} \psi_{i_1}^1 \cdots \psi_{i_q}^q + i^{\frac{q}{2}} \sum_{i_1, \dots, i_q} J_{i_1, \dots, i_q} \bar{\psi}_{i_1}^1 \cdots \bar{\psi}_{i_q}^q \right). \quad (3.2.1)$$

Here J_{i_1, \dots, i_q} is a rank q tensor that plays the role of a coupling constant. This model is close in spirit to tensor models and is a particular case of the Gross-Rosenhaus generalisation of the SYK model.

For the sake of completeness, let us mention that a bipartite complex SYK-like tensor model (without any fermion flavors and) with $O(N)^3$ symmetry was studied in the TASI lectures [41]. It was then found that one of the operators has a complex scaling dimension, which suggests that the nearly-conformal large N phase of the bipartite model is unstable.

The model (3.2.1) is subject to quenched disorder - we average the free energy (or connected correlation functions) over the couplings J . The most convenient way to perform this is through the use of replicas. We thus add an extra replica index $r = 1, \dots, n$ to the fermions. One has:

$$\langle \log Z(J) \rangle_J = \lim_{n \rightarrow 0} \frac{\langle Z^n(J) \rangle_J - 1}{n}, \quad (3.2.2)$$

with

$$Z^n(J) = \int \prod_{1 \leq r \leq n} [d\psi_r][d\bar{\psi}_r] \exp \sum_r S_J(\psi_r, \bar{\psi}_r). \quad (3.2.3)$$

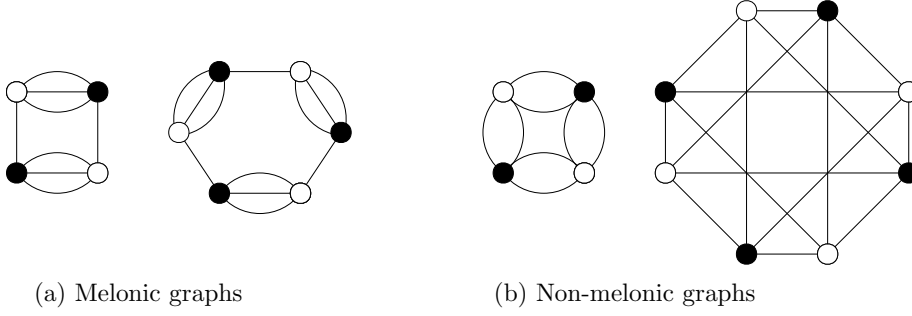


Figure 3.1: Examples of melonic and non-melonic graphs for $q = 4$.

The averaging over J is performed with a possibly non-Gaussian weight:

$$\langle Z^n(J) \rangle_J = \frac{\int dJ d\bar{J} Z^n(J) \exp \left[- \left[\frac{N^{q-1}}{\sigma^2} J\bar{J} + V_N(J, \bar{J}) \right] \right]}{\int dJ d\bar{J} \exp \left[- \left[\frac{N^{q-1}}{\sigma^2} J\bar{J} + V_N(J, \bar{J}) \right] \right]}. \quad (3.2.4)$$

We further impose that the potential V_N is invariant under independent unitary transformations:

$$J_{i_1, \dots, i_q} \rightarrow \sum_{j_1, \dots, j_q} U_{i_1 j_1}^1 \cdots U_{i_q j_q}^q J_{j_1, \dots, j_q}, \quad \bar{J}_{i_1, \dots, i_q} \rightarrow \sum_{\bar{j}_1, \dots, \bar{j}_q} \bar{U}_{i_1 \bar{j}_1}^1 \cdots \bar{U}_{i_q \bar{j}_q}^q \bar{J}_{\bar{j}_1, \dots, \bar{j}_q}. \quad (3.2.5)$$

Assuming that the potential V_N is a polynomial (or an analytic function) in the couplings J and \bar{J} , this invariance imposes that the potential can be expanded over particular graphs, as follows. Let us consider (non necessarily connected) graphs¹ Γ with black and white vertices of valence q . The edges of such a graph connect only black to white vertices (we thus have bipartite graphs) and are labelled by a colour $a = 1, \dots, q$ in such a way that, at each vertex, the q incident edges carry distinct colours (we thus have edge-coloured graphs). Let us mention that each edge colour of these graphs Γ corresponds to a fermion flavor of the model. See Fig. 3.1 for some examples of such graphs: melonic graphs on figure (a) and non-melonic graphs on figure (b). A graph is called melonic if for any vertex v , there is another vertex \bar{v} such that the removal of v and \bar{v} yields exactly q connected components (including isolated lines).

The most general form of the potential is expanded over these graphs as:

$$V_N(J, \bar{J}) = \sum_{\text{graph } \Gamma} \lambda_\Gamma \frac{N^{q-k(\Gamma)}}{\text{Sym}(\Gamma)} \langle J, \bar{J} \rangle_\Gamma, \quad (3.2.6)$$

where we have used the shorthand for the contraction of tensors along the graph Γ

$$\langle J, \bar{J} \rangle_\Gamma = \sum_{1 \leq i_{v,a}, \dots, i_{\bar{v},a} \leq N} \prod_{\substack{\text{white} \\ \text{vertices } v}} J_{i_{v,1}, \dots, i_{v,q}} \prod_{\substack{\text{black} \\ \text{vertices } \bar{v}}} \bar{J}_{i_{\bar{v},1}, \dots, i_{\bar{v},q}} \prod_{\substack{\text{edges} \\ e=(v, \bar{v})}} \delta_{i_{v,c(e)}, i_{\bar{v},c(e)}}. \quad (3.2.7)$$

In this expression, λ_Γ is a real number, $k(\Gamma)$ is the number of connected components of Γ and $\text{Sym}(\Gamma)$ its symmetry factor. The contraction of indices means that each white vertex carries a tensor J , each black vertex a tensor \bar{J} and that the indices have to be

¹These graphs are called bubbles in the tensor model literature (see again the book [86]).

contracted by identifying two indices on both sides of an edge, the place of the index in the tensor being defined by the colour of the edge denoted by $c(e)$.

The Gaussian term corresponds to a dipole graph (a white vertex and a black vertex, related by q lines) and reads

$$\frac{N^{q-1}}{\sigma^2} J \bar{J} = \frac{N^{q-1}}{\sigma^2} \sum_{1 \leq i_1, \dots, i_q \leq N} J_{i_1, \dots, i_q} \bar{J}_{i_1, \dots, i_q}. \quad (3.2.8)$$

Introducing the pair of complex conjugate tensors K and \bar{K} defined by

$$K_{i_1, \dots, i_q} = i^{\frac{q}{2}} \sum_r \int dt \psi_{i_1, r}^1 \cdots \psi_{i_q, r}^q, \quad \bar{K}_{i_1, \dots, i_q} = i^{\frac{q}{2}} \sum_r \int dt \bar{\psi}_{i_1, r}^1 \cdots \bar{\psi}_{i_q, r}^q, \quad (3.2.9)$$

the averaged partition function reads

$$\langle Z^n(J) \rangle_J = \frac{\int [d\psi][d\bar{\psi}] \exp \left[-\int dt \sum_{a, i_a, r} \bar{\psi}_{i_a, r}^a \partial_t \psi_{i_a, r}^a \right] \int dJ d\bar{J} \exp \left[-\left[\frac{N^{q-1}}{\sigma^2} J \bar{J} + V_N(J, \bar{J}) + J \bar{K} + \bar{J} K \right] \right]}{\int dJ d\bar{J} \exp \left[-\left[\frac{N^{q-1}}{\sigma^2} J \bar{J} + V_N(J, \bar{J}) \right] \right]}. \quad (3.2.10)$$

After a shift of variables in the integral over J and \bar{J} , the integral on J and \bar{J} in the numerator reads

$$\exp \left[-\frac{\sigma^2}{N^{q-1}} K \bar{K} \right] \int dJ d\bar{J} \exp \left[-\left[\frac{N^{q-1}}{\sigma^2} J \bar{J} + V_N \left(J - \frac{\sigma^2}{N^{q-1}} K, \bar{J} - \frac{\sigma^2}{N^{q-1}} \bar{K} \right) \right] \right]. \quad (3.2.11)$$

In order to study the large N limit of the average (3.2.10), we introduce the background field effective potential, with $L = -\frac{\sigma^2}{N^{q-1}} K$ and $\bar{L} = -\frac{\sigma^2}{N^{q-1}} \bar{K}$. One has:

$$V_N(s, L, \bar{L}) = -\log \int dJ d\bar{J} \exp \left[-\left[\frac{N^{q-1}}{s} J \bar{J} + V_N \left(J + L, \bar{J} + \bar{L} \right) \right] \right] + N^q \log \frac{\pi s}{N^{q-1}}. \quad (3.2.12)$$

In this framework, s is a parameter that interpolates between the integral we have to compute, at $s = \sigma^2$ (up to a trivial multiplicative constant) and the potential we started with at $s = 0$ (no integration and $J = \bar{J} = 0$). The inclusion of the constant ensures that the effective potential remains zero when we start with a vanishing potential. This comes to:

$$\begin{aligned} & \int dJ d\bar{J} \exp \left[-\left[\frac{N^{q-1}}{\sigma^2} J \bar{J} + V_N \left(J - \frac{\sigma^2}{N^{q-1}} K, \bar{J} - \frac{\sigma^2}{N^{q-1}} \bar{K} \right) \right] \right] \\ &= \left(\frac{N^{q-1}}{\pi \sigma^2} \right)^{N^q} \exp \left[-V_N \left(s = \sigma^2, L = -\frac{\sigma^2}{N^{q-1}} K, \bar{L} = -\frac{\sigma^2}{N^{q-1}} \bar{K} \right) \right]. \end{aligned} \quad (3.2.13)$$

In the next section, we will derive the large N behaviour of the effective potential using a Polchinski-like flow equation.

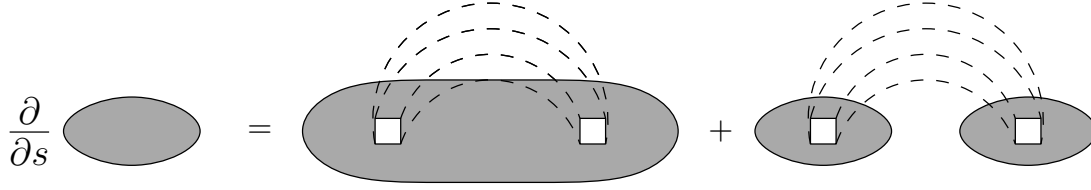


Figure 3.2: Graphical representation of equation (3.3.1) for $q = 4$.

3.3 Gaussian universality

This section follows the approach proposed in [91] (see also [92], [66] or [93]). Using standard QFT manipulations (see for example, the book [98]), one can show that the effective potential $V_N(s, L, \bar{L})$ (see eq. (3.2.12)) obeys the following differential equation:

$$\frac{\partial V}{\partial s} = \frac{1}{N^{q-1}} \sum_{1 \leq i_1, \dots, i_q \leq N} \left(\frac{\partial^2 V}{\partial L_{i_1, \dots, i_q} \partial \bar{L}_{i_1, \dots, i_q}} - \frac{\partial V}{\partial L_{i_1, \dots, i_q}} \frac{\partial V}{\partial \bar{L}_{i_1, \dots, i_q}} \right). \quad (3.3.1)$$

One can represent this equation in a graphical way as shown in Fig. 3.2. The first term on the RHS corresponds to an edge closing a loop in the graph and the second term in the RHS corresponds to a bridge (or an 1PR) edge. This equation is formally a Polchinski-like equation [99], albeit there are no short distance degrees of freedom over which we integrate. In our context it simply describes a partial integration with a weight s and will be used to control the large N limit of the effective potential.

Since the effective potential is also invariant under the unitary transformations defined in eq. (3.2.5), it may also be expanded over graphs as in (3.2.7),

$$V_N(s, L, \bar{L}) = \sum_{\text{graph } \Gamma} \lambda_\Gamma(s) \frac{N^{q-k(\Gamma)}}{\text{Sym}(\Gamma)} \langle L, \bar{L} \rangle_\Gamma, \quad (3.3.2)$$

with s dependent couplings $\lambda_\Gamma(s)$.

Inserting this graphical expansion in the differential equation (3.3.1), we obtain a system of differential equations for the couplings,

$$\frac{d\lambda_\Gamma}{ds} = \sum_{\Gamma' / (\bar{v}v) = \Gamma} N^{k(\Gamma) - k(\Gamma') + e(v, \bar{v}) - q + 1} \lambda_{\Gamma'} - \sum_{(\Gamma' \cup \Gamma'') / (\bar{v}v) = \Gamma} \lambda_{\Gamma'} \lambda_{\Gamma''}. \quad (3.3.3)$$

A derivation of the potential V with respect to L_{i_1, \dots, i_q} (resp. $\bar{L}_{i_1, \dots, i_q}$) removes a white vertex (resp. a black vertex). Then, the summation over the indices in i_1, \dots, i_q in (3.3.1) reconnects the edges, respecting the colours.

In the first term on the RHS of (3.3.1), given a graph Γ in the expansion of the LHS, we have to sum over all graphs Γ' and pairs of a white vertex v and a black vertex \bar{v} in Γ' such that the graph $\Gamma' / (\bar{v}v)$ obtained after reconnecting the edges (discarding the connected components made of single lines) is equal to Γ - see Fig. 3.3 and Fig. 3.4.

The number $e(v, \bar{v})$ is the number of edges directly connecting v and \bar{v} in Γ . After summation over the indices, each of these lines yields a power of N , which gives the factor of $N^{e(v, \bar{v})}$.

The operation of removing two vertices and reconnecting the edges can at most increase the number of connected components (including the graphs made of single closed lines)

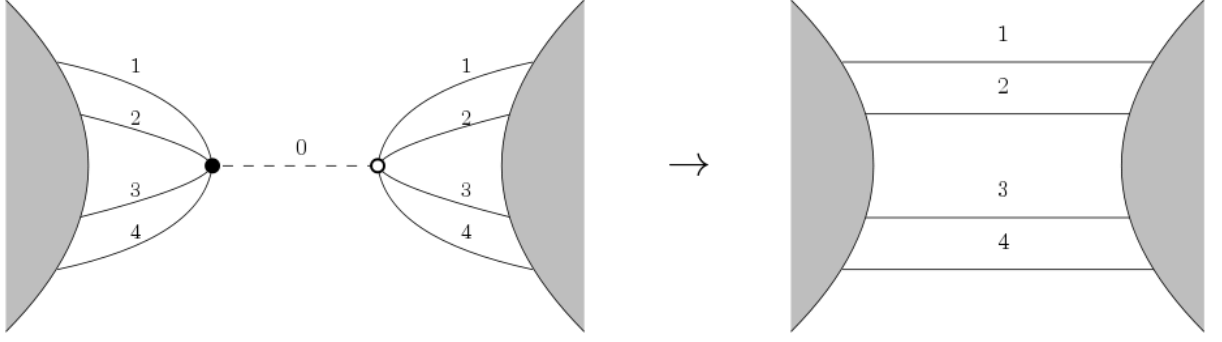


Figure 3.3: Removal of a white and a black vertex and reconnection of the edges.

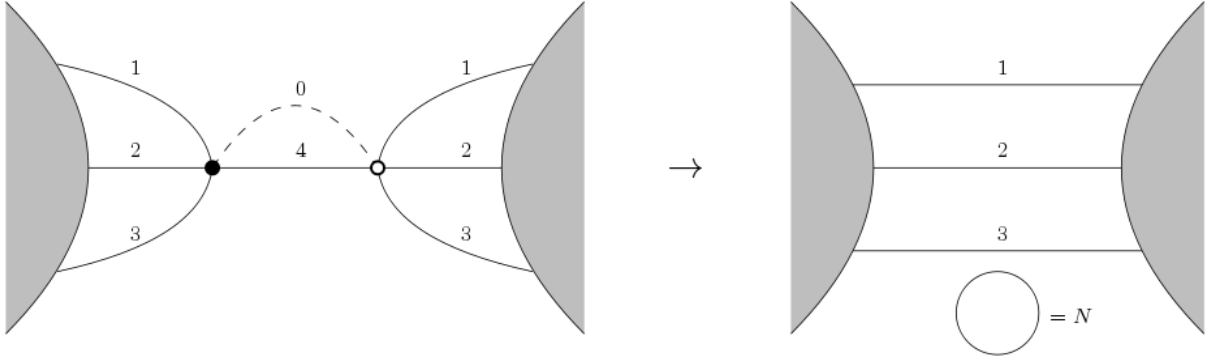


Figure 3.4: Removal of a white and a black vertex and reconnection of the edges creating a loop.

by $q-1$, so that we always have $k(\Gamma) - k(\Gamma') + e(v, \bar{v}) - q + 1 \leq 0$. We obtain the equality if and only if Γ' is a melonic graph. Therefore, in the large N limit, only melonic graphs survive in the first term on the RHS of (3.3.3).

In the second term, we sum over graphs Γ' and white vertices $v \in \Gamma'$ and graphs Γ'' and black vertices $\bar{v} \in \Gamma''$, with the condition that the graph obtained after removing the vertices and reconnecting the lines $(\Gamma' \cup \Gamma'') / (\bar{v}v)$ is equal to Γ . In that case, the number of connected components necessarily diminishes by 1, so that all powers of N cancel.

The crucial point in the system (3.3.3) is that only negative (or null) powers of N appear. It can be written as

$$\frac{d\lambda_\Gamma}{ds} = \beta_0(\{\lambda_\Gamma\}) + \frac{1}{N}\beta_1(\{\lambda_\Gamma\}) + \dots \quad (3.3.4)$$

As a consequence, if $\lambda_\Gamma(s=0)$ is bounded, then $\lambda_\Gamma(s)$ is also bounded for all s (i.e. it does not contain positive powers of N).

Let us now substitute $L = -\frac{\sigma^2}{N^{q-1}}K$ and $\bar{L} = -\frac{\sigma^2}{N^{q-1}}\bar{K}$ in the expansion of the effective potential (3.2.7),

$$V_N\left(s = \sigma^2, L = -\frac{\sigma^2}{N^{q-1}}K, \bar{L} = -\frac{\sigma^2}{N^{q-1}}\bar{K}\right) = \sum_{\text{graph } \Gamma} \lambda_\Gamma(\sigma^2) \frac{(-\sigma^2)^{v(\Gamma)} N^{q-k(q)-(q-1)v(\Gamma)}}{\text{Sym}(\Gamma)} \langle K, \bar{K} \rangle_\Gamma. \quad (3.3.5)$$

Here $v(\Gamma)$ the number of vertices of Γ . The exponent of N can be rewritten as $(q-1)(1-v(\Gamma)) + 1 - k(\Gamma)$. It has its maximal value for $v(\Gamma) = 2$ and $k(\Gamma) = 1$, which corresponds

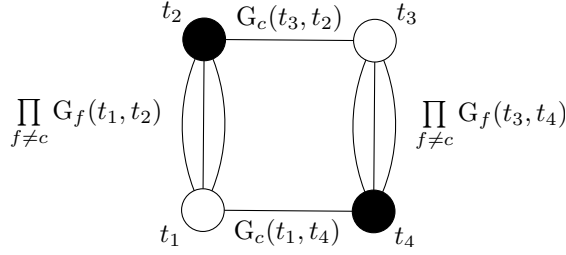


Figure 3.5: Graphical representation of the term $\langle G \rangle_\Gamma$ for the quartic melonic graph for $q = 4$.

to the dipole graph. This is a re-expression the Gaussian universality property of random tensors.

3.4 Effective action

Taking into account the non-Gaussian quenched disorder, we derive the effective action for the bilocal invariants,

$$G_{r,r'}^a(t, t') = \frac{1}{N} \sum_i \psi_{i,r}^a(t_1) \bar{\psi}_{i,r'}^a(t'). \quad (3.4.1)$$

Note that these invariants carry one flavour label a and two replica indices r, r' .

To this end, let us come back to the partition function (3.2.10). We then express the result of the average over J and \bar{J} as a sum over graphs Γ using the expansion of the effective potential (3.3.5) and replacing the tensors K and \bar{K} in terms of the fermions ψ and $\bar{\psi}$ (see eq. (3.2.9)).

Each graph Γ then involves the combination

$$\langle K, \bar{K} \rangle_\Gamma = \sum_{1 \leq i_v, a, \dots, i_{\bar{v}}, a \leq N} \prod_{\substack{\text{white} \\ \text{vertices } v}} \sum_{r_v} \int dt_v \psi_{i_v, 1, r_v}^1(t_v) \cdots \psi_{i_v, q, r_v}^q(t_v) \\ \prod_{\substack{\text{black} \\ \text{vertices } \bar{v}}} \sum_{r_{\bar{v}}} \int dt_{\bar{v}} \bar{\psi}_{i_{\bar{v}}, 1, r_{\bar{v}}}^1 \cdots \bar{\psi}_{i_{\bar{v}}, q, r_{\bar{v}}}^q(t_{\bar{v}}) \prod_{\substack{\text{edges} \\ e=(v, \bar{v})}} \delta_{i_v, c(e), i_{\bar{v}}, c(e)}. \quad (3.4.2)$$

After introducing the Lagrange multiplier Σ to enforce the constraint (3.4.1) and assuming a replica symmetric saddle-point, the effective action of our model writes:

$$\frac{\mathcal{S}_{eff}[\mathbf{G}, \Sigma]}{N} = - \sum_{f=1}^q \log \det (\delta(t_1 - t_2) \partial_t - \Sigma_f(t_1, t_2)) + \int dt \sum_{f=1}^4 \Sigma_f(\mathbf{t}) G_f(\mathbf{t}) \\ - \sum_{\Gamma} N^{-(v(\Gamma)-2)(q/2-1)+1-k(\Gamma)} \mu_\Gamma(\sigma^2, \{\lambda_{\Gamma'}\}) \langle G \rangle_\Gamma, \quad (3.4.3)$$

The term $\langle G \rangle_\Gamma$ associated to a graph Γ is constructed as follows:

- to each vertex associate a real variable t_v ;
- to an edge of colour c joining v to v' associate $G_c(t_v, t_{v'})$;

- multiply all edge contributions and integrate over vertex variables.

We then add up these contributions, with a weight λ_Γ and a power of N given by (with $e(\gamma)$ the number of edges of Γ , obeying $2e(\Gamma) = qv(\Gamma)$)

$$N^{q-k(\Gamma)} \times (N^{-(q-1)})^{v(\Gamma)} \times N^{e(\Gamma)} = N \times N^{-(v(\Gamma)-2)(q/2-1)+1-k(\Gamma)}. \quad (3.4.4)$$

At leading order in N , only the Gaussian terms survives (*i. e.* the graph Γ with ($v(\Gamma) = 2$ and $k(\Gamma) = 1$)), except for the matrix model case ($q = 2$). In this case, all terms corresponding to connected graphs survive. Let us emphasise that the variance of the Gaussian distribution of coupling is thus modified, as a consequence of the non-Gaussian averaging of our model. Remarkably, for $q > 2$, this is the only modification at leading order in N .

Moreover, the actual value of the covariance (which we denote by σ') induced by non Gaussian disorder is most easily computed using a Schwinger-Dyson equation, see [100]. In our context, the latter arises from

$$\sum_{i_1 \dots i_q} \int dJ d\bar{J} \frac{\partial}{\partial \bar{J}_{i_1 \dots i_q}} \left\{ J_{i_1 \dots i_q} \exp \left[- \left[\frac{N^{q-1}}{\sigma^2} J \bar{J} + V_N(J, \bar{J}) \right] \right] \right\} = 0. \quad (3.4.5)$$

At large N , it leads to the algebraic equation

$$1 = \frac{\sigma'^2}{\sigma^2} + \sum_{\text{melonic graph } \Gamma} \frac{\lambda_\Gamma}{\text{Sym}(\Gamma)} (\sigma')^{v(\Gamma)}. \quad (3.4.6)$$

Let us end this section by emphasising that the new terms induced by non-Gaussian randomness do not lead to any terms that could break reparametrisation invariance in situations where the kinetic term can be omitted.

This effective action, despite being non local, is invariant under reparametrisation (in the IR) at all orders in $1/N$:

$$G(t, t') \rightarrow \left(\frac{d\varphi}{dt}(t) \right)^\Delta \left(\frac{d\varphi}{dt'}(t') \right)^\Delta G(\varphi(t), \varphi(t')). \quad (3.4.7)$$

Indeed, changing the vertex variables as $t_v \rightarrow \varphi(t_v)$, the jacobians exactly cancel with the rescaling of G since $\Delta = 1/q$ and all vertices are q -valent.

3.5 A quartic perturbation computation

In this section we consider the case $q = 4$ with a quartic perturbation of the disorder. We explicitly compute the modification of the variance with respect to the Gaussian averaged model and we write down the effective action.

3.5.1 The quartic perturbed model

The action writes:

$$\mathcal{S}[\psi, \bar{\psi}] = \int dt \left(\sum_{f=1}^4 \sum_{i=1} \bar{\psi}_i^f \frac{d}{dt} \psi_i^f - \sum_{i,j,k,l} \bar{J}_{ijkl} \psi_i^1 \psi_j^2 \psi_k^3 \psi_l^4 - \sum_{i,j,k,l} J_{ijkl} \bar{\psi}_i^1 \bar{\psi}_j^2 \bar{\psi}_k^3 \bar{\psi}_l^4 \right). \quad (3.5.1)$$

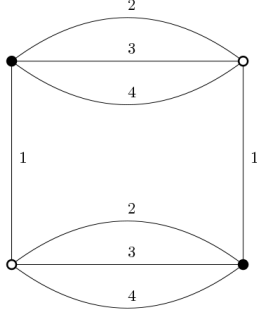


Figure 3.6: The pillow interaction for a particular choice of colours of its edges.

The coupling constant is a random tensor of rank 4 with the non-Gaussian potential given by:

$$V_N(J, \bar{J}) = N^3 \lambda \sum_{c=1}^4 \sum_{I, K} J_I \bar{J}_{I_{\hat{c}k_c}} J_K \bar{J}_{K_{\hat{c}i_c}}, \quad (3.5.2)$$

where $I = (i_1, i_2, i_3, i_4)$, $I_{\hat{c}k_c}$ means that i_c is replaced by k_c . It is the rank 4 pillow interaction as we have seen for arbitrary rank in Chapter 1, see Fig. 3.6 for its graphical representation.

We need to integrate over the disorder the replicated generating functional

$$\begin{aligned} \langle Z^n \rangle_J = & \int \mathcal{D}\psi_i^{f,a} \mathcal{D}\bar{\psi}_i^{f,a} \mathcal{D}J \mathcal{D}\bar{J} \exp \left(- \int dt \left(\sum_{a=1}^n \sum_{f=1}^4 \sum_i \bar{\psi}_i^{f,a} \frac{d}{dt} \psi_i^{f,a} \right) - \frac{N^3}{\sigma^2} \sum_{i,j,k,l} J_{ijkl} \bar{J}_{ijkl} \right. \\ & \left. + \int dt \left(\sum_{a=1}^n \sum_{i,j,k,l} \bar{J}_{ijkl} \psi_i^{1,a} \psi_j^{2,a} \psi_k^{3,a} \psi_l^{4,a} + \sum_{a=1}^n \sum_{i,j,k,l} J_{ijkl} \bar{\psi}_i^{1,a} \bar{\psi}_j^{2,a} \bar{\psi}_k^{3,a} \bar{\psi}_l^{4,a} \right) - V_N(J, \bar{J}) \right). \end{aligned} \quad (3.5.3)$$

3.5.2 Hubbard-Stratonovich transformation for the disorder

We start by rewriting the quartic term in J and \bar{J} using a Hubbard-Stratonovich transformation (or intermediate field representation, see for example [101] or [97])

$$e^{-N^3 \lambda \sum_{I,K} J_I \bar{J}_{I_{\hat{c}k_c}} J_K \bar{J}_{K_{\hat{c}i_c}}} = \sqrt{\frac{N^3}{2\pi}} \int dM^{(c)} e^{-\frac{N^3}{2} \text{Tr}((M^{(c)})^2) - iN^3 \left(\frac{\lambda}{2}\right)^{\frac{1}{2}} \sum_{I,j} \bar{J}_{I_{\hat{c}j}} M_{ij}^{(c)} J_I}, \quad (3.5.4)$$

where $M^{(c)}$ is an $N \times N$ Hermitian matrix, for $c \in \{1, 2, 3, 4\}$. In (3.5.3), keeping only the terms in J and \bar{J} , we get

$$\begin{aligned} \int \mathcal{D}J \mathcal{D}\bar{J} \exp \left(- \frac{N^3}{\sigma^2} \sum_{i,j,k,l} J_{ijkl} \bar{J}_{ijkl} - iN^3 \left(\frac{\lambda}{2}\right)^{\frac{1}{2}} \sum_{c=1}^4 \sum_{I,j} J_I M_{ij}^{(c)} \bar{J}_{I_{\hat{c}j}} \right. \\ \left. + \int dt \sum_{a=1}^n \sum_{i,j,k,l} \left(\bar{J}_{ijkl} \psi_i^{1,a} \psi_j^{2,a} \psi_k^{3,a} \psi_l^{4,a} + J_{ijkl} \bar{\psi}_i^{1,a} \bar{\psi}_j^{2,a} \bar{\psi}_k^{3,a} \bar{\psi}_l^{4,a} \right) \right). \end{aligned} \quad (3.5.5)$$

Following [97], we introduce the notation $\mathcal{M}_c = 1^{\otimes(c-1)} \otimes M^{(c)} \otimes 1^{\otimes(4-c)}$ for $c \in \{1, 2, 3, 4\}$. We can thus rewrite eq. (3.5.5) as

$$\int \mathcal{D}J \mathcal{D}\bar{J} \exp \left(-N^3 \bar{J} \left(\frac{1}{\sigma^2} 1^{\otimes 4} + i \left(\frac{\lambda}{2} \right)^{\frac{1}{2}} \sum_{c=1}^4 \mathcal{M}_c \right) J + \int dt \sum_{a=1}^n \sum_{i,j,k,l} \left(\bar{J}_{ijkl} \psi_i^{1,a} \psi_j^{2,a} \psi_k^{3,a} \psi_l^{4,a} + J_{ijkl} \bar{\psi}_i^{1,a} \bar{\psi}_j^{2,a} \bar{\psi}_k^{3,a} \bar{\psi}_l^{4,a} \right) \right). \quad (3.5.6)$$

Then, after rescaling $(J, \bar{J}) \rightarrow N^{\frac{3}{2}}(J, \bar{J})$, we can perform the integral over the disorder. Eq. (3.5.6) thus rewrites:

$$\frac{(2\pi)^N}{\det \left(\frac{1}{\sigma^2} 1^{\otimes 4} + i \left(\frac{\lambda}{2} \right)^{\frac{1}{2}} \sum_{c=1}^4 \mathcal{M}_c \right)} \exp \left(N^{-3} \int dt_1 dt_2 \sum_{a,b=1}^n \prod_{f=1}^4 \psi^{f,a}(t_1) \left(\frac{1}{\sigma^2} 1^{\otimes 4} + i \left(\frac{\lambda}{2} \right)^{\frac{1}{2}} \sum_{c=1}^4 \mathcal{M}_c \right)^{-1} \prod_{f=1}^4 \bar{\psi}^{f,b}(t_2) \right). \quad (3.5.7)$$

Hence, the replicated generating functional (3.5.3) writes

$$\begin{aligned} \langle Z^n \rangle_J &= \int \mathcal{D}\psi_i^{f,a} \mathcal{D}\bar{\psi}_i^{f,a} \mathcal{D}M^{(c)} \exp \left(- \int dt \sum_{a=1}^n \sum_{f=1}^4 \sum_i \bar{\psi}_i^{f,a} \frac{d}{dt} \psi_i^{f,a} \right. \\ &\quad - \text{Tr} \log \left(\frac{1}{\sigma^2} 1^{\otimes 4} + i \left(\frac{\lambda}{2} \right)^{\frac{1}{2}} \sum_{c=1}^4 \mathcal{M}_c \right) - \frac{1}{2} \sum_{c=1}^4 \text{Tr}(\mathcal{M}_c^2) \\ &\quad \left. + \frac{1}{N^3} \int dt_1 dt_2 \sum_{a,b=1}^n \psi^{1,a} \psi^{2,a} \psi^{3,a} \psi^{4,a} \left(\frac{1}{\sigma^2} 1^{\otimes 4} + i \left(\frac{\lambda}{2} \right)^{\frac{1}{2}} \sum_{c=1}^4 \mathcal{M}_c \right)^{-1} \bar{\psi}^{1,b} \bar{\psi}^{2,b} \bar{\psi}^{3,b} \bar{\psi}^{4,b} \right). \end{aligned} \quad (3.5.8)$$

One has:

$$\begin{aligned} \left(\frac{1}{\sigma^2} 1^{\otimes 4} + i \left(\frac{\lambda}{2} \right)^{\frac{1}{2}} \sum_{c=1}^4 \mathcal{M}_c \right)^{-1} &= \sigma^2 1^{\otimes 4} + \sigma^2 \sum_{k \geq 1} \frac{(-i \left(\frac{\lambda}{2} \right)^{\frac{1}{2}} \sigma^2)^k}{k!} \left(\sum_{c=1}^4 \mathcal{M}_c \right)^k \\ &= \sigma^2 1^{\otimes 4} + \sigma^2 \sum_{k \geq 1} \frac{(-i \left(\frac{\lambda}{2} \right)^{\frac{1}{2}} \sigma^2)^k}{k!} \sum_{k_1+k_2+k_3+k_4=k} \binom{k}{k_1, k_2, k_3, k_4} \prod_{c=1}^4 \mathcal{M}_c^{k_c}, \end{aligned} \quad (3.5.9)$$

$$\begin{aligned} \log \left(\frac{1}{\sigma^2} 1^{\otimes 4} + i \left(\frac{\lambda}{2} \right)^{\frac{1}{2}} \sum_{c=1}^4 \mathcal{M}_c \right) &= -2 \log(\sigma 1^{\otimes 4}) + \log \left(1^{\otimes 4} + i \sigma^2 \left(\frac{\lambda}{2} \right)^{\frac{1}{2}} \sum_{c=1}^4 \mathcal{M}_c \right) \\ &= -2 \log(\sigma 1^{\otimes 4}) - \sum_{k \geq 1} \frac{(-i \left(\frac{\lambda}{2} \right)^{\frac{1}{2}} \sigma^2)^k}{k} \sum_{k_1+k_2+k_3+k_4=k} \binom{k}{k_1, k_2, k_3, k_4} \prod_{c=1}^4 \mathcal{M}_c^{k_c}. \end{aligned} \quad (3.5.10)$$

Inserting these series in (3.5.8) and keeping only the terms in \mathcal{M}_c we have:

$$\begin{aligned} & - \frac{1}{2} \sum_{c=1}^4 \text{Tr}(\mathcal{M}_c^2) + \sum_{k \geq 1} \frac{(-i \left(\frac{\lambda}{2} \right)^{\frac{1}{2}} \sigma^2)^k}{k} \sum_{k_1+k_2+k_3+k_4=k} \binom{k}{k_1, k_2, k_3, k_4} \text{Tr} \left(\prod_{c=1}^4 \mathcal{M}_c^{k_c} \right) \\ & + \frac{\sigma^2}{N^3} \int dt \sum_{a,b=1}^n \prod_{c=1}^4 \psi^{c,a} \sum_{k \geq 1} \frac{(-i \left(\frac{\lambda}{2} \right)^{\frac{1}{2}} \sigma^2)^k}{k!} \sum_{k_1+k_2+k_3+k_4=k} \binom{k}{k_1, k_2, k_3, k_4} \prod_{c=1}^4 \mathcal{M}_c^{k_c} \prod_{c=1}^4 \bar{\psi}^{c,b}, \end{aligned} \quad (3.5.11)$$

with $dt = dt_1 dt_2$. Eq. (3.5.11) can be rewritten in the form

$$\begin{aligned}
& -\frac{1}{2} \sum_{c=1}^4 \text{Tr}(\mathcal{M}_c^2) \\
& + \text{Tr} \left(\sum_{k \geq 1} \sum_{k_1+k_2+k_3+k_4=k} \frac{(-i(\frac{\lambda}{2})^{\frac{1}{2}} \sigma^2)^k}{k_1! k_2! k_3! k_4!} \left((k-1)! 1^{\otimes 4} + \frac{\sigma^2}{N^3} \int dt \sum_{a,b=1}^n (\bar{\psi}_b^4 \cdot \psi_a^4) \right) \prod_{c=1}^4 \mathcal{M}_c^{k_c} \right),
\end{aligned} \tag{3.5.12}$$

where $(\bar{\psi}_b^4 \cdot \psi_a^4) = \bigotimes_{f=1}^4 (\bar{\psi}^{f,b} \cdot \psi^{f,a})$ with $(\bar{\psi}^{f,b} \cdot \psi^{f,a})_{ij} = \bar{\psi}_i^{f,b} \psi_j^{f,a}$.

We can note that the term proportional to the identity in (3.5.9) contributes to the effective action as the Gaussian part of the disorder.

3.5.3 First order correction of the effective action

The integration on the intermediate fields $M^{(c)}$ cannot be explicitly performed. We can however truncate the series in λ and compute perturbatively the first order of the effective action. Keeping only the linear and quadratic terms in the intermediate fields in equation (3.5.12), we get

$$-\frac{1}{2} \sum_{c=1}^4 \text{Tr}(\mathcal{M}_c^2) - i\sigma^2 \left(\frac{\lambda}{2}\right)^{\frac{1}{2}} \sum_{c=1}^4 \text{Tr}(\mathcal{M}_c) + \frac{\sigma^2}{N^3} \int dt_1 dt_2 \sum_{a,b=1}^n \psi_a^4 \left(-i \left(\frac{\lambda}{2}\right)^{\frac{1}{2}} \sigma^2 \sum_{c=1}^4 \mathcal{M}_c \right) \bar{\psi}_b^4, \tag{3.5.13}$$

where we have introduced the notations $\psi_a^4 = \psi^{1,a} \psi^{2,a} \psi^{3,a} \psi^{4,a}$ and $\bar{\psi}_b^4 = \bar{\psi}^{1,b} \bar{\psi}^{2,b} \bar{\psi}^{3,b} \bar{\psi}^{4,b}$. By performing partial traces on the identity part of \mathcal{M}_c , equation (3.5.13) can be further simplified:

$$\int \prod_{c=1}^4 dM^{(c)} \exp \left\{ -\frac{N^3 \lambda}{2} \sum_{c=1}^4 \text{Tr}((M^{(c)})^2) - \sum_{c=1}^4 \text{Tr} \left[\left(i \left(\frac{\lambda}{2}\right)^{\frac{1}{2}} \left(N^3 \sigma^2 1 + \frac{\sigma^4}{N^3} \int dt \sum_{a,b=1}^n (\bar{\psi}_b^4 \cdot \psi_a^4)_c \right) M^{(c)} \right) \right] \right\}, \tag{3.5.14}$$

where $(\bar{\psi}_b^4 \cdot \psi_a^4)_c = \prod_{d \neq c} \text{Tr}(\bar{\psi}^{d,b} \cdot \psi^{d,a}) (\bar{\psi}^{c,b} \cdot \psi^{c,a})$. Let us now perform the Gaussian integrals on the intermediate fields. We get:

$$\begin{aligned}
& \exp \left(-\frac{N^3 \lambda}{4} \sum_{c=1}^4 \text{Tr} \left(\sigma^2 1 + \frac{\sigma^4}{N^3} \int dt \sum_{a,b=1}^n (\bar{\psi}_b^4 \cdot \psi_a^4)_c \right)^2 \right) \\
& = \exp \left(-N^4 \lambda \sigma^4 - \frac{2\lambda \sigma^6}{N^3} \int dt \sum_{a,b=1}^n \text{Tr}(\bar{\psi}_b^4 \cdot \psi_a^4) \right. \\
& \quad \left. - \frac{\lambda \sigma^8}{4N^9} \sum_{c=1}^4 \int dt dt' \sum_{a,b,p,q=1}^n \text{Tr}[(\bar{\psi}_b^4 \cdot \psi_a^4)_c (\bar{\psi}_p^4 \cdot \psi_q^4)_c] \right).
\end{aligned} \tag{3.5.15}$$

This leads to the the following expression for the effective action

$$\begin{aligned} \mathcal{S}_{eff}[\psi, \bar{\psi}] &= \int dt \sum_{a=1}^n \sum_{f=1}^4 \sum_i \bar{\psi}_i^{f,a} \frac{d}{dt} \psi_i^{f,a} - \frac{\sigma^2 - 2\lambda\sigma^6}{N^3} \int dt \sum_{a,b=1}^n \text{Tr}(\bar{\psi}_b^4 \cdot \psi_a^4) \\ &+ \frac{\lambda\sigma^8}{4N^9} \sum_{c=1}^4 \int dt dt' \sum_{a,b,p,q=1}^n \text{Tr}[(\bar{\psi}_b^4 \cdot \psi_a^4)_c (\bar{\psi}_p^4 \cdot \psi_q^4)_c], \end{aligned} \quad (3.5.16)$$

with $dt' = dt_3 dt_4$. We can directly see the effect of the non-Gaussian perturbation, on the effective action. Taking $\lambda = 0$, we recover the action of the model without quartic perturbation in the disorder. We then define the bi-local fields

$$G_f^{ab}(t_1, t_2) = \frac{1}{N} \sum_i \psi_i^{f,b}(t_1) \bar{\psi}_i^{f,a}(t_2), \quad (3.5.17)$$

and introduce the Lagrange multipliers $\Sigma_f^{ab}(t_1, t_2)$:

$$\int \mathcal{D}\Sigma_f^{ab} \exp \left(-N \int dt \sum_{a,b=1}^n \sum_{f=1}^4 \Sigma_f^{ab}(\mathbf{t}) \left(G_f^{ab}(\mathbf{t}) - \frac{1}{N} \sum_i \psi_i^{f,b}(t_1) \bar{\psi}_i^{f,a}(t_2) \right) \right). \quad (3.5.18)$$

The effective action (3.5.16) rewrites as:

$$\begin{aligned} \mathcal{S}_{eff}[\psi, \bar{\psi}, G, \Sigma] & \quad (3.5.19) \\ &= \int dt \sum_{a,b=1}^n \sum_{f=1}^4 \sum_i \bar{\psi}_i^{f,a} (\delta_{ab} \delta(t_1 - t_2) \partial_t - \Sigma_f^{ab}(\mathbf{t})) \psi_i^{f,a} - N(\sigma^2 - 2\lambda\sigma^6) \int dt \sum_{a,b=1}^n \prod_{f=1}^4 G_f^{ab}(\mathbf{t}) \\ &+ N \sum_{a,b=1}^n \int dt \sum_{f=1}^4 \Sigma_f^{ab}(\mathbf{t}) G_f^{ab}(\mathbf{t}) + \frac{\lambda\sigma^8}{4N} \int dt dt' \sum_{a,b,p,q=1}^n \sum_{c=1}^4 G_c^{ap}(t_1, t_4) G_c^{qb}(t_3, t_2) \prod_{f \neq c} G_f^{ab}(\mathbf{t}) G_f^{qp}(\mathbf{t}'). \end{aligned} \quad (3.5.20)$$

We now perform the Gaussian integral on the fermionic fields

$$\begin{aligned} \langle Z^n \rangle_J &= \int \mathcal{D}\psi_i^{f,a} \mathcal{D}\bar{\psi}_i^{f,a} \mathcal{D}G_f^{ab} \mathcal{D}\Sigma_f^{ab} \exp(-\mathcal{S}_{eff}[\psi, \bar{\psi}, G, \Sigma]) \quad (3.5.21) \\ &= \int \mathcal{D}G_f^{ab} \mathcal{D}\Sigma_f^{ab} \exp \left(\frac{N}{2} \sum_{a,b=1}^n \sum_{f=1}^4 \log \det (\delta_{ab} \delta(t_1 - t_2) \partial_t - \Sigma_f^{ab}(t_1, t_2)) \right. \\ &+ N(\sigma^2 - 2\lambda\sigma^6) \int dt \sum_{a,b=1}^n \prod_{f=1}^4 G_f^{ab}(\mathbf{t}) - N \sum_{a,b=1}^n \int dt \sum_{f=1}^4 \Sigma_f^{ab}(\mathbf{t}) G_f^{ab}(\mathbf{t}) \\ &\left. - \frac{\lambda\sigma^8}{4N} \int dt dt' \sum_{a,b,p,q=1}^n \sum_{c=1}^4 G_c^{ap}(t_1, t_4) G_c^{qb}(t_3, t_2) \prod_{f \neq c} G_f^{ab}(\mathbf{t}) G_f^{qp}(\mathbf{t}') \right). \end{aligned}$$

We then assume a symmetric saddle point for the replicas and get the effective action:

$$\begin{aligned} \frac{\mathcal{S}_{eff}[G, \Sigma]}{N} &= - \sum_{f=1}^4 \log \det (\delta(t_1 - t_2) \partial_t - \Sigma_f(t_1, t_2)) - (\sigma^2 - 2\lambda\sigma^6) \int dt \prod_{f=1}^4 G_f(\mathbf{t}) \\ &+ \int dt \sum_{f=1}^4 \Sigma_f(\mathbf{t}) G_f(\mathbf{t}) - \frac{\lambda\sigma^8}{4N^2} \int dt dt' \sum_{c=1}^4 G_c(t_1, t_4) G_c(t_3, t_2) \prod_{f \neq c} G_f(\mathbf{t}) G_f(\mathbf{t}'). \end{aligned} \quad (3.5.22)$$

Let us emphasise that the effective action formula above implies that the variance of the Gaussian disorder is modified by the non-Gaussian perturbation:

$$\sigma^2 \rightarrow \sigma^2 - 2\lambda\sigma^6. \quad (3.5.23)$$

Moreover, let us notice that every term in (3.5.22) is of order 1, except for the last term which is of order $\frac{1}{N^2}$, as expected from the universality result. This term can be represented graphically as in Fig 3.5.

3.6 Gross-Rosenhaus SYK model with non-Gaussian disorder

In this section we follow the steps of the calculation of the previous section and we compute the modification of the covariance and of the effective action for a quartic melonic perturbation of the disorder of the Gross-Rosenhaus SYK model.

The Gross-Rosenhaus model [33] is a generalisation of the SYK model containing f flavors of fermions, with N_a fermions of flavor a , appearing q_a times in the interaction, so that $q = \sum_{a=1}^f q_a$. The complex model treated in the previous section can thus be seen as a particular case of a complex version of the Gross-Rosenhaus model treated in this section.

The action of the model writes

$$\mathcal{S} = \int dt \left(\sum_{a=1}^f \sum_{i=1}^{N_a} \psi_i^a \frac{d}{dt} \psi_i^a + \frac{(i)^{\frac{q}{2}}}{\prod_{a=1}^f q_a!} \sum_I J_I \prod_{a=1}^f \prod_{p=1}^{q_a} (\psi_{i_p^a}^a) \right), \quad (3.6.1)$$

where $I = i_1^1, \dots, i_{q_1}^1, \dots, i_1^f, \dots, i_{q_f}^f$. The coupling tensor J is now antisymmetric under permutations of indices in the same family of flavors, with the probability distribution

$$P(J) = C \exp \left(-\frac{1}{2\sigma^2 N} \prod_a \frac{N_a^{q_a}}{(q_a - 1)!} \sum_I J_I^2 - \frac{\lambda}{4} \frac{\prod_a N_a^{q_a}}{N} \sum_{c=1}^q \sum_{I,K} J_I J_{I_{\hat{c}k_c}} J_K J_{K_{\hat{c}i_c}} \right), \quad (3.6.2)$$

where $N = \sum_a N_a$ and $\sigma^2 = \prod_a q_a! \tilde{\sigma}^2$, with $\tilde{\sigma}^2$ the variance of the Gaussian distribution.

We use again the intermediate field

$$e^{-\frac{\lambda}{4} \frac{\prod_a N_a^{q_a}}{N} \sum_{I,K} J_I J_{I_{\hat{c}k_c}} J_K J_{K_{\hat{c}i_c}}} \propto \int dM^{(c)} e^{-\frac{1}{2} \frac{\prod_a N_a^{q_a}}{N} \text{Tr}((M^{(c)})^2) - i \frac{\prod_a N_a^{q_a}}{N} \left(\frac{\lambda}{2}\right)^{\frac{1}{2}} \sum_{I,j} J_{I_{\hat{c}j}} M_{ij}^{(c)} J_I}, \quad (3.6.3)$$

where $M^{(c)}$ is a symmetric real $N_c \times N_c$ matrix. Using the replica trick and keeping the terms in J we have

$$\int \mathcal{D}J \exp \left(-\prod_a \frac{N_a^{q_a}}{(q_a - 1)!} \sum_I \frac{J_I^2}{2\sigma^2 N} - i \frac{\prod_a N_a^{q_a}}{N} \left(\frac{\lambda}{2}\right)^{\frac{1}{2}} \sum_{c=1}^q \sum_{I,j} J_{I_{\hat{c}j}} M_{ij}^{(c)} J_I - \frac{(i)^{\frac{q}{2}}}{\prod_{a=1}^f q_a!} \int dt \sum_{r=1}^n \sum_I J_I \prod_{a=1}^f \prod_{p=1}^{q_a} (\psi_{i_p^a}^{a,r}) \right). \quad (3.6.4)$$

As above, let $\mathcal{M}_c = 1^{\otimes(c-1)} \otimes M^{(c)} \otimes 1^{\otimes(q-c)}$, where 1 is implicitly the identity $N_a \times N_a$ matrix, for $a = 1, \dots, f$. One then has

$$\begin{aligned}
& \int \mathcal{D}J \exp \left(-\frac{\prod_a N_a^{q_a}}{2N} J \left(\frac{1}{\sigma^2} \prod_{a=1}^f \frac{1}{(q_a-1)!} 1^{\otimes q} + i(2\lambda)^{\frac{1}{2}} \sum_{c=1}^q \mathcal{M}_c \right) J \right. \\
& \left. - \frac{(i)^{\frac{q}{2}}}{\prod_{a=1}^f q_a!} \int dt \sum_{r=1}^n \sum_I J_I \prod_{a=1}^f \prod_{p=1}^{q_a} (\psi_{i_p}^{a,r}) \right) \\
& \propto \left(\det \left(\frac{1}{\sigma^2} \prod_{a=1}^f \frac{1}{(q_a-1)!} 1^{\otimes q} + i(2\lambda)^{\frac{1}{2}} \sum_{c=1}^q \mathcal{M}_c \right) \right)^{-\frac{1}{2}} \\
& \exp \left(\frac{i^q N}{2 \prod_{a=1}^f N_a^{q_a} (q_a!)^2} \int dt_1 dt_2 \sum_{r,s=1}^n \prod_{a=1}^f \prod_{p=1}^{q_a} (\psi_p^{a,r}) \left(\frac{1}{\sigma^2} \prod_{a=1}^f \frac{1}{(q_a-1)!} 1^{\otimes q} + i(2\lambda)^{\frac{1}{2}} \sum_{c=1}^q \mathcal{M}_c \right)^{-1} (\psi_p^{a,s}) \right).
\end{aligned} \tag{3.6.5}$$

The replicated generating functional thus writes:

$$\begin{aligned}
\langle Z^n \rangle_J &= \int \mathcal{D}\psi_i^{f,a} \mathcal{D}M^{(c)} \exp \left[- \int dt \sum_{r=1}^n \sum_{a=1}^f \sum_{i=1}^{N_a} \psi_i^{a,r} \frac{d}{dt} \psi_i^{a,r} \right. \\
& \left. - \frac{1}{2} \text{Tr} \log \left(\frac{1}{\sigma^2} \prod_{a=1}^f \frac{1}{(q_a-1)!} 1^{\otimes q} + i(2\lambda)^{\frac{1}{2}} \sum_{c=1}^q \mathcal{M}_c \right) - \frac{1}{2} \frac{\prod_a N_a^{q_a}}{N} \sum_{c=1}^q \text{Tr}((M^{(c)})^2) \right. \\
& \left. + \frac{i^q N}{2 \prod_{a=1}^f N_a^{q_a} (q_a!)^2} \int dt_1 dt_2 \sum_{r,s=1}^n \prod_{a=1}^f \prod_{p=1}^{q_a} (\psi_p^{a,r}) \left(\frac{1}{\sigma^2} \prod_{a=1}^f \frac{1}{(q_a-1)!} 1^{\otimes q} + i(2\lambda)^{\frac{1}{2}} \sum_{c=1}^q \mathcal{M}_c \right)^{-1} (\psi_p^{a,s}) \right].
\end{aligned} \tag{3.6.6}$$

As above, we now write the following series:

$$\begin{aligned}
& \left(\frac{1}{\sigma^2} \prod_{a=1}^f \frac{1}{(q_a-1)!} 1^{\otimes q} + i(2\lambda)^{\frac{1}{2}} \sum_{c=1}^q \mathcal{M}_c \right)^{-1} \\
& = \sigma^2 \prod_{a=1}^f (q_a-1)! 1^{\otimes q} + \sigma^2 \prod_{a=1}^f (q_a-1)! \sum_{k \geq 1} \left(-i\sigma^2 (2\lambda)^{\frac{1}{2}} \prod_{a=1}^f (q_a-1)! \right)^k \sum_{\substack{k \\ \sum_i k_i = k}} \binom{k}{k_1, \dots, k_q} \prod_{c=1}^q \mathcal{M}_c^{k_c},
\end{aligned} \tag{3.6.7}$$

$$\begin{aligned}
& \log \left(\frac{1}{\sigma^2} \prod_{a=1}^f \frac{1}{(q_a-1)!} 1^{\otimes q} + i(2\lambda)^{\frac{1}{2}} \sum_{c=1}^q \mathcal{M}_c \right) \\
& = -2 \log(\sigma 1^{\otimes q}) - \sum_{a=1}^f \log((q_a-1)! 1^{\otimes q}) + \log \left(1^{\otimes q} + i(2\lambda)^{\frac{1}{2}} \sigma^2 \prod_{a=1}^f (q_a-1)! \sum_{c=1}^q \mathcal{M}_c \right)
\end{aligned}$$

$$\begin{aligned}
&= -2 \log(\sigma 1^{\otimes q}) - \sum_{a=1}^f \log((q_a - 1)! 1^{\otimes q}) \\
&- \sum_{k \geq 1} \frac{\left(-i(2\lambda)^{\frac{1}{2}} \sigma^2 \prod_{a=1}^f (q_a - 1)!\right)^k}{k} \sum_{\sum_i^q k_i = k} \binom{k}{k_1, \dots, k_q} \prod_{c=1}^q \mathcal{M}_c^{k_c}. \tag{3.6.8}
\end{aligned}$$

This leads to:

$$\begin{aligned}
&- \frac{1}{2} \frac{\prod_a N_a^{q_a}}{N} \sum_{c=1}^q \text{Tr}((M^{(c)})^2) \\
&+ \frac{1}{2} \sum_{k \geq 1} \frac{\left(-i(2\lambda)^{\frac{1}{2}} \sigma^2 \prod_{a=1}^f (q_a - 1)!\right)^k}{k} \sum_{\sum_i^q k_i = k} \binom{k}{k_1, \dots, k_q} \text{Tr} \left(\prod_{c=1}^q \mathcal{M}_c^{k_c} \right) \\
&+ \frac{i^q N \sigma^2}{2 \prod_{a=1}^f N_a^{q_a} q_a (q_a!)} \\
&\times \sum_{k \geq 1} \left(-i \sigma^2 (2\lambda)^{\frac{1}{2}} \prod_{a=1}^f (q_a - 1)!\right)^k \sum_{\sum_i^q k_i = k} \binom{k}{k_1, \dots, k_q} \int dt \text{Tr} \left((\psi_r^q \cdot \psi_s^q) \prod_{c=1}^q \mathcal{M}_c^{k_c} \right), \tag{3.6.9}
\end{aligned}$$

where we used the notation $(\psi_r^q \cdot \psi_s^q) = \sum_{r,s=1}^n \bigotimes_{a=1}^f \bigotimes_{p=1}^{q_a} (\psi_p^{a,r} \cdot \psi_p^{a,s})$ and $(\psi_p^{a,r} \cdot \psi_p^{a,s})_{ij} = \psi_{i_p^a}^{a,r} \psi_{j_p^a}^{a,s}$.

For the sake of simplicity, we can rewrite this term in the more compact form

$$- \frac{1}{2} \frac{\prod_a N_a^{q_a}}{N} \sum_{c=1}^q \text{Tr}((M^{(c)})^2) + \frac{1}{2} \text{Tr} \left[\sum_{k \geq 1} \left(-i(2\lambda)^{\frac{1}{2}} \sigma^2 \prod_{a=1}^f (q_a - 1)!\right)^k \sum_{\sum_i^q k_i = k} \binom{k}{k_1, \dots, k_q} \hat{A}_k \prod_{c=1}^q \mathcal{M}_c^{k_c} \right], \tag{3.6.10}$$

where we denoted

$$\hat{A}_k = \frac{1^{\otimes q}}{k} + \frac{i^q N \sigma^2}{\prod_{a=1}^f N_a^{q_a} q_a (q_a!)} \int dt (\psi_r^q \cdot \psi_s^q). \tag{3.6.11}$$

Keeping only the terms in $\sqrt{\lambda}$ in (3.6.10), we get:

$$- \frac{1}{2} \frac{\prod_a N_a^{q_a}}{N} \sum_{c=1}^q \text{Tr}((M^{(c)})^2) - i \sigma^2 \prod_{a=1}^f (q_a - 1)! \sqrt{\frac{\lambda}{2}} \sum_{c=1}^q \text{Tr}(\hat{A}_1 \mathcal{M}_c). \tag{3.6.12}$$

This allows to perform the Gaussian integral over the intermediate fields:

$$\begin{aligned}
& \int \prod_{c=1}^q dM^{(c)} \exp \left(-\frac{1}{2} \frac{\prod_a N_a^{q_a}}{N} \sum_{c=1}^q \text{Tr}((M^{(c)})^2) - i\sigma^2 \prod_{a=1}^f (q_a - 1)! \sqrt{\frac{\lambda}{2}} \sum_{c=1}^q \text{Tr}(\hat{A}_1 \mathcal{M}_c) \right) \\
& \propto \exp \left(-\frac{i^q \lambda N^2 \sigma^6}{2 \prod_{a=1}^f N_a^{2q_a} q_a^3 (q_a!)^{-1}} \int dt \text{Tr}(\psi_r^q \cdot \psi_s^q) \right. \\
& \quad \left. - \frac{(-1)^q \lambda N^3 \sigma^8}{4 \prod_{a=1}^f N_a^{3q_a} q_a^4} \sum_{c=1}^f \sum_{k=1}^{q_c} \int dt dt' \text{Tr}[(\psi_r^q \cdot \psi_s^q)_{c,k} (\psi_u^q \cdot \psi_v^q)_{c,k}] \right), \tag{3.6.13}
\end{aligned}$$

where $(\psi_r^q \cdot \psi_s^q)_{c,k} = \sum_{r,s=1}^n \prod_{a \neq c} \prod_{p \neq k} \text{Tr}[(\psi_p^{a,r} \cdot \psi_p^{a,s})](\psi_k^{c,r} \cdot \psi_k^{c,s})$. This leads to the following expression for the effective action:

$$\begin{aligned}
\mathcal{S}_{eff}[\psi] &= \int dt \sum_{a=1}^f \sum_{r=1}^n \sum_{i=1}^{N_a} \psi_i^{a,r} \frac{d}{dt} \psi_i^{a,r} - \frac{i^q N}{2 \prod_{a=1}^f N_a^{q_a} q_a q_a!} \left(\sigma^2 - \lambda N \sigma^6 \prod_{a=1}^f \frac{(q_a!)^2}{q_a^2 N_a^{q_a}} \right) \int dt \text{Tr}(\psi_r^q \cdot \psi_s^q) \\
& \quad + \frac{(-1)^q \lambda N^3 \sigma^8}{4 \prod_{a=1}^f N_a^{3q_a} q_a^4} \sum_{c=1}^f \sum_{k=1}^{q_c} \int dt dt' \text{Tr}[(\psi_r^q \cdot \psi_s^q)_{c,k} (\psi_u^q \cdot \psi_v^q)_{c,k}]. \tag{3.6.14}
\end{aligned}$$

In order to evaluate the fermionic integral in the expression of the replicated generating function, we introduce the bi-local fields

$$G_a^{rs}(t_1, t_2) = \frac{1}{N_a} \sum_{i=1}^{N_a} \psi_i^{a,r}(t_1) \psi_i^{a,s}(t_2), \tag{3.6.15}$$

and the Lagrange multipliers $\Sigma_a^{rs}(t_1, t_2)$:

$$\int \mathcal{D}\Sigma_a^{rs} \exp \left(-\int dt \sum_{r,s=1}^n \sum_{a=1}^f \frac{N_a}{2} \Sigma_a^{rs}(t_1, t_2) \left(G_a^{rs}(t_1, t_2) - \frac{1}{N_a} \sum_{i=1}^{N_a} \psi_i^{a,r} \psi_i^{a,s} \right) \right). \tag{3.6.16}$$

The effective action (3.6.14) then writes:

$$\begin{aligned}
\mathcal{S}_{eff}[\psi, G, \Sigma] &= \int dt \sum_{a=1}^f \sum_{r,s=1}^n \sum_{i=1}^{N_a} \psi_i^{a,r} (\delta_{rs} \delta(t_1 - t_2) \partial_t - \Sigma_a^{rs}(\mathbf{t})) \psi_i^{a,s} \\
& \quad + \int dt \sum_{r,s=1}^n \sum_{a=1}^f \frac{N_a}{2} \Sigma_a^{rs}(\mathbf{t}) G_a^{rs}(\mathbf{t}) - \frac{i^q N}{2 \prod_{a=1}^f q_a q_a!} \left(\sigma^2 - \lambda N \sigma^6 \prod_{a=1}^f \frac{(q_a!)^2}{q_a^2 N_a^{q_a}} \right) \int dt \sum_{r,s=1}^n \prod_{a=1}^f (G_a^{rs}(\mathbf{t}))^{q_a} \\
& \quad + \frac{(-1)^q \lambda N^3 \sigma^8}{4 \prod_{a=1}^f N_a^{q_a} q_a^4} \int dt dt' \sum_{r,s,u,v=1}^n \sum_{c=1}^f q_c G_c^{su}(t_2, t_3) G_c^{rv}(t_1, t_4) (G_c^{rs}(\mathbf{t}) G_c^{uv}(\mathbf{t}'))^{q_c-1} \prod_{a \neq c} (G_a^{rs}(\mathbf{t}) G_a^{uv}(\mathbf{t}'))^{q_a}. \tag{3.6.17}
\end{aligned}$$

This allows to perform the Gaussian integral on the fermionic fields:

$$\begin{aligned}
\langle Z^n \rangle_J &= \int \mathcal{D}\psi \mathcal{D}G \mathcal{D}\Sigma e^{-\mathcal{S}_{eff}[\psi, G, \Sigma]} \\
&= \int \mathcal{D}\psi \mathcal{D}G \mathcal{D}\Sigma \exp \left(- \int dt \sum_{a=1}^f \sum_{r,s=1}^n \frac{N_a}{2} \log \det (\delta_{rs} \delta(t_1 - t_2) \partial_t - \Sigma_a^{rs}(\mathbf{t})) \right. \\
&\quad - \int dt \sum_{r,s=1}^n \sum_{a=1}^f \frac{N_a}{2} \Sigma_a^{rs}(\mathbf{t}) G_a^{rs}(\mathbf{t}) \\
&\quad + \frac{i^q N}{2 \prod_{a=1}^f q_a q_a!} \left(\sigma^2 - \lambda N \sigma^6 \prod_{a=1}^f \frac{(q_a!)^2}{q_a^2 N_a^{q_a}} \right) \int dt \sum_{r,s=1}^n \prod_{a=1}^f (G_a^{rs}(\mathbf{t}))^{q_a} \\
&\quad - \frac{(-1)^q \lambda N^3 \sigma^8}{4 \prod_{a=1}^f N_a^{q_a} q_a^4} \\
&\quad \left. \times \int dt dt' \sum_{r,s,u,v=1}^n \sum_{c=1}^f q_c G_c^{su}(t_2, t_3) G_c^{rv}(t_1, t_4) (G_c^{rs}(\mathbf{t}) G_c^{uv}(\mathbf{t}'))^{q_c-1} \prod_{a \neq c} (G_a^{rs}(\mathbf{t}) G_a^{uv}(\mathbf{t}'))^{q_a} \right). \tag{3.6.18}
\end{aligned}$$

Assuming a symmetric saddle point for the replicas, we get the following expression for the effective action:

$$\begin{aligned}
\mathcal{S}_{eff}[G, \Sigma] &= \int dt \sum_{a=1}^f \frac{N_a}{2} \log \det (\delta(t_1 - t_2) \partial_t - \Sigma_a(\mathbf{t})) + \int dt \sum_{a=1}^f \frac{N_a}{2} \Sigma_a(\mathbf{t}) G_a(\mathbf{t}) \\
&\quad - \frac{i^q N}{2 \prod_{a=1}^f q_a} \left(\tilde{\sigma}^2 - \lambda N \tilde{\sigma}^6 \prod_{a=1}^f \frac{(q_a!)^4}{q_a^2 N_a^{q_a}} \right) \int dt \prod_{a=1}^f (G_a(\mathbf{t}))^{q_a} \\
&\quad + (-1)^q \frac{\lambda}{4} N^3 \tilde{\sigma}^8 \prod_{a=1}^f \frac{(q_a!)^4}{N_a^{q_a} q_a^4} \int dt dt' \sum_{c=1}^f q_c G_c(t_2, t_3) G_c(t_1, t_4) (G_c(\mathbf{t}) G_c(\mathbf{t}'))^{q_c-1} \prod_{a \neq c} (G_a(\mathbf{t}) G_a(\mathbf{t}'))^{q_a}. \tag{3.6.19}
\end{aligned}$$

Let us emphasise that the Gaussian variance is now modified by the non-Gaussian perturbation:

$$\tilde{\sigma}^2 \rightarrow \tilde{\sigma}^2 - \lambda N \tilde{\sigma}^6 \prod_{a=1}^f \frac{(q_a!)^4}{q_a^2 N_a^{q_a}}. \tag{3.6.20}$$

This expression is a generalisation of the modification (3.5.23) of the Gaussian variance of the complex model treated in the previous sections.

3.7 Conclusions and perspectives

In this chapter we have investigated the effects of a non-Gaussian average over the random couplings J in a complex SYK model, as well as in a (real) SYK generalisation proposed

by Gross and Rosenhaus. To our knowledge, this is the first study of the effects of the relaxation of the Gaussianity condition in SYK models when no double scaling limit is taken.

An interesting perspective appears to us to be the investigation of the effects of such a perturbation from Gaussianity in the case of $q = 2$ (fermions with a random mass matrix) and in the case of the real SYK model - a first step towards this latter case having been already made in this chapter (since the real SYK model is a particular case of the Gross-Rosenhaus model). The main technical complication in this latter case comes from the fact that one has to deal with graphs which are not necessary bipartite - the removal and reconnection of edges of these graphs (which is the main technical ingredient of our approach) being much more involved.

It would thus be interesting to check whether or not in this case also, non-Gaussian perturbation leads to a modification of the variance of the Gaussian distributions of the couplings J at leading order in N , as we proved to be the case for the complex version of the SYK model studied here.

Another perspective farther from the content on this chapter is to compute the analytic contributions of the NLO graphs determined in [47] for a coloured (or flavoured) SYK model. So far, only the dominant term in the large N expansion is fully understood in the original SYK framework. The building block for this computation is the leading 4-point function, which is composed of a conformal part and a singular part which breaks the emergent conformal invariance in the IR.

In [29] and [30], Gross and Rosenhaus obtained the conformal part of the 6-point and 8-point functions of the SYK at leading order in the large N limit, and derived a way to compute the conformal part of any correlation function also at leading order.

One could adapt and generalise these techniques for the computation of the next-to-leading (in the large N expansion) conformal part of the 2-point, 4-point functions and Bethe-Salpeter equation. This involves challenging integration of hypergeometric functions. These computations would give insights on corrections to the anomalous dimension and OPE coefficients of the fermions, and the dimensions of the bilinear operators in the conformal sector of the SYK model.

Chapter 4

On the variance of Sobolev norms in resonant systems

This chapter is based on a work in progress in collaboration with S. Dartois and A. Tanasa. It is a follow up to [60] by S. Dartois *et al.* which we edited into section 4.1 with some added content. Section 4.2 then presents our new developments and section 4.3 presents the next steps of our work. We use throughout this chapter a more probabilistic language than in the rest of the thesis, where the QFT correlation functions correspond to the moments of the probability distribution, or cumulants if we consider only connected graphs.

4.1 Resonant systems

4.1.1 The model

In this chapter we study typical phenomenon of non-linear random flows in many variables. We consider the following Hamiltonian

$$H = \frac{1}{2} \sum_{S=0}^{\infty} \sum_{j,k=0}^S C_{jk}^S \bar{\alpha}_j(t) \bar{\alpha}_{S-j}(t) \alpha_k(t) \alpha_{S-k}(t), \quad (4.1.1)$$

where the tensor coupling C is an infinite family of real symmetric $(S+1) \times (S+1)$ matrices C_{jk}^S (where S runs over non-negative integers, that is, $S \in \mathbb{N}$) and has the following symmetries

$$C_{jk}^S = C_{kj}^S = C_{S-j,k}^S = C_{j,S-k}^S. \quad (4.1.2)$$

The equations of motion is

$$i \frac{d\alpha_j}{dt} = \sum_{S=j}^{\infty} \sum_{k=0}^S C_{jk}^S \bar{\alpha}_{S-j}(t) \alpha_k(t) \alpha_{S-k}(t), \quad (4.1.3)$$

where α_n with $n \geq 0$ are an infinite sequence of complex-valued functions of time (whose physical origin is in complex amplitudes of linear normal modes of a weakly non-linear system). Such equations naturally emerge in weakly non-linear analysis of PDEs whose

frequency spectra of linearized perturbations are highly resonant (more specifically, differences of any two frequencies of the linearized normal modes are integer in appropriate units). Moreover the tensor coupling C depends on the model from which this equation emerges.

In [60], the authors focus on the question of energy cascades characteristic of turbulent flows, and in order to study the spread of energy over modes, introduced the Sobolev norms

$$S_\gamma(t) = \sum_{r \geq 0} r^\gamma \bar{\alpha}_r(t) \alpha_r(t) = \sum_{n \geq 0} s_{\gamma,n} t^n. \quad (4.1.4)$$

The evolve over time of Sobolev norms was then studied. Two specific cases, $S_0(t)$ and $S_1(t)$, are in fact independent of t , and correspond to known conserved quantities of (4.1.3). For resonant systems emerging from weakly nonlinear analysis of PDEs, S_0 can be thought of as a ‘‘particle number’’ quantifying excitations of the linearized modes, while S_1 is the total energy of the normal modes in the linearized theory. On the other hand, $S_\gamma(t)$ for $\gamma > 1$ are generically not conserved, and can be used to quantify the transfer of energy from the long wavelength modes to those with shorter wavelengths. The growth of these quantities indicates that the excitation of higher modes is getting stronger.

Since we are interested in typical features of this type of models, we do not pick a particular choice of coupling but rather consider the family of symmetric matrices C_{jk}^S as Gaussian i.i.d. variables. This corresponds to imposing the covariance

$$\begin{aligned} \langle C_{jk}^S C_{j'k'}^{S'} \rangle_C = \frac{\delta_{SS'}}{8} & \left(\delta_{jj'} \delta_{kk'} + \delta_{j,S-j'} \delta_{kk'} + \delta_{jj'} \delta_{k,S-k'} + \delta_{j,S-j'} \delta_{k,S-k'} \right. \\ & \left. + \delta_{jk'} \delta_{kj'} + \delta_{j,S-k'} \delta_{kj'} + \delta_{jk'} \delta_{k,S-j'} + \delta_{j,S-k'} \delta_{k,S-j'} \right). \end{aligned} \quad (4.1.5)$$

on the infinite family of real $(S+1) \times (S+1)$ matrices $\{C_{jk}^S\}_{S \in \mathbb{N}}$ with *no symmetries*. Indeed, the necessary symmetries are automatically implemented by the eight terms in (4.1.5).

We choose initial conditions for the modes α_j in which the higher modes are suppressed. More precisely, we draw the initial conditions from a random Gaussian ensemble, in which they are independently but *not* identically distributed with respect to j , and they spread over a large number $N \gg 1$ of low-lying modes. This is expressed by the following covariance

$$\langle \alpha_j(0) \bar{\alpha}_{j'}(0) \rangle_\alpha = \frac{\delta_{jj'}}{N} \chi_N(j), \quad \langle \alpha_j(0) \alpha_{j'}(0) \rangle_\alpha = \langle \bar{\alpha}_j(0) \bar{\alpha}_{j'}(0) \rangle_\alpha = 0, \quad (4.1.6)$$

where the function $\chi_N(j)$ is such that $\sum_{j \geq 0} \chi_N(j) = N$. This implies that we have the normalisation condition:

$$\sum_{j=0}^{\infty} \langle |\alpha_j(0)|^2 \rangle_\alpha = 1. \quad (4.1.7)$$

In practice, the distribution that we use decays exponentially over j , so that

$$\chi_N(j) = p^j \quad \text{and} \quad N = \frac{1}{1-p}, \quad (4.1.8)$$

where $0 < p < 1$ is fixed. The limit $N \rightarrow \infty$ corresponds to the limit $p \rightarrow 1$.

The main quantities studied in [60] are the averaged Sobolev norms

$$\bar{S}_\gamma(t) := \langle S_\gamma(t) \rangle_{C,\alpha} = \sum_{n \text{ even}} \bar{s}_{\gamma,n} t^n. \quad (4.1.9)$$

Note that only even integers contribute in the sum, since the Gaussian distribution for C is even. Defining $\bar{S}_\gamma(t)$ may be subtle, even though the individual coefficients of its time-series expansion are perfectly well-defined and algorithmically computable. For instance, the ensemble-averaged S_γ could blow up for all finite times and its time series would have a zero radius of convergence. Such behaviour has been seen to happen with couplings C outside our ensemble of resonant systems. Whether such complications actually occur in our context, is an open, interesting and complicated mathematical question. Nevertheless, the dominant melonic part extracted from the expansion is always convergent, and should convey some information on the dynamics of initial configurations with a large spread over energies (a large number of initially excited low-lying modes).

When $N \rightarrow \infty$ in (4.1.6), hence $p \rightarrow 1$, *more and more* low-lying modes are excited by the initial conditions. We will identify in $\bar{s}_{\gamma,n}$ the amplitudes that scale in the leading way as $N \rightarrow \infty$ at each fixed order n of the perturbation series, and to *restrict* the perturbation theory for $\bar{S}_\gamma(t)$ to these contributions. As for tensor models, the dominant term will correspond to melonic graphs. At any fixed order in t , it was established in [60] that

$$\bar{s}_{\gamma,n} = s_{\gamma,n}^{melo} + o_{\gamma,n}(1/N). \quad (4.1.10)$$

Accordingly, the melonic approximation

$$S_\gamma^{melo}(t) := \sum_{n \in 2\mathbb{N}} s_{\gamma,n}^{melo} t^n \quad (4.1.11)$$

to the averaged Sobolev norm \bar{S}_γ includes only graphs of the melonic type and we have

$$\bar{S}_\gamma(t) = S_\gamma^{melo}(t) + o_{\gamma,t}(1/N). \quad (4.1.12)$$

In [60] it was proved that the time series for $S_\gamma^{melo}(t)$ has a finite, non-zero radius of convergence, hence it is well-defined and in fact *analytic* at least for a finite time interval (in essence, this is because the melonic family has far *fewer* graphs than the general family). The $1/N$ analysis can be summarised as

Theorem 4.1.1. *The dominant graphs as $N \rightarrow \infty$ for the averaged Sobolev norm $\bar{S}_\gamma(t)$ are exactly the melonic graphs and the corresponding approximation $S_\gamma^{melo}(t)$ is an analytic function of time in a disk $|t| < \rho$ of finite radius $\rho > 0$.*

Through an explicit computation of $s_{\gamma,2}^{melo}$ one can check that

Theorem 4.1.2. *For any $\gamma > 1$ there exists a constant δ such that $S_\gamma^{melo}(t)$ grows monotonically in time for $t \in [0, \delta]$.*

These are the main results of [60] and they mean that, *in the melonic approximation*, energy spreads at least for a while from the low modes to the higher modes, as expected in a turbulent cascade. In this chapter we will go beyond these results.

At this point we do not know if the average Sobolev norm is representative of our ensemble of resonant systems. For that we need to characterise on average the fluctuation around the mean value, namely the variance of Sobolev norms. Indeed, if the distribution of Sobolev norms happens to be similar to a uniform law, then the mean value would not be representative of the ensemble. However, if this distribution is a Gaussian law, the mean value is a good characterisation of the distribution. Moreover, it would be completely characterised by its mean value and variance.

We can already make some statement in this direction for the cases $\gamma = 0, 1$ using the fact that $S_{\gamma=0,1}(t)$ are independent of t , as we will show in Proposition 4.1.3. There is two regimes to consider: the first one is the $p = 1$ where the central limit theorem tells us that the fluctuation around the mean value of $NS_{\gamma=0,1}$ are distributed along a Gaussian law. This leads us to hope that at early times and in the limit $p \rightarrow 1$ the same results holds for $\gamma > 1$. The second regime is for $0 < p < 1$ where the central limit theorem cannot be used since the sum of variance squared on the different modes $\alpha_j \bar{\alpha}_j$ is always finite. Nevertheless, one has:

Proposition 4.1.3. *For $\gamma = 0, 1$ the Sobolev norms $S_{\gamma=0,1}(t)$ are independent of t and converge almost surely¹ for $0 < p < 1$.*

Proof. The time invariance is straightforward when we recast the equations of motion in the following form

$$\frac{d}{dt}\alpha_j(t) = -i \sum_{\substack{j',k,k'=0 \\ j+j'=k+k'}}^{\infty} C_{jj'kk'} \bar{\alpha}_{j'}(t) \alpha_k(t) \alpha_{k'}(t), \quad (4.1.13)$$

$$\frac{d}{dt}\bar{\alpha}_j(t) = i \sum_{\substack{j',k,k'=0 \\ j+j'=k+k'}}^{\infty} C_{jj'kk'} \alpha_{j'}(t) \bar{\alpha}_k(t) \bar{\alpha}_{k'}(t), \quad (4.1.14)$$

where $S = j + j' = k + k'$ is the resonance condition and $C_{jj'kk'}$ is symmetric under the exchange of j and j' , k and k' and of the pairs (j, j') and (k, k') . Making use of the equations of motion and the symmetry of the tensor couplings C under the exchange of the pairs of its indices, the derivative of the Sobolev norm with respect to time can be written as:

$$\dot{S}_1(t) = i \sum_{\substack{j,j',k,k'=0 \\ j+j'=k+k'}}^{\infty} (j - k) C_{jj'kk'} \alpha_j(t) \alpha_{j'}(t) \bar{\alpha}_k(t) \bar{\alpha}_{k'}(t). \quad (4.1.15)$$

The same manipulation for $\gamma = 0$ gives $\dot{S}_0(t) = 0$. Using the resonance condition, $j - k = k' - j'$ and the other symmetries of C under the exchange of j and j' , k and k' we also get $\dot{S}_1(t) = 0$.

Let us note $X_1 = N\alpha_1(0)\bar{\alpha}_1(0)$ which is distributed along a χ_2 law of density $e^{-x/2}/2$, and $X_j = N\alpha_j(0)\bar{\alpha}_j(0) \sim p^j X_1$ (equal in law). For a constant c , we consider

$$r_j = \mathbb{P}(X_j \geq jc^j) = \mathbb{P}(X_1 \geq jc^j/p^{j/2}), \quad (4.1.16)$$

¹We would like to thank Jean-François Marckert for discussions on this point.

Taking $c = \sqrt{p}$, we get

$$r_j = \mathbb{P}(X_1 \geq j) = e^{-j/2}. \quad (4.1.17)$$

Since $\sum_{j=0}^{\infty} r_j = \frac{\sqrt{e}}{\sqrt{e-1}}$ is finite, by Borel-Cantelli theorem, only a finite number of the events $X_j \geq jp^{j/2}$ occur. Hence $\sum_{j=0}^{\infty} X_j$ converge almost surely. \square

Once again, this results inclines us to think that similar statement can be made on the existence of the Sobolev norm for $\gamma > 1$.

These previous discussions present our motivation to study the variance of Sobolev norms which will at worst tell us if the mean value is a good characterisation of the distribution and at best enable us to completely characterise this same distribution.

In the following subsections, we will recall the tree expansion and explicit computations of the average Sobolev norms at order t^2 which prove Theorem 4.1.2 and from which we will build upon in section 4.2.

4.1.2 Tree expansion

We return to our pair of evolution equations (4.1.3), which we write as

$$\frac{d}{dt}\alpha_j(t) = -i \sum_{S=j}^{\infty} \sum_{k=0}^S C_{jk}^S \bar{\alpha}_{S-j}(t) \alpha_k(t) \alpha_{S-k}(t), \quad (4.1.18)$$

$$\frac{d}{dt}\bar{\alpha}_j(t) = i \sum_{S=j}^{\infty} \sum_{k=0}^S C_{jk}^S \alpha_{S-j}(t) \bar{\alpha}_k(t) \bar{\alpha}_{S-k}(t). \quad (4.1.19)$$

There is an iterative solution to these equations in terms of *suitably oriented and indexed* trees T (for (4.1.18)) and anti-trees \bar{T} (for (4.1.19)) in $\mathcal{T}_{1,3}^h$ (they are heap-ordered 3-ary 1-rooted trees) as defined in the following. The idea is to compute the h^{th} derivative $\alpha_j^{(h)}(t)$ recursively using (4.1.18) and (4.1.19). We start with a particular vertex (the root) and connect it with an edge to a first vertex of valency 4. In this way we get a tree with one root, one vertex of valency 4, and 3 leaves. To the vertex is associated a tensor couplings C and to each leaf a factor $\alpha(t)$ or $\bar{\alpha}(t)$, so that this first tree corresponds to $\dot{\alpha}_j$ as given in (4.1.18). In the same way, we can connect any of those leafs to a second vertex of valency 4, and we can then compute recursively $\alpha_j^{(h)}(t)$ and $\bar{\alpha}_j^{(h)}(t)$. The order in which the vertices of valency have been added in the recursion matters as well.

Ordered trees. The trees arising in the iteration of this process are *heap-ordered, 3-ary, 1-rooted trees*, which we now introduce. In this chapter, a *1-rooted tree* is a tree drawn on the plane, i.e. a tree together with an ordering of the edges around each vertex, which in addition has a distinguished vertex of valency one, called the root. The leaves are the vertices of valency 1 distinct from the root. It will be convenient in what follows to consider amputated leaves, hence to represent leaves simply as dashed half-edges hooked at another vertex but with no vertex at the end (see Figure 4.1), and to represent the root as a black square of valency one.

A rooted tree is said to be q -ary if its vertices are all of valency $q+1$ (we also call these the “true” vertices), except the root and the leaves. Around each vertex v of a rooted tree distinct from the root, there is a unique edge which belongs to the only path connecting this vertex to the root. We call this edge the parent-edge of v . The other edges incident to v are the children-edges. This provides a kinship among vertices as well.

We define a *heap-ordered tree* as a rooted tree together with a labelling σ of its h true vertices from 1 to h , which respects the kinship of the vertices, that is $\sigma(v) < \sigma(v')$ whenever v is the parent of v' . We denote $\mathcal{T}_{1,q}^h$ the set of q -ary 1-rooted heap-ordered trees with h true vertices.

When iterating the computation of derivatives $\alpha_j^{(h)}(t)$ and $\bar{\alpha}_j^{(h)}(t)$ one obtains a representation the following expansions

$$\alpha_r(t) = \sum_{h \in \mathbb{N}} \frac{t^h}{h!} \sum_{T \in \mathcal{T}_{1,3}^h} A_r(T), \quad (4.1.20)$$

$$\bar{\alpha}_r(t) = \sum_{\bar{h} \in \mathbb{N}} \frac{t^{\bar{h}}}{\bar{h}!} \sum_{\bar{T} \in \mathcal{T}_{1,3}^{\bar{h}}} A_r(\bar{T}). \quad (4.1.21)$$

where the amplitudes $A_r(T)$ and $A_r(\bar{T})$ take into account the orientation and indexation of the trees and anti-trees T and \bar{T} in a way that we now explain.

Orientation of the trees. The h 4-valent vertices of a tree in $\mathcal{T}_{1,3}^h$ represent the way in which the α factors have been recursively differentiated. The heap-ordering precisely keeps track of the differentiation history: the vertex labeled σ corresponds to the σ th differentiation step. The root of a tree (resp. an anti-tree) initially represents an α (resp. an $\bar{\alpha}$) factor, which we picture as out-going (resp. in-going). The first true vertex resulted from the differentiation of this initial factor. Our graphical rule at a true vertex v is to orient the children-edges which carried α factors at the $\sigma(v)$ th differentiation step as out-going and those which carried $\bar{\alpha}$ factors as in-going. The orientation of the full tree then results from recursively applying this “parent” rule to the true vertices while following the heap-ordering of the vertices as follows. Around a vertex v we denote the parent-edge $e_1(v)$.² The children-edges, which are ordered from 2 to 4, are denoted respectively by $e_2(v)$, $e_3(v)$, and $e_4(v)$. Among children-edges at a vertex v , the edge $e_2(v)$ is endowed with the same orientation (in-going or out-going) as the parent-edge $e_1(v)$, and the remaining two edges incident to v are endowed with the opposite orientation.

We remind the reader that, importantly, in a tree, only the leaves carry α or $\bar{\alpha}$ factors, the root and the solid edges do not. The leaves are half-edges and carry arrows: an arrow pointing out of the tree corresponds to a leaf and to an α factor whereas an arrow pointing into the tree corresponds to what we call an *anti-leaf* and to an $\bar{\alpha}$ factor.³ Note that a tree in $\mathcal{T}_{1,3}^h$ with h vertices has exactly $h+1$ leaves and h anti-leaves; conversely an anti-tree with \bar{h} vertices has exactly \bar{h} leaves and $\bar{h}+1$ anti-leaves. See some examples in Figure 4.1.

²Note that for the leaves it is the only incident (dashed) edge.

³We stress however that in this amputated representation, the root (which also has valency one), is still represented as a vertex and does not bring any α or $\bar{\alpha}$ factor.

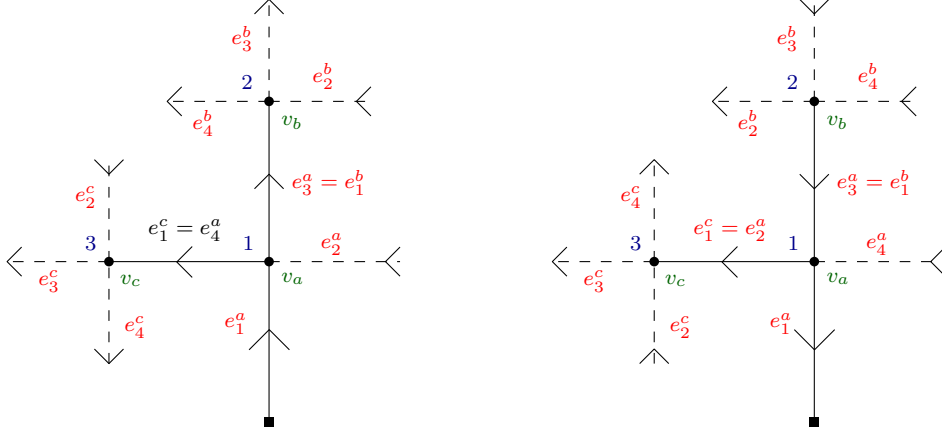


Figure 4.1: A heap-ordered tree oriented as a tree (left) or an anti-tree (right).

Momenta. In analogy with the Feynman graph terminology, let us call now the indices $j, S - j, k, S - k$ in (4.1.18-4.1.19) *momenta*.⁴ For a given 1-rooted tree with root index r entering the root, we now define its *momentum attribution* \mathcal{I}_T . It is a set of integers, defined first by a choice, for each 4-valent vertex v of the tree, of three non-negative integers $S_v \in \mathbb{N}$, $j_v \leq S_v$, and $k_v \leq S_v$. The two momenta j_v and $S_v - j_v$ are respectively attributed to the parent-edge $e_1(v)$ and the edge $e_2(v)$ and the two momenta, k_v and $S_v - k_v$, are respectively attributed to the edges $e_3(v)$ and $e_4(v)$. These choices furthermore satisfy the constraints that if a vertex v is incident to the root, the momentum of its parent-edge is the root momentum $j_v = r$, and the momenta of the two half-edges forming any edge must be the same. To each leaf ℓ is thus associated a momentum $j(\mathcal{I}_T, \ell)$ and to each anti-leaf $\bar{\ell}$ is associated a momentum $j(\mathcal{I}_T, \bar{\ell})$, namely those of their parent-vertex.

Amplitude of a tree. We then have the following ‘‘Feynman rules’’:

- to each (4-valent) vertex v of the tree or anti-tree, one associates a factor $C_{j_v k_v}^{S_v}$;
- to each leaf ℓ is associated a factor $\alpha_{j(\mathcal{I}_T, \ell)}(0)$ and to each anti-leaf $\bar{\ell}$, one associates a factor $\bar{\alpha}_{j(\mathcal{I}_T, \bar{\ell})}(0)$, where we stress again that the root vertex is not counted among leaves;
- each 4-valent vertex v of the tree or anti-tree whose unique parent-edge $e_1(v)$ is in-going (resp. out-going) is weighted by $(-i)$ (resp. $(+i)$).

The amplitude $A_r(T)$ is defined by multiplying all these factors and summing over all indices \mathcal{I}_T :

$$A_r(T) = \sum_{\mathcal{I}_T} \prod_v (\pm i) C_{j_v k_v}^{S_v} \prod_{\ell} \alpha_{j(\mathcal{I}_T, \ell)}(0) \prod_{\bar{\ell}} \bar{\alpha}_{j(\mathcal{I}_T, \bar{\ell})}(0). \quad (4.1.22)$$

The summation over \mathcal{I}_T more precisely stands for the following summations and constraints

$$\left(\sum_{S_{v_1} \geq r} \sum_{k_{v_1}=0}^{S_{v_1}} \right) \left(\prod_{\substack{v \text{ true} \\ \text{vertex}}} \sum_{S_v \geq 0} \sum_{j_v, k_v=0}^{S_v} \right) \left(\prod_{\substack{l \text{ leaf} \\ j_l \geq 0}} \sum_{j_l} \right) \prod_{e \text{ edge}} \delta_{a_e}^{b_e}, \quad (4.1.23)$$

⁴The symmetries of C is indeed reminiscent of energy-momentum conservation at each vertex.

where for every edge e , a_e and b_e are the momenta of its two half-edges (including the leaves), and the vertex v_1 is the true vertex incident to the root ($\sigma(v_1) = 1$). The amplitude $A_r(T)$ is a function of the entering momentum r , of the couplings C and of the initial data $\{\alpha_j(0), \bar{\alpha}_j(0)\}_{j \in \mathbb{N}}$.

Let us return to the Sobolev norms $S_\gamma(t) = \sum_{r \geq 0} r^\gamma \bar{\alpha}_r(t) \alpha_r(t)$. Using (4.1.20)-(4.1.21), one has the following time evolutions

$$S_\gamma(t) = \sum_{r \geq 0} \frac{r^\gamma}{N} G_2(r, t), \quad (4.1.24)$$

$$G_2(r, t) = N \bar{\alpha}_r(t) \alpha_r(t) = N \sum_{h \in \mathbb{N}, \bar{h} \in \mathbb{N}} \frac{t^{h+\bar{h}}}{h! \bar{h}!} \sum_{T \in \mathcal{T}_{1,3}^h, \bar{T} \in \mathcal{T}_{1,3}^{\bar{h}}} A_r(T) A_r(\bar{T}), \quad (4.1.25)$$

where we included a factor N in $G_2(r, t)$ for optimised scaling properties.

2-rooted tree. It is possible to simplify the factorial factors in the expansion (4.1.25) by using a slightly different notion of trees. By merging the roots of a tree T with h vertices and an anti-tree \bar{T} with \bar{h} vertices, we obtain a tree U with $n = h + \bar{h}$, 4-valent (true) vertices, $2n + 2$ leaves, and a single distinguished root-vertex of valency two. We call such trees *2-rooted trees*. Note that in the case where the tree is trivial ($h = 0$), the bivalent root is directly linked to a leaf (a dashed half-edge) and not to a true vertex, and similarly for the anti-tree. Most of what has been said for 1-rooted trees (ordering, parent-edge, heap-ordering) still holds for 2-rooted trees, and we denote $\mathcal{T}_{2,3}^n$ the set of heap-ordered 3-ary 2-rooted trees with n true vertices. The 2-rooted tree U inherits the orientations of T and \bar{T} : its bivalent root has one in-going edge and one out-going edge, and its $2n + 2$ leaves divide into $n + 1$ leaves and $n + 1$ anti-leaves. The momentum attribution \mathcal{I}_U of U follows the exact same rules as the momentum attributions for T and \bar{T} , the only difference being that there are now two vertices incident to the root.

Note however that when merging the roots of two heap-ordered 1-rooted trees, the resulting 2-rooted tree is not heap-ordered, and in order to heap-order it, we need to relabel its vertices. There are several ways to define a heap-ordering on U given the heap-orderings of T and \bar{T} . Indeed, there is one such heap-ordering on U for every set injection $\iota_T : \{1, \dots, h\} \rightarrow \{1, \dots, n = h + \bar{h}\}$ that preserves the natural order of integers. In fact, such an injection induces a relabeling of the vertices of T seen as a subgraph of U . Meanwhile, the complement in $\{1, \dots, n\}$ of the image $\text{Im } \iota_T$ induces a relabeling of the vertices of \bar{T} seen as a subgraph of U . The above constructed relabelings thus indeed defines a heap-ordering of U . Therefore, for each pair of heap-ordered T, \bar{T} there are as many heap-ordered 2-rooted trees as there are order-preserving injections ι_T , namely $\frac{n!}{h! \bar{h}!}$. It follows that if we define the amplitude of U as $A_r(U) := A_r(T) A_r(\bar{T})$, we have:

$$\sum_{U \in \mathcal{T}_{2,3}^n} A_r(U) = \sum_{U \in \mathcal{T}_{2,3}^n} A_r(T) A_r(\bar{T}) = \frac{n!}{h! \bar{h}!} \sum_{T \in \mathcal{T}_{1,3}^h, \bar{T} \in \mathcal{T}_{1,3}^{\bar{h}}} A_r(T) A_r(\bar{T}). \quad (4.1.26)$$

From this we conclude, using (4.1.25), that $G_2(r, t)$ is rewritten as a sum over heap-ordered 2-rooted trees as

$$G_2(r, t) = N \sum_{n \in \mathbb{N}} \frac{t^n}{n!} \sum_{U \in \mathcal{T}_{2,3}^n} A_r(U). \quad (4.1.27)$$

4.1.3 Averaged Sobolev norms

Averaging over C and α commutes. It is more convenient to first average over α , then over C .

Averaging over α . We recall that the initial conditions are Gaussian distributed random variables of zero mean and covariance (4.1.6)

$$\langle \alpha_j(0) \bar{\alpha}_{j'}(0) \rangle_\alpha = \frac{\delta_{jj'}}{N} \chi_N(j). \quad (4.1.28)$$

A tree $U \in \mathcal{T}_{2,3}^n$ has a binary root plus n , 4-valent true vertices forming a set $\mathcal{V}(U)$, and $n+1$ leaves and $n+1$ anti-leaves. The averaging over α pairs together in all the $(n+1)!$ possible ways the $n+1$ leaves with the $n+1$ anti-leaves of U into $n+1$ new α -edges. We call $\mathcal{W}_\alpha(U)$ the set of the $(n+1)!$ different pairings of leaves with anti-leaves and $\mathcal{E}_\alpha(w)$ the set of α -edges obtained for a given $w \in \mathcal{W}_\alpha(U)$. Any pair $(U \in \mathcal{T}_{2,3}^n, w \in \mathcal{W}_\alpha(U))$ defines a new oriented diagrams with a bivalent root-vertex. Its α -edges are naturally represented as *dashed*, and oriented from the leaf to the anti-leaf. An example is shown in Figure 4.2 (note that the 2-rooted tree in this example is composed of the tree on the left of Fig. 4.1, and of the only anti-tree with one true vertex). The remaining n edges in the diagram are not dashed (they link rooted or true vertices of U), and are depicted as solid, to distinguish them from the dashed edges, because only the latter carry a $\frac{\chi_N}{N}$ factor. As a consequence of (4.1.28), any dashed edge e constrains the two indices j_e, \bar{j}_e of the leaf and anti-leaf that it joins to be equal.

Note that any $w \in \mathcal{W}_\alpha(U)$ must connect the T and \bar{T} pieces of U because the number of leaves and anti-leaves differ by one in T and also in \bar{T} .

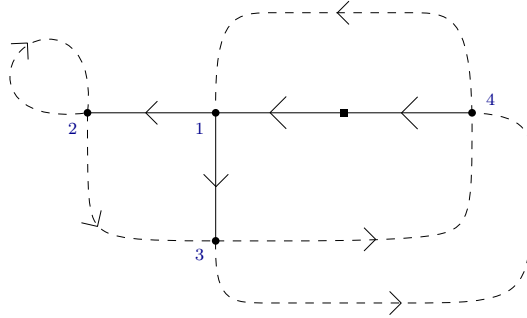


Figure 4.2: Oriented diagram defined by a tree in $U \in \mathcal{T}_{2,3}^n$ and a pairing $w \in \mathcal{W}_\alpha(U)$.

The α -averaged G_2 function is therefore a sum over trees $U \in \mathcal{T}_{2,3}^n$ and pairings $w \in \mathcal{W}_\alpha(U)$ of an associated amplitude in which the leaf factor $\prod_\ell \alpha_{j(\mathcal{I}_U, \ell)}(0) \prod_{\bar{\ell}} \bar{\alpha}_{j(\mathcal{I}_U, \bar{\ell})}(0)$ in the tree amplitudes has been replaced by a dashed edge factor $\prod_{e \in \mathcal{E}_\alpha(w)} \frac{\chi_N(j_e)}{N}$. Hence, since $|\mathcal{E}_\alpha(w)| = n+1$ and $\chi_N(j_e) = p^{j_e}$, we have

$$\langle G_2(r, t) \rangle_\alpha = \sum_{n \in \mathbb{N}} \frac{1}{N^n} \frac{t^n}{n!} \sum_{U \in \mathcal{T}_{2,3}^n} \sum_{\mathcal{I}_U} \prod_{v \in \mathcal{V}(U)} (\pm i) C_{j_v k_v}^{S_v} \sum_{w \in \mathcal{W}_\alpha(U)} \prod_{e \in \mathcal{E}_\alpha(w)} \delta_{j_e \bar{j}_e} p^{j_e}, \quad (4.1.29)$$

where \mathcal{I}_U is the momentum attribution of U .

Averaging over C . Recall that the tensor coefficients of C are Gaussian distributed variables of zero mean and covariance (4.1.5)

$$\begin{aligned} \langle C_{jk}^S C_{j'k'}^{S'} \rangle_C &= \frac{\delta_{SS'}}{8} \left(\delta_{jj'} \delta_{kk'} + \delta_{j,S-j'} \delta_{kk'} + \delta_{jj'} \delta_{k,S-k'} + \delta_{j,S-j'} \delta_{k,S-k'} \right. \\ &\quad \left. + \delta_{jk'} \delta_{kj'} + \delta_{j,S-k'} \delta_{kj'} + \delta_{jk'} \delta_{k,S-j'} + \delta_{j,S-k'} \delta_{k,S-j'} \right). \end{aligned} \quad (4.1.30)$$

A first consequence is that when averaged over C , the terms in the expansion (4.1.29) of $\langle G_2(r, t) \rangle_\alpha$ that correspond to diagrams (U, w) with an odd number n of true vertices vanish.

Let us focus on the contribution to the expansion $\langle G_2(r, t) \rangle_\alpha$ of a diagram with an even number of true vertices. The averaging over C of the corresponding term is expressed as a sum over all the possible ways of pairing the true vertices of the diagram two-by-two. For each such partition in pairs of vertices, the coefficients C associated with the vertices of a given pair are replaced with the covariance (4.1.30) (the indices S, j, k and S', j', k' correspond to the indices S_v, j_v, k_v and $S_{v'}, j_{v'}, k_{v'}$ associated with the two true vertices v and v'). This is known as the Wick theorem, and it is common to call such a pairing of two C 's a *Wick contraction*. For a diagram (U, w) with n true vertices, there are $n!! := n \cdot (n-1) \cdot (n-3) \cdot \dots \cdot 3 \cdot 1$ possible ways of performing the $n/2$ Wick contractions.

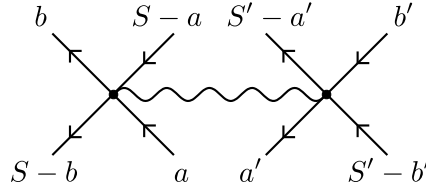


Figure 4.3: A wavy edge represents the averaging of two tensors C .

We represent a Wick contraction between two tensors C as a wavy line between the two corresponding true vertices, as depicted in Fig. 4.3 (the half-edges are solid in the figure, but up to three of them at each true vertex might be dashed). In Fig. 4.3, depending on whether the parent-edge is in-going or out-going, the indices a and b take the value j_v or k_v , and similarly for a', b' and $j_{v'}, k_{v'}$. The graphs obtained after averaging over C thus have a new set of $n/2$ wavy edges. For each such edge, there is a sum implementing the eight different terms in (4.1.30).

We denote by \mathcal{W}_C the set of Wick contractions of all the C factors together with one of the eight different possibilities for each wavy line. In the following, we call the eight terms in (4.1.30) *propagators*. An element of \mathcal{W}_C is then a choice of a partition of all of the true vertices in pairs of vertices (represented by wavy lines), together with a choice of propagator, *i.e.* of one of the eight terms in (4.1.30), for each wavy line. Each $w' \in \mathcal{W}_C$ gives a set of new momentum identifications, which we denote for the moment as $\delta_{w'}(\mathcal{I}_U)$. Moreover we call a **diagram** $G = (U, w)$ with the added $w' \in \mathcal{W}_C$ a **graph**.

Note that $|\mathcal{W}_C| = 8^{n/2} n!!$. Indeed, the number of pairings of all the true vertices is $n!!$, and it should be multiplied by $8^{n/2}$, because there are eight choices of possible propagators for each wavy line. Then to each diagram there is $8^{n/2} n!!$ associated graphs.

In this way, the expansion for the function G_2 , when averaged over α and C , is expressed as a sum over graphs $G = (U, w, w')$ which have a set \mathcal{V} of n true vertices

(which are now *five-valent* if we count the wavy edges) and one bivalent root, a set \mathcal{E}_s of n solid edges, a set \mathcal{E}_α of $n + 1$ dashed edges, and a set \mathcal{E}_C of $n/2$ wavy edges. The root constrains the momenta of the two edges attached to be r . We write this expansion as follows

$$\langle G_2(r, t) \rangle_{\alpha, C} = \sum_{n \text{ even}} \frac{t^n}{n!} 8^{-n/2} \sum_{U \in \mathcal{T}_{2,3}^n} \epsilon(U) \sum_{\substack{w \in \mathcal{W}_\alpha(U) \\ w' \in \mathcal{W}_C(U)}} \mathcal{A}_r(G), \quad (4.1.31)$$

$$\mathcal{A}_r(G) = \frac{1}{N^n} \sum_{\mathcal{I}_U} \delta_{w'}(\mathcal{I}_U) \prod_{e \in \mathcal{E}_\alpha(w)} \delta_{j_e \bar{j}_e} p^{j_e}, \quad (4.1.32)$$

where $\epsilon(U)$ is the sign obtained by collecting all the n factors $\pm i$ in the previous formula (since $n = h + \bar{h}$ is even, these factors must multiply to a real sign ± 1), and $\mathcal{A}_r(G)$ is the *amplitude* associated to the graph $G = (U, w, w')$, which is now obviously strictly positive. Indeed, at fixed root-momentum r , it evaluates the sum over all the $\{S_v, j_v, k_v\}$ integers using the delta constraints in $\delta_{w'}(\mathcal{I}_U) \prod_{e \in \mathcal{E}_\alpha(w)} \delta_{j_e \bar{j}_e}$, the exponential decays $\prod_{e \in \mathcal{E}_\alpha(w)} p^{j_e}$ for the momenta of the dashed edges and the root constraint that the two incident edges have fixed momentum r .

4.1.4 Explicit computations at order t^2

We now recall the computation of the first non-trivial order of perturbation theory, namely $n = 2$. In that case, there is a single possible Wick contraction w' , hence, in the figures, the corresponding wavy edge will be omitted, but of course the indices identification that it implies will be included in the computations.

Amplitudes at order 2

We now list the leading contributions at order two in t , and compute the corresponding graph amplitudes. We do not represent the heap-orderings on the diagrams in the figures, as they simply provide a counting factor which we will indicate explicitly in each case. We arrange the contributions into three different groups and will only treat in detail the first case (more details for the other groups can be found in [60]).

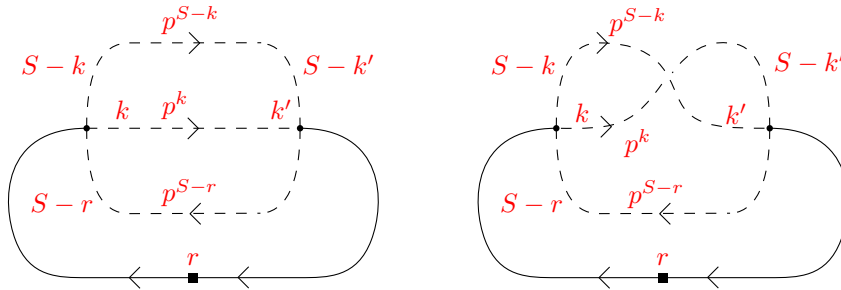


Figure 4.4: Type-I diagram.

Each one of the diagrams in Fig. 4.4 has two heap-orderings (the root is labeled 1 and there are two ways of labelling the two other true vertices). These four diagrams give the same total contribution to $\langle G_2(r, t) \rangle_{\alpha, C}$ at order 2, which can be understood from

the symmetries of C . However, for a given choice of propagator for the wavy edge, the amplitudes of the corresponding graphs for the diagrams on the left and on the right of Fig. 4.4 actually differ. In total, there are $2 \times 2 \times 8$ graphs corresponding to the diagrams shown in Fig. 4.4. We call them graphs of type I. In the following, we provide step-by-step details for the computation of the amplitude associated with any one of the 2×8 graphs $G = (U, w, w')$ corresponding to the diagram on the left of Fig. 4.4.

Using (4.1.32), the amplitude of a graph corresponding to the left diagram of Fig. 4.4 reads

$$\mathcal{A}_r(G) = \frac{1}{N^2} \sum_{S \geq r} \sum_{j, k=0}^S \sum_{S' \geq r} \sum_{j', k'=0}^{S'} \delta_{w'}(\mathcal{I}_U) p^{S-k} \delta_{S-k}^{S'-k'} p^k \delta_k^{k'} p^{S-j} \delta_{S-j}^{S'-j'} \delta_j^r \delta_r^{j'}, \quad (4.1.33)$$

where $\delta_{w'}(\mathcal{I}_U)$ is one of the eight propagators in (4.1.30). As a first step, we use the identification between S and S' in $\delta_{w'}(\mathcal{I}_U)$ to sum over S' , and sum over j and j' , which are fixed to r , so that we obtain

$$\mathcal{A}_r(G) = \frac{1}{N^2} \sum_{S \geq r} \sum_{k, k'=0}^S \tilde{\delta}_{w'}(\mathcal{I}_U) p^{2S-r} \delta_k^{k'}, \quad (4.1.34)$$

where $\tilde{\delta}_{w'}(\mathcal{I}_U)$ is now one of the eight propagators $1, \delta_k^{S-k'}, \delta_r^{S-r}, \delta_k^{S-k'} \delta_r^{S-r}, \delta_k^r, \delta_k^{S-r} \delta_r^{k'}, \delta_k^r \delta_r^{S-k'},$ or δ_k^{S-r} . The contribution from the first trivial propagator $\tilde{\delta}_{w'}(\mathcal{I}_U) = 1$ (originally $\delta_{w'}(\mathcal{I}_U) = \delta_S^r \delta_j^r \delta_k^{k'}$) is

$$\mathcal{A}_r(G_m^I) = p^r \left(\frac{p^2}{(1+p)^2} + \frac{1}{N} \frac{r+1}{1+p} \right). \quad (4.1.35)$$

The sum of the contributions from the other seven propagators is

$$\frac{1}{N} \left[\frac{p^r}{(1+p)(1+p^2)} (\delta_{r[2]}^0 + p^2 \delta_{r[2]}^1) + \frac{2p^r}{1+p} \right] + \frac{1}{N^2} 2p^{3r} (r+2), \quad (4.1.36)$$

where $\delta_{r[2]}^0$ vanishes if r is even, and conversely for $\delta_{r[2]}^1$. In particular, the contributions of these seven propagators for the wavy line are subdominant when $p \rightarrow 1$.

Using the same reasoning, the amplitude of a graph corresponding to the diagram on the right of Fig. 4.4 is

$$\mathcal{A}_r(G') = \frac{1}{N^2} \sum_{S \geq r} \sum_{k, k'=0}^S \tilde{\delta}_{w'}(\mathcal{I}_U) p^{2S-r} \delta_k^{S-k'}, \quad (4.1.37)$$

where $\tilde{\delta}_{w'}(\mathcal{I}_U)$ is one of the eight propagators $\delta_k^{k'}, \delta_k^{k'} \delta_r^{S-r}, 1, \delta_r^{S-r}, \delta_k^r, \delta_k^{S-r} \delta_r^{k'}, \delta_k^r \delta_r^{S-k'},$ or δ_r^{S-r} . In this case, the dominant contribution only comes from the third propagator $\tilde{\delta}_{w'}(\mathcal{I}_U) = \delta_S^{S'} \delta_j^{j'} \delta_k^{S-k'}$ and gives the same result as (4.1.35). The same holds for the seven other propagators and for the sum (4.1.36).

Therefore, we observe that the total sum of the contributions of the graphs from the left and from the right of Fig. 4.4 is the same. This result can actually be traced back to the symmetries of C . Indeed, using these symmetries, one can untwist the dashed edges of the graphs from the right of Fig. 4.4. Then, by a local relabelling $k' \rightarrow S' - k'$, we

directly obtain the graphs from the left of the figure. Moreover, this also explains why it is the first propagator $\delta_S^{S'} \delta_j^{j'} \delta_k^{k'}$ that gives the dominant contribution for the graphs from the left of the figure whereas it is the third propagator $\delta_S^{S'} \delta_j^{j'} \delta_k^{S-k'}$ for the graphs from the right. In both cases, it is obtained for the trivial propagator $\tilde{\delta}_{w'}(\mathcal{I}_U) = 1$.

We will call *leading propagator* δ_{lead} the particular choice of propagator for the wavy edge of a graph, which leads to a dominant contribution. For each one of the diagrams presented in Fig. 4.4, 4.5a, and 4.5b, and similar diagrams, there is a unique leading propagator. This unique leading propagator always corresponds to the trivial propagator $\tilde{\delta}_{w'}(\mathcal{I}_U) = 1$, i.e. to the propagator which does not add additional constraints to the constraints imposed by the edges. This is quite intuitive, since constraints lower the number of free sums thus also lowering the number of potential N factors. In the following we will only be interested in the dominant contribution of each graph amplitudes.

In total, the sum of the dominant amplitudes among the 32 graphs of type I, denoted \mathcal{A}_r^{I} , is four times (4.1.35). The total contribution of these graphs to $\langle G_2(r, t) \rangle_{\alpha, C}$ is $\frac{t^2}{16} \mathcal{A}_r^{\text{I}}$.

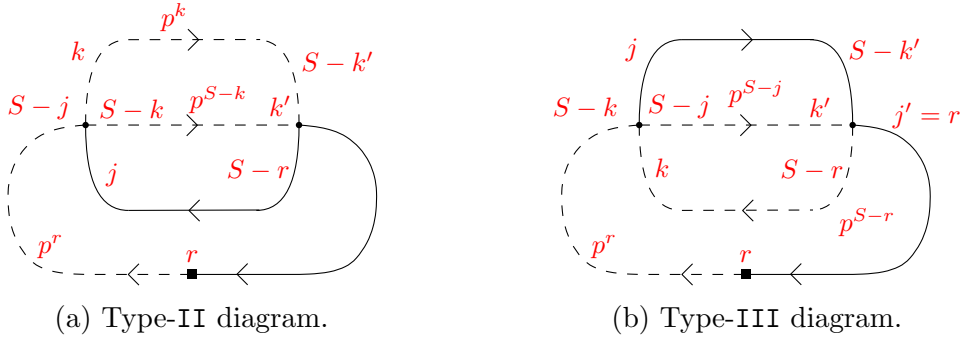


Figure 4.5: Remaining leading diagram types.

The second kind of diagrams is shown in Fig. 4.5a. We only draw one example, however there are four diagrams which all give the same contribution due to the symmetries of C : they are obtained by exchanging the role of the tree and the anti-tree, and by crossing the k and $S - k$ edges as in Fig. 4.4. Each one of these four diagrams gives 8 graphs, thus a total of 32 graphs (here, the trees have a unique heap-ordering).

The dominant term in the amplitude of any one of the 4 diagrams $G = (U, w, w')$ as in the example of Fig. 4.5a is:

$$\mathcal{A}_r(G_m^{\text{II}}) = p^{2r} \left(p + \frac{r+1}{N} \right). \quad (4.1.38)$$

In total, the sum of the dominant term in the amplitudes of the 4 diagrams of type II, denoted $\mathcal{A}_r^{\text{II}}$, is four times (4.1.38), and the contribution of these diagrams to $\langle G_2(r, t) \rangle_{\alpha, C}$ is $\frac{t^2}{16} \mathcal{A}_r^{\text{II}}$.

The third type of diagrams is shown in Fig. 4.5b. Again, we only draw one of them, however there are now eight diagrams which all give the same contribution due to the symmetries of C , and which we obtain by exchanging the role of the tree and the anti-tree, by crossing the two upper edges as on the right of Fig. 4.4, or by choosing which one of the two upper edges is solid and which one is dashed. Each one of these 8 diagrams gives 8 graphs, thus a total of 64 graphs (again, the tree has a unique heap-ordering).

Importantly, here the total contribution from these 64 graphs to $\langle G_2(r, t) \rangle_{\alpha, C}$ comes with a *minus sign* (i.e. $\epsilon(U) = -1$), because the two true vertices have parent-edges with the same orientation: both in-going or both out-going. The dominant terms in the amplitude of the diagram of Fig. 4.5b is

$$\mathcal{A}_r(G_m^{\text{III}}) = p^r - \frac{p^{2r+1}}{1+p}. \quad (4.1.39)$$

In total, the sum of the dominant terms in the amplitudes of the 8 diagrams of type III, denoted $\mathcal{A}_r^{\text{III}}$, is eight times (4.1.38), and the contribution of these diagrams to $\langle G_2(r, t) \rangle_{\alpha, C}$ is $-\frac{t^2}{16}\mathcal{A}_r^{\text{III}}$.

Sobolev norms at order 2

The leading contribution to $\langle G_2(r, t) \rangle_{\alpha, C}$ at order 2 is given by

$$\begin{aligned} \langle G_2(r, t) \rangle_{\alpha, C}^{(2)} &= \frac{t^2}{16}(\mathcal{A}_r^{\text{I}} + \mathcal{A}_r^{\text{II}} - \mathcal{A}_r^{\text{III}}) + o(N^{-1}) \\ &= \frac{t^2 p^r}{4} \left[p^{r+1} \frac{p+3}{p+1} + \frac{p^2}{(p+1)^2} - 2 \right] + \frac{(r+1)t^2 p^r}{4N} \left[\frac{1}{1+p} + p^r \right] + o(N^{-1}), \end{aligned} \quad (4.1.40)$$

$$(4.1.41)$$

Indeed only the terms from \mathcal{A}_r^{I} , $\mathcal{A}_r^{\text{II}}$, and $\mathcal{A}_r^{\text{III}}$ give dominant contributions (because when summed over r , a typical term of the form $\sum r^\gamma p^r$ behaves as $(1-p)^{-1-\gamma}$ as $p \rightarrow 1$). We make more precise statements in the following paragraph.

We are interested in the averaged Sobolev norms at order 2,

$$\bar{S}_\gamma^{(2)}(t) := \langle S_\gamma(t) \rangle_{\alpha, C}^{(2)} = \sum_{r \geq 0} \frac{r^\gamma}{N} \langle G_2(r, t) \rangle_{\alpha, C}^{(2)}. \quad (4.1.42)$$

In general, for $\gamma > 0$, we express the various terms involved in $\bar{S}_\gamma^{(2)}(t)$ using the series $L_\gamma(z) = \sum_{r \geq 1} r^\gamma z^r$ (they are polylogarithm functions⁵). We have for $\gamma > 0$

$$\begin{aligned} \bar{S}_\gamma^{(2)}(t) &= \frac{t^2}{4N} \left[p \frac{p+3}{p+1} L_\gamma(p^2) + \left(\frac{p^2}{(p+1)^2} - 2 \right) L_\gamma(p) \right] \\ &\quad + \frac{t^2}{4N^2} \left[\frac{L_{\gamma+1}(p) + L_\gamma(p)}{1+p} + L_{\gamma+1}(p^2) + L_\gamma(p^2) \right] + o(N^\gamma), \end{aligned} \quad (4.1.43)$$

To obtain the asymptotic behavior of the order 2 Sobolev norms, let us take a closer look at the behavior of L_γ near 1, when γ is a positive integer. In that case,

$$L_\gamma(z) = \frac{1}{(1-z)^{\gamma+1}} \sum_{k=0}^{\gamma-1} A(\gamma, k) z^{\gamma-k}, \quad (4.1.44)$$

⁵In the standard notation, this series corresponds to the polylogarithm $L_{-\gamma}(z)$, however all the polylogarithm functions appearing in this chapter have similar negative coefficient, hence the introduction of our notation.

where the $A(\gamma, k)$ are the Eulerian numbers, which satisfy the identity

$$\sum_{k=0}^{\gamma-1} A(\gamma, k) = \gamma!, \quad (4.1.45)$$

so that when approaching 1,

$$L_\gamma(z) = \frac{\gamma!}{(1-z)^{\gamma+1}} + o\left(\frac{1}{(1-z)^{\gamma+1}}\right). \quad (4.1.46)$$

We find that when N goes to infinity (p goes to 1),

$$\bar{S}_\gamma^{(2)}(t) = \frac{t^2 N^\gamma \gamma!}{16} \left[\frac{5+\gamma}{2^\gamma} + 2\gamma - 5 \right] + o(N^\gamma), \quad (4.1.47)$$

In particular, we see that since $\frac{5+\gamma}{2^\gamma} + 2\gamma - 5$ does not vanish for $\gamma > 1$, the only dominant contributions are obtained for the leading propagators. Furthermore, very importantly, *the order 2 averaged Sobolev norms are positive when p is close to 1*, which proves theorem 4.1.2.

4.2 Variance of the Sobolev norm at order t^4

We can adapt the tree and diagram expansions discussed in section 4.1.2 and 4.1.3 to the computation of the variance of Sobolev norms. We need to compute

$$\langle S_\gamma(t)^2 \rangle_{C,\alpha,c} = \sum_{r_1 \geq 0} \sum_{r_2 \geq 0} (r_1 r_2)^\gamma \langle \alpha_{r_1}(t) \bar{\alpha}_{r_1}(t) \alpha_{r_2}(t) \bar{\alpha}_{r_2}(t) \rangle_{C,\alpha,c}, \quad (4.2.1)$$

at order t^4 which is the first non-trivial order in t , where

$$\langle \alpha_{r_1}(t) \bar{\alpha}_{r_1}(t) \alpha_{r_2}(t) \bar{\alpha}_{r_2}(t) \rangle_{C,\alpha,c} = \langle \alpha_{r_1}(t) \bar{\alpha}_{r_1}(t) \alpha_{r_2}(t) \bar{\alpha}_{r_2}(t) \rangle_{C,\alpha} - \langle \alpha_{r_1}(t) \bar{\alpha}_{r_1}(t) \rangle_{C,\alpha} \langle \alpha_{r_2}(t) \bar{\alpha}_{r_2}(t) \rangle_{C,\alpha}. \quad (4.2.2)$$

Similarly to the G_2 computation, we need to consider

$$G_4(r_1, r_2, t) = N^2 \alpha_{r_1}(t) \bar{\alpha}_{r_1}(t) \alpha_{r_2}(t) \bar{\alpha}_{r_2}(t). \quad (4.2.3)$$

This expression can be written as a tree expansion

$$G_4(r_1, r_2, t) = N^2 \sum_{h_1, \bar{h}_1 \in \mathbb{N}} \sum_{h_2, \bar{h}_2 \in \mathbb{N}} \frac{t^{h_1 + \bar{h}_1 + h_2 + \bar{h}_2}}{h_1! \bar{h}_1! h_2! \bar{h}_2!} \sum_{T_1, \bar{T}_1 \in \mathcal{T}_{1,3}^h} \sum_{T_2, \bar{T}_2 \in \mathcal{T}_{1,3}^h} A_{r_1}(T_1) A_{r_1}(\bar{T}_1) A_{r_2}(T_2) A_{r_2}(\bar{T}_2), \quad (4.2.4)$$

and then rewritten as a sum over a pair of heap-ordered 2-rooted trees

$$G_4(r_1, r_2, t) = N^2 \sum_{n_1, n_2 \in \mathbb{N}} \frac{t^{n_1 + n_2}}{n_1! n_2!} \sum_{U_1, U_2 \in \mathcal{T}_{2,3}^h} A_{r_1}(U_1) A_{r_2}(U_2), \quad (4.2.5)$$

where n_1 and n_2 are the numbers of true vertices of U_1 and U_2 respectively. Noting by U the pair of heap-ordered 2-rooted trees (U_1, U_2) , and averaging on both α and C , we obtain

$$\langle G_4(r_1, r_2, t) \rangle_{C,\alpha} = \sum_{n_1 + n_2 \text{ even}} \frac{t^{n_1 + n_2}}{n_1! n_2!} 8^{-\frac{n_1 + n_2}{2}} \sum_{U \in \mathcal{T}_{2,3}^h \times \mathcal{T}_{2,3}^h} \epsilon(U) \sum_{\substack{w \in \mathcal{W}_\alpha(U) \\ w' \in \mathcal{W}_C(U)}} A_{r_1, r_2}(G), \quad (4.2.6)$$

where $\mathcal{W}_\alpha(U)$ is the set of different pairings of leaves with anti-leaves in U (which means that some pairings can happen between U_1 and U_2 or inside each 2-rooted tree), $\mathcal{W}_C(U)$ is the set of different Wick contractions of all the tensor couplings C , $\epsilon(U)$ is the global ± 1 factor depending on the orientation of the solid edges in U . We note $A_{r_1, r_2}(G)$ as the amplitude associated to the graph $G = (U, w, w')$ which reads

$$A_{r_1, r_2}(G) = \frac{1}{N^{n_1+n_2}} \sum_{\mathcal{I}_U} \delta_{w'}(\mathcal{I}_U) \prod_{e \in \mathcal{E}_\alpha(w)} \delta_{j_e \bar{j}_e} p^{j_e}, \quad (4.2.7)$$

where \mathcal{I}_U is the moment attribution of U , $\delta_{w'}(\mathcal{I}_U)$ are the momentum constraints imposed by the Wick contraction of C and $\mathcal{E}_\alpha(w)$ the set of dashed edges of G .

In the following, we are only interested in connected graphs⁶, we will compute

$$\langle G_4(r_1, r_2, t) \rangle_{C, \alpha} - \langle G_2(r_1, t) \rangle_{C, \alpha} \langle G_2(r_2, t) \rangle_{C, \alpha}. \quad (4.2.8)$$

We want to emphasise again that a diagram is consisted only of solid and dashed edges. For each diagram, many graphs are obtained by choosing how to add wavy-lines and for each wavy-lines we have to pick one of the eight possible propagators. Only one choice of wavy-lines and propagators gives a leading order graph amplitude. In the following, we will mention which wavy-lines choice is the dominant one but not represent them. Moreover, diagrams are grouped in types which are the different ways one can draw a diagram and obtain the same leading order graph amplitude. When summing all dominant graph amplitudes, this leads to a combinatorial factor which counts the number of diagrams grouped within the same type.

We now determine which diagrams give leading order graphs with the right choice of Wick contractions and propagators for C , and we only compute these dominant contributions. We use the notation $\mathcal{A}_{r_1, r_2}(G)$ as the sum of the dominant graph amplitudes belonging to the same diagram type G . This means that we include the combinatorial factor coming from the perturbative expansion, namely $\frac{1}{n_1! n_2!} 8^{-\frac{n_1+n_2}{2}}$, the factor counting the number of diagram of type G , and the global ± 1 factor $\epsilon(U)$.

There are three classes of diagrams contributing to the variance of Sobolev norms at leading order. We thus split up the variance at order t^4 in three parts:

$$\bar{S}_\gamma^{(4)}(t) = \sum_{r_1 \geq 0} \sum_{r_2 \geq 0} \frac{(r_1 r_2)^\gamma}{N^2} \left(\langle G_4(r_1, r_2, t) \rangle_{C, \alpha}^{(4)} - \langle G_2(r_1, t) \rangle_{C, \alpha}^{(2)} \langle G_2(r_2, t) \rangle_{C, \alpha}^{(2)} \right) \quad (4.2.9)$$

$$= \bar{S}_{\gamma, M}^{(4)}(t) + \bar{S}_{\gamma, L1}^{(4)}(t) + \bar{S}_{\gamma, L2}^{(4)}(t). \quad (4.2.10)$$

The first class are melonic diagrams which are very similar to the diagrams obtained in the computation of the average Sobolev norms. These diagrams come in 4 different types and we compute their contribution $\bar{S}_{\gamma, M}^{(4)}(t)$ in subsection 4.2.1. Then there are two class of ladder diagrams that are computed in subsection 4.2.2. For the first class, we compute their contributions to the variance of Sobolev norms $\bar{S}_{\gamma, L1}^{(4)}(t)$. The second class is more involved and at the time of the writing of this chapter we only computed the dominant graphs amplitudes. Their contribution to the Sobolev variance $\bar{S}_{\gamma, L2}^{(4)}(t)$ is a work in progress.

⁶Note that a graph disconnected with respect to dashed edges but connected by wavy-edges (or the opposite) doesn't contribute at leading order.

4.2.1 Melonic diagrams

The four diagram types treated in this section are drawn in Figure 4.6 and their graph amplitudes are square or product of the graphs amplitudes found in subsection 4.1.4. We give some details for the diagram type M_I shown in Figure 4.6a and directly give the results for the other types. The Wick contractions for C are pairing the true vertices already linked by three dashed edges so that to obtain melonic sub-graphs with four edges (three dashed edges and one wavy-line). The wavy-lines are taken in an analogous way for the other diagram types except on of the dashed edge in replace by a solid edge. The dominant graph amplitudes for M_I is then

$$\mathcal{A}_r(M_I) = \delta_{r_1, r_2} \frac{16}{8^2 4} \left(\frac{1}{N^2} \sum_{S \geq r} (S+1) p^{2S-r} \right)^2 = \frac{\delta_{r_1, r_2}}{16} p^{2r} \left(\frac{p^2}{(1+p)^2} + \frac{1}{N} \frac{r+1}{1+p} \right)^2, \quad (4.2.11)$$

where the root indices r_1 and r_2 are identified and by a slight abuse of notation are both called r . The combinatorial factor 16 comes first from the 4 possible heap-orderings of the 2-rooted trees and then from a factor 4 which is obtained by interchanging the dashed lines of similar orientations.

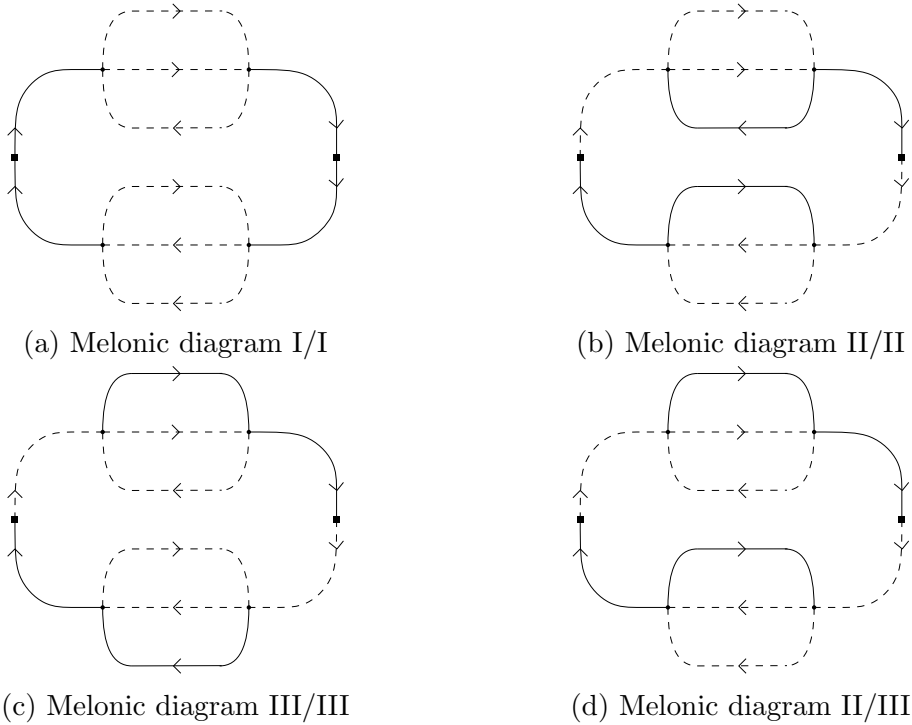


Figure 4.6: Melonic diagram types contributing at leading order to the variance of Sobolev norms at order t^4 .

The leading amplitudes for the other types are computed to be:

$$\mathcal{A}_r(M_{II}) = \frac{\delta_{r_1, r_2}}{32} \left(p^{2r} \left(p + \frac{r+1}{N} \right) \right)^2 \quad (4.2.12)$$

$$\mathcal{A}_r(M_{III}) = \frac{\delta_{r_1, r_2}}{8} \left(p^r - \frac{p^{2r+1}}{1+p} \right)^2 \quad (4.2.13)$$

$$\mathcal{A}_r(M_{II/III}) = -\frac{\delta_{r_1, r_2}}{8} p^{2r} \left(p + \frac{r+1}{N} \right) \left(p^r - \frac{p^{2r+1}}{1+p} \right). \quad (4.2.14)$$

Knowing these amplitudes we can proceed to compute their contribution to the variance. As above, we treat in detail M_I , the computational details for the other types can be found in Appendix F. The contribution to the Sobolev 2-point of $\mathcal{A}_r(M_I)$ is

$$\begin{aligned} & \sum_{r \geq 0} \frac{r^{2\gamma}}{16N^2} p^{2r} \left(\frac{p^2}{(1+p)^2} + \frac{1}{N} \frac{r+1}{1+p} \right)^2 \\ &= \sum_{r \geq 0} \frac{r^{2\gamma}}{16N^2} p^{2r} \left(\frac{p^4}{(1+p)^4} + \frac{2p^2}{N} \frac{r+1}{(1+p)^3} + \frac{1}{N^2} \left(\frac{r+1}{1+p} \right)^2 \right) \\ &= \frac{1}{16N^2} \left(\frac{p^4}{(1+p)^4} L_{2\gamma}(p^2) + \frac{2p^2}{N(1+p)^3} (L_{2\gamma}(p^2) + L_{2\gamma+1}(p^2)) \right. \\ & \quad \left. + \frac{1}{N^2(1+p)^2} (L_{2\gamma}(p^2) + 2L_{2\gamma+1}(p^2) + L_{2\gamma+2}(p^2)) \right). \end{aligned} \quad (4.2.15)$$

From equation (4.1.46), we know that $L_\gamma(p)$ is of order $N^{\gamma+1}$ in the limit $p \rightarrow 1$. At leading order the only contributing terms are

$$\frac{1}{16N^2} \left(\frac{p^4}{(1+p)^4} L_{2\gamma}(p^2) + \frac{2p^2}{N(1+p)^3} L_{2\gamma+1}(p^2) + \frac{1}{N^2(1+p)^2} L_{2\gamma+2}(p^2) \right). \quad (4.2.16)$$

In the limit $p \rightarrow 1$, this expression simplifies to

$$\begin{aligned} & \frac{N^{2\gamma-1}}{16} \left(\frac{p^4}{(1+p)^4} \frac{(2\gamma)!}{(1+p)^{2\gamma+1}} + \frac{2p^2}{(1+p)^3} \frac{(2\gamma+1)!}{(1+p)^{2\gamma+2}} + \frac{1}{(1+p)^2} \frac{(2\gamma+2)!}{(1+p)^{2\gamma+3}} \right) \\ & \stackrel{p \rightarrow 1}{=} \frac{N^{2\gamma-1}}{2^{2\gamma+9}} (2\gamma)! (4\gamma^2 + 10\gamma + 5) + o(N^{2\gamma-1}). \end{aligned} \quad (4.2.17)$$

Thus, in the limit $p \rightarrow 1$, the total contribution of melonic diagrams to the variance of Sobolev norms at order t^4 is:

$$\bar{S}_{\gamma, M}^{(4)}(t) = \frac{t^4 N^{2\gamma-1}}{8} (2\gamma)! \left(\frac{1}{2^{2\gamma+6}} (4\gamma^2 + 10\gamma + 5) + \frac{1}{2^{4\gamma+7}} (2\gamma^2 + 11\gamma + 13) \right) \quad (4.2.18)$$

$$+ (2\gamma+1) \left(\frac{1}{2^{4\gamma+5}} - \frac{1}{3^{2\gamma+2}} \right) + \frac{1}{2^{2\gamma+1}} + \frac{3}{2^{4\gamma+4}} - \frac{2}{3^{2\gamma+1}} \Big) + o(N^{2\gamma-1}). \quad (4.2.19)$$

4.2.2 Ladder diagrams

In this subsection we compute the amplitude of ladder diagrams (here a rail with 2 rungs). There is a total of 18 different types of such diagrams shown in figure 4.7. We further split these diagram types into two classes. The first class is constituted of 11 diagrams whose dominant graph amplitudes are straightforward to compute. The remaining 7 types belonging to the second class are more involved. For each of these two classes of ladder diagrams, we will detail the computation of the dominant graph amplitudes of one type. The details for other types can be found in Appendix F.

We name the different types of diagrams in the following way, each 2-rooted trees in the pair used to construct the diagram can be of type *I*, *II* or *III* depending of its solid

edges. For a given type of trees, when contracting the leaves, several pattern of dashed edges can occur. We refer to these patterns by adding A , B or C to the original type. When the two sides of a diagram are the same, we simplify the notation such that, for instance the type IIA/IIA is noted L_{IIA} . Moreover, for each diagrams, the wavy-lines are drawn between the two true vertices of a same vertical rung and we pick the leading propagators to get the dominant graph contribution.

We consider for example the diagram type $L_{IA/IB}$ showed on Figure 4.7b. It is made of two part, the left part is of type IA , and the right part of type IB . Its dominant graph amplitude writes

$$\mathcal{A}_{r_1, r_2}(L_{IA/IB}) = \frac{64}{8^2 4 N^4} \sum_{S_1 \geq r_1} \sum_{S_2 \geq r_2} p^{2(S_1+S_2)-r_1-r_2} \sum_{k_1=0}^{S_1} \sum_{k_2=0}^{S_2} \delta_{S_1-r_1}^{k_2} \quad (4.2.20)$$

$$= \frac{p^{r_1+r_2}}{4N^4} \sum_{S_2 \geq 0} p^{2S_2} \sum_{S_1=0}^{S_2+r_2} (S_1 + r_1 + 1) p^{2S_1} \quad (4.2.21)$$

$$= \frac{p^{r_1+r_2}}{4N^4} \left(\frac{1 + r_1(1 - p^2)}{(1 - p^2)^3} - \frac{p^{2(r_2+1)}}{(1 - p^4)(1 - p^2)^2} \right. \\ \left. - \frac{p^{2(r_2+2)}}{(1 - p^2)(1 - p^4)^2} ((r_1 + r_2)(1 - p^4) + 1) \right) \quad (4.2.22)$$

$$= \frac{p^{r_1+r_2}}{4N(1+p)^2} \left(\frac{1}{(1+p)} + \frac{r_1}{N} - \frac{p^{2(r_2+1)}}{(1+p)(1+p^2)} \right. \\ \left. - \frac{p^{2(r_2+2)}}{(1+p)(1+p^2)^2} - \frac{(r_1 + r_2)p^{2(r_2+2)}}{N(1+p^2)} \right). \quad (4.2.23)$$

The combinatorial factor 64 is obtain in the following way. We get a factor 4 from the different heap-orderings and a factor 2 from the fact that the pair of 2-rooted trees (U_1, U_2) gives a diagram of type IA/IB or IB/IA . Then by interchanging the two dashed half-edges of same orientation at each true vertex of the IA side, we get a factor 4. Finally, we have to take as well into consideration a factor 2 by interchanging the two dashed edges in the rung of the IB side.

The dominant amplitudes for the other type of diagrams are computed to be:

$$\mathcal{A}_{r_1, r_2}(L_{IB}) = \frac{p^{r_1+r_2}}{16N(1+p)(1+p^2)} \left(\frac{1 + p^4}{(1+p)^2(1+p^2)^2} + \frac{r_1 + r_2}{N(1+p)(1+p^2)} + \frac{r_1 r_2}{N^2} \right), \quad (4.2.24)$$

$$\mathcal{A}_{r_1, r_2}(L_{IB/IIIB}) = \frac{p^{r_1+2r_2}}{8N(1+p)^2} \left(1 + \frac{r_1(1+p)}{N} - \frac{p^{2(r_2+1)}}{1+p+p^2} \right. \\ \left. - \frac{(1+p)p^{2(r_2+1)}}{(1+p+p^2)^2} \left(1 + (r_1 + r_2) \frac{(1+p+p^2)}{N} \right) \right), \quad (4.2.25)$$

$$\mathcal{A}_{r_1, r_2}(L_{IB/IIIB}) = -\frac{p^{r_1+r_2}}{16N(1+p)^2} \left(1 + \frac{r_1(1+p+p^2)}{N} - \frac{(p^3 + 2(1+p+p^2))p^{3(r_2+1)}}{(1+p)^2(1+p^2)^2} \right. \\ \left. - \frac{(1+p+p^2)p^{3(r_2+1)}(r_1 + r_2)}{N(1+p)(1+p^2)} \right), \quad (4.2.26)$$

$$\mathcal{A}_{r_1, r_2}(L_{IIA}) = \frac{p^{2(r_1+r_2)}}{64N} \left(\frac{1 + p^2}{(1+p)^3} + \frac{(r_1 + r_2)}{N(1+p)^2} + \frac{r_1 r_2}{N^2(1+p)} \right), \quad (4.2.27)$$

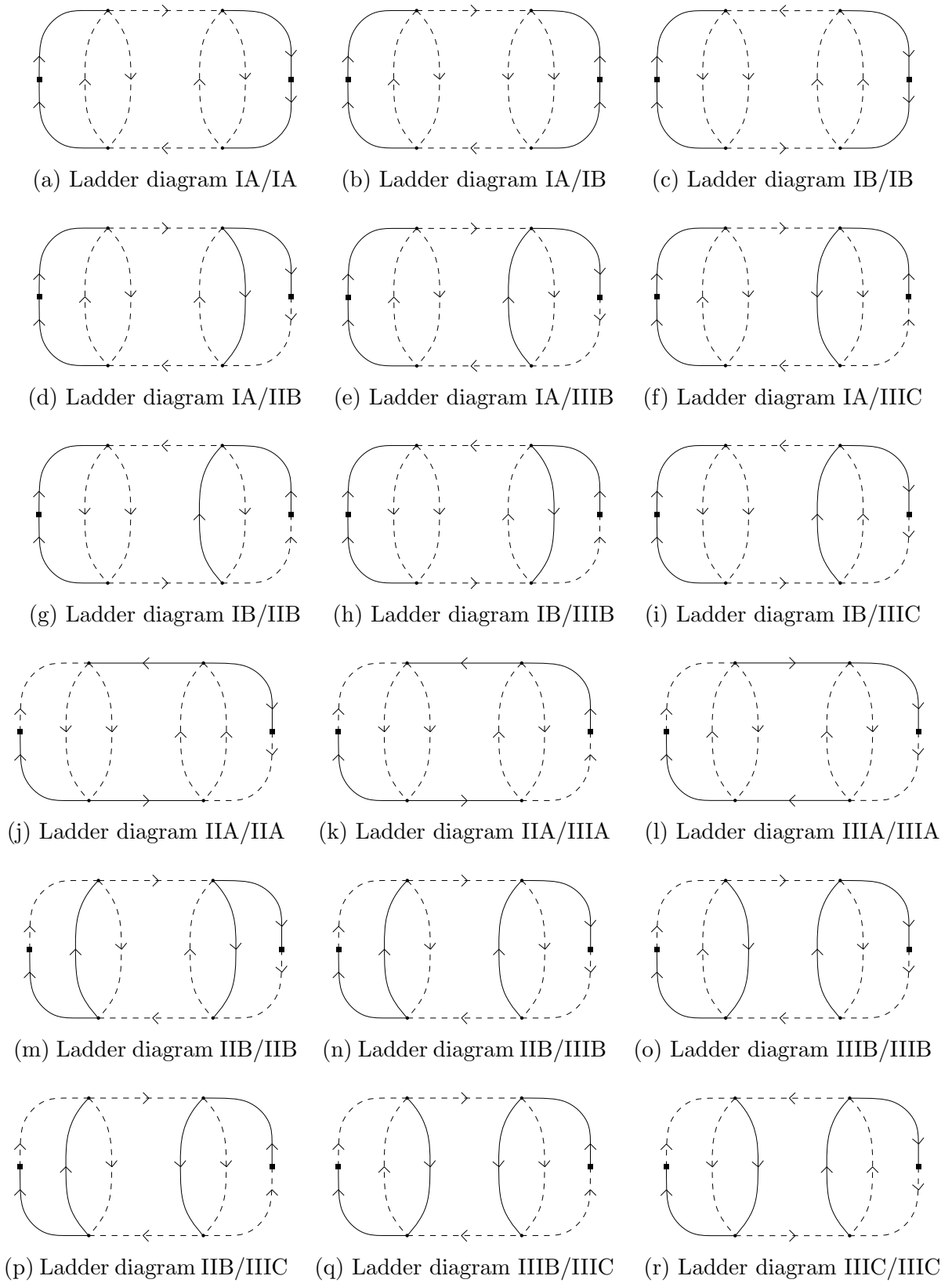


Figure 4.7: Ladder diagram types contributing at leading order to the variance at order t^4 .

$$\mathcal{A}_{r_1, r_2}(L_{IIA}/IIIA) = -\frac{p^{2(r_1+r_2)}}{32N(1+p)} \left(\frac{1}{(1+p)^2} + \frac{r_2(r_2+1)}{2N^2} + \frac{r_1+r_2}{N(1+p)} + \frac{r_1r_2}{N^2} \right), \quad (4.2.28)$$

$$\mathcal{A}_{r_1, r_2}(L_{IIIC}) = \frac{p^{r_1+r_2}}{16N} \left(\frac{1}{1+p} - \frac{p(p^{r_1+r_2})}{1+p+p^2} + \frac{p^{r_1+r_2+2}}{(1+p)(1+p^2)} \right), \quad (4.2.29)$$

$$\begin{aligned} \mathcal{A}_{r_1, r_2}(L_{IIIB}/IIIC) &= \frac{p^{r_1+r_2}}{16N} \left(\frac{1}{1+p} - \frac{p^{r_2+1}}{1+p+p^2} - \frac{p^{2r_1+2}}{(1+p)(1+p+p^2)} \right. \\ &\quad \left. - \frac{p^{3r_1+r_2+4}}{(1+p)(1+p^2)(1+p+p^2)} \right), \end{aligned} \quad (4.2.30)$$

$$\mathcal{A}_{r_1, r_2}(L_{IIB}/IIIC) = -\frac{p^{2r_1+r_2}}{8N} \left(1 - \frac{p}{1+p}(p^{r_1}+p^{r_2}) + \frac{p^{2r_1+r_2+3}}{(1+p)(1+p+p^2)} \right), \quad (4.2.31)$$

$$\mathcal{A}_{r_1, r_2}(L_{IA}/IIIC) = -\frac{p^{r_1+r_2}}{4N} \left(1 - \frac{p^{r_2+1}}{(1+p)^2} - \frac{p^{r_1+1}}{1+p+p^2} + \frac{p^{2r_1+r_2+3}}{(1+p)^2(1+p^2)} \right), \quad (4.2.32)$$

$$\begin{aligned} \mathcal{A}_{r_1, r_2}(L_{IB}/IIIC) &= -\frac{p^{r_1+r_2}}{8N} \left(\frac{1}{(1+p+p^2)^2} + \frac{r_1}{N(1+p+p^2)} \right. \\ &\quad \left. - \frac{p^{r_2+1}}{(1+p)(1+p^2)} \left(\frac{1}{(1+p)(1+p^2)} + \frac{r_1}{N} \right) \right). \end{aligned} \quad (4.2.33)$$

The details of their contributions to the variance can be found in Appendix F, summing all of them gives

$$\begin{aligned} \bar{S}_{\gamma, L1}^{2(4)}(t) &= t^4 N^{2\gamma-1} (\gamma!)^2 \left(\frac{1}{16} \left(\frac{1}{2} + \gamma + 1 - \frac{1}{2^{2\gamma+4}} - \frac{1}{3^{\gamma+18}} - \frac{2(\gamma+1)}{3^{2\gamma+2}} \right) \right. \\ &\quad + \frac{1}{64} \left(\frac{1}{8} + \frac{\gamma+1}{2} + (\gamma+1)^2 \right) + \frac{1}{32} \left(\frac{1}{2^{\gamma+1}} + \frac{\gamma+1}{2^\gamma} - \frac{3}{2^{2\gamma+1}} - \frac{5(\gamma+1)}{2^{2\gamma+33}} \right) \\ &\quad - \frac{1}{64} \left(1 + 3(\gamma+1) - \frac{15\gamma+22}{2^{2\gamma+6}} \right) + \frac{1}{2^{2\gamma+10}} \left(3 + 2\gamma + \frac{\gamma^2+1}{2} \right) \\ &\quad - \frac{1}{2^{2\gamma+4}} \left(\gamma^2 + 4\gamma + \frac{\gamma^2+3\gamma}{2} + 5 \right) + \frac{1}{32} \left(1 - \frac{1}{2^{\gamma-13}} + \frac{1}{2^{2\gamma+3}} \right) \\ &\quad + \frac{1}{32} \left(1 - \frac{1}{2^\gamma 3} - \frac{1}{3^{\gamma+2}} - \frac{1}{2^{3\gamma+4}} \right) - \frac{1}{16} \left(\frac{1}{2^\gamma} - \frac{1}{2^{2\gamma+2}} - \frac{1}{3^{\gamma+1}} + \frac{1}{2^{\gamma+1} 3^{\gamma+2}} \right) \\ &\quad \left. - \frac{1}{4} \left(1 - \frac{7}{2^{\gamma+33}} + \frac{1}{2^{\gamma+4} 3^{\gamma+1}} \right) - \frac{1}{8} \left(\frac{1}{9} + \frac{\gamma+1}{3} - \frac{5}{2^{\gamma+5}} \right) \right) + o(N^{2\gamma-1}). \end{aligned} \quad (4.2.34)$$

For the second class of ladder diagrams, let us now compute in detail the dominant amplitudes for the diagram of type $L_{IA}/IIIB$ shown in Figure 4.7e. It comes with a combinatorial factor 32 when taking into account the 2 heap-orderings, the exchange of the two types IA and $IIIB$, and the way one can rearrange the dashed half-edge of same orientation at a true vertex gives a factor 4 for the IA side and 2 for the $IIIB$ side. The amplitudes also comes with a minus sign because of the relative orientation of solid edges in the $IIIB$ side. We then get

$$\mathcal{A}_{r_1, r_2}(L_{IA}/IIIB) = -\frac{32}{8^2 4 N^4} p^{-r_1} \sum_{S_1 \geq r_1} \sum_{S_2 \geq r_2} p^{2S_1+S_2} \sum_{k_1=0}^{S_1} \sum_{k_2=0}^{S_2} p^{k_2} \delta_{k_1}^{k_2} \quad (4.2.35)$$

$$= -\frac{p^{-r_1}}{8N^4} \sum_{S_1 \geq r_1} \sum_{S_2 \geq r_2} p^{2S_1+S_2} \sum_{k_1=0}^{S_1} \sum_{k_2=0}^{S_2} p^{k_2} \delta_{k_1}^{k_2} \quad (4.2.36)$$

$$= -\frac{p^{-r_1}}{8N^4} \sum_{S_1 \geq r_1} \sum_{S_2 \geq r_2} p^{2S_1+S_2} \frac{1 - p^{\min(S_1, S_2)+1}}{1-p} \quad (4.2.37)$$

$$= -\frac{p^{r_1+r_2}}{8N^4} \sum_{S_1 \geq 0} \sum_{S_2 \geq 0} p^{2S_1+S_2} \frac{1 - p^{\min(S_1+r_1, S_2+r_2)+1}}{1-p} \quad (4.2.38)$$

$$= -\frac{p^{r_1+r_2}}{8N^4(1-p)} \left(\frac{1}{(1-p)^2(1+p)} - \sum_{S_1 \geq 0} \sum_{S_2 \geq 0} p^{2S_1+S_2+\min(S_1+r_1, S_2+r_2)+1} \right). \quad (4.2.39)$$

If $r_1 > r_2$ then one has

$$\begin{aligned} & \sum_{S_1 \geq 0} \sum_{S_2 \geq 0} p^{2S_1+S_2+\min(S_1+r_1, S_2+r_2)+1} \\ &= \sum_{S_1 \geq 0} \left(\sum_{S_2=0}^{r_1-r_2-1} p^{2S_1+2S_2+r_2+1} + \sum_{S_2 \geq r_1-r_2} p^{2S_1+S_2+\min(S_1+r_1, S_2+r_2)+1} \right) \end{aligned} \quad (4.2.40)$$

$$= p^{r_2+1} \frac{1 - p^{2(r_1-r_2)}}{(1-p^2)^2} + p^{r_1-r_2+1} \sum_{S_1 \geq 0} \sum_{S_2 \geq 0} p^{2S_1+S_2+\min(S_1+r_2, S_2+r_2)} \quad (4.2.41)$$

$$= p^{r_2+1} \left(\frac{1 - p^{2(r_1-r_2)}}{(1-p^2)^2} + p^{2(r_1-r_2)} \frac{1 + 2p + 3p^2 + 2p^3 + p^4}{(1-p^2)^2(1+p^2)(1+p+p^2)} \right), \quad (4.2.42)$$

and if $r_1 < r_2$,

$$\begin{aligned} & \sum_{S_1 \geq 0} \sum_{S_2 \geq 0} p^{2S_1+S_2+\min(S_1+r_1, S_2+r_2)+1} \\ &= \sum_{S_2 \geq 0} \left(\sum_{S_1=0}^{r_2-r_1-1} p^{3S_1+S_2+r_1+1} + \sum_{S_1 \geq r_2-r_1} p^{2S_1+S_2+\min(S_1+r_1, S_2+r_2)+1} \right) \end{aligned} \quad (4.2.43)$$

$$= p^{r_1+1} \left(\frac{1 - p^{3(r_2-r_1)}}{(1-p)(1-p^3)} + p^{3(r_2-r_1)} \frac{1 + 2p + 3p^2 + 2p^3 + p^4}{(1-p^2)^2(1+p^2)(1+p+p^2)} \right). \quad (4.2.44)$$

Hence the amplitude can be written as

$$\mathcal{A}_{r_1, r_2}(L_{IA}/III B) = -\frac{p^{r_1+r_2}}{8N^4(1-p)^3(1+p)} \left(1 - p^{\min(r_1, r_2)+1} \left(\theta(r_1 - r_2) \frac{1 - p^{2(r_1-r_2)}}{(1+p)} \right. \right. \quad (4.2.45)$$

$$\left. \left. + \theta(r_2 - r_1) \frac{(1+p)(1 - p^{3(r_2-r_1)})}{(1+p+p^2)} + p^{(2\theta(r_1-r_2)+3\theta(r_2-r_1))|r_1-r_2|} \frac{1+p+p^2}{(1+p^2)(1+p)} \right) \right). \quad (4.2.46)$$

In an analogous way, we obtain the amplitudes for the other types listed above:

$$\mathcal{A}_{r_1, r_2}(L_{IA}) = \frac{p^{r_1+r_2}}{4N^4(1-p^2)^3(1+p^2)} (1 + p^2 + \min(r_1, r_2)(1 - p^4) - p^{2|r_1-r_2|+2}), \quad (4.2.47)$$

$$\mathcal{A}_{r_1, r_2}(L_{IIB}) = \frac{p^{2(r_1+r_2)}}{16N^4(1-p)^3(1+p)}(1+p+\min(r_1, r_2)(1-p^2) - p^{|r_1-r_2|+1}), \quad (4.2.48)$$

$$\mathcal{A}_{r_1, r_2}(L_{IIIA}) = \frac{p^{2(r_1+r_2)}}{64N^4(1-p^2)^3} \left((1+p^2+|r_1-r_2|(1-p^2))p^{|r_1-r_2|-r_1-r_2} - p^2 \right), \quad (4.2.49)$$

$$\begin{aligned} \mathcal{A}_{r_1, r_2}(L_{IIIB}) &= \frac{p^{r_1+r_2}}{64N^4(1-p^2)(1-p)^2} \\ &\times \left(1 - \frac{p^{2+2\min(r_1, r_2)}}{(1+p+p^2)(1+p^2)} (1+p^2+p^{3|r_1-r_2|+1}) \right), \end{aligned} \quad (4.2.50)$$

$$\mathcal{A}_{r_1, r_2}(L_{IIB/IIIB}) = -\frac{p^{2(r_1+r_2)}}{16N^4(1-p)^3(1+p)} \left(1 - \frac{p^{2|r_1-r_2|+2}}{(1+p+p^2)} \right), \quad (4.2.51)$$

$$\begin{aligned} \mathcal{A}_{r_1, r_2}(L_{IA/IIIB}) &= \frac{p^{r_1+2r_2}}{4N^4(1-p)^2(1+p)} \left(1 + \min(r_1, r_2) + \frac{p^3}{(1-p)(1+p+p^2)} \right. \\ &+ \theta(r_1-r_2)p(1+p) \frac{1-p^{r_1-r_2}}{(1-p)(1+p+p^2)} \\ &\left. + \theta(r_2-r_1)p^2 \frac{1-p^{2(r_2-r_1)}}{(1-p)(1+p)(1+p+p^2)} \right). \end{aligned} \quad (4.2.52)$$

The first step of the computation for each amplitude can be found in Appendix F.

4.3 Perspectives

A first immediate perspective is the computations of the contribution of the second class of ladder diagrams to the variance. This is more involved than the contribution of the previous amplitudes and is currently in progress. As an example, let us show the contribution of the ladder diagram of type L_{IA} ,

$$\begin{aligned} &\sum_{r_1 \geq 0} \sum_{r_2 \geq 0} \frac{(r_1 r_2)^\gamma}{N^2} \mathcal{A}_{r_1, r_2}(L_{IA}) \\ &= \sum_{r_1 \geq 0} \sum_{r_2 \geq 0} \frac{(r_1 r_2)^\gamma p^{r_1+r_2}}{4N^3(1+p)^3(1+p^2)} (1+p^2+\min(r_1, r_2)(1-p^4) - p^{2|r_1-r_2|+2}) \end{aligned} \quad (4.3.1)$$

$$= \frac{1}{4N^3} \left(\frac{L_\gamma(p)^2}{(1+p)^3} + 2 \sum_{r_1 \geq 0} \sum_{r_2=0}^{r_1} \frac{(r_1 r_2)^\gamma p^{r_1+r_2}}{(1+p)^3(1+p^2)} (r_2(1-p^4) - p^{2(r_1-r_2)+2}) \right) \quad (4.3.2)$$

$$= \frac{1}{4N^3} \left(\frac{L_\gamma(p)^2}{(1+p)^3} + 2 \sum_{r_1 \geq 0} r_1^\gamma p^{r_1} \sum_{r_2=0}^{r_1} \frac{r_2^{\gamma+1} p^{r_2}}{N(1+p)^2} - 2p^2 \sum_{r_1 \geq 0} r_1^\gamma p^{3r_1} \sum_{r_2=0}^{r_1} \frac{r_2^\gamma p^{-r_2}}{(1+p)^3(1+p^2)} \right) \quad (4.3.3)$$

$$\begin{aligned} &= \frac{1}{4N^3} \left(\frac{L_\gamma(p)^2}{(1+p)^3} + \frac{2}{N(1+p)^2} (L_{\gamma, \gamma+1}(p, p) + L_{2\gamma+1}(p^2)) \right. \\ &\left. - \frac{2p^2}{(1+p)^3(1+p^2)} (L_{\gamma, \gamma}(p^3, \frac{1}{p}) + L_{2\gamma}(p^2)) \right), \end{aligned} \quad (4.3.4)$$

where we introduced the multiple polylogarithm functions⁷ [102]

$$L_{\gamma_1, \gamma_2}(z_1, z_2) = \sum_{r_1 > r_2 > 0}^{\infty} r_1^{s_1} r_2^{s_2} z_1^{r_1} z_2^{r_2}. \quad (4.3.5)$$

Using the facts that $L_0(z) = \frac{z}{1-z}$ and $z \frac{d}{dz} L_\gamma(z) = L_{\gamma+1}(z)$ and following the lines of [103] for standard polylogarithm, we can express the multiple polylogarithm functions as sums of polylogarithm,

$$L_{0,0}(z_1, z_2) = \frac{z_1}{(1-z_1)(1-z_1 z_2)}, \quad (4.3.6)$$

$$L_{n,m}(z_1, z_2) = \sum_{k=0}^n \binom{n}{k} L_k(z_1) L_{n+m-k}(z_1 z_2) \quad \text{with } n, m > 0. \quad (4.3.7)$$

With these formulas, we can express the contribution of ladder diagrams of type L_{IA} as

$$\begin{aligned} & \sum_{r_1 \geq 0}^{\infty} \sum_{r_2 \geq 0}^{\infty} \frac{(r_1 r_2)^\gamma}{N^2} \mathcal{A}_{r_1, r_2}(L_{IA}) \\ &= \frac{1}{4N^3} \left(\frac{L_\gamma(p)^2}{(1+p)^3} + \frac{2}{N(1+p)^2} \left(\sum_{k=0}^{\gamma} \binom{\gamma}{k} L_k(p) L_{2\gamma+1-k}(p^2) + L_{2\gamma+1}(p^2) \right) \right. \\ & \quad \left. - \frac{2p^2}{(1+p)^3(1+p^2)} \left(\sum_{k=0}^{\gamma} \binom{\gamma}{k} L_k(p^3) L_{2\gamma-k}(p^2) + L_{2\gamma}(p^2) \right) \right) \end{aligned} \quad (4.3.8)$$

$$\begin{aligned} &=_{LO} \frac{1}{4N^3} \left(\frac{L_\gamma(p)^2}{(1+p)^3} + \frac{2}{N(1+p)^2} \sum_{k=0}^{\gamma} \binom{\gamma}{k} L_k(p) L_{2\gamma+1-k}(p^2) \right. \\ & \quad \left. - \frac{2p^2}{(1+p)^3(1+p^2)} \sum_{k=0}^{\gamma} \binom{\gamma}{k} L_k(p^3) L_{2\gamma-k}(p^2) \right) \end{aligned} \quad (4.3.9)$$

$$\begin{aligned} &=_{p \rightarrow 1} \frac{N^{2\gamma-1}}{4} \left(\frac{(\gamma!)^2}{2^3} + \sum_{k=0}^{\gamma} \binom{\gamma}{k} \frac{k!(2\gamma+1-k)!}{2^{2\gamma+2-k}} - \sum_{k=0}^{\gamma} \binom{\gamma}{k} \frac{k!(2\gamma-k)!}{3^{k+1} 2^{2\gamma+4-k}} \right) + o(N^{2\gamma-1}). \end{aligned} \quad (4.3.10)$$

A second perspective is to prove that the dominant graph in the limit $p \rightarrow 1$ are indeed the one we computed, namely melonic and ladder diagrams. The combinatorics are very similar to the SYK model, hence a first step for this proof would be to prove the dominance of ladder diagrams in the large N expansion of the 4-point function of the SYK model. One possible way to do so is by adapting to the 4-point function, the method used in [104] for the proof of the melonic dominance in the large N expansion of the 2-point function. We then need to take into account the specific momentum attribution of the diagrams in our model in order to prove the analogue of Theorem 4.1.1 for the variance (see [60] for the proof of Theorem 4.1.1).

A third perspective that appears to us is the study of other cumulants of the distribution of Sobolev norms in the limit $p \rightarrow 1$. We can expect that the leading order

⁷As for the standard polylogarithm functions, we use a different notation for the coefficient, in the usual convention the series corresponds to $L_{-\gamma_1, -\gamma_2}(z_1, z_2)$.

diagrams are similar to the ones in the 6-point and higher-point function of the SYK model described in [29] and [30]. We hope to prove that it is indeed the case and from this knowledge that at leading order in the limit $p \rightarrow 1$ and at early time the fluctuation around the mean value of Solobev norms is distributed along a Gaussian law, as is the case for $\gamma = 0, 1$. Naturally, the next step would be to extend these results at all times but this task goes beyond the perturbative techniques used in this chapter.

Appendices

A Proof of Lemma 1.4.1

Proof. The proof is lengthy but straightforward. Let us explicitly compute here some of the necessary terms:

$$\begin{aligned} \frac{1}{2! \cdot 2^2} \langle\langle G_{|\overline{a\emptyset}|\overline{a\emptyset}|}^{(8)}, \overline{a} \sqcup \overline{a} \rangle\rangle_{s_a} & \quad (\text{A.1a}) \\ &= \frac{1}{8} \left(\sum_{r=1,2} \Delta_{s_a,r} G_{|\overline{a\emptyset}|\overline{a\emptyset}|}^{(8)} + \sum_{r=3,4} (123)^* (\Delta_{s_a,r} G_{|\overline{a\emptyset}|\overline{a\emptyset}|}^{(8)}) \right) \star \mathbb{J}(\overline{\emptyset} \sqcup \overline{a}) \end{aligned}$$

$$\begin{aligned} \frac{1}{2! \cdot 2^2} \sum_{i \neq a} \langle\langle G_{|\overline{i\emptyset}|\overline{i\emptyset}|}^{(8)}, \overline{i} \sqcup \overline{i} \rangle\rangle_{s_a} & \quad (\text{A.1b}) \\ &= \frac{1}{8} \sum_{i \neq a} \left(\sum_{r=1,2} \Delta_{s_a,r} G_{|\overline{i\emptyset}|\overline{i\emptyset}|}^{(8)} + \sum_{r=3,4} (123)^* \Delta_{s_a,r} G_{|\overline{i\emptyset}|\overline{i\emptyset}|}^{(8)} \right) \star \mathbb{J}(\overline{\emptyset} \sqcup \overline{i}) \end{aligned}$$

$$\begin{aligned} \frac{1}{2^2} \sum_{i \neq a} \langle\langle G_{|\overline{i\emptyset}|\overline{a\emptyset}|}^{(8)}, \overline{i} \sqcup \overline{a} \rangle\rangle_{s_a} & \quad (\text{A.1c}) \\ &= \frac{1}{4} \sum_{i \neq a} \left(\left(\sum_{r=1,2} \Delta_{s_a,r} G_{|\overline{i\emptyset}|\overline{a\emptyset}|}^{(8)} \right) \star \mathbb{J}(\overline{\emptyset} \sqcup \overline{a}) \right. \\ & \quad \left. + \left(\sum_{p=3,4} (123)^* \Delta_{s_a,p} G_{|\overline{i\emptyset}|\overline{a\emptyset}|}^{(8)} \right) \star \mathbb{J}(\overline{\emptyset} \sqcup \overline{i}) \right) \end{aligned}$$

$$\begin{aligned} \frac{1}{2^2} \langle\langle G_{|\overline{b\emptyset}|\overline{c\emptyset}|}^{(8)}, \overline{b} \sqcup \overline{c} \rangle\rangle_{s_a} & \quad (\text{A.1d}) \\ &= \frac{1}{4} \left(\left(\sum_{r=1,2} \Delta_{s_a,r} G_{|\overline{b\emptyset}|\overline{c\emptyset}|}^{(8)} \right) \star \mathbb{J}(\overline{\emptyset} \sqcup \overline{c}) \right. \\ & \quad \left. + \left(\sum_{p=3,4} (123)^* \Delta_{s_a,p} G_{|\overline{b\emptyset}|\overline{c\emptyset}|}^{(8)} \right) \star \mathbb{J}(\overline{\emptyset} \sqcup \overline{b}) \right) \end{aligned}$$

$$\begin{aligned} \frac{1}{3} \langle\langle G_{|\overline{\emptyset}|\overline{\emptyset}|}^{(8)}, \overline{\emptyset} \sqcup \overline{\emptyset} \rangle\rangle_{s_a} & \quad (\text{A.1e}) \\ &= \frac{1}{3} \Delta_{s_a,1} G_{|\overline{\emptyset}|\overline{\emptyset}|}^{(8)} \star \mathbb{J}(\overline{\emptyset}) + \frac{1}{3} \sum_{q=2,3,4} \Delta_{s_a,q} G_{|\overline{\emptyset}|\overline{\emptyset}|}^{(8)} \star \mathbb{J}(\overline{\emptyset} \sqcup \overline{a}) \end{aligned}$$

$$\frac{1}{3} \sum_{i \neq a} \langle\langle G_{|\overline{\emptyset}|\overline{i\emptyset}|}^{(8)}, \overline{\emptyset} \sqcup \overline{i} \rangle\rangle_{s_a} \quad (\text{A.1f})$$

$$= \frac{1}{3} \sum_{i \neq a} \left\{ \Delta_{s_a,1} G_{|\Theta|\langle i \rangle}^{(8)} \star \mathbb{J}(\langle i \rangle) + \sum_{q=2,3,4} \Delta_{s_a,q} G_{|\Theta|\langle i \rangle}^{(8)} \star \mathbb{J}(\Theta \sqcup \langle a \rangle) \right\}$$

$$\frac{1}{3} \langle\langle G_{|\Theta|\langle a \rangle}^{(8)}, \Theta \sqcup \langle a \rangle \rangle\rangle_{s_a} \quad (\text{A.1g})$$

$$= \frac{1}{3} \left\{ \Delta_{s_a,1} G_{|\Theta|\langle a \rangle}^{(8)} \star \mathbb{J}(\langle a \rangle) + \sum_{q=2,3,4} \Delta_{s_a,q} G_{|\Theta|\langle a \rangle}^{(8)} \right\} \star \mathbb{J}(\Theta \sqcup \langle a \rangle)$$

$$\sum_{i \neq a} \langle\langle G_{|\Theta| \langle i \rangle \langle i \rangle}^{(8)}, \Theta \sqcup \langle i \rangle \rangle\rangle_{s_a} \quad (\text{A.1h})$$

$$= \Delta_{s_a,1} G_{|\Theta| \langle a \rangle \langle b \rangle}^{(8)} \star \mathbb{J}(\langle a \rangle \langle b \rangle) + \sum_{h=2,3} \Delta_{s_a,h} G_{|\Theta| \langle a \rangle \langle b \rangle}^{(8)} \star \mathbb{J}(\Theta \sqcup \langle b \rangle)$$

$$+ \Delta_{s_a,1} G_{|\Theta| \langle a \rangle \langle c \rangle}^{(8)} \star \mathbb{J}(\langle a \rangle \langle c \rangle) + \sum_{h=2,3} \Delta_{s_a,h} G_{|\Theta| \langle a \rangle \langle c \rangle}^{(8)} \star \mathbb{J}(\Theta \sqcup \langle c \rangle)$$

$$+ (\Delta_{s_a,4} G_{|\Theta| \langle a \rangle \langle b \rangle}^{(8)} + \Delta_{s_a,4} G_{|\Theta| \langle a \rangle \langle c \rangle}^{(8)}) \star \mathbb{J}(\Theta \sqcup \langle a \rangle)$$

$$\langle\langle G_{|\Theta| \langle b \rangle \langle c \rangle}^{(8)}, \Theta \sqcup \langle b \rangle \rangle\rangle_{s_a} \quad (\text{A.1i})$$

$$= \Delta_{s_a,1} G_{|\Theta| \langle b \rangle \langle c \rangle}^{(8)} \star \mathbb{J}(\langle b \rangle \langle c \rangle) + \Delta_{s_a,2} G_{|\Theta| \langle b \rangle \langle c \rangle}^{(8)} \star \mathbb{J}(\Theta \sqcup \langle c \rangle)$$

$$+ \Delta_{s_a,3} G_{|\Theta| \langle b \rangle \langle c \rangle}^{(8)} \star \mathbb{J}(\Theta \sqcup \Theta \sqcup \Theta) + \Delta_{s_a,4} G_{|\Theta| \langle b \rangle \langle c \rangle}^{(8)} \star \mathbb{J}(\Theta \sqcup \langle b \rangle)$$

$$\frac{1}{2 \cdot 2!} \sum_{i \neq a} \langle\langle G_{|\Theta|\Theta|\langle i \rangle}^{(8)}, \Theta \sqcup \Theta \sqcup \langle i \rangle \rangle\rangle_{s_a} \quad (\text{A.1j})$$

$$= \frac{1}{4} \left\{ \sum_{i \neq a} \sum_{r=1,2} \Delta_{s_a,r} G_{|\Theta|\Theta|\langle i \rangle}^{(8)} \star \mathbb{J}(\Theta \sqcup \langle i \rangle) \right.$$

$$\left. + \sum_{p=3,4} \Delta_{s_a,p} G_{|\Theta|\Theta|\langle i \rangle}^{(8)} \star \mathbb{J}(\Theta^{\sqcup 3}) \right\}$$

$$\frac{1}{2 \cdot 2!} \sum_{i \neq a} \langle\langle G_{|\Theta|\Theta|\langle a \rangle}^{(8)}, \Theta \sqcup \Theta \sqcup \langle a \rangle \rangle\rangle_{s_a} \quad (\text{A.1k})$$

$$= \frac{1}{4} \left\{ \sum_{r=1,2} \Delta_{s_a,r} G_{|\Theta|\Theta|\langle a \rangle}^{(8)} \star \mathbb{J}(\Theta \sqcup \langle a \rangle) \right.$$

$$\left. + \sum_{p=3,4} \Delta_{s_a,p} G_{|\Theta|\Theta|\langle a \rangle}^{(8)} \star \mathbb{J}(\Theta \sqcup \Theta \sqcup \Theta) \right\}$$

$$\frac{1}{4!} \langle\langle G_{|\Theta|\Theta|\Theta|\Theta|}^{(8)}, \Theta \sqcup \Theta \sqcup \Theta \sqcup \Theta \rangle\rangle_{s_a} \quad (\text{A.1l})$$

$$= \frac{1}{4!} \sum_{u=1}^4 (\Delta_{s_a,u} G_{|\Theta|\Theta|\Theta|\Theta|}^{(8)}) \star \mathbb{J}(\Theta \sqcup \Theta \sqcup \Theta)$$

$$\langle\langle G_{\overline{(b)j(a)c}}^{(8)}, a \begin{array}{c} b \quad a \quad c \\ \left(\begin{array}{ccc} c & c & b \\ b & a & c \end{array} \right) a \end{array} \rangle\rangle_{s_a} \quad (\text{A.1m})$$

$$\begin{aligned} &= \Delta_{s_a,1} G_{\overline{(b)j(a)c}}^{(8)} \star \mathbb{J} \left(\begin{array}{c} a \quad c \\ \left(\begin{array}{c} b \end{array} \right) \end{array} \right) + \Delta_{s_a,2} G_{\overline{(b)j(a)c}}^{(8)} \star \mathbb{J} \left(\begin{array}{c} b \quad c \\ \left(\begin{array}{c} a \end{array} \right) \end{array} \right) \\ &+ \Delta_{s_a,3} G_{\overline{(b)j(a)c}}^{(8)} \star \mathbb{J} \left(\begin{array}{c} b \quad c \\ \left(\begin{array}{c} a \end{array} \right) \end{array} \right) + \Delta_{s_a,4} G_{\overline{(b)j(a)c}}^{(8)} \star \mathbb{J} \left(\begin{array}{c} b \quad a \\ \left(\begin{array}{c} c \end{array} \right) \end{array} \right) \\ &= \Delta_{s_a,1} G_{\overline{(b)j(a)c}}^{(8)} \star \mathbb{J} \left(\begin{array}{c} a \quad c \\ \left(\begin{array}{c} b \end{array} \right) \end{array} \right) + \Delta_{s_a,2} G_{\overline{(b)j(a)c}}^{(8)} \star \mathbb{J} \left(\begin{array}{c} b \quad c \\ \left(\begin{array}{c} a \end{array} \right) \end{array} \right) \\ &+ \Delta_{s_a,3} G_{\overline{(b)j(a)c}}^{(8)} \star \mathbb{J} \left(\begin{array}{c} b \quad c \\ \left(\begin{array}{c} a \end{array} \right) \end{array} \right) + (13)^* (\Delta_{s_a,4} G_{\overline{(b)j(a)c}}^{(8)}) \star \mathbb{J} \left(\begin{array}{c} a \quad b \\ \left(\begin{array}{c} c \end{array} \right) \end{array} \right) \end{aligned}$$

$$\langle\langle G_{\overline{(c)j(b)a}}^{(8)}, b \begin{array}{c} c \quad b \quad a \\ \left(\begin{array}{ccc} a & a & c \\ c & b & a \end{array} \right) b \end{array} \rangle\rangle_{s_a} \quad (\text{A.1n})$$

$$\begin{aligned} &= (13)^* (\Delta_{s_a,1} G_{\overline{(c)j(b)a}}^{(8)}) \star \mathbb{J} \left(\begin{array}{c} a \quad b \\ \left(\begin{array}{c} c \end{array} \right) \end{array} \right) + \Delta_{s_a,2} G_{\overline{(c)j(b)a}}^{(8)} \star \mathbb{J} \left(\bigoplus \sqcup \begin{array}{c} a \\ \left(\begin{array}{c} \end{array} \right) \end{array} \right) \\ &+ [(13)^* (\Delta_{s_a,3} G_{\overline{(c)j(b)a}}^{(8)}) + (13)^* (\Delta_{s_a,4} G_{\overline{(c)j(b)a}}^{(8)})] \star \mathbb{J} \left(\begin{array}{c} b \quad c \\ \left(\begin{array}{c} a \end{array} \right) \end{array} \right) \end{aligned}$$

$$\langle\langle G_{\overline{(a)j(c)b}}^{(8)}, c \begin{array}{c} a \quad c \quad b \\ \left(\begin{array}{ccc} b & b & a \\ a & c & b \end{array} \right) c \end{array} \rangle\rangle_{s_a}$$

$$\begin{aligned} &= [(13)^* (\Delta_{s_a,1} G_{\overline{(a)j(c)b}}^{(8)}) + (13)^* (\Delta_{s_a,2} G_{\overline{(a)j(c)b}}^{(8)})] \star \mathbb{J} \left(\begin{array}{c} b \quad c \\ \left(\begin{array}{c} a \end{array} \right) \end{array} \right) \\ &+ (123)^* (\Delta_{s_a,3} G_{\overline{(a)j(c)b}}^{(8)}) \star \mathbb{J} \left(\bigoplus \sqcup \begin{array}{c} a \\ \left(\begin{array}{c} \end{array} \right) \end{array} \right) + \Delta_{s_a,4} G_{\overline{(a)j(c)b}}^{(8)} \star \mathbb{J} \left(\begin{array}{c} a \quad c \\ \left(\begin{array}{c} b \end{array} \right) \end{array} \right) \end{aligned}$$

$$\frac{1}{2} \sum_{\substack{i=b,c \\ (a \neq j \neq i)}} \langle\langle G_{\overline{(a)j(i)i}}^{(8)}, j \begin{array}{c} a \quad j \quad a \\ \left(\begin{array}{ccc} i & i & i \\ a & j & a \end{array} \right) i \end{array} \rangle\rangle_{s_a} \quad (\text{A.1o})$$

$$= \frac{1}{2} \sum_{\substack{i=b,c \\ (a \neq j \neq i)}} \left[\sum_{r=1,2} \Delta_{s_a,r} G_{\overline{(a)j(i)i}}^{(8)} \star \mathbb{J} \left(\begin{array}{c} j \quad a \\ \left(\begin{array}{c} i \end{array} \right) \end{array} \right) + \sum_{p=3,4} \Delta_{s_a,p} G_{\overline{(a)j(i)i}}^{(8)} \star \mathbb{J} \left(\begin{array}{c} a \quad j \\ \left(\begin{array}{c} i \end{array} \right) \end{array} \right) \right]$$

$$= \frac{1}{2} \sum_{\substack{i=b,c \\ (a \neq j \neq i)}} \left[\left(\sum_{r=1,2} (13)^* (\Delta_{s_a,r} G_{\overline{(a)j(i)i}}^{(8)}) + \sum_{p=3,4} \Delta_{s_a,p} G_{\overline{(a)j(i)i}}^{(8)} \right) \star \mathbb{J} \left(\begin{array}{c} a \quad j \\ \left(\begin{array}{c} i \end{array} \right) \end{array} \right) \right]$$

$$= \frac{1}{2} \left[\left(\sum_{r=1,2} (13)^* (\Delta_{s_a,r} G_{\overline{(a)j(i)i}}^{(8)}) + \sum_{p=3,4} \Delta_{s_a,p} G_{\overline{(a)j(i)i}}^{(8)} \right) \star \mathbb{J} \left(\begin{array}{c} a \quad c \\ \left(\begin{array}{c} b \end{array} \right) \end{array} \right) \right]$$

$$+ \left(\sum_{r=1,2} (13)^* (\Delta_{s_a,r} G_{\overline{(c)j(i)i}}^{(8)}) + \sum_{p=3,4} \Delta_{s_a,p} G_{\overline{(c)j(i)i}}^{(8)} \right) \star \mathbb{J} \left(\begin{array}{c} a \quad b \\ \left(\begin{array}{c} c \end{array} \right) \end{array} \right) \right]$$

$$\frac{1}{2} \sum_{\substack{i=b,c \\ (a \neq j \neq i)}} \langle\langle G_{\overline{(a)j(i)i}}^{(8)}, i \begin{array}{c} j \quad i \quad j \\ \left(\begin{array}{ccc} a & a & a \\ j & i & j \end{array} \right) a \end{array} \rangle\rangle_{s_a} \quad (\text{A.1p})$$

$$\begin{aligned}
& + \sum_{p=3,4} (\Delta_{s_a,p} G_{\substack{a \\ b \\ c}}^{(8)} + (13)^* \Delta_{s_a,p} G_{\substack{a \\ c \\ b}}^{(8)}) \star \mathbb{J}(\langle \langle \begin{array}{c} b \quad c \\ a \end{array} \rangle \rangle) \\
\sum_{i \neq a} \langle \langle G_{\substack{a \\ b \\ c}}^{(8)}, \langle \langle \begin{array}{c} a \\ i \quad j \\ a \end{array} \rangle \rangle \rangle_{s_a} & \tag{A.1t}
\end{aligned}$$

$$\begin{aligned}
& = \sum_{r=1,2} \Delta_{s_a,r} G_{\substack{a \\ b \\ c}}^{(8)} \star \mathbb{J}(\langle \langle \begin{array}{c} c \\ a \end{array} \rangle \rangle) + \sum_{p=3,4} \Delta_{s_a,p} G_{\substack{a \\ b \\ c}}^{(8)} \star \mathbb{J}(\langle \langle \begin{array}{c} a \quad c \\ b \end{array} \rangle \rangle) \\
& + \sum_{r=1,2} \Delta_{s_a,r} G_{\substack{a \\ b \\ c}}^{(8)} \star \mathbb{J}(\langle \langle \begin{array}{c} b \\ a \end{array} \rangle \rangle) + \sum_{p=3,4} \Delta_{s_a,p} G_{\substack{a \\ b \\ c}}^{(8)} \star \mathbb{J}(\langle \langle \begin{array}{c} a \quad b \\ c \end{array} \rangle \rangle) \\
\sum_{i,j \neq a; i \neq j} \langle \langle G_{\substack{a \\ b \\ c}}^{(8)}, \langle \langle \begin{array}{c} i \\ j \\ i \end{array} \rangle \rangle \rangle_{s_a} & \tag{A.1u}
\end{aligned}$$

$$\begin{aligned}
& = (\Delta_{s_a,1} G_{\substack{a \\ b \\ c}}^{(8)} + \Delta_{s_a,1} G_{\substack{a \\ c \\ b}}^{(8)}) \star \mathbb{J}(\langle \langle \begin{array}{c} a \\ a \end{array} \rangle \rangle) \\
& + \sum_{q=2,3,4} \{ (13)^* \Delta_{s_a,q} G_{\substack{a \\ b \\ c}}^{(8)} \star \mathbb{J}(\langle \langle \begin{array}{c} a \quad c \\ b \end{array} \rangle \rangle) + (13)^* \Delta_{s_a,q} G_{\substack{a \\ c \\ b}}^{(8)} \star \mathbb{J}(\langle \langle \begin{array}{c} a \quad b \\ c \end{array} \rangle \rangle) \}
\end{aligned}$$

$$\begin{aligned}
\sum_{i \neq a} \langle \langle G_{\substack{a \\ b \\ c}}^{(8)}, \langle \langle \begin{array}{c} i \quad a \\ j \\ i \quad a \end{array} \rangle \rangle \rangle_{s_a} & \tag{A.1v}
\end{aligned}$$

$$\begin{aligned}
& = (\Delta_{s_a,1} G_{\substack{a \\ b \\ c}}^{(8)} + \Delta_{s_a,1} G_{\substack{a \\ c \\ b}}^{(8)}) \star \mathbb{J}(\langle \langle \begin{array}{c} a \\ a \end{array} \rangle \rangle) \\
& + \sum_{q=2,3,4} (13)^* \Delta_{s_a,q} G_{\substack{a \\ b \\ c}}^{(8)} \star \mathbb{J}(\langle \langle \begin{array}{c} a \quad b \\ c \end{array} \rangle \rangle) + (13)^* \Delta_{s_a,q} G_{\substack{a \\ c \\ b}}^{(8)} \star \mathbb{J}(\langle \langle \begin{array}{c} a \quad c \\ b \end{array} \rangle \rangle)
\end{aligned}$$

$$\begin{aligned}
\langle \langle G_{\substack{a \\ b \\ c}}^{(8)}, \langle \langle \begin{array}{c} a \quad b \\ c \\ a \quad b \\ a \end{array} \rangle \rangle \rangle_{s_a} & \tag{symmetric in } b, c \tag{A.1w}
\end{aligned}$$

$$\begin{aligned}
& = \sum_{r=1,2} \Delta_{s_a,r} G_{\substack{a \\ b \\ c}}^{(8)} \star \mathbb{J}(\langle \langle \begin{array}{c} a \\ a \end{array} \rangle \rangle) + \sum_{p=3,4} \Delta_{s_a,p} G_{\substack{a \\ b \\ c}}^{(8)} \star \mathbb{J}(\langle \langle \begin{array}{c} a \\ a \end{array} \rangle \rangle)
\end{aligned}$$

$$\begin{aligned}
\langle \langle G_{\substack{a \\ b \\ c}}^{(8)}, \langle \langle \begin{array}{c} a \quad c \\ b \\ a \quad c \end{array} \rangle \rangle \rangle_{s_a} & \tag{A.1x}
\end{aligned}$$

$$\begin{aligned}
& = \sum_{r=1,2} \Delta_{s_a,r} G_{\substack{a \\ b \\ c}}^{(8)} \star \mathbb{J}(\langle \langle \begin{array}{c} c \\ a \end{array} \rangle \rangle) \\
& + \Delta_{s_a,3} G_{\substack{a \\ b \\ c}}^{(8)} \star \mathbb{J}(\langle \langle \begin{array}{c} a \quad c \\ b \end{array} \rangle \rangle) + \Delta_{s_a,4} G_{\substack{a \\ b \\ c}}^{(8)} \star \mathbb{J}(\langle \langle \begin{array}{c} a \quad b \\ c \end{array} \rangle \rangle) \\
& = \sum_{r=1,2} (13)^* (\Delta_{s_a,r} G_{\substack{a \\ b \\ c}}^{(8)}) \star \mathbb{J}(\langle \langle \begin{array}{c} b \quad c \\ a \end{array} \rangle \rangle) + \Delta_{s_a,3} G_{\substack{a \\ b \\ c}}^{(8)} \star \mathbb{J}(\langle \langle \begin{array}{c} a \quad c \\ b \end{array} \rangle \rangle) \\
& + \sum_{p=3,4} (13)^* (\Delta_{s_a,p} G_{\substack{a \\ b \\ c}}^{(8)}) \star \mathbb{J}(\langle \langle \begin{array}{c} a \quad b \\ c \end{array} \rangle \rangle)
\end{aligned}$$

$$\frac{1}{4} \langle\langle G^{(8)}, \text{graph} \rangle\rangle_{s_a} \quad (\text{A.1y})$$

$$= \frac{1}{4} \left\{ (23)^* \Delta_{s_a,1} G^{(8)} + \Delta_{s_a,2} G^{(8)} + (13)^* \Delta_{s_a,3} G^{(8)} + (123)^* \Delta_{s_a,4} G^{(8)} \right\} \star \mathbb{J}(\text{graph})$$

$$\frac{1}{4} \sum_{\substack{i=b,c; \\ (i \neq j \neq a)}} \langle\langle G^{(8)}, \text{graph} \rangle\rangle_{s_a} \quad (\text{A.1z})$$

$$= \frac{1}{4} \left[\left\{ \Delta_{s_a,1} G^{(8)} + (123)^* \Delta_{s_a,2} G^{(8)} + (23)^* \Delta_{s_a,3} G^{(8)} + (13)^* \Delta_{s_a,4} G^{(8)} \right\} \star \mathbb{J}(\text{graph}) + \left\{ \Delta_{s_a,1} G^{(8)} + (123)^* \Delta_{s_a,2} G^{(8)} + (23)^* \Delta_{s_a,3} G^{(8)} + (13)^* \Delta_{s_a,4} G^{(8)} \right\} \star \mathbb{J}(\text{graph}) \right]$$

$$\frac{1}{4} \langle\langle G^{(8)}, \text{graph} \rangle\rangle_{s_a} = \frac{1}{4} \sum_{r=1}^4 G^{(8)} \star \mathbb{J}(\text{graph}). \quad (\text{A.1aa})$$

One adds all the previous equations and associates by $\mathbb{J}(\mathcal{B})$, for \mathcal{B} one of the 11 graphs with 6 vertices. \square

B Rank-four and five melonic quartic theories

In this appendix we treat in detail the SDE for connected boundary graphs up to the 6-point function for the rank-4 quartic theory with pillow interactions and give some early steps on the rank-5 theory.

B.1 Four-coloured graphs and melonic quartic rank-4 theories

We count the graphs with $2k$ vertices for $k < 4$ in order to obtain free energy expansion until $\mathcal{O}(J^4, \bar{J}^4)$.

Figure 1.3 summarizes some properties of these graphs that the free energy expansion depends on. Although they had been enumerated, neither had they been identified nor their symmetry factors (the order of the coloured automorphism groups) found. We can now expand the free energy until sixth order, which would in theory allow the computation of 4-point function's equations starting from (1.2.3). For the φ_m^4 -theory, the sum is over all $\partial \text{Feyn}_D(\varphi_m^4) = \text{Grph}_D^{\text{II,cl}}$, as shown in [62]. For that model (and also for any other model containing those interaction vertices and thus the same boundary sector), the free

energy $W_{D=4}[J, \bar{J}]$ to $\mathcal{O}(6)$ is then given by the following expansion, where $b = b_{a,c} = \min(\{1, 2, 3, 4\} \setminus \{a, c\})$ and $d = d_{a,c} = \max(\{1, 2, 3, 4\} \setminus \{a, c\})$ and $(i_1(a), i_2(a), i_3(a))$ is the ordered set of $\{1, 2, 3, 4\} \setminus \{a\}$:

$$\begin{aligned}
W_{D=4}[J, \bar{J}] &= G_{\ominus}^{(2)} \star \mathbb{J}(\text{⊖}) + \frac{1}{2!} G_{|\ominus|\ominus}^{(4)} \star \mathbb{J}(\text{⊖}|\text{⊖}) + \sum_{j=1}^4 \frac{1}{2} G_{\text{⊖}|\text{⊖}}^{(4)} \star \mathbb{J}(\text{⊖}|\text{⊖}) \\
&+ \sum_{i<j} \frac{1}{2} G_{\text{⊖}|\text{⊖}}^{(4)} \star \mathbb{J}(\text{⊖}|\text{⊖}) + \frac{1}{3!} G_{|\ominus|\ominus|\ominus}^{(6)} \star \mathbb{J}(\text{⊖}|\text{⊖}|\text{⊖}) \\
&+ \frac{1}{2} \sum_{j=1}^4 G_{|\ominus|\text{⊖}|\text{⊖}}^{(6)} \star \mathbb{J}(\text{⊖}|\text{⊖}|\text{⊖}) + \frac{1}{2} \sum_{i<j} G_{|\ominus|\text{⊖}|\text{⊖}}^{(6)} \star \mathbb{J}(\text{⊖}|\text{⊖}|\text{⊖}) \\
&+ \sum_{i<j} G_{\text{⊖}|\text{⊖}}^{(6)} \star \mathbb{J}(\text{⊖}|\text{⊖}) + \sum_{i \neq j} G_{\text{⊖}|\text{⊖}}^{(6)} \star \mathbb{J}(\text{⊖}|\text{⊖}) \\
&+ \frac{1}{3} \sum_{i<j} G_{\text{⊖}|\text{⊖}}^{(6)} \star \mathbb{J}(\text{⊖}|\text{⊖}) + \frac{1}{3} \sum_{i=1}^4 G_{\text{⊖}|\text{⊖}}^{(6)} \star \mathbb{J}(\text{⊖}|\text{⊖}) \\
&+ \sum_{i<j} \sum_{\substack{k \neq i \\ k \neq j}} G_{\text{⊖}|\text{⊖}}^{(6)} \star \mathbb{J}(\text{⊖}|\text{⊖}) + \frac{1}{3} \sum_{i<j} G_{\text{⊖}|\text{⊖}}^{(6)} \star \mathbb{J}(\text{⊖}|\text{⊖}) \\
&+ \sum_{k=1}^4 \left\{ G_{\text{⊖}|\text{⊖}}^{(6)} \star \mathbb{J}(\text{⊖}|\text{⊖}) \right\} \Big|_{\{i_1, i_2, i_3\} = \{k\}^c} + O(J^4, \bar{J}^4)
\end{aligned}$$

It is convenient to single a particular colour a we want to use the WTI for. Care has been taken in order to colour the graph's edges in non-redundant, but univocal way. In particular, edges are labeled strictly by the closest letter next to them.

$$\begin{aligned}
W_{D=4}[J, \bar{J}] &= G_{\ominus}^{(2)} \star \mathbb{J}(\text{⊖}) + \frac{1}{2!} G_{|\ominus|\ominus}^{(4)} \star \mathbb{J}(\text{⊖}|\text{⊖}) + \sum_{c \neq a} \frac{1}{2} G_{\text{⊖}|\text{⊖}}^{(4)} \star \mathbb{J}(\text{⊖}|\text{⊖}) + \frac{1}{2} G_{\text{⊖}|\text{⊖}}^{(4)} \star \mathbb{J}(\text{⊖}|\text{⊖}) \\
&+ \sum_{c \neq a} \frac{1}{2} G_{\text{⊖}|\text{⊖}}^{(4)} \star \mathbb{J}(\text{⊖}|\text{⊖}) + \frac{1}{3!} G_{|\ominus|\ominus|\ominus}^{(6)} \star \mathbb{J}(\text{⊖}|\text{⊖}|\text{⊖}) \\
&+ \frac{1}{2} G_{|\ominus|\text{⊖}|\text{⊖}}^{(6)} \star \mathbb{J}(\text{⊖}|\text{⊖}|\text{⊖}) + \frac{1}{2} \sum_{c \neq a} G_{|\ominus|\text{⊖}|\text{⊖}}^{(6)} \star \mathbb{J}(\text{⊖}|\text{⊖}|\text{⊖}) \\
&+ \frac{1}{2} \sum_{c \neq a} G_{|\ominus|\text{⊖}|\text{⊖}}^{(6)} \star \mathbb{J}(\text{⊖}|\text{⊖}|\text{⊖}) + \sum_{c \neq a} G_{\text{⊖}|\text{⊖}}^{(6)} \star \mathbb{J}(\text{⊖}|\text{⊖}) \\
&+ \sum_{c \neq a} G_{\text{⊖}|\text{⊖}}^{(6)} \star \mathbb{J}(\text{⊖}|\text{⊖}) + \sum_{c \neq a} G_{\text{⊖}|\text{⊖}}^{(6)} \star \mathbb{J}(\text{⊖}|\text{⊖}) \\
&+ \sum_{c \neq a} G_{\text{⊖}|\text{⊖}}^{(6)} \star \mathbb{J}(\text{⊖}|\text{⊖}) + \sum_{c \neq a} \sum_{f=b,d} G_{\text{⊖}|\text{⊖}}^{(6)} \star \mathbb{J}(\text{⊖}|\text{⊖})
\end{aligned}$$

$$\begin{aligned}
& + \frac{1}{3} \sum_{c \neq a} G_a^{(6)} \star \mathbb{J} \left(\begin{array}{c} a \\ \text{---} \\ c \quad c \\ \text{---} \\ a \end{array} \right) + \frac{1}{3} G_a^{(6)} \star \mathbb{J} \left(\begin{array}{c} a \\ \text{---} \\ a \\ \text{---} \\ c \end{array} \right) + \frac{1}{3} \sum_{c \neq a} G_c^{(6)} \star \mathbb{J} \left(\begin{array}{c} c \\ \text{---} \\ c \\ \text{---} \\ c \end{array} \right) \\
& + \sum_{c \neq a} \sum_{f=b,d} G_a^{(6)} \star \mathbb{J} \left(\begin{array}{c} a \\ \text{---} \\ f \quad f \\ \text{---} \\ a \end{array} \right) + \frac{1}{3} \sum_{c \neq a} G_a^{(6)} \star \mathbb{J} \left(\begin{array}{c} a \\ \text{---} \\ c \quad c \\ \text{---} \\ a \end{array} \right) + \frac{1}{3} \sum_{c \neq a} G_a^{(6)} \star \mathbb{J} \left(\begin{array}{c} c \\ \text{---} \\ a \quad a \\ \text{---} \\ c \end{array} \right) \\
& + \sum_{c \neq a} \left\{ G_a^{(6)} \star \mathbb{J} \left(\begin{array}{c} a \\ \text{---} \\ c \quad c \\ \text{---} \\ a \end{array} \right) \right\} + G_a^{(6)} \star \mathbb{J} \left(\begin{array}{c} a \\ \text{---} \\ i_1 \quad i_2 \\ \text{---} \\ i_3 \end{array} \right) + O(J^4, \bar{J}^4)
\end{aligned}$$

For the sequel, we adopt the notation of writing entries of \mathbb{Z}^D as unordered sets, even though we mean them having a colour-ordering (by the subindices). Hence, the D -tuple $(q_{p_1}, q_{p_2}, \dots, q_{p_{D-1}}, q_{p_D})$ actually means $(q_r, q_s, \dots, q_t, q_u)$ where $r < s < \dots < t < u$, being $\{r, s, \dots, t, u\} = \{p_i\}_{i=1}^D$ as sets.

The simplified $Y_{m_a}^{(a)}$ -term given by (1.2.7) and by the Ward Takahashi identity after taking the $(m_a n_a)$ -entry of a generator of the a -th summand of $\text{Lie}(\text{U}(N)^D)$, reads then:

$$\begin{aligned}
& \sum_{q_{i_1}, q_{i_2}, q_{i_3}} G_{\ominus}^{(2)}(m_a, q_{i_1}, q_{i_2}, q_{i_3}) \\
& + \frac{1}{2} \left\{ \sum_{s=1,2} \Delta_{m_a, s} G_{|\ominus||\ominus|}^{(4)} + \sum_{i=1}^4 \sum_{s=1,2} \Delta_{m_a, s} G_{\text{---}}^{(4)} + \sum_{c \neq a} \sum_{s=1,2} \Delta_{m_a, s} G_a^{(4)} \right\} \star \mathbb{J}(\ominus) \quad (\text{B.1})
\end{aligned}$$

$$\begin{aligned}
& + \left\{ \frac{1}{3!} \sum_{r=1}^3 \Delta_{m_a, r} G_{|\ominus||\ominus||\ominus|}^{(6)} + \frac{1}{2} \sum_{i=1}^4 \sum_{s=2,3} \Delta_{m_a, s} G_{|\ominus||\text{---}|}^{(6)} + \frac{1}{2} \sum_{c \neq a} \left[\sum_{s=2,3} \Delta_{m_a, s} G_{|\ominus||\text{---}|}^{(6)} \right. \right. \\
& \left. \left. + \Delta_{m_a, 2} G_{\text{---}}^{(6)} + \Delta_{m_a, 2} G_a^{(6)} \right] \right\} \star \mathbb{J}(\ominus|\ominus) \quad (\text{B.2})
\end{aligned}$$

$$\begin{aligned}
& + \left\{ \frac{1}{2} \Delta_{m_a, 1} G_{|\ominus||\text{---}|}^{(6)} + \frac{1}{3} \sum_{r=1}^3 \Delta_{m_a, r} G_{\text{---}}^{(6)} + \sum_{c \neq a} \left[\Delta_{m_a, 1} G_{\text{---}}^{(6)} + \frac{1}{3} \sum_{r=1}^3 \Delta_{m_a, r} G_a^{(6)} \right. \right. \\
& \left. \left. + \Delta_{m_a, 2} G_{\text{---}}^{(6)} + \Delta_{m_a, 3} G_{\text{---}}^{(6)} \right] \right\} \star \mathbb{J}(\text{---})
\end{aligned}$$

$$\begin{aligned}
& + \sum_{\alpha=1}^3 \left\{ \frac{1}{2} \Delta_{m_a, 1} G_{|\ominus||i_\alpha|}^{(6)} + \Delta_{m_a, \alpha} G_{i_1 \text{---} i_2 \text{---} i_3}^{(6)} \right\} \star \mathbb{J}(\text{---} i_\alpha)
\end{aligned}$$

$$\begin{aligned}
& + \sum_{c \neq a} \left\{ \left[\sum_{s=1,2} \Delta_{m_a, s} G_{\text{---}}^{(6)} + \Delta_{m_a, 1} G_a^{(6)} + \frac{1}{3} \sum_{r=1}^3 \Delta_{m_a, r} G_c^{(6)} \right. \right. \\
& \left. \left. + \Delta_{m_a, 1} G_{\text{---}}^{(6)} + \Delta_{m_a, 1} G_{\text{---}}^{(6)} \right] \star \mathbb{J}(\text{---} c) \right. \\
& \left. + \left[\Delta_{m_a, 3} G_{\text{---}}^{(6)} + \sum_{s=1,2} \Delta_{m_a, s} G_{\text{---}}^{(6)} \right] \star \mathbb{J}(\text{---} b_{a,c}) \right. \\
& \left. + \left[\Delta_{m_a, 1} G_{\text{---}}^{(6)} + \sum_{s=1,2} \Delta_{m_a, s} G_{\text{---}}^{(6)} \right] \star \mathbb{J}(\text{---} d_{a,c}) \right\}
\end{aligned}$$

$$\begin{aligned}
& + \sum_{c \neq a} \left\{ \left[\frac{1}{2} \Delta_{m_a, 1} G_{|\ominus| \ominus| a|}^{(6)} + \sum_{s=2,3} \Delta_{m_a, s} G_{\text{cylinder}}^{(6)} + \Delta_{m_a, 3} G_{\text{cylinder}}^{(6)} \right. \right. \\
& \quad \left. \left. + \frac{1}{3} \sum_{r=1}^3 \Delta_{m_a, r} G_{\text{cylinder}}^{(6)} + \frac{1}{3} \sum_{r=1}^3 \Delta_{m_a, r} G_{\text{triangle}}^{(6)} + \sum_{\ell=1,3} \Delta_{m_a, \ell} G_{\text{triangle}}^{(6)} \right] \star \mathbb{J} \left(a \begin{array}{c} c \\ c \\ a \end{array} \right) \right. \\
& \quad \left. + \left[\Delta_{m_a, 3} G_{\text{cylinder}}^{(6)} + \Delta_{m_a, 2} G_{\text{triangle}}^{(6)} + \Delta_{m_a, 3} G_{\text{triangle}}^{(6)} \right] \star \mathbb{J} \left(b_{a,c} \begin{array}{c} a \\ a \\ b_{a,c} \end{array} \right) \right. \\
& \quad \left. + \left[\Delta_{m_a, 3} G_{\text{cylinder}}^{(6)} + \Delta_{m_a, 3} G_{\text{triangle}}^{(6)} + \Delta_{m_a, 2} G_{\text{triangle}}^{(6)} \right] \star \mathbb{J} \left(d_{a,c} \begin{array}{c} a \\ a \\ d_{a,c} \end{array} \right) \right\} + O(J^3, \bar{J}^3).
\end{aligned}$$

B.2 Two-point equation for rank-4 theories

Also rank-4 theories are also an active topic [105]. We think it is instructive to derive directly, without using the theorem the SDE for the 2-point function:

$$\begin{aligned}
G_{\ominus}^{(2)}(\mathbf{a}) &= \frac{1}{Z_0} \left\{ \frac{\delta}{\delta J_{\mathbf{a}}} \left[\exp(-\mathcal{S}_{\text{int}}(\delta/\delta \bar{J}, \delta/\delta J)) \frac{1}{E_{\mathbf{a}}} J_{\mathbf{a}} e^{\sum_{\mathbf{q}} \bar{J}_{\mathbf{q}} E_{\mathbf{q}}^{-1} J_{\mathbf{q}}} \right] \right\}_{J=\bar{J}=0} \\
&= \frac{1}{Z_0 E_{\mathbf{a}}} \left[\exp(-\mathcal{S}_{\text{int}}(\delta/\delta \bar{J}, \delta/\delta J)) e^{\sum_{\mathbf{q}} \bar{J}_{\mathbf{q}} E_{\mathbf{q}}^{-1} J_{\mathbf{q}}} \right]_{J=\bar{J}=0} \\
& \quad + \frac{1}{Z_0 E_{\mathbf{a}}} \left(\exp(-\mathcal{S}_{\text{int}}(\delta/\delta \bar{J}, \delta/\delta J)) J_{\mathbf{a}} \frac{\delta}{\delta J_{\mathbf{a}}} e^{\sum_{\mathbf{q}} \bar{J}_{\mathbf{q}} E_{\mathbf{q}}^{-1} J_{\mathbf{q}}} \right)_{J=\bar{J}=0} \\
&= \frac{1}{E_{\mathbf{a}}} + \frac{1}{Z_0} \frac{1}{E_{\mathbf{a}}} \left(\bar{\varphi}_{\mathbf{a}} \frac{\partial}{\partial \bar{\varphi}_{\mathbf{a}}} (-\mathcal{S}_{\text{int}}(\varphi, \bar{\varphi})) \right)_{\varphi^b \rightarrow \delta/\delta J^{\sharp}} \left. Z[J, \bar{J}] \right|_{J=\bar{J}=0},
\end{aligned} \tag{B.3}$$

$$\begin{aligned}
& \bar{\varphi}_{\mathbf{x}} \frac{\partial(-\mathcal{S}_{\text{int}}(\varphi, \bar{\varphi}))}{\partial \bar{\varphi}_{\mathbf{x}}} \Big|_{\varphi^b \rightarrow \delta/\delta J^{\sharp}} \\
&= -2\lambda \left\{ \frac{\delta}{\delta J_{x_1 x_2 x_3 x_4}} \sum_{y_1} \frac{\delta}{\delta \bar{J}_{y_1 x_2 x_3 x_4}} \sum_{y_2, y_3, y_4} \frac{\delta}{\delta J_{y_1 y_2 y_3 y_4}} \frac{\delta}{\delta \bar{J}_{x_1 y_2 y_3 y_4}} \quad (\mathbf{x} \in \mathbb{Z}^4) \right. \\
& \quad + \frac{\delta}{\delta J_{x_1 x_2 x_3 x_4}} \sum_{y_2} \frac{\delta}{\delta \bar{J}_{x_1 y_2 x_3 x_4}} \sum_{y_1, y_3, y_4} \frac{\delta}{\delta J_{y_1 y_2 y_3 y_4}} \frac{\delta}{\delta \bar{J}_{y_1 x_2 y_3 y_4}} \\
& \quad + \frac{\delta}{\delta J_{x_1 x_2 x_3 x_4}} \sum_{y_3} \frac{\delta}{\delta \bar{J}_{x_1 x_2 y_3 x_4}} \sum_{y_1, y_2, y_4} \frac{\delta}{\delta J_{y_1 y_2 y_3 y_4}} \frac{\delta}{\delta \bar{J}_{y_1 y_2 x_3 y_4}} \\
& \quad \left. + \frac{\delta}{\delta J_{x_1 x_2 x_3 x_4}} \sum_{y_4} \frac{\delta}{\delta \bar{J}_{x_1 x_2 x_3 y_4}} \sum_{y_1, y_2, y_3} \frac{\delta}{\delta J_{y_1 y_2 y_3 y_4}} \frac{\delta}{\delta \bar{J}_{y_1 y_2 y_3 x_4}} \right\} \left. Z[J, \bar{J}] \right|_{J=\bar{J}=0}.
\end{aligned}$$

One uses the WTI for the double derivatives of the form

$$\sum_{y_2, y_3, y_4} \frac{\delta^2 Z[J, \bar{J}]}{\delta J_{y_1 y_2 y_3 y_4} \delta \bar{J}_{x_1 y_2 y_3 y_4}}, \dots, \sum_{y_1, y_2, y_3} \frac{\delta^2 Z[J, \bar{J}]}{\delta J_{y_1 y_2 y_3 y_4} \delta \bar{J}_{y_1 y_2 y_3 x_4}}.$$

Then

$$\begin{aligned}
& \bar{\varphi}_{\mathbf{x}} \frac{\partial(-\mathcal{S}_{\text{int}}(\varphi, \bar{\varphi}))}{\partial \bar{\varphi}_{\mathbf{x}}} \Big|_{\varphi^b \rightarrow \delta/\delta J^\#} \\
&= -2\lambda Z_0 \left\{ \sum_{a=1}^4 \left[\frac{\delta^2 Y_{x_a}^{(a)}[J, \bar{J}]}{\delta J_{\mathbf{x}} \delta \bar{J}_{\mathbf{x}}} \Big|_{J=\bar{J}=0} + Y_{x_a}^{(a)}[0, 0] \cdot G_{\ominus}^{(2)}(\mathbf{x}) \right. \right. \\
&\quad \left. \left. - \sum_{y_a} \frac{1}{|x_a|^2 - |y_a|^2} (G_{\ominus}^{(2)}(\mathbf{x}) - G_{\ominus}^{(2)}(y_a, x_{i_1(a)}, x_{i_2(a)}, x_{i_3(a)})) \right] \right\}. \tag{B.4}
\end{aligned}$$

Recall that (q_i, q_j, q_k, q_l) implies an ordering of the entries, that is, reordering so that q_s appears to the left of q_r if and only if $s < r$, $s, r \in \{i, j, k, l\} = \{1, 2, 3, 4\}$. Twice the double derivative appearing there, $2\delta^2 Y_{x_a}^{(a)}[J, \bar{J}]/\delta J_{\mathbf{x}} \delta \bar{J}_{\mathbf{x}}$, is given by

$$\begin{aligned}
& \sum_{q_{i_1(a)}, q_{i_2(a)}, q_{i_3(a)}} \left(G_{|\ominus| \ominus| \ominus|}^{(4)}(x_a, q_{i_1(a)}, q_{i_2(a)}, q_{i_3(a)}; \mathbf{x}) + G_{|\ominus| \ominus| \ominus|}^{(4)}(\mathbf{x}; x_a, q_{i_1(a)}, q_{i_2(a)}, q_{i_3(a)}) \right) \\
&+ \sum_{c \neq a} \sum_{q_{b(a,c)}, q_{d(a,c)}} \left(G_{\underbrace{\ominus}_{c \ominus}}^{(4)}(x_a, x_c, q_b, q_d; \mathbf{x}) + G_{\underbrace{\ominus}_{c \ominus}}^{(4)}(\mathbf{x}; x_a, x_c, q_b, q_d) \right) \\
&+ 2G_{\underbrace{\ominus}_{a \ominus}}^{(4)}(\mathbf{x}; \mathbf{x}) + \sum_{c \neq a} \sum_{q_c} \left(G_{\underbrace{\ominus}_{a \ominus c}}^{(4)}(x_a, x_b, q_c, x_d; \mathbf{x}) + G_{\underbrace{\ominus}_{a \ominus c}}^{(4)}(\mathbf{x}; x_a, x_b, q_c, x_d) \right).
\end{aligned}$$

Thus, since $Y_{m_a}^{(a)}[0, \bar{0}] = \sum_{q_{i_1}, q_{i_2}, q_{i_3}} G_{\ominus}^{(2)}(m_a, q_{i_1}, q_{i_2}, q_{i_3})$, one has

$$\begin{aligned}
G_{\ominus}^{(2)}(\mathbf{x}) &= \frac{1}{E_{\mathbf{x}}} + \frac{1}{Z_0} \frac{1}{E_{\mathbf{x}}} \left(\bar{\varphi}_{\mathbf{x}} \frac{\partial}{\partial \bar{\varphi}_{\mathbf{x}}} (-\mathcal{S}_{\text{int}}(\varphi, \bar{\varphi})) \Big|_{\varphi^b \rightarrow \delta/\delta J^\#} Z[J, \bar{J}] \Big|_{J=\bar{J}=0} \right) \\
&= \frac{1}{E_{\mathbf{x}}} + \frac{(-\lambda)}{E_{\mathbf{x}}} \left\{ \sum_{a=1}^4 \left[2 \cdot G_{\ominus}^{(2)}(\mathbf{x}) \cdot \left(\sum_{q_{i_1(a)}} \sum_{q_{i_2(a)}} \sum_{q_{i_3(a)}} G_{\ominus}^{(2)}(x_a, q_{i_1(a)}, q_{i_2(a)}, q_{i_3(a)}) \right) \right. \right. \\
&\quad + \sum_{q_{i_1(a)}} \sum_{q_{i_2(a)}} \sum_{q_{i_3(a)}} \left(G_{|\ominus| \ominus| \ominus|}^{(4)}(x_a, q_{i_1(a)}, q_{i_2(a)}, q_{i_3(a)}; \mathbf{x}) \right. \\
&\quad \quad \left. \left. + G_{|\ominus| \ominus| \ominus|}^{(4)}(\mathbf{x}; x_a, q_{i_1(a)}, q_{i_2(a)}, q_{i_3(a)}) \right) \right. \\
&\quad + \sum_{c \neq a} \sum_{q_{b(a,c)}} \sum_{q_{d(a,c)}} \left(G_{\underbrace{\ominus}_{c \ominus}}^{(4)}(x_a, x_c, q_b, q_d; \mathbf{x}) + G_{\underbrace{\ominus}_{c \ominus}}^{(4)}(\mathbf{x}; x_a, x_c, q_b, q_d) \right) \\
&\quad + \sum_{c \neq a} \sum_{q_c} \left(G_{\underbrace{\ominus}_{a \ominus c}}^{(4)}(x_a, x_b, q_c, x_d; \mathbf{x}) + G_{\underbrace{\ominus}_{a \ominus c}}^{(4)}(\mathbf{x}; x_a, x_b, q_c, x_d) \right) + 2G_{\underbrace{\ominus}_{a \ominus}}^{(4)}(\mathbf{x}; \mathbf{x}) \\
&\quad \left. \left. - \sum_{y_a} \frac{2}{|x_a|^2 - |y_a|^2} (G_{\ominus}^{(2)}(\mathbf{x}) - G_{\ominus}^{(2)}(y_a, x_{i_1(a)}, x_{i_2(a)}, x_{i_3(a)})) \right] \right\}.
\end{aligned}$$

B.3 Four-point equation for $G_{\mathbb{1}\overline{\mathbb{1}}\mathbb{1}}^{(4)}$ in rank-4 theories

Since \mathcal{V}_1 has \mathbb{Z}_2 as automorphism group, according to Theorem 1.3.1, the equation satisfied by $G_{\mathbb{1}\overline{\mathbb{1}}\mathbb{1}}^{(4)}$ is the following:

$$\begin{aligned} & \left(1 + \frac{2\lambda}{E_{x_1, y_2, y_3, y_4}} \sum_{a=1}^4 \sum_{\mathbf{q}\hat{a}} G_{\ominus}^{(2)}(s_a, \mathbf{q}\hat{a}) \right) G_{\mathbb{1}\overline{\mathbb{1}}\mathbb{1}}^{(4)}(\mathbf{X}) \\ &= \frac{(-2\lambda)}{E_{\mathbf{s}}} \sum_{a=1}^4 \left\{ \sum_{\hat{\sigma} \in \mathbb{Z}_2} \sigma^* \mathfrak{f}_{\mathbb{1}\overline{\mathbb{1}}\mathbb{1}}^{(a)}(\mathbf{X}) + \sum_{\rho > 1} \frac{Z_0^{-1}}{E(y_a^\rho, s_a)} \left[\frac{\partial Z[J, J]}{\partial \varsigma_a(\mathbb{1}\overline{\mathbb{1}}; 1, \rho)}(\mathbf{X}) - \frac{\partial Z[J, J]}{\partial \varsigma_a(\mathbb{1}\overline{\mathbb{1}}; 1, \rho)}(\mathbf{X}|_{s_a \rightarrow y_a^\rho}) \right] \right. \\ & \quad \left. - \sum_{b_a} \frac{1}{E(s_a, b_a)} [G_{\mathbb{1}\overline{\mathbb{1}}\mathbb{1}}^{(4)}(\mathbf{X}) - G_{\mathbb{1}\overline{\mathbb{1}}\mathbb{1}}^{(4)}(\mathbf{X}|_{s_a \rightarrow b_a})] \right\}, \end{aligned} \quad (\text{B.5})$$

for $\mathbf{x}, \mathbf{y} \in \mathbb{Z}^4$, $\mathbf{X} = (\mathbf{x}, \mathbf{y})$, and $\mathbf{s} = (x_1, y_2, y_3, y_4)$. We write down first the term in square brackets in the RHS, which one finds trivially:

$$\begin{aligned} \sum_{a=1}^4 \frac{Z_0^{-1}}{E(y_a^2, s_a)} \frac{\partial Z[J, J]}{\partial \varsigma_a(\mathbb{1}\overline{\mathbb{1}}; 1, 2)}(\mathbf{X}) &= \frac{1}{E(y_1, x_1)} (G_{|\ominus|\ominus|\ominus|}^{(4)}(\mathbf{X}) + G_{\ominus}^{(2)}(\mathbf{x}) \cdot G_{\ominus}^{(2)}(\mathbf{y})) \\ &+ \sum_{c \neq 1} \frac{1}{E(x_c, y_c)} G_{\mathbb{1}\overline{\mathbb{1}}\mathbb{1}}^{(4)}(\mathbf{X}). \end{aligned}$$

Less so is to find $\sum_a \mathfrak{f}_{\mathbb{1}\overline{\mathbb{1}}\mathbb{1}}^{(a)}$. The contributions to $\mathfrak{f}_{\mathbb{1}\overline{\mathbb{1}}\mathbb{1}}^{(a)}$, for fixed colour a , are all functions occurring in front of a $\mathbb{J}(\overline{\mathbb{1}}\mathbb{1})$ -source term. These functions come from coefficients of the following source terms in (B.1) $\mathbb{J}(\overline{\mathbb{1}}_a\mathbb{1})$ and $\mathbb{J}(\overline{\mathbb{1}}_c\mathbb{1})$ for the values⁸ when $a = 1$ or $c = 1$ (in the sum over c), but also form the following values:

$$\begin{aligned} & \mathbb{J}(\overline{\mathbb{1}}^{i_a}\mathbb{1}), \text{ for } a \in \{2, 3, 4\}; \quad \mathbb{J}(\overline{\mathbb{1}}^{b_a c}\mathbb{1}), \text{ for } (a, c) \in \{(2, 3), (2, 4), (3, 2), (3, 4), (4, 2), (4, 3)\}; \\ & \text{none from } \mathbb{J}(\overline{\mathbb{1}}^{d_a c}\mathbb{1}). \end{aligned}$$

Hence

$$\begin{aligned} \mathfrak{f}_{\mathbb{1}\overline{\mathbb{1}}\mathbb{1}}^{(1)} &= \left\{ \frac{1}{2} \Delta_{x_1, 1} G_{|\ominus|\ominus|\ominus|}^{(6)} + \frac{1}{3} \sum_{r=1}^3 \Delta_{x_1, r} G_{\mathbb{1}\overline{\mathbb{1}}\mathbb{1}}^{(6)} + \sum_{c \neq a} \left[\Delta_{x_1, 1} G_{\mathbb{1}\overline{\mathbb{1}}\mathbb{1}}^{(6)} + \frac{1}{3} \sum_{r=1}^3 \Delta_{x_1, r} G_{\mathbb{1}\overline{\mathbb{1}}\mathbb{1}}^{(6)} \right. \right. \\ & \quad \left. \left. + \Delta_{x_1, 2} G_{\mathbb{1}\overline{\mathbb{1}}\mathbb{1}}^{(6)} + \Delta_{x_1, 3} G_{\mathbb{1}\overline{\mathbb{1}}\mathbb{1}}^{(6)} \right] \right\}, \end{aligned} \quad (\text{B.6})$$

$$\begin{aligned} \mathfrak{f}_{\mathbb{1}\overline{\mathbb{1}}\mathbb{1}}^{(2)} &= \sum_{s=1, 2} \Delta_{y_2, s} G_{\mathbb{1}\overline{\mathbb{1}}\mathbb{1}}^{(6)} + \Delta_{y_2, 1} G_{\mathbb{1}\overline{\mathbb{1}}\mathbb{1}}^{(6)} + \frac{1}{3} \sum_{r=1}^3 \Delta_{y_2, r} G_{\mathbb{1}\overline{\mathbb{1}}\mathbb{1}}^{(6)} + \Delta_{y_2, 1} G_{\mathbb{1}\overline{\mathbb{1}}\mathbb{1}}^{(6)} + \Delta_{y_2, 1} G_{\mathbb{1}\overline{\mathbb{1}}\mathbb{1}}^{(6)} \\ & \quad (\text{B.7}) \end{aligned}$$

⁸Recall that c ($c \neq a$) in that expansion (B.1) is seen as running variable, while $b < d$ are defined in terms of a and c by $\{a, b, c, d\} = \{1, 2, 3, 4\}$. Also $i_1(a) < i_2(a) < i_3(a)$, and $\{i_1, i_2, i_3, a\} = \{1, 2, 3, 4\}$.

$$\begin{aligned}
& + \frac{1}{2} \Delta_{y_2,1} G_{|\ominus| \ominus| \ominus|}^{(6)} + \Delta_{y_2,\alpha} G_{\text{1} \begin{array}{c} \diagup \diagdown \\ \text{2} \end{array} \text{4}}^{(6)} + \sum_{c=3,4} \left[\Delta_{y_2,3} G_{\text{1} \begin{array}{c} \diagup \diagdown \\ c \end{array} \text{2}}^{(6)} + \sum_{s=1,2} \Delta_{y_2,s} G_{\text{c} \begin{array}{c} \diagup \diagdown \\ c \end{array} \text{2}}^{(6)} \right], \\
\mathbf{f}_{\text{1} \begin{array}{c} \diagup \diagdown \\ \text{1} \end{array} \text{1}}^{(3)} &= \sum_{s=1,2} \Delta_{y_3,s} G_{\text{3} \begin{array}{c} \diagup \diagdown \\ \text{1} \end{array} \text{1}}^{(6)} + \Delta_{y_3,1} G_{\text{3} \begin{array}{c} \diagup \diagdown \\ \text{3} \end{array} \text{1}}^{(6)} + \frac{1}{3} \sum_{r=1}^3 \Delta_{y_3,r} G_{\text{3} \begin{array}{c} \diagup \diagdown \\ r \end{array} \text{1}}^{(6)} + \Delta_{y_3,1} G_{\text{3} \begin{array}{c} \diagup \diagdown \\ \text{3} \end{array} \text{3}}^{(6)} + \Delta_{y_3,1} G_{\text{3} \begin{array}{c} \diagup \diagdown \\ \text{3} \end{array} \text{4}}^{(6)} \\
& + \frac{1}{2} \Delta_{y_3,1} G_{|\ominus| \ominus| \ominus|}^{(6)} + \Delta_{y_3,\alpha} G_{\text{1} \begin{array}{c} \diagup \diagdown \\ \text{3} \end{array} \text{4}}^{(6)} + \sum_{c=2,4} \left[\Delta_{y_3,3} G_{\text{1} \begin{array}{c} \diagup \diagdown \\ c \end{array} \text{3}}^{(6)} + \sum_{s=1,2} \Delta_{y_3,s} G_{\text{c} \begin{array}{c} \diagup \diagdown \\ c \end{array} \text{3}}^{(6)} \right], \\
\mathbf{f}_{\text{1} \begin{array}{c} \diagup \diagdown \\ \text{1} \end{array} \text{1}}^{(4)} &= \sum_{s=1,2} \Delta_{y_4,s} G_{\text{4} \begin{array}{c} \diagup \diagdown \\ \text{1} \end{array} \text{1}}^{(6)} + \Delta_{y_4,1} G_{\text{4} \begin{array}{c} \diagup \diagdown \\ \text{4} \end{array} \text{1}}^{(6)} + \frac{1}{3} \sum_{r=1}^3 \Delta_{y_4,r} G_{\text{4} \begin{array}{c} \diagup \diagdown \\ r \end{array} \text{1}}^{(6)} + \Delta_{y_4,1} G_{\text{4} \begin{array}{c} \diagup \diagdown \\ \text{4} \end{array} \text{3}}^{(6)} + \Delta_{y_4,1} G_{\text{4} \begin{array}{c} \diagup \diagdown \\ \text{4} \end{array} \text{4}}^{(6)} \\
& + \frac{1}{2} \Delta_{y_4,1} G_{|\ominus| \ominus| \ominus|}^{(6)} + \Delta_{y_4,\alpha} G_{\text{1} \begin{array}{c} \diagup \diagdown \\ \text{4} \end{array} \text{3}}^{(6)} + \sum_{c=2,3} \left[\Delta_{y_4,3} G_{\text{1} \begin{array}{c} \diagup \diagdown \\ c \end{array} \text{4}}^{(6)} + \sum_{s=1,2} \Delta_{y_4,s} G_{\text{c} \begin{array}{c} \diagup \diagdown \\ c \end{array} \text{4}}^{(6)} \right].
\end{aligned} \tag{B.8}$$

One inserts the sum of these four terms in equation (B.5).

B.4 Four-point equation for $G_{\text{1} \begin{array}{c} \diagup \diagdown \\ \text{2} \end{array} \text{2}}^{(4)}$ in rank-4 theories

In order to get the equation for $G_{\text{1} \begin{array}{c} \diagup \diagdown \\ \text{2} \end{array} \text{2}}^{(4)}$, we calculate first $\sum_a \mathbf{f}_{\text{1} \begin{array}{c} \diagup \diagdown \\ \text{2} \end{array} \text{2}}^{(a)}$.

$$\begin{aligned}
\mathbf{f}_{\text{1} \begin{array}{c} \diagup \diagdown \\ \text{2} \end{array} \text{2}}^{(1)} &= \left[\frac{1}{2} \Delta_{x_1,1} G_{|\ominus| \ominus| \text{1} \begin{array}{c} \diagup \diagdown \\ \text{2} \end{array} \text{2}}^{(6)} + \sum_{s=2,3} \Delta_{x_1,s} G_{\text{2} \begin{array}{c} \diagup \diagdown \\ s \end{array} \text{1}}^{(6)} + \Delta_{x_1,3} G_{\text{1} \begin{array}{c} \diagup \diagdown \\ \text{1} \end{array} \text{2}}^{(6)} \right. \\
& + \frac{1}{3} \sum_{r=1}^3 \Delta_{x_1,r} G_{\text{1} \begin{array}{c} \diagup \diagdown \\ \text{2} \end{array} \text{2} \text{1}}^{(6)} + \frac{1}{3} \sum_{r=1}^3 \Delta_{x_1,r} G_{\text{2} \begin{array}{c} \diagup \diagdown \\ r \end{array} \text{2}}^{(6)} + \sum_{\ell=1,3} \Delta_{x_1,\ell} G_{\text{2} \begin{array}{c} \diagup \diagdown \\ \ell \end{array} \text{2}}^{(6)} \left. \right] \\
& + \sum_{c=3,4} \left[\Delta_{x_1,3} G_{\text{c} \begin{array}{c} \diagup \diagdown \\ c \end{array} \text{1}}^{(6)} + \Delta_{x_1,2} G_{\text{1} \begin{array}{c} \diagup \diagdown \\ c \end{array} \text{1}}^{(6)} + \Delta_{x_1,3} G_{\text{1} \begin{array}{c} \diagup \diagdown \\ c \end{array} \text{1}}^{(6)} \right],
\end{aligned} \tag{B.10a}$$

$$\begin{aligned}
\mathbf{f}_{\text{1} \begin{array}{c} \diagup \diagdown \\ \text{2} \end{array} \text{2}}^{(2)} &= \left[\frac{1}{2} \Delta_{x_2,1} G_{|\ominus| \ominus| \text{1} \begin{array}{c} \diagup \diagdown \\ \text{2} \end{array} \text{2}}^{(6)} + \sum_{s=2,3} \Delta_{x_2,s} G_{\text{1} \begin{array}{c} \diagup \diagdown \\ s \end{array} \text{2}}^{(6)} + \Delta_{x_2,3} G_{\text{2} \begin{array}{c} \diagup \diagdown \\ \text{2} \end{array} \text{1}}^{(6)} \right. \\
& + \frac{1}{3} \sum_{r=1}^3 \Delta_{x_2,r} G_{\text{1} \begin{array}{c} \diagup \diagdown \\ \text{2} \end{array} \text{2} \text{1}}^{(6)} + \frac{1}{3} \sum_{r=1}^3 \Delta_{x_2,r} G_{\text{1} \begin{array}{c} \diagup \diagdown \\ r \end{array} \text{2}}^{(6)} + \sum_{\ell=1,3} \Delta_{x_2,\ell} G_{\text{1} \begin{array}{c} \diagup \diagdown \\ \ell \end{array} \text{2}}^{(6)} \left. \right] \\
& + \sum_{c=3,4} \left[\Delta_{x_2,3} G_{\text{c} \begin{array}{c} \diagup \diagdown \\ c \end{array} \text{2}}^{(6)} + \Delta_{x_2,2} G_{\text{2} \begin{array}{c} \diagup \diagdown \\ c \end{array} \text{2}}^{(6)} + \Delta_{x_2,3} G_{\text{2} \begin{array}{c} \diagup \diagdown \\ c \end{array} \text{2}}^{(6)} \right],
\end{aligned} \tag{B.10b}$$

$$\begin{aligned}
\mathbf{f}_{\text{1} \begin{array}{c} \diagup \diagdown \\ \text{2} \end{array} \text{2}}^{(3)} &= \left[\frac{1}{2} \Delta_{y_3,1} G_{|\ominus| \ominus| \text{3} \begin{array}{c} \diagup \diagdown \\ \text{2} \end{array} \text{2}}^{(6)} + \sum_{s=2,3} \Delta_{y_3,s} G_{\text{4} \begin{array}{c} \diagup \diagdown \\ s \end{array} \text{3}}^{(6)} + \Delta_{y_3,3} G_{\text{3} \begin{array}{c} \diagup \diagdown \\ \text{3} \end{array} \text{4}}^{(6)} \right. \\
& + \frac{1}{3} \sum_{r=1}^3 \Delta_{y_3,r} G_{\text{3} \begin{array}{c} \diagup \diagdown \\ \text{4} \end{array} \text{3}}^{(6)} + \frac{1}{3} \sum_{r=1}^3 \Delta_{y_3,r} G_{\text{3} \begin{array}{c} \diagup \diagdown \\ r \end{array} \text{3}}^{(6)} + \sum_{\ell=1,3} \Delta_{y_3,\ell} G_{\text{3} \begin{array}{c} \diagup \diagdown \\ \ell \end{array} \text{3}}^{(6)} \left. \right] \\
& + \sum_{c=2,4} \left[\Delta_{y_3,3} G_{\text{c} \begin{array}{c} \diagup \diagdown \\ c \end{array} \text{3}}^{(6)} + \Delta_{y_3,3} G_{\text{3} \begin{array}{c} \diagup \diagdown \\ c \end{array} \text{3}}^{(6)} + \Delta_{y_3,2} G_{\text{3} \begin{array}{c} \diagup \diagdown \\ c \end{array} \text{3}}^{(6)} \right],
\end{aligned} \tag{B.10c}$$

$$\begin{aligned}
\mathbf{f}_{\mathbb{1}\mathbb{2}}^{(4)} &= \left[\frac{1}{2} \Delta_{y_4,1} G_{|\mathbb{1}\mathbb{2}|}^{(6)} + \sum_{s=2,3} \Delta_{y_4,s} G_{\mathbb{3}\mathbb{4}}^{(6)} + \Delta_{y_4,3} G_{\mathbb{4}\mathbb{3}}^{(6)} \right. \\
&\quad \left. + \frac{1}{3} \sum_{r=1}^3 \Delta_{y_4,r} G_{\mathbb{3}\mathbb{4}\mathbb{3}}^{(6)} + \frac{1}{3} \sum_{r=1}^3 \Delta_{y_4,r} G_{\mathbb{3}\mathbb{4}\mathbb{3}}^{(6)} + \sum_{\ell=1,3} \Delta_{y_4,\ell} G_{\mathbb{4}\mathbb{3}\mathbb{4}}^{(6)} \right] \\
&\quad + \sum_{c=2,3} \left[\Delta_{y_4,3} G_{\mathbb{c}\mathbb{4}\mathbb{c}}^{(6)} + \Delta_{y_4,3} G_{\mathbb{4}\mathbb{c}\mathbb{4}}^{(6)} + \Delta_{y_4,2} G_{\mathbb{4}\mathbb{c}\mathbb{4}}^{(6)} \right].
\end{aligned} \tag{B.10d}$$

The remaining terms from swapping edges are:

$$\begin{aligned}
\sum_{a=1}^4 \frac{Z_0^{-1}}{E(y_a^2, s_a)} \frac{\partial Z[J, J]}{\partial \varsigma_a(\mathbb{1}\mathbb{2}; 1, 2)}(\mathbf{X}) &= \frac{1}{E(y_1, x_1)} G_{\mathbb{2}\mathbb{2}}^{(4)}(\mathbf{x}, \mathbf{y}) + \frac{1}{E(y_2, x_2)} G_{\mathbb{1}\mathbb{1}}^{(4)}(\mathbf{x}, \mathbf{y}) \\
&\quad + \frac{1}{E(x_3, y_3)} G_{\mathbb{4}\mathbb{4}}^{(4)}(\mathbf{x}, \mathbf{y}) + \frac{1}{E(x_4, y_4)} G_{\mathbb{3}\mathbb{3}}^{(4)}(\mathbf{x}, \mathbf{y}),
\end{aligned}$$

whence the SDE for $G_{\mathbb{1}\mathbb{2}}^{(4)}$ is

$$\begin{aligned}
&\left(1 + \frac{2\lambda}{E_s} \sum_{a=1}^4 \sum_{\mathbf{q}_{\hat{a}}} G_{\mathbb{1}\mathbb{2}}^{(2)}(s_a, \mathbf{q}_{\hat{a}}) \right) \cdot G_{\mathbb{1}\mathbb{2}}^{(4)}(\mathbf{X}) \\
&= \frac{(-2\lambda)}{E_s} \sum_{a=1}^4 \left\{ \sum_{\hat{\sigma} \in \mathbb{Z}_2} \sigma^* \mathbf{f}_{\mathbb{1}\mathbb{2}}^{(a)}(\mathbf{X}) + \frac{1}{E(y_1, x_1)} [G_{\mathbb{2}\mathbb{2}}^{(4)}(\mathbf{x}, \mathbf{y}) - G_{\mathbb{2}\mathbb{2}}^{(4)}(y_1, x_2, x_3, x_4, \mathbf{y})] + \right. \\
&\quad + \frac{1}{E(y_2, x_2)} [G_{\mathbb{1}\mathbb{1}}^{(4)}(\mathbf{x}, \mathbf{y}) - G_{\mathbb{1}\mathbb{1}}^{(4)}(x_1, y_2, x_3, x_4, \mathbf{y})] \\
&\quad + \frac{1}{E(x_3, y_3)} [G_{\mathbb{4}\mathbb{4}}^{(4)}(\mathbf{x}, \mathbf{y}) - G_{\mathbb{4}\mathbb{4}}^{(4)}(\mathbf{x}, y_1, y_2, x_3, y_4)] \\
&\quad + \frac{1}{E(x_4, y_4)} [G_{\mathbb{3}\mathbb{3}}^{(4)}(\mathbf{x}, \mathbf{y}) - G_{\mathbb{3}\mathbb{3}}^{(4)}(\mathbf{x}, y_1, y_2, y_3, x_4)] \\
&\quad \left. - \sum_{b_a} \frac{1}{E(s_a, b_a)} [G_{\mathbb{1}\mathbb{2}}^{(4)}(\mathbf{X}) - G_{\mathbb{1}\mathbb{2}}^{(4)}(\mathbf{X}|_{s_a \rightarrow b_a})] \right\},
\end{aligned}$$

with $\mathbf{X} = (\mathbf{x}, \mathbf{y})$ and $\mathbf{s} = (x_1, x_2, y_3, y_4)$ with the functions $\mathbf{f}_{\mathbb{1}\mathbb{2}}^{(a)}$ given by eqs. (B.10).

B.5 Rank-five melonic quartic theory

The generating function that enumerates the rank-5 connected boundary graphs (and interaction vertices) is the OEIS [A057007](#):

$$Z_{\text{conn},5}(x) = x + 15x^2 + 235x^3 + 14120x^4 + 1712845x^5 + 371515454x^6 + \dots$$

We will not classify the 235 connected graphs with six vertices, but, aiming only at obtaining the 2-point function's equation, we will compute the free energy up to $\mathcal{O}(J^3, \bar{J}^3)$:

$$W_{D=5}[J, \bar{J}] = G_{\mathbb{1}\mathbb{2}}^{(2)} \star \mathbb{J}(\mathbb{1}\mathbb{2}) + \frac{1}{2!} G_{|\mathbb{1}\mathbb{2}|}^{(4)} \star \mathbb{J}(\mathbb{1}\mathbb{2}|\mathbb{1}\mathbb{2})$$

$$\begin{aligned}
& + \sum_{j=1}^5 \frac{1}{2} G_{\text{diag}_j}^{(4)} \star \mathbb{J}(\text{diag}_j) + \sum_{i<j} \frac{1}{2} G_{\text{diag}_{ij}}^{(4)} \star \mathbb{J}(\text{diag}_{ij}) + O(J^3, \bar{J}^3) \\
& = G_{\text{diag}_1}^{(2)} \star \mathbb{J}(\text{diag}_1) + \frac{1}{2!} G_{\text{diag}_{12}}^{(4)} \star \mathbb{J}(\text{diag}_{12}) + \frac{1}{2} G_{\text{diag}_2}^{(4)} \star \mathbb{J}(\text{diag}_2) \\
& + \sum_{c \neq a} \frac{1}{2} G_{\text{diag}_c}^{(4)} \star \mathbb{J}(\text{diag}_c) + \sum_{c \neq a} \frac{1}{2} G_{\text{diag}_{ac}}^{(4)} \star \mathbb{J}(\text{diag}_{ac}) \\
& + \sum_{\substack{c,d \neq a \\ c < d}} \frac{1}{2} G_{\text{diag}_{cd}}^{(4)} \star \mathbb{J}(\text{diag}_{cd}) + O(J^3, \bar{J}^3).
\end{aligned}$$

For an arbitrary model in rank 5 one has, up to $\mathcal{O}(J^2, \bar{J}^2)$ -terms,

$$\begin{aligned}
Y_{m_a}^{(a)}[J, \bar{J}] & \sim \sum_{q_{i_1}, \dots, q_{i_4}} G_{\text{diag}_1}^{(2)}(m_a, q_{i_1}, q_{i_2}, q_{i_3}, q_{i_4}) + \frac{1}{2} \left\{ \sum_{s=1,2} \Delta_{m_a,s} G_{\text{diag}_{1s}}^{(4)} + \sum_{c \neq a} \sum_{s=1,2} \Delta_{m_a,s} G_{\text{diag}_{cs}}^{(4)} \right. \\
& \left. + \sum_{\substack{c,d \neq a \\ c < d}} \sum_{s=1,2} \Delta_{m_a,s} G_{\text{diag}_{cds}}^{(4)} + \sum_{c \neq a} \sum_{s=1,2} \Delta_{m_a,s} G_{\text{diag}_{acs}}^{(4)} + \sum_{s=1,2} \Delta_{m_a,s} G_{\text{diag}_{cs}}^{(4)} \right\} \star \mathbb{J}(\text{diag}_1).
\end{aligned}$$

One straightforwardly gets

$$\begin{aligned}
G_{\text{diag}_1}^{(2)}(\mathbf{x}) & = \frac{1}{E_{\mathbf{x}}} + \frac{(-\lambda)}{E_{\mathbf{x}}} \left\{ \sum_{a=1}^5 \left[2 \cdot G_{\text{diag}_1}^{(2)}(\mathbf{x}) \cdot \left(\sum_{q_{i_1(a)}} \sum_{q_{i_2(a)}} \sum_{q_{i_3(a)}} \sum_{q_{i_4(a)}} G_{\text{diag}_1}^{(2)}(x_a, q_{i_1(a)}, q_{i_2(a)}, q_{i_3(a)}) \right) \right. \right. \\
& + \sum_{q_{i_1(a)}} \sum_{q_{i_2(a)}} \sum_{q_{i_3(a)}} \sum_{q_{i_4(a)}} \left(G_{\text{diag}_{1s}}^{(4)}(x_a, q_{i_1(a)}, q_{i_2(a)}, q_{i_3(a)}, q_{i_4(a)}; \mathbf{x}) \right. \\
& \quad \left. \left. + G_{\text{diag}_{1s}}^{(4)}(\mathbf{x}; x_a, q_{i_1(a)}, q_{i_2(a)}, q_{i_3(a)}, q_{i_4(a)}) \right) \right. \\
& + \sum_{c \neq a} \sum_{q_{b(a,c)}} \sum_{q_{d(a,c)}} \sum_{q_{e(a,c)}} \left(G_{\text{diag}_{bc}}^{(4)}(x_a, x_c, q_b, q_d, q_e; \mathbf{x}) + G_{\text{diag}_{bc}}^{(4)}(\mathbf{x}; x_a, x_c, q_b, q_d, q_e) \right) \\
& + \sum_{\substack{d,e \neq a \\ d < e}} \sum_{q_c} \sum_{q_b} \left(G_{\text{diag}_{bcd}}^{(4)}(x_a, x_b, x_c, q_d, q_e; \mathbf{x}) + G_{\text{diag}_{bcd}}^{(4)}(\mathbf{x}; x_a, x_b, x_c, q_d, q_e) \right) \\
& + \sum_{c \neq a} \sum_{q_c} \left(G_{\text{diag}_{acd}}^{(4)}(x_a, x_b, q_c, x_d, x_e; \mathbf{x}) + G_{\text{diag}_{acd}}^{(4)}(\mathbf{x}; x_a, x_b, q_c, x_d, x_e) \right) + 2G_{\text{diag}_{cd}}^{(4)}(\mathbf{x}; \mathbf{x}) \\
& \left. + \sum_{y_a} \frac{2}{|x_a|^2 - |y_a|^2} \left(G_{\text{diag}_1}^{(2)}(\mathbf{x}) - G_{\text{diag}_1}^{(2)}(y_a, x_{i_1(a)}, x_{i_2(a)}, x_{i_3(a)}, x_{i_4(a)}) \right) \right\}.
\end{aligned}$$

C Perturbative expansion

In this appendix, we perform a perturbative check of the SDE up to second order of the coupling constant, before and after taking the large N limit. For simplicity, we do not write the powers in N in the equations.

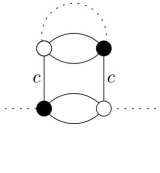
2-point function

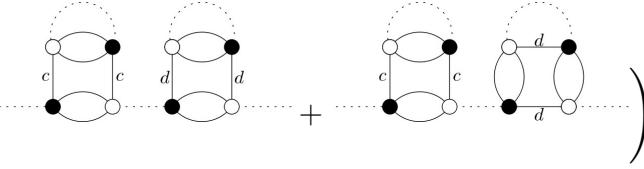
The SDE for the 2-point function is

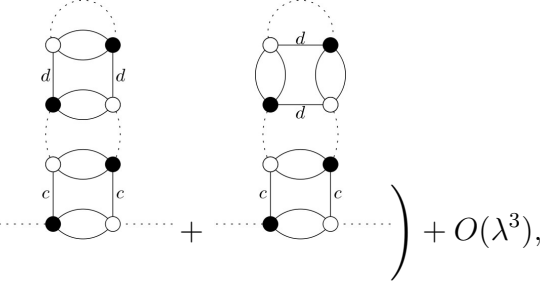
$$G^{(2)}(\mathbf{x}) = \frac{1}{1 + |\mathbf{x}|^2} - \frac{2\lambda}{1 + |\mathbf{x}|^2} \sum_c \left(\sum_{\mathbf{q}_c} G^{(2)}(\mathbf{q}_c x_c) G^{(2)}(\mathbf{x}) + G_c^{(4)}(\mathbf{x}, \mathbf{x}) \right) \quad (\text{C.1})$$

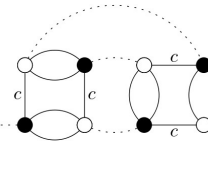
$$+ \sum_{\mathbf{q}_c} G_m^{(4)}(\mathbf{q}_c x_c, \mathbf{x}) + \sum_{q_c} \frac{1}{x_c^2 - q_c^2} (G^{(2)}(\mathbf{x}_c q_c) - G^{(2)}(\mathbf{x})) + \sum_{d \neq c} \sum_{q_c} G_d^{(4)}(\mathbf{x}, \mathbf{x}_c q_c),$$

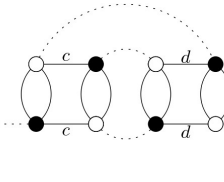
Let us look at the perturbative equation up to 2^{nd} order in the coupling constant. We can first remark that the term with $\lambda G_m^{(4)}$ will only start contributing at order λ^3 . The other terms give

$$- \frac{2\lambda}{1 + |\mathbf{x}|^2} \sum_c \sum_{\mathbf{q}_c} G^{(2)}(\mathbf{q}_c x_c) G^{(2)}(\mathbf{x}) = 2 \sum_{c=1}^3 \dots \quad (\text{C.2})$$


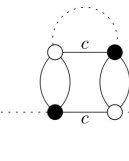
$$+ 4 \sum_{c=1}^3 \sum_{d=1}^3 \left(\dots + \dots \right)$$


$$+ 4 \sum_{c=1}^3 \sum_{d=1}^3 \left(\dots + \dots \right) + O(\lambda^3),$$


$$- \frac{2\lambda}{1 + |\mathbf{x}|^2} \sum_c G_c^{(4)}(\mathbf{x}, \mathbf{x}) = 4 \sum_{c=1}^3 \dots + O(\lambda^3), \quad (\text{C.3})$$


$$- \frac{2\lambda}{1 + |\mathbf{x}|^2} \sum_{c=1}^3 \sum_{c \neq d} \sum_{q_c} G_d^{(4)}(\mathbf{x}, \mathbf{x}_c q_c) = 4 \sum_{c=1}^3 \sum_{c \neq d} \dots + O(\lambda^3), \quad (\text{C.4})$$


It is more involved to obtain the perturbative expansion from the difference of 2-point functions. At first order, we have

$$- \frac{2\lambda}{1 + |\mathbf{x}|^2} \sum_{c=1}^3 \sum_{q_c} \frac{1}{x_c^2 - q_c^2} (G^{(2)}(\mathbf{x}_c q_c) - G^{(2)}(\mathbf{x})) = 2 \sum_c \dots + O(\lambda^2). \quad (\text{C.5})$$


We are going to take the example of $c = 1$ and compute explicitly the diagrams at 2nd order in the coupling constant.

$$\begin{aligned}
& - \frac{2\lambda}{1 + |\mathbf{x}|^2} \sum_{a_1} \frac{1}{x_1^2 - a_1^2} \left(G^{(2)}(a_1, x_2, x_3) - G^{(2)}(\mathbf{x}) \right) \Big|_{\lambda^2} = \tag{C.6} \\
& \frac{4\lambda^2}{1 + |\mathbf{x}|^2} \sum_{a_1} \frac{1}{x_1^2 - a_1^2} \left\{ \frac{1}{(1 + a_1^2 + x_2^2 + x_3^2)^2} \left[\sum_{b_1, b_2} \frac{1}{1 + b_1^2 + b_2^2 + x_3^2} + \sum_{b_1, b_3} \frac{1}{1 + b_1^2 + x_2^2 + b_3^2} \right. \right. \\
& + \sum_{b_2, b_3} \frac{1}{1 + a_1^2 + b_2^2 + b_3^2} + \sum_{b_1} \frac{1}{1 + b_1^2 + x_2^2 + x_3^2} + \sum_{b_2} \frac{1}{1 + a_1^2 + b_2^2 + x_3^2} \\
& + \left. \sum_{b_3} \frac{1}{1 + a_1^2 + x_2^2 + b_3^2} \right] - \frac{1}{(1 + |\mathbf{x}|^2)^2} \left[\sum_{b_1, b_2} \frac{1}{1 + b_1^2 + b_2^2 + x_3^2} + \sum_{b_1, b_3} \frac{1}{1 + b_1^2 + x_2^2 + b_3^2} \right. \\
& + \sum_{b_2, b_3} \frac{1}{1 + x_1^2 + b_2^2 + b_3^2} + \sum_{b_1} \frac{1}{1 + b_1^2 + x_2^2 + x_3^2} + \sum_{b_2} \frac{1}{1 + x_1^2 + b_2^2 + x_3^2} \\
& \left. + \sum_{b_3} \frac{1}{1 + x_1^2 + x_2^2 + b_3^2} \right] \Big\}.
\end{aligned}$$

Half of the terms are straightforward to combine, let us look first at

$$\begin{aligned}
& \frac{4\lambda^2}{1 + |\mathbf{x}|^2} \sum_{b_1} \frac{1}{1 + b_1^2 + x_2^2 + x_3^2} \sum_{a_1} \frac{1}{a_1^2 - x_1^2} \left(\frac{1}{(1 + |\mathbf{x}|^2)^2} - \frac{1}{(1 + a_1^2 + x_2^2 + x_3^2)^2} \right) \tag{C.7} \\
& = \frac{4\lambda^2}{(1 + |\mathbf{x}|^2)^2} \sum_{a_1, b_1} \frac{1}{(1 + b_1^2 + x_2^2 + x_3^2)(1 + a_1^2 + x_2^2 + x_3^2)} \left(\frac{1}{|\mathbf{x}|^2} + \frac{1}{1 + a_1^2 + x_2^2 + x_3^2} \right)
\end{aligned}$$

$$= 2 \cdot \text{diagram 1} + 2 \cdot \text{diagram 2} \tag{C.8}$$

And combining the terms with sums on b_1, b_2 and b_1, b_3 gives

$$= 4 \cdot \text{diagram 3} + 4 \cdot \text{diagram 4} \tag{C.9}$$

Now let us look at the two terms

$$\frac{4\lambda^2}{1 + |\mathbf{x}|^2} \sum_{a_1} \frac{1}{a_1^2 - x_1^2} \left(\frac{1}{(1 + |\mathbf{x}|^2)^2} \sum_{b_2, b_3} \frac{1}{1 + x_1^2 + b_2^2 + b_3^2} \right)$$

$$- \frac{1}{(1 + a_1^2 + x_2^2 + x_3^2)^2} \sum_{b_2, b_3} \frac{1}{1 + a_1^2 + b_2^2 + b_3^2} \Big), \quad (\text{C.10})$$

and compute

$$\begin{aligned} & (1 + a_1^2 + x_2^2 + x_3^2)^2(1 + a_1^2 + b_2^2 + b_3^2) - (1 + |\mathbf{x}|^2)^2(1 + x_1^2 + b_2^2 + b_3^2) = \\ & a_1^6 - x_1^6 + (a_1^4 - x_1^4)(1 + b_2^2 + b_3^2 + 2(1 + x_2^2 + x_3^2)) \\ & + (a_1^2 - x_1^2)(1 + x_2^2 + x_3^2)(1 + x_2^2 + x_3^2 + 2(1 + b_2^2 + b_3^2)). \end{aligned} \quad (\text{C.11})$$

By writing

$$a_1^6 - x_1^6 = (a_1^2 - x_1^2)(a_1^4 + x_1^4) + x_1^2 a_1^4 - x_1^4 a_1^2 = (a_1^2 - x_1^2)(a_1^4 + x_1^4 + a_1^2 x_1^2), \quad (\text{C.12})$$

$$(a_1^4 - x_1^4) = (a_1^2 - x_1^2)(a_1^2 + x_1^2), \quad (\text{C.13})$$

we get

$$\frac{4\lambda^2}{1 + |\mathbf{x}|^2} \sum_{a_1, b_2, b_3} \frac{a_1^4 + x_1^4 + a_1^2 x_1^2 + (1 + b_2^2 + b_3^2 + 2(1 + x_2^2 + x_3^2))(a_1^2 + x_1^2) + (1 + x_2^2 + x_3^2)(1 + x_2^2 + x_3^2 + 2(1 + b_2^2 + b_3^2))}{(1 + |\mathbf{x}|^2)^2(1 + x_1^2 + b_2^2 + b_3^2)(1 + a_1^2 + x_2^2 + x_3^2)^2(1 + a_1^2 + b_2^2 + b_3^2)}. \quad (\text{C.14})$$

Now we can factorise

$$\begin{aligned} & a_1^4 + x_1^4 + a_1^2 x_1^2 + (1 + b_2^2 + b_3^2 + 2(1 + x_2^2 + x_3^2))(a_1^2 + x_1^2) \\ & + (1 + x_2^2 + x_3^2)(1 + x_2^2 + x_3^2 + 2(1 + b_2^2 + b_3^2)) \\ & = (1 + |\mathbf{x}|^2)(1 + a_1^2 + x_2^2 + x_3^2) + (1 + a_1^2 + x_2^2 + x_3^2)(1 + a_1^2 + b_2^2 + b_3^2) \\ & + (1 + |\mathbf{x}|^2)(1 + x_1^2 + b_2^2 + b_3^2), \end{aligned} \quad (\text{C.15})$$

which gives

$$\begin{aligned} & \frac{4\lambda^2}{1 + |\mathbf{x}|^2} \sum_{a_1, b_2, b_3} \left(\frac{1}{(1 + |\mathbf{x}|^2)(1 + x_1^2 + b_2^2 + b_3^2)(1 + a_1^2 + x_2^2 + x_3^2)(1 + a_1^2 + b_2^2 + b_3^2)} \right. \\ & + \frac{1}{(1 + |\mathbf{x}|^2)^2(1 + x_1^2 + b_2^2 + b_3^2)(1 + a_1^2 + x_2^2 + x_3^2)} \\ & \left. + \frac{1}{(1 + |\mathbf{x}|^2)(1 + a_1^2 + x_2^2 + x_3^2)^2(1 + a_1^2 + b_2^2 + b_3^2)} \right) \\ & = 4 \dots + 4 \dots + 4 \dots \end{aligned} \quad (\text{C.16})$$

Then by combining the terms with a sum on b_2 or on b_3 , we get an analogous result which correspond to replace b_3 by x_3 or b_2 by x_2 in the previous equation. And we obtain the

following diagrams

$$4 \dots + 4 \dots + 4 \dots \quad (\text{C.17})$$

This computation is completely analogous for $c = 2, 3$. Collecting all the diagrams we get

$$G^{(2)}(\mathbf{x}) = \dots + \sum_{c=1}^3 \left\{ 2 \dots + 2 \dots \right. \quad (\text{C.18})$$

$$+ \sum_{d=1}^3 \left[4 \dots + 4 \dots + 8 \dots \right.$$

$$+ 4 \dots + 4 \dots + 4 \dots + 4 \dots$$

$$+ 4 \dots \left. \right\} + O(\lambda^3).$$

Once we take the large N limit, we get the following expansion and SDE

$$G^{(2)}(\mathbf{x}) = \dots + \sum_{c=1}^3 \left\{ 2 \dots \right.$$

$$+ 4 \sum_{d=1}^3 \left[\dots + \dots \right] \left. \right\} + O(\lambda^3)$$

$$= \left(1 + |\mathbf{x}|^2 + 2\lambda \sum_{c=1}^3 \int d\mathbf{q}_c G^{(2)}(\mathbf{q}_c x_c) \right)^{-1}. \quad (\text{C.19})$$

4-point function with connected boundary

The full SDE for the 4-point function is

$$\begin{aligned}
G_1^{(4)}(\mathbf{x}, \mathbf{y}) = & -\frac{2\lambda}{1+x_1^2+y_2^2+y_3^2} \left\{ \sum_{c=1}^3 f_c(\mathbf{x}, \mathbf{y}; s_c; V_c) + \sum_{c=1}^3 \sum_{\mathbf{q}_c} G^{(2)}(\mathbf{q}_c s_c) G_1^{(4)}(\mathbf{x}, \mathbf{y}) \right. \\
& + \sum_{b_1} \frac{1}{b_1^2 - x_1^2} \left(G_1^{(4)}(\mathbf{x}, \mathbf{y}) - G_1^{(4)}(b_1, x_2, x_3, \mathbf{y}) \right) \\
& + \sum_{b_2} \frac{1}{b_2^2 - y_2^2} \left(G_1^{(4)}(\mathbf{x}, \mathbf{y}) - G_1^{(4)}(\mathbf{x}, y_1, b_2, y_3) \right) \\
& + \sum_{b_3} \frac{1}{b_3^2 - y_3^2} \left(G_1^{(4)}(\mathbf{x}, \mathbf{y}) - G_1^{(4)}(\mathbf{x}, y_1, y_2, b_3) \right) \\
& + \frac{1}{y_2^2 - x_2^2} \left(G_3^{(4)}(\mathbf{x}, y_1, x_2, y_3) - G_3^{(4)}(\mathbf{x}, \mathbf{y}) \right) \\
& + \frac{1}{y_3^2 - x_3^2} \left(G_2^{(4)}(\mathbf{x}, y_1, y_2, x_3) - G_2^{(4)}(\mathbf{x}, \mathbf{y}) \right) + \frac{G^{(2)}(\mathbf{y})}{y_1^2 - x_1^2} \left(G^{(2)}(\mathbf{x}) - G^{(2)}(y_1, x_2, x_3) \right) \\
& \left. + \frac{1}{y_1^2 - x_1^2} \left(G_m^{(4)}(\mathbf{x}, \mathbf{y}) - G_m^{(4)}(y_1, x_2, x_3, \mathbf{y}) \right) \right\}, \tag{C.20}
\end{aligned}$$

where $\mathbf{s} = (x_1, y_2, y_3)$. We can remark that the terms in λf_c involve only 6-point functions and start to contribute to the perturbative expansion only at order λ^3 , and so does the terms in $\lambda G_m^{(4)}$. Hence up to the 2nd order in the coupling constant the other terms give

$$\begin{aligned}
\sum_{d=1}^3 \sum_{\mathbf{q}_d} G^{(2)}(\mathbf{q}_d s_d) G_1^{(4)}(\mathbf{x}, \mathbf{y}) = & 4 \sum_{d=1}^3 \text{diagram} + O(\lambda^3), \tag{C.21} \\
-\frac{2\lambda}{1+x_1^2+y_2^2+y_3^2} G^{(2)}(\mathbf{y}) \frac{G^{(2)}(\mathbf{x}) - G^{(2)}(y_1, x_2, x_3)}{y_1^2 - x_1^2} = & 2 \text{diagram} + 4 \text{diagram} \\
+ 4 \text{diagram} + 4 \sum_{d=1}^3 \left(\text{diagram} + \text{diagram} \right) & \\
+ \text{diagram} + \text{diagram} + \text{diagram} &
\end{aligned}$$

$$\left. \begin{aligned}
& + \text{diagram 1} + \text{diagram 2} + \text{diagram 3} \\
& + \text{diagram 4} + \text{diagram 5} + \text{diagram 6}
\end{aligned} \right) + O(\lambda^3). \tag{C.26}$$

After taking the large N limit, we get the following SDE and perturbative expansion

$$\begin{aligned}
G_1^{(4)}(\mathbf{x}, \mathbf{y}) &= -\frac{2\lambda}{1 + x_1^2 + y_2^2 + y_3^2} \left(\sum_{c=1}^3 \int d\mathbf{q}_{\hat{c}} G^{(2)}(\mathbf{q}_{\hat{c}} s_c) G_1^{(4)}(\mathbf{x}, \mathbf{y}) \right. \\
&\quad \left. + G^{(2)}(\mathbf{y}) \frac{G^{(2)}(\mathbf{x}) - G^{(2)}(y_1, x_2, x_3)}{y_1^2 - x_1^2} \right)
\end{aligned}$$

$$\begin{aligned}
& = 2 \text{diagram} + 4 \text{diagram} + 4 \sum_{d=1}^3 \left(\text{diagram} \right. \\
& + \text{diagram} + \text{diagram} + \text{diagram} \left. \right) + O(\lambda^3). \tag{C.27}
\end{aligned}$$

4-point function with disconnected boundary

The SDE for the 4-point function with a disconnected boundary graph is

$$\begin{aligned}
G_m^{(4)}(\mathbf{x}, \mathbf{y}) &= -\frac{2\lambda}{1 + |\mathbf{x}|^2} \sum_{c=1}^3 \left\{ \sum_{\mathbf{q}_{\hat{c}}} G^{(2)}(\mathbf{q}_{\hat{c}} x_c) G_m^{(4)}(\mathbf{x}, \mathbf{y}) + \mathfrak{f}_{m|m, x_c}^{(c)}(\mathbf{x}, \mathbf{y}) + \mathfrak{f}_{m|m, x_c}^{(c)}(\mathbf{y}, \mathbf{x}) \right. \\
&\quad + \sum_{b_c} \frac{1}{b_c^2 - x_c^2} (G_m^{(4)}(\mathbf{x}, \mathbf{y}) - G_m^{(4)}(\mathbf{x}_{\hat{c}} b_c, \mathbf{y})) + \frac{1}{y_c^2 - x_c^2} (G_c^{(4)}(\mathbf{x}, \mathbf{y}) - G_c^{(4)}(\mathbf{x}_{\hat{c}} y_c, \mathbf{y})) \\
&\quad \left. + G^{(2)}(\mathbf{x}) \left(G_c^{(4)}(\mathbf{y}_{\hat{c}} x_c, \mathbf{y}) + \sum_{d \neq c} \sum_{\substack{q_b \\ b \neq c, d}} G_d^{(4)}(x_c, q_b, y_d, \mathbf{y}) + \sum_{\mathbf{q}_{\hat{c}}} G_m^{(4)}(\mathbf{q}_{\hat{c}} x_c, \mathbf{y}) \right) \right\}, \tag{C.28}
\end{aligned}$$

where (x_c, q_b, y_d) with $\{b, c, d\} = \{1, 2, 3\}$ is implicitly reordered. Let us again check the perturbative expansion up to 2nd order in the coupling constant. We can note that the first graphs appearing in $G_m^{(4)}$ are of order λ^2 , hence all terms in the SDE involving $\lambda G_m^{(4)}$ will start to contribute only at order λ^3 , and the same goes for the terms $\lambda \mathbf{f}_{|m}$. The other terms give

$$-\frac{2\lambda}{1+|\mathbf{x}|^2} G^{(2)}(\mathbf{x}) \sum_{c=1}^3 G_c^{(4)}(\mathbf{y}_{\hat{c}} x_c, \mathbf{y}) = 4 \sum_{c=1}^3 \left(\text{diagram 1} + \text{diagram 2} \right) + O(\lambda^3), \quad (\text{C.29})$$

$$-\frac{2\lambda}{1+|\mathbf{x}|^2} G^{(2)}(\mathbf{x}) \sum_{c=1}^3 \sum_{d \neq c} \sum_{\substack{q_b \\ b \neq c, d}} G_d^{(4)}(x_c, q_b, y_d, \mathbf{y}) = 4 \sum_{c=1}^3 \sum_{d \neq c} \left(\text{diagram 3} + \text{diagram 4} \right) + O(\lambda^3), \quad (\text{C.30})$$

$$-\frac{2\lambda}{1+|\mathbf{x}|^2} \sum_{c=1}^3 \frac{G_c^{(4)}(\mathbf{x}, \mathbf{y}) - G_c^{(4)}(\mathbf{x}_{\hat{c}} y_c, \mathbf{y})}{y_c^2 - x_c^2} \quad (\text{C.31})$$

$$= 4 \sum_{c=1}^3 \left(\text{diagram 5} + \text{diagram 6} \right) + O(\lambda^3).$$

In the large N limit, only one of these graphs survives and the SDE becomes

$$\begin{aligned} G_m^{(4)}(\mathbf{x}, \mathbf{y}) &= 4 \sum_{c=1}^3 \sum_{d \neq c} \left(\text{diagram 7} \right) + O(\lambda^3) \quad (\text{C.32}) \\ &= -\frac{2\lambda}{1+|\mathbf{x}|^2} \sum_{c=1}^3 \left\{ \int d\mathbf{q}_{\hat{c}} G^{(2)}(\mathbf{q}_{\hat{c}} x_c) G_m^{(4)}(\mathbf{x}, \mathbf{y}) \right. \\ &\quad \left. + G^{(2)}(\mathbf{x}) \left(\sum_{d \neq c} \int d\mathbf{q}_b G_d^{(4)}(x_c, q_b, y_d, \mathbf{y}) + \int d\mathbf{q}_{\hat{c}} G_m^{(4)}(\mathbf{q}_{\hat{c}} x_c, \mathbf{y}) \right) \right\}. \end{aligned}$$

D Recurrence relations

In this appendix, we will use the recursive equation (2.6.2) to determine recurrence relations on the numbers $a_{n,k,m}$. We first perform the integration

$$\int d\mathbf{q}_{\hat{1}} G_p^{(2)}(\mathbf{q}_{\hat{1}} x_1) = -\frac{\pi}{4} \log(1+x_1^2) \quad \text{if } p=0, \quad (\text{D.1})$$

$$= \left(\frac{\pi}{2} \right)^{p+1} \left(\frac{\log^p(1+x_1^2)}{2p(1+x_1^2)^p} + \frac{(-1)^p}{2(1+x_1^2)^p} \sum_{r=1}^{p-1} (-1)^r \log^r(1+x_1^2) \sum_{m=1}^r \frac{a_{p,r,m}}{m} \right) \quad \text{if } p > 0, \quad (\text{D.2})$$

where for $p = 1$ the sum on r does not appear. Plugging back the ansatz (2.6.10) in the recurrence relation (2.6.2) with $c = 1$ gives

$$\begin{aligned} G_n^{(2)}(\mathbf{x}) = & -\frac{2}{|\mathbf{x}|^2 + 1} \left\{ -\frac{\pi}{4} \log(1 + x_1^2) G_{n-1}^{(2)}(\mathbf{x}) + \sum_{p=1}^{n-1} \left(\frac{\pi}{2}\right)^{p+1} \frac{\log^p(1 + x_1^2)}{2p(1 + x_1^2)^p} G_{n-p-1}^{(2)}(\mathbf{x}) \right. \\ & \left. + \sum_{p=2}^{n-1} \left(\frac{\pi}{2}\right)^{p+1} \left(\frac{(-1)^p}{2(1 + x_1^2)^p} \sum_{r=1}^{p-1} (-1)^r \log^r(1 + x_1^2) \sum_{m=1}^r \frac{a_{p,r,m}}{m} \right) G_{n-p-1}^{(2)}(\mathbf{x}) \right\}. \end{aligned} \quad (\text{D.3})$$

The first term of (D.3) gives

$$\begin{aligned} & \frac{\pi \log(1 + x_1^2)}{2(|\mathbf{x}|^2 + 1)} \left(\frac{\pi}{2}\right)^{n-1} \left(\frac{\log^{n-1}(1 + x_1^2)}{(1 + |\mathbf{x}|^2)^n} \right) \\ & + \frac{(-1)^{n-1}}{(1 + x_1^2)^{n-1}} \sum_{k=1}^{n-2} (-1)^k \log^k(1 + x_1^2) \sum_{m=1}^k a_{n-1,k,m} \frac{(1 + x_1^2)^m}{(1 + |\mathbf{x}|^2)^{m+1}} \\ & = \left(\frac{\pi}{2}\right)^n \left(\frac{\log^n(1 + x_1^2)}{(1 + |\mathbf{x}|^2)^{n+1}} + \frac{(-1)^{n-1}}{(1 + x_1^2)^{n-1}} \sum_{k=1}^{n-2} (-1)^k \log^{k+1}(1 + x_1^2) \sum_{m=1}^k a_{n-1,k,m} \frac{(1 + x_1^2)^m}{(1 + |\mathbf{x}|^2)^{m+2}} \right) \\ & = \left(\frac{\pi}{2}\right)^n \left(\frac{\log^n(1 + x_1^2)}{(1 + |\mathbf{x}|^2)^{n+1}} + \frac{(-1)^n}{(1 + x_1^2)^n} \sum_{k=2}^{n-1} (-1)^k \log^k(1 + x_1^2) \sum_{m=2}^k a_{n-1,k-1,m-1} \frac{(1 + x_1^2)^m}{(1 + |\mathbf{x}|^2)^{m+1}} \right), \end{aligned} \quad (\text{D.4})$$

where we sent $k \rightarrow k + 1$ and $m \rightarrow m + 1$ to get to the last line. The second term of (D.3) gives

$$\begin{aligned} & -\frac{2}{|\mathbf{x}|^2 + 1} \left(\sum_{p=1}^{n-1} \left(\frac{\pi}{2}\right)^{p+1} \frac{\log^p(1 + x_1^2)}{2p(1 + x_1^2)^p} \left(\frac{\pi}{2}\right)^{n-p-1} \frac{\log^{n-p-1}(1 + x_1^2)}{(1 + |\mathbf{x}|^2)^{n-p}} \right. \\ & + \sum_{p=1}^{n-3} \left(\frac{\pi}{2}\right)^{p+1} \frac{\log^p(1 + x_1^2)}{2p(1 + x_1^2)^p} \left(\frac{\pi}{2}\right)^{n-p-1} \frac{(-1)^{n-p-1}}{(1 + x_1^2)^{n-p-1}} \\ & \left. \sum_{k=1}^{n-p-2} (-1)^k \log^k(1 + x_1^2) \sum_{m=1}^k a_{n-p-1,k,m} \frac{(1 + x_1^2)^m}{(1 + |\mathbf{x}|^2)^{m+1}} \right) \\ & = -\left(\frac{\pi}{2}\right)^n \frac{\log^{n-1}(1 + x_1^2)}{(1 + x_1^2)^n} \sum_{p=1}^{n-1} \frac{1}{p} \frac{(1 + x_1^2)^{n-p}}{(1 + |\mathbf{x}|^2)^{n-p+1}} \\ & + \left(\frac{\pi}{2}\right)^n \frac{(-1)^n}{(1 + x_1^2)^n} \sum_{p=1}^{n-3} \sum_{k=1}^{n-p-2} (-1)^{k-p} \log^{p+k}(1 + x_1^2) \sum_{m=1}^k \frac{a_{n-p-1,k,m}}{p} \frac{(1 + x_1^2)^{m+1}}{(1 + |\mathbf{x}|^2)^{m+2}}. \end{aligned} \quad (\text{D.5})$$

Setting $r = p + k$ in the line of the previous equation, let us rewrite the double sum as

$$\sum_{k=1}^{n-3} \sum_{r=k+1}^{n-2} \frac{(-1)^r}{r-k} \log^r(1 + x_1^2) a_{n-r+k-1,k,m} = \sum_{r=2}^{n-2} \sum_{k=1}^{r-1} \frac{(-1)^r}{r-k} \log^r(1 + x_1^2) a_{n-r+k-1,k,m}. \quad (\text{D.6})$$

Then we send $m \rightarrow m + 1$ and rewrite double sum to get

$$\sum_{k=1}^{r-1} \sum_{m=2}^{k+1} \frac{a_{n-r+k-1,k,m-1}}{r-k} \frac{(1+x_1^2)^m}{(1+|\mathbf{x}|^2)^{m+1}} = \sum_{m=2}^r \sum_{k=m-1}^{r-1} \frac{a_{n-r+k-1,k,m-1}}{r-k} \frac{(1+x_1^2)^m}{(1+|\mathbf{x}|^2)^{m+1}}. \quad (\text{D.7})$$

Hence, sending $p \rightarrow n - p$ and collecting the results we get

$$\begin{aligned} & - \left(\frac{\pi}{2}\right)^n \frac{\log^{n-1}(1+x_1^2)}{(1+x_1^2)^n} \sum_{p=1}^{n-1} \frac{1}{n-p} \frac{(1+x_1^2)^p}{(1+|\mathbf{x}|^2)^{p+1}} \\ & + \left(\frac{\pi}{2}\right)^n \frac{(-1)^n}{(1+x_1^2)^n} \sum_{r=2}^{n-2} (-1)^r \log^r(1+x_1^2) \sum_{m=2}^r \sum_{k=m-1}^{r-1} \frac{a_{n-1+k-r,k,m-1}}{r-k} \frac{(1+x_1^2)^m}{(1+|\mathbf{x}|^2)^{m+1}}. \end{aligned} \quad (\text{D.8})$$

The third term of (D.3) gives

$$\begin{aligned} & - \frac{2}{|\mathbf{x}|^2 + 1} \left\{ \sum_{p=2}^{n-1} \left(\frac{\pi}{2}\right)^{p+1} \left(\frac{(-1)^p}{2(1+x_1^2)^p} \sum_{r=1}^{p-1} (-1)^r \log^r(1+x_1^2) \sum_{m=1}^r \frac{a_{p,r,m}}{m} \right) \right. \\ & \left. \left(\frac{\pi}{2}\right)^{n-p-1} \frac{\log^{n-p-1}(1+x_1^2)}{(1+|\mathbf{x}|^2)^{n-p}} + \sum_{p=2}^{n-3} \left(\frac{\pi}{2}\right)^{p+1} \left(\frac{(-1)^p}{2(1+x_1^2)^p} \sum_{r=1}^{p-1} (-1)^r \log^r(1+x_1^2) \sum_{m=1}^r \frac{a_{p,r,m}}{m} \right) \right. \\ & \left. \left(\frac{\pi}{2}\right)^{n-p-1} \frac{(-1)^{n-p-1}}{(1+x_1^2)^{n-p-1}} \sum_{k=1}^{n-p-2} (-1)^k \log^k(1+x_1^2) \sum_{l=1}^k a_{n-p-1,k,l} \frac{(1+x_1^2)^l}{(1+|\mathbf{x}|^2)^{l+1}} \right\}. \end{aligned} \quad (\text{D.9})$$

The first term of equation (D.9) gives

$$\begin{aligned} & - \left(\frac{\pi}{2}\right)^n \sum_{p=2}^{n-1} \sum_{r=1}^{p-1} (-1)^{p+r} \frac{\log^{n-p+r-1}(1+x_1^2)}{(1+x_1^2)^n} \sum_{m=1}^r \frac{a_{p,r,m}}{m} \frac{(1+x_1^2)^{n-p}}{(1+|\mathbf{x}|^2)^{n-p+1}} \\ & = - \left(\frac{\pi}{2}\right)^n \sum_{r=1}^{n-2} \sum_{k=1}^{n-1-r} (-1)^k \frac{\log^{n-k-1}(1+x_1^2)}{(1+x_1^2)^n} \sum_{m=1}^r \frac{a_{r+k,r,m}}{m} \frac{(1+x_1^2)^{n-r-k}}{(1+|\mathbf{x}|^2)^{n-r-k+1}}, \end{aligned} \quad (\text{D.10})$$

by setting $k = p - r$. Then by setting $l = n - 1 - k$ and rewriting the sums we get

$$\begin{aligned} & \left(\frac{\pi}{2}\right)^n \frac{(-1)^n}{(1+x_1^2)^n} \sum_{r=1}^{n-2} \sum_{l=r}^{n-2} (-1)^l \log^l(1+x_1^2) \sum_{m=1}^r \frac{a_{n-1+r-l,r,m}}{m} \frac{(1+x_1^2)^{l-r+1}}{(1+|\mathbf{x}|^2)^{l-r+2}} \\ & = \left(\frac{\pi}{2}\right)^n \frac{(-1)^n}{(1+x_1^2)^n} \sum_{l=1}^{n-2} (-1)^l \log^l(1+x_1^2) \sum_{r=1}^l \sum_{m=1}^r \frac{a_{n-1+r-l,r,m}}{m} \frac{(1+x_1^2)^{l-r+1}}{(1+|\mathbf{x}|^2)^{l-r+2}}. \end{aligned} \quad (\text{D.11})$$

Then we set $k = l - r + 1$ and obtain

$$\left(\frac{\pi}{2}\right)^n \frac{(-1)^n}{(1+x_1^2)^n} \sum_{l=1}^{n-2} (-1)^l \log^l(1+x_1^2) \sum_{k=1}^l \sum_{m=1}^{l-k+1} \frac{a_{n-k,l-k+1,m}}{m} \frac{(1+x_1^2)^k}{(1+|\mathbf{x}|^2)^{k+1}}. \quad (\text{D.12})$$

The second term of (D.9) gives, by rewriting the sums,

$$\left(\frac{\pi}{2}\right)^n \frac{(-1)^n}{(1+x_1^2)^n} \sum_{p=2}^{n-3} \sum_{k=1}^{n-p-2} \sum_{r=1}^{p-1} (-1)^{k+r} \log^{k+r}(1+x_1^2) \sum_{l=1}^k \sum_{m=1}^r \frac{a_{p,r,m}}{m} a_{n-p-1,k,l} \frac{(1+x_1^2)^{l+1}}{(1+|\mathbf{x}|^2)^{l+2}}$$

$$= \left(\frac{\pi}{2}\right)^n \frac{(-1)^n}{(1+x_1^2)^n} \sum_{r=1}^{n-4} \sum_{k=1}^{n-3-r} (-1)^{k+r} \log^{r+k}(1+x_1^2) \sum_{l=1}^k \sum_{m=1}^r \sum_{p=r+1}^{n-2-k} \frac{a_{p,r,m}}{m} a_{n-p-1,k,l} \frac{(1+x_1^2)^{l+1}}{(1+|\mathbf{x}|^2)^{l+2}}. \quad (\text{D.13})$$

First by setting $q = k + r$ and by several rewriting of the sums we get

$$\begin{aligned} & \left(\frac{\pi}{2}\right)^n \frac{(-1)^n}{(1+x_1^2)^n} \sum_{k=1}^{n-4} \sum_{q=k+1}^{n-3} (-1)^q \log^q(1+x_1^2) \sum_{l=1}^k \sum_{m=1}^{q-k} \sum_{p=q-k+1}^{n-2-k} \frac{a_{p,q-k,m}}{m} a_{n-p-1,k,l} \frac{(1+x_1^2)^{l+1}}{(1+|\mathbf{x}|^2)^{l+2}} \\ &= \left(\frac{\pi}{2}\right)^n \frac{(-1)^n}{(1+x_1^2)^n} \sum_{q=2}^{n-3} (-1)^q \log^q(1+x_1^2) \sum_{k=1}^{q-1} \sum_{l=1}^k \sum_{m=1}^{q-k} \sum_{p=q-k+1}^{n-2-k} \frac{a_{p,q-k,m}}{m} a_{n-p-1,k,l} \frac{(1+x_1^2)^{l+1}}{(1+|\mathbf{x}|^2)^{l+2}} \\ &= \left(\frac{\pi}{2}\right)^n \frac{(-1)^n}{(1+x_1^2)^n} \sum_{q=2}^{n-3} (-1)^q \log^q(1+x_1^2) \sum_{l=1}^{q-1} \sum_{k=l}^{q-1} \sum_{m=1}^{q-k} \sum_{p=q-k+1}^{n-2-k} \frac{a_{p,q-k,m}}{m} a_{n-p-1,k,l} \frac{(1+x_1^2)^{l+1}}{(1+|\mathbf{x}|^2)^{l+2}} \\ &= \left(\frac{\pi}{2}\right)^n \frac{(-1)^n}{(1+x_1^2)^n} \sum_{q=2}^{n-3} (-1)^q \log^q(1+x_1^2) \sum_{l=2}^q \sum_{k=l-1}^{q-1} \sum_{m=1}^{q-k} \sum_{p=q-k+1}^{n-2-k} \frac{a_{p,q-k,m}}{m} a_{n-p-1,k,l-1} \frac{(1+x_1^2)^l}{(1+|\mathbf{x}|^2)^{l+1}}, \end{aligned} \quad (\text{D.14})$$

where we send $l \rightarrow l + 1$ in the last line.

Now collecting all the results we obtain recurrence relations on $a_{n,k,m}$:

$$a_{n,1,1} = a_{n-1,1,1}, \quad (\text{D.15})$$

$$a_{n,n-1,1} = \frac{1}{n-1}, \quad (\text{D.16})$$

$$a_{n,n-1,m} = \frac{1}{n-m} + a_{n-1,n-2,m-1}, \quad \text{for } m \in \llbracket 2, n-1 \rrbracket, \quad (\text{D.17})$$

$$a_{n,n-2,m} = a_{n-1,n-3,m-1} + \sum_{r=m-1}^{n-3} \frac{a_{r+1,r,m-1}}{n-2-r} + \sum_{l=1}^{n-1-m} \frac{a_{n-m,n-1-m,l}}{l}, \quad (\text{D.18})$$

for $m \in \llbracket 2, n-2 \rrbracket$,

$$a_{n,k,1} = \sum_{l=1}^k \frac{a_{n-1,k,l}}{l}, \quad \text{for } k \in \llbracket 1, n-3 \rrbracket, \quad (\text{D.19})$$

$$\begin{aligned} a_{n,k,m} &= a_{n-1,k-1,m-1} + \sum_{r=m-1}^{k-1} \frac{a_{n-1+r-k,r,m-1}}{k-r} + \sum_{l=1}^{k-m+1} \frac{a_{n-m,k-m+1,l}}{l} \\ &+ \sum_{r=m-1}^{k-1} \sum_{l=1}^{k-r} \sum_{p=k-r+1}^{n-2-r} \frac{a_{p,k-r,l} a_{n-p-1,r,m-1}}{l}, \quad \text{for } k \in \llbracket 2, n-3 \rrbracket \text{ and } m \in \llbracket 2, k \rrbracket. \end{aligned} \quad (\text{D.20})$$

Rewriting these equations gives explicit relations on Stirling numbers of the first kind, harmonic numbers and binomial coefficients. Indeed, from equation (D.19) we recover

$$\frac{1}{(n-1)!} \begin{bmatrix} n-1 \\ n-k \end{bmatrix} = \sum_{l=1}^k \frac{1}{(n-l)!} \begin{bmatrix} n-1-l \\ n-1-k \end{bmatrix}, \quad \text{for } k \in \llbracket 1, n-3 \rrbracket, \quad (\text{D.21})$$

which correspond to the equation (6.21) in [106]. Setting $l = n - 2 - r$, $k = n - m - 1$ and sending $n - 3 \rightarrow n$, equation (D.18) gives

$$H_k = \frac{k+1}{2n+3-k} \sum_{l=1}^k \frac{n+1-k+l}{l(k+1-l)}, \quad \text{for } k \in \llbracket 1, n \rrbracket. \quad (\text{D.22})$$

Sending $r \rightarrow k - l$ and in the last term $l \rightarrow r$ of equation (D.20), we get

$$\begin{aligned} & ((n-1)m - k(m-1)) \frac{(n-2)!}{k!(n-m)!} \begin{bmatrix} n-m \\ n-k \end{bmatrix} \\ &= \sum_{l=1}^{k-m+1} \frac{1}{(n-m-l)!} \begin{bmatrix} n-m-l \\ n-k-1 \end{bmatrix} \left(\frac{(n-1-m)!}{(k-m+1)!} + \frac{m-1}{l} \frac{(n-l-2)!}{(k-l)!} \right) \\ &+ \sum_{l=1}^{k-m+1} \frac{m-1}{l!(k-l)!} \sum_{p=l+1}^{n-2-k+l} \frac{(p-1)!(n-2-p)!}{(n-m-p)!} \begin{bmatrix} n-m-p \\ n-k-1-p+l \end{bmatrix} \sum_{r=1}^l \frac{1}{(p-r)!} \begin{bmatrix} p-r \\ p-l \end{bmatrix}, \end{aligned} \quad (\text{D.23})$$

for $k \in \llbracket 2, n-3 \rrbracket$ and $m \in \llbracket 2, k \rrbracket$.

E Schwinger-Dyson equations for the intermediate field

In this appendix we construct the Schwinger-Dyson equations for the matrix intermediate field used in Chapter 3. As already announced, our calculations follow the lines of [97]. The following subsection deals with the complex SYK model and the last subsection deals with the real Gross-Rosenhaus SYK generalization.

E.1 Complex SYK

We first perform the following change of variables:

$$M^{(c)} \rightarrow \alpha 1 + \frac{1}{N} M^{(c)}. \quad (\text{E.1})$$

The effective action for the intermediate field in equation (3.5.12) leads to the following expression

$$\begin{aligned} & -\frac{N}{2} \sum_{c=1}^4 \text{Tr}(M^{(c)2}) - \alpha N^2 \sum_{c=1}^4 \text{Tr}(M^{(c)}) \\ &+ \text{Tr} \left(\sum_{k \geq 1} \sum_{k_1+k_2+k_3+k_4=k} \frac{(-i(\frac{\lambda}{2})^{\frac{1}{2}} \sigma^2)^k}{k_1!k_2!k_3!k_4!} \left((k-1)! 1^{\otimes 4} + \frac{\sigma^2}{N^3} \int dt \sum_{a,b=1}^n (\bar{\psi}_b^4 \cdot \psi_a^4) \right) \right. \\ & \quad \left. \prod_{c=1}^4 \left(\alpha 1^{\otimes 4} + \frac{1}{N} \mathcal{M}_c \right)^{k_c} \right) \end{aligned}$$

$$\begin{aligned}
&= -\frac{N}{2} \sum_{c=1}^4 \text{Tr}(M^{(c)2}) - \alpha N^2 \sum_{c=1}^4 \text{Tr}(M^{(c)}) \\
&+ \text{Tr} \left(\sum_{k \geq 1} \sum_{k_1+k_2+k_3+k_4=k} \frac{(-i(\frac{\lambda}{2})^{\frac{1}{2}} \sigma^2 \alpha)^k}{k_1!k_2!k_3!k_4!} \left((k-1)!1^{\otimes 4} + \frac{\sigma^2}{N^3} \int dt \sum_{a,b=1}^n (\bar{\psi}_b^4 \cdot \psi_a^4) \right) \right. \\
&\quad \left. \prod_{c=1}^4 \sum_{p_c=0}^{k_c} \binom{k_c}{p_c} \frac{\mathcal{M}_c^{p_c}}{(\alpha N)^{p_c}} \right), \tag{E.2}
\end{aligned}$$

where we recall the notation $\mathcal{M}_c = 1^{\otimes(c-1)} \otimes M^{(c)} \otimes 1^{\otimes(4-c)}$. Using the expression above of the action, we can now derive the Schwinger-Dyson equations (recall that these equations can be derived by exploiting the fact that the integration of a total derivative is vanishing):

$$\begin{aligned}
0 &= \sum_{ij} \int \prod_{c=1}^4 dM^{(c)} \frac{\partial}{\partial M_{ij}^{(d)}} \left[\left(M^{(d)} \right)_{ij}^q \exp \left(-\frac{N}{2} \sum_{c=1}^4 \text{Tr}(M_c^2) - \alpha N^2 \sum_{c=1}^4 \text{Tr}(M_c) \right) \right. \\
&+ \text{Tr} \left(\sum_{k \geq 1} \sum_{k_1+k_2+k_3+k_4=k} \frac{(-i(\frac{\lambda}{2})^{\frac{1}{2}} \sigma^2 \alpha)^k}{k_1!k_2!k_3!k_4!} \left((k-1)!1^{\otimes 4} + \frac{\sigma^2}{N^3} \int dt \sum_{a,b=1}^n (\bar{\psi}_b^4 \cdot \psi_a^4) \right) \right. \\
&\quad \left. \left. \prod_{c=1}^4 \sum_{p_c=0}^{k_c} \binom{k_c}{p_c} \frac{\mathcal{M}_c^{p_c}}{(\alpha N)^{p_c}} \right) \right]. \tag{E.3}
\end{aligned}$$

This leads to:

$$\begin{aligned}
0 &= \left\langle \sum_{i=0}^{q-1} \text{Tr}(M^{(d)i}) \text{Tr}(M^{(d)q-i-1}) \right\rangle - N \langle \text{Tr}(M^{(d)q+1}) \rangle - \alpha N^2 \langle \text{Tr}(M^{(d)q}) \rangle \\
&+ \left\langle \text{Tr} \left[\sum_{k \geq 1} \sum_{k_1+k_2+k_3+k_4=k} \frac{(-i(\frac{\lambda}{2})^{\frac{1}{2}} \sigma^2 \alpha)^k}{k_1!k_2!k_3!k_4!} \left((k-1)!1^{\otimes 4} + \frac{\sigma^2}{N^3} \int dt \sum_{a,b=1}^n (\bar{\psi}_b^4 \cdot \psi_a^4) \right) \right. \right. \\
&\quad \left. \left. \left(\prod_{\substack{c=1 \\ c \neq d}}^4 \sum_{p_c=0}^{k_c} \binom{k_c}{p_c} \frac{\mathcal{M}_c^{p_c}}{(\alpha N)^{p_c}} \sum_{p_d=1}^{k_d} \binom{k_d}{p_d} \frac{p_d}{\alpha N} \frac{\mathcal{M}_d^{q+p_d-1}}{(\alpha N)^{p_d-1}} \right) \right] \right\rangle. \tag{E.4}
\end{aligned}$$

Let us now compute in detail the Leading Order (LO) and the Next to Leading Order (NLO) of the above Schwinger-Dyson Equation. Notice that the LO is of order N^3 and it writes:

$$0 = -\alpha \langle \text{Tr}(M^{(d)q}) \rangle + \frac{1}{\alpha} \sum_{k \geq 1} \frac{1}{k} \sum_{k_1+k_2+k_3+k_4=k} \left(-i \left(\frac{\lambda}{2} \right)^{\frac{1}{2}} \sigma^2 \alpha \right)^k \frac{k!k_d}{k_1!k_2!k_3!k_4!} \langle \text{Tr}(M^{(d)q}) \rangle. \tag{E.5}$$

This LO equation rewrites as:

$$\alpha^2 = \sum_{k \geq 1} \frac{1}{k} \left(-i \left(\frac{\lambda}{2} \right)^{\frac{1}{2}} \sigma^2 \alpha \right)^k \sum_{k_1+k_2+k_3+k_4=k} \frac{k!k_d}{k_1!k_2!k_3!k_4!}. \tag{E.6}$$

Let us now recall the following identity:

$$\sum_{k_1+\dots+k_D=k} \frac{k!}{k_1! \dots k_D!} \prod_{i=1}^D x_i^{k_i} = (x_1 + \dots + x_D)^k. \quad (\text{E.7})$$

We now derive the above identity with respect to x_d ; this leads to:

$$\sum_{k_1+\dots+k_D=k} \frac{k!k_d}{k_1! \dots k_D!} \prod_{i \neq d} x_i^{k_i} x_d^{k_d-1} = k(x_1 + \dots + x_D)^{k-1}, \quad (\text{E.8})$$

Setting all the x_i 's equal to 1, we have:

$$kD^{k-1} = \sum_{k_1+\dots+k_D=k} \frac{k!k_d}{k_1! \dots k_D!}. \quad (\text{E.9})$$

Using the above result for $D = 4$, the LO equation reduces to:

$$\alpha^2 = \sum_{k \geq 1} \left(-i \left(\frac{\lambda}{2} \right)^{\frac{1}{2}} \sigma^2 \alpha \right)^k 4^{k-1} = \frac{-i\alpha\sigma^2\sqrt{\lambda/2}}{1 + 4i\alpha\sigma^2\sqrt{\lambda/2}}. \quad (\text{E.10})$$

Finally, we can solve the LO of the Schwinger-Dyson equation and find the values of α :

$$\alpha_{\pm} = \frac{-1 \pm \sqrt{1 + 8\sigma^4\lambda}}{8i\sigma^2\sqrt{\lambda/2}}. \quad (\text{E.11})$$

Notice that these are the same values of α_{\pm} found in [97] through a careful use of the saddle point method.

Let us now evaluate the NLO of the Schwinger-Dyson equation. Collecting the terms of order N^2 in the Schwinger-Dyson equation (E.4), we get:

$$\begin{aligned} 0 = & \left\langle \sum_{i=0}^{q-1} \text{Tr} (M^{(d)i}) \text{Tr} (M^{(d)q-i-1}) \right\rangle - N \langle \text{Tr} (M^{(d)q+1}) \rangle \\ & + \frac{1}{\alpha^2} \left\langle \sum_{k \geq 1} \frac{1}{k} \sum_{k_1+k_2+k_3+k_4=k} \left(-i \left(\frac{\lambda}{2} \right)^{\frac{1}{2}} \sigma^2 \alpha \right)^k \frac{k!}{k_1!k_2!k_3!k_4!} \right. \\ & \left. \sum_{c=1}^4 k_d(k_c - \delta_{cd}) \text{Tr} (M^{(c)1-\delta_{cd}}) \text{Tr} (M^{(d)q+\delta_{cd}}) \right\rangle. \end{aligned} \quad (\text{E.12})$$

In order to solve the NLO equation, we first have to evaluate the third term in RHS of the equation above. In order to do this, we derive eq. (E.8) with respect to x_c , and we sum over all flavours c . This leads to:

$$\begin{aligned} \sum_{c=1}^D \frac{d}{dx_c} k(x_1 + \dots + x_D)^{k-1} &= Dk(k-1)(x_1 + \dots + x_D)^{k-2} = \\ \sum_{c=1}^D \sum_{k_1+\dots+k_D=k} \frac{k!k_d(k_c - \delta_{cd})}{k_1! \dots k_D!} &\prod_{i \neq c,d} x_i^{k_i} x_c^{k_c-\delta_{cd}} x_d^{k_d-1-\delta_{cd}}. \end{aligned} \quad (\text{E.13})$$

As above, let us set all the x_i 's equal to 1, and insert the resulting identity for $D = 4$ in the NLO Schwinger-Dyson equation (E.12). We get:

$$0 = \left\langle \sum_{i=0}^{q-1} \text{Tr} (M^{(d)i}) \text{Tr} (M^{(d)q-i-1}) \right\rangle - N \langle \text{Tr} (M^{(d)q+1}) \rangle + \\ + \frac{1}{\alpha^2} \sum_{k \geq 1} \left(-i \left(\frac{\lambda}{2} \right)^{\frac{1}{2}} \sigma^2 \alpha \right)^k (k-1) 4^{k-1} \left\langle \sum_{c=1}^4 \text{Tr} (M^{(c)1-\delta_{cd}}) \text{Tr} (M^{(d)q+\delta_{cd}}) \right\rangle. \quad (\text{E.14})$$

Using eq. (E.11) the NLO term of the Schwinger-Dyson equation reduces to

$$0 = \left\langle \sum_{i=0}^{q-1} \text{Tr} (M^{(d)i}) \text{Tr} (M^{(d)q-i-1}) \right\rangle + (\alpha^2 - 1) N \langle \text{Tr} (M^{(d)q+1}) \rangle \\ + \alpha^2 \left\langle \sum_{\substack{c=1 \\ c \neq d}}^4 \text{Tr} (M^{(c)}) \text{Tr} (M^{(d)q}) \right\rangle. \quad (\text{E.15})$$

Notice that, also in the NLO term of the Schwinger-Dyson equation, we recovered exactly the same result of [97]. Even if we considered a non-Gaussian distribution (a Gaussian term plus a quartic pillow term potential), the first orders of the Schwinger-Dyson equation are the same as in the Gaussian case.

E.2 Gross-Rosenhaus SYK generalization

Let us first consider the formula (3.6.10) for the field $M^{(c)}$ and perform the following change of variables:

$$M^{(c)} \rightarrow \alpha 1 + \frac{N}{\prod_{a=1}^f N_a^{\frac{q_a}{2}}} M^{(c)}. \quad (\text{E.16})$$

The action (3.6.10) thus rewrites:

$$\mathcal{S}[M^{(c)}] = \frac{1}{2} N \sum_{c=1}^q \text{Tr} ((M^{(c)})^2) + \alpha \prod_{a=1}^f N_a^{\frac{q_a}{2}} \sum_{c=1}^q \text{Tr} (M^{(c)}) \\ - \frac{1}{2} \text{Tr} \left[\sum_{k \geq 1} \left(-i \alpha \sqrt{2\lambda} \sigma^2 \prod_{a=1}^f (q_a - 1)! \right)^k \sum_{\sum_i^q k_i = k} \binom{k}{k_1, \dots, k_q} \hat{A}_k \right. \\ \left. \prod_{c=1}^q \sum_{p_c=0}^{k_c} \binom{k_c}{p_c} \left(\frac{N}{\alpha \prod_{a=1}^f N_a^{\frac{q_a}{2}}} \right)^{p_c} \mathcal{M}_c^{p_c} \right]. \quad (\text{E.17})$$

The Schwinger-Dyson equation for the intermediate field writes:

$$0 = \sum_{ij} \int \prod_{c=1}^q dM^{(c)} \frac{\partial}{\partial M_{ij}^{(d)}} \left[(M^{(d)})_{ij}^h e^{-\mathcal{S}[M]} \right], \quad (\text{E.18})$$

This leads to:

$$0 = \left\langle \sum_{i=0}^{h-1} \text{Tr} (M^{(d)i}) \text{Tr} (M^{(d)h-i-1}) \right\rangle - N \langle \text{Tr} (M^{(d)h+1}) \rangle - \alpha \prod_{a=1}^f N_a^{\frac{q_a}{2}} \langle \text{Tr} (M^{(d)h}) \rangle +$$

$$\begin{aligned}
& + \left\langle \text{Tr} \left[\sum_{k \geq 1} \left(-i\alpha\sqrt{2\lambda}\sigma^2 \prod_{a=1}^f (q_a - 1)! \right)^k \sum_{\sum_i^q k_i = k} \binom{k}{k_1, \dots, k_q} \hat{A}_k \right. \right. \\
& \left. \left. \left(\prod_{\substack{c=1 \\ c \neq d}}^q \sum_{p_c=0}^{k_c} \binom{k_c}{p_c} \left(\frac{N}{\alpha \prod_{a=1}^f N_a^{\frac{q_a}{2}}} \right)^{p_c} \mathcal{M}_c^{p_c} \sum_{p_d=1}^{k_d} \binom{k_d}{p_d} p_d \left(\frac{N}{\alpha \prod_{a=1}^f N_a^{\frac{q_a}{2}}} \right)^{p_d} \mathcal{M}_d^{h+p_d-1} \right) \right] \right\rangle.
\end{aligned} \tag{E.19}$$

Let us define $\kappa_a = \frac{N_a}{N}$, so that the LO of the Schwinger-Dyson equation in the large N limit is of the order of $N^{\frac{q_a+2}{2}}$. The LO contribution thus writes:

$$\begin{aligned}
0 & = -\alpha N^{\frac{q_a}{2}+1} \prod_{a=1}^f \kappa_a^{\frac{q_a}{2}} \langle \text{Tr} (M^{(d)h}) \rangle \\
& + \frac{N^{\frac{q_a}{2}+1} \prod_{a=1}^f \kappa_a^{\frac{q_a}{2}}}{\alpha \kappa_d} \sum_{k \geq 1} \frac{1}{k} \sum_{\sum_i^q k_i = k} \binom{k}{k_1, \dots, k_q} \left(-i \left(\frac{\lambda}{2} \right)^{\frac{1}{2}} \sigma^2 \alpha \prod_{a=1}^f (q_a - 1)! \right)^k k_d \langle \text{Tr} (M^{(d)h}) \rangle.
\end{aligned} \tag{E.20}$$

which becomes

$$\alpha^2 = \frac{1}{\kappa_d} \sum_{k \geq 1} \left(-i \left(\frac{\lambda}{2} \right)^{\frac{1}{2}} \sigma^2 \alpha \prod_{a=1}^f (q_a - 1)! \right)^k q^{k-1} = \frac{1}{\kappa_d} \frac{-i\alpha\sigma^2\sqrt{\lambda/2} \prod_{a=1}^f (q_a - 1)!}{1 + qi\alpha\sigma^2\sqrt{\lambda/2} \prod_{a=1}^f (q_a - 1)!}, \tag{E.21}$$

with

$$\alpha_{\pm} = \frac{-1 \pm \sqrt{1 + 2q\sigma^4 \frac{\lambda}{\kappa_d} (\prod_{a=1}^f (q_a - 1)!)^2}}{2iq\sigma^2\sqrt{\lambda/2} \prod_{a=1}^f (q_a - 1)!}. \tag{E.22}$$

We can note that the saddle point is parametrized by κ_d .

The NLO part of the Schwinger-Dyson equations writes:

$$\begin{aligned}
0 & = \left\langle \sum_{i=0}^{h-1} \text{Tr} (M^{(d)i}) \text{Tr} (M^{(d)h-i-1}) \right\rangle - N \langle \text{Tr} (M^{(d)h+1}) \rangle \\
& + \sum_{k \geq 1} \sum_{\sum_i^q k_i = k} \binom{k}{k_1, \dots, k_q} \left(-i \left(\frac{\lambda}{2} \right)^{\frac{1}{2}} \sigma^2 \alpha \prod_{a=1}^f (q_a - 1)! \right)^k \\
& \sum_{c=1}^q \frac{k_d(k_c - \delta_{cd})}{k\kappa_d\kappa_c\alpha^2} \langle \text{Tr} (M^{(c)1-\delta_{cd}}) \text{Tr} (M^{(d)h+\delta_{cd}}) \rangle.
\end{aligned} \tag{E.23}$$

This can be rewritten as:

$$\begin{aligned}
0 & = \left\langle \sum_{i=0}^{h-1} \text{Tr} (M^{(d)i}) \text{Tr} (M^{(d)h-i-1}) \right\rangle - N \langle \text{Tr} (M^{(d)h+1}) \rangle \\
& + \sum_{k \geq 1} \left(-i \left(\frac{\lambda}{2} \right)^{\frac{1}{2}} \sigma^2 \alpha \prod_{a=1}^f (q_a - 1)! \right)^k (k-1) q^{k-1} \sum_{c=1}^q \frac{1}{\kappa_d\kappa_c\alpha^2} \langle \text{Tr} (M^{(c)1-\delta_{cd}}) \text{Tr} (M^{(d)h+\delta_{cd}}) \rangle,
\end{aligned} \tag{E.24}$$

Finally, we get the following equation:

$$\begin{aligned}
0 &= \left\langle \sum_{i=0}^{h-1} \text{Tr} (M^{(d)i}) \text{Tr} (M^{(d)h-i-1}) \right\rangle - N \langle \text{Tr} (M^{(d)h+1}) \rangle \\
&+ q\alpha^2 \sum_{c=1}^q \frac{\kappa_d}{\kappa_c} \langle \text{Tr} (M^{(c)1-\delta_{cd}}) \text{Tr} (M^{(d)h+\delta_{cd}}) \rangle.
\end{aligned} \tag{E.25}$$

F Explicit computation of the variance at order t^4

In this appendix we detail some of the computations of the dominant graph amplitudes and their contribution to the variance of Sobolev norms at order t^4 . We start by the contribution of melonic diagrams to the variance $\bar{S}_{\gamma, M}^{(4)}(t)$, then we show the explicit computation of the first class of ladder graph amplitudes and their contribution to $\bar{S}_{\gamma, L_1}^{(4)}(t)$.

F.1 Melonic diagrams

The contribution of $\mathcal{A}_r(M_{II})$ is

$$\begin{aligned}
&\sum_{r \geq 0} \frac{r^{2\gamma}}{32N^2} p^{4r} \left(p^2 + \frac{2p(r+1)}{N} + \frac{r^2 + 2r + 1}{N^2} \right) \\
&= \frac{1}{32N^2} \left(p^2 L_{2\gamma}(p^4) + \frac{2p}{N} (L_{2\gamma}(p^4) + L_{2\gamma+1}(p^4)) + \frac{1}{N^2} (L_{2\gamma}(p^4) + 2L_{2\gamma+1}(p^4) + L_{2\gamma+2}(p^4)) \right) \\
&= \frac{1}{32N^2} \left(p^2 L_{2\gamma}(p^4) + \frac{2p}{N} L_{2\gamma+1}(p^4) + \frac{1}{N^2} L_{2\gamma+2}(p^4) \right) + o(N^{2\gamma-1}) \\
&\stackrel{p \rightarrow 1}{=} \frac{N^{2\gamma-1}}{2^{4\gamma+10}} (2\gamma)! (2\gamma^2 + 11\gamma + 13) + o(N^{2\gamma-1}),
\end{aligned} \tag{F.1}$$

Similarly for $\mathcal{A}_r(M_{III})$,

$$\begin{aligned}
&\sum_{r \geq 0} \frac{r^{2\gamma}}{8N^2} \left(p^{2r} - \frac{2p^{3r+1}}{1+p} + \frac{p^{4r+2}}{(1+p)^2} \right) = \frac{1}{8N^2} \left(L_{2\gamma}(p^2) - \frac{2p}{1+p} L_{2\gamma}(p^3) + \frac{p^2}{(1+p)^2} L_{2\gamma}(p^4) \right) \\
&\stackrel{p \rightarrow 1}{=} \frac{N^{2\gamma-1}}{8} (2\gamma)! \left(\frac{1}{2^{2\gamma+1}} - \frac{1}{3^{2\gamma+1}} + \frac{1}{2^{4\gamma+4}} \right) + o(N^{2\gamma-1}),
\end{aligned} \tag{F.2}$$

and for $\mathcal{A}_r(M_{II/III})$,

$$\begin{aligned}
&-\sum_{r \geq 0} \frac{r^{2\gamma}}{8N^2} p^{2r} \left(p^{r+1} + \frac{r+1}{N} p^r - \frac{p^{2r+2}}{1+p} - \frac{r+1}{N} \frac{p^{2r+1}}{1+p} \right) \\
&= -\frac{1}{8N^2} \left(p L_{2\gamma}(p^3) + \frac{1}{N} (L_{2\gamma}(p^3) + L_{2\gamma+1}(p^3)) - \frac{p^{2r+2}}{1+p} L_{2\gamma}(p^4) \right) \\
&- \frac{1}{N} \frac{p}{1+p} (L_{2\gamma}(p^4) + L_{2\gamma+1}(p^4))
\end{aligned}$$

$$=_{LO} -\frac{1}{8N^2} \left(pL_{2\gamma}(p^3) + \frac{1}{N}L_{2\gamma+1}(p^3) - \frac{p^2}{1+p}L_{2\gamma}(p^4) - \frac{1}{N} \frac{p}{(1+p)}L_{2\gamma+1}(p^4) \right) \quad (F.3)$$

$$\stackrel{=}{=} \frac{N^{2\gamma-1}}{8} (2\gamma)! \left((2\gamma+1) \left(\frac{1}{2^{4\gamma+5}} - \frac{1}{3^{2\gamma+2}} \right) + \frac{1}{2^{4\gamma+3}} - \frac{1}{3^{2\gamma+1}} \right) + o(N^{2\gamma-1}). \quad (F.4)$$

F.2 Ladder diagrams

We recall the dominant amplitude of $L_{IA/IB}$,

$$\begin{aligned} \mathcal{A}_{r_1, r_2}(L_{IA/IB}) &= \frac{p^{r_1+r_2}}{4N(1+p)^2} \left(\frac{1}{(1+p)} + \frac{r_1}{N} - \frac{p^{2(r_2+1)}}{(1+p)(1+p^2)} \right. \\ &\quad \left. - \frac{p^{2(r_2+2)}}{(1+p)(1+p^2)^2} - \frac{(r_1+r_2)p^{2(r_2+2)}}{N(1+p^2)} \right). \end{aligned} \quad (F.5)$$

Its contribution to the variance of the Sobolev norm is

$$\begin{aligned} &\frac{1}{4N^3(1+p)^2} \left(\frac{L_\gamma(p)^2}{(1+p)} + \frac{L_{\gamma+1}(p)L_\gamma(p)}{N} - \frac{p^2L_\gamma(p)L_\gamma(p^2)}{(1+p)(1+p^2)} - \frac{p^4L_\gamma(p)L_\gamma(p^3)}{(1+p)(1+p^2)^2} \right. \\ &\quad \left. - \frac{p^4}{N(1+p^2)} (L_{\gamma+1}(p)L_\gamma(p^3) + L_\gamma(p)L_{\gamma+1}(p^3)) \right) \end{aligned} \quad (F.6)$$

$$\stackrel{=}{=} \frac{N^{2\gamma-1}}{16} (\gamma!)^2 \left(\frac{1}{2} + \gamma + 1 - \frac{1}{2^{2\gamma+4}} - \frac{1}{3^{\gamma+1}8} - \frac{2(\gamma+1)}{3^{2\gamma+2}} \right) + o(N^{2\gamma-1}). \quad (F.7)$$

Then we compute one by one the dominant amplitudes of each type of diagrams. The dominant amplitudes for L_{IB} is

$$\mathcal{A}_{r_1, r_2}(L_{IB}) = \frac{16}{8^2 4N^4} \sum_{S_1 \geq r_1} \sum_{S_2 \geq r_2} p^{2(S_1+S_2)-r_1-r_2} \sum_{k_1=0}^{S_1} \sum_{k_2=0}^{S_2} \delta_{S_1-r_1}^{S_2-r_2} \quad (F.8)$$

$$= \frac{p^{r_1+r_2}}{16N^4} \sum_{S \geq 0} (S+r_1+1)(S+r_2+1)p^{4S} \quad (F.9)$$

$$= \frac{p^{r_1+r_2}}{16N^4} \left(\frac{1+p^4}{(1-p^4)^3} + \frac{r_1+r_2}{(1-p^4)^2} + \frac{r_1r_2}{1-p^4} \right) \quad (F.10)$$

$$= \frac{p^{r_1+r_2}}{16N(1+p)(1+p^2)} \left(\frac{1+p^4}{(1+p)^2(1+p^2)^2} + \frac{r_1+r_2}{N(1+p)(1+p^2)} + \frac{r_1r_2}{N^2} \right). \quad (F.11)$$

Its contribution to the variance of the Sobolev norm is

$$\frac{1}{16N^3(1+p)(1+p^2)} \left(\frac{(1+p^4)L_\gamma(p)^2}{(1+p)^2(1+p^2)^2} + \frac{2L_\gamma(p)L_{\gamma+1}(p)}{N(1+p)(1+p^2)} + \frac{L_{\gamma+1}(p)^2}{N^2} \right) \quad (F.12)$$

$$\stackrel{=}{=} \frac{N^{2\gamma-1}}{64} (\gamma!)^2 \left(\frac{1}{8} + \frac{\gamma+1}{2} + (\gamma+1)^2 \right) + o(N^{2\gamma-1}). \quad (F.13)$$

The dominant amplitudes for $L_{IB/IIB}$ gives

$$\mathcal{A}_{r_1, r_2}(L_{IB/IIB}) = \frac{32}{8^2 4N^4} \sum_{S_1 \geq r_1} \sum_{S_2 \geq r_2} p^{2S_1+S_2+r_2-r_1} \sum_{k_1=0}^{S_1} \sum_{k_2=0}^{S_2} \delta_{S_1-r_1}^{S_2-k_2} \quad (F.14)$$

$$= \frac{p^{r_1+2r_2}}{8N^4} \sum_{S_2 \geq 0} p^{S_2} \sum_{S_1=0}^{S_2+r_2} (S_1 + r_1 + 1) p^{2S_1} \quad (\text{F.15})$$

$$= \frac{p^{r_1+2r_2}}{8N^4(1-p^2)^2} \left(\frac{1+r_1(1-p^2)}{1-p} - \frac{p^{2(r_2+1)}}{1-p^3} - \frac{(1-p^2)p^{2(r_2+1)}}{(1-p^3)^2} ((r_1+r_2)(1-p^3)+1) \right) \quad (\text{F.16})$$

$$= \frac{p^{r_1+2r_2}}{8N(1+p)^2} \left(1 + \frac{r_1(1+p)}{N} - \frac{p^{2(r_2+1)}}{1+p+p^2} - \frac{(1+p)p^{2(r_2+1)}}{(1+p+p^2)^2} \left(1 + (r_1+r_2) \frac{(1+p+p^2)}{N} \right) \right). \quad (\text{F.17})$$

Its contribution to the variance of the Sobolev norm is

$$\frac{1}{8N^3(1+p)^2} \left(L_\gamma(p)L_\gamma(p^2) + \frac{(1+p)L_\gamma(p^2)L_{\gamma+1}(p)}{N} - \frac{(2(1+p)p^2+p^4)L_\gamma(p)L_\gamma(p^4)}{(1+p+p^2)^2} - \frac{p^4(1+p)}{N(1+p+p^2)} (L_{\gamma+1}(p)L_\gamma(p^4) + L_\gamma(p)L_{\gamma+1}(p^4)) \right) \quad (\text{F.18})$$

$$\stackrel{p \rightarrow 1}{=} \frac{N^{2\gamma-1}}{32} (\gamma!)^2 \left(\frac{1}{2^{\gamma+1}} + \frac{\gamma+1}{2^\gamma} - \frac{3}{2^{2\gamma+1}} - \frac{5(\gamma+1)}{2^{2\gamma+3}3} \right) + o(N^{2\gamma-1}). \quad (\text{F.19})$$

The dominant amplitudes for $L_{IB/IIIB}$ gives

$$\mathcal{A}_{r_1, r_2}(L_{IB/IIIB}) = -\frac{16}{8^2 4 N^4} \sum_{S_1 \geq r_1} \sum_{S_2 \geq r_2} p^{2S_1 - r_1 + S_2} \sum_{k_1=0}^{S_1} \sum_{k_2=0}^{S_2} p^{k_2} \delta_{S_1 - r_1}^{k_2} \quad (\text{F.20})$$

$$= -\frac{p^{r_1+r_2}}{16N^4} \sum_{S_2 \geq r_2} p^{S_2} \sum_{S_1=0}^{S_2+r_2} (S_1 + r_1 + 1) p^{3S_2} \quad (\text{F.21})$$

$$= -\frac{p^{r_1+r_2}}{16N^4(1-p^2)^2} \left(\frac{1+r_1(1-p^3)}{1-p} - \frac{p^{3(r_2+1)}}{1-p^4} - \frac{(1-p^3)p^{3(r_2+1)}}{(1-p^4)^2} ((r_1+r_2)(1-p^4)+1) \right) \quad (\text{F.22})$$

$$= -\frac{p^{r_1+r_2}}{16N(1+p)^2} \left(1 + \frac{r_1(1+p+p^2)}{N} - \frac{p^{3(r_2+1)}}{(1+p)(1+p^2)} - \frac{(1+p+p^2)p^{3(r_2+1)}}{(1+p)^2(1+p^2)^2} \left((r_1+r_2) \frac{(1+p)(1+p^2)}{N} + 1 \right) \right) \quad (\text{F.23})$$

$$= -\frac{p^{r_1+r_2}}{16N(1+p)^2} \left(1 + \frac{r_1(1+p+p^2)}{N} - \frac{(p^3+2(1+p+p^2))p^{3(r_2+1)}}{(1+p)^2(1+p^2)^2} - \frac{(1+p+p^2)p^{3(r_2+1)}(r_1+r_2)}{N(1+p)(1+p^2)} \right). \quad (\text{F.24})$$

Its contribution to the variance of the Sobolev norm is

$$- \frac{1}{16N^3(1+p)^2} \left(L_\gamma(p)^2 + \frac{(1+p+p^2)L_\gamma(p)L_{\gamma+1}(p)}{N} - \frac{(p^3+2(1+p+p^2))p^3}{(1+p)^2(1+p^2)^2} L_\gamma(p)L_\gamma(p^4) \right)$$

$$- \frac{(1+p+p^2)p^3}{N(1+p)(1+p^2)} (\mathbb{L}_{\gamma+1}(p)\mathbb{L}_\gamma(p^4) + \mathbb{L}_\gamma(p)\mathbb{L}_{\gamma+1}(p^4)) \quad (\text{F.25})$$

$$\stackrel{p \rightarrow 1}{=} - \frac{N^{2\gamma-1}}{64} (\gamma!)^2 \left(1 + 3(\gamma+1) - \frac{7}{2^{2\gamma+6}} - \frac{15(\gamma+1)}{2^{2\gamma+6}} \right) + o(N^{2\gamma-1}). \quad (\text{F.26})$$

The dominant amplitudes for L_{IIA} writes

$$\mathcal{A}_{r_1, r_2}(L_{IIA}) = \frac{4}{8^2 4 N^4} p^{r_1+r_2} \sum_{S_1 \geq r_1} \sum_{S_2 \geq r_2} p^{S_1+S_2} \sum_{k_1=0}^{S_1} \sum_{k_2=0}^{S_2} \delta_{S_1-r_1}^{S_2-r_2} \quad (\text{F.27})$$

$$= \frac{p^{2(r_1+r_2)}}{64 N^4} \sum_{S \geq 0} p^{2S} (S+r_1+1)(S+r_2+1) \quad (\text{F.28})$$

$$= \frac{p^{2(r_1+r_2)}}{64 N} \left(\frac{1+p^2}{(1+p)^3} + \frac{(r_1+r_2)}{N(1+p)^2} + \frac{r_1 r_2}{N^2(1+p)} \right). \quad (\text{F.29})$$

Its contribution to the variance of the Sobolev norm is

$$\frac{1}{64 N^3 (1+p)} \left(\frac{1+p^2}{(1+p)^2} \mathbb{L}_\gamma(p^2)^2 + \frac{2}{N(1+p)} \mathbb{L}_\gamma(p^2) \mathbb{L}_{\gamma+1}(p^2) + \frac{\mathbb{L}_{\gamma+1}(p^2)^2}{N^2} \right) \quad (\text{F.30})$$

$$\stackrel{p \rightarrow 1}{=} \frac{N^{2\gamma-1}}{2^{2\gamma+10}} (\gamma!)^2 \left(3 + 2\gamma + \frac{\gamma^2+1}{2} \right) + o(N^{2\gamma-1}). \quad (\text{F.31})$$

For the dominant amplitudes of $L_{IIA}/III A$ we obtain

$$\mathcal{A}_{r_1, r_2}(L_{IIA}/III A) = - \frac{8}{8^2 4 N^4} \sum_{S_1 \geq 0} \sum_{S_2 \geq r_2} p^{2r_1} p^{S_1+S_2} (S_1+r_1+1) \sum_{k_2=0}^{S_2} p^{k_2} \delta_{k_2}^{S_2-S_1} \quad (\text{F.32})$$

$$= - \frac{1}{32 N^4} \sum_{S_1 \geq 0} \sum_{S_2 \geq r_2} p^{2r_1} p^{S_1+S_2} (S_1+r_1+1) p^{S_2-S_1} \Theta(S_2-S_1) \quad (\text{F.33})$$

$$= - \frac{p^{2(r_1+r_2)}}{32 N^4} \sum_{S_2 \geq 0} \sum_{S_1 \geq 0} p^{2S_2} (S_1+r_1+1) \quad (\text{F.34})$$

$$= - \frac{p^{2(r_1+r_2)}}{32 N^4} \sum_{S_2 \geq 0} p^{2S_2} (S_2+r_2+1) \left(r_1+1 + \frac{r_2+S_2}{2} \right) \quad (\text{F.35})$$

$$= - \frac{p^{2(r_1+r_2)}}{32 N^4 (1-p^2)} \left(\frac{1}{(1-p^2)^2} + \frac{r_2(r_2+1)}{2} + \frac{r_1+r_2}{1-p^2} + r_1 r_2 \right) \quad (\text{F.36})$$

$$= - \frac{p^{2(r_1+r_2)}}{32 N (1+p)} \left(\frac{1}{(1+p)^2} + \frac{r_2(r_2+1)}{2 N^2} + \frac{r_1+r_2}{N(1+p)} + \frac{r_1 r_2}{N^2} \right). \quad (\text{F.37})$$

Its contribution to the variance of the Sobolev norm is

$$- \frac{1}{32 N^3 (1+p)} \left(\frac{1}{(1+p)^2} \mathbb{L}_\gamma(p^2)^2 + \mathbb{L}_\gamma(p^2) \frac{\mathbb{L}_{\gamma+1}(p^2) + \mathbb{L}_{\gamma+2}(p^2)}{2 N^2} \right. \\ \left. + \frac{2 \mathbb{L}_\gamma(p^2) \mathbb{L}_{\gamma+1}(p^2)}{N(1+p)} + \frac{\mathbb{L}_{\gamma+1}(p^2)^2}{N^2} \right) \quad (\text{F.38})$$

$$\stackrel{LO}{=} - \frac{1}{32 N^3 (1+p)} \left(\frac{1}{(1+p)^2} \mathbb{L}_\gamma(p^2)^2 + \mathbb{L}_\gamma(p^2) \frac{\mathbb{L}_{\gamma+2}(p^2)}{2 N^2} + \frac{2 \mathbb{L}_\gamma(p^2) \mathbb{L}_{\gamma+1}(p^2)}{N(1+p)} + \frac{\mathbb{L}_{\gamma+1}(p^2)^2}{N^2} \right) \quad (\text{F.39})$$

$$\stackrel{=}{p \rightarrow 1} - \frac{N^{2\gamma-1}}{2^{2\gamma+4}} (\gamma!)^2 \left(\gamma^2 + 4\gamma + \frac{\gamma^2 + 3\gamma}{2} + 5 \right) + o(N^{2\gamma-1}). \quad (\text{F.40})$$

For the dominant amplitudes of L_{IHC} we get

$$\mathcal{A}_{r_1, r_2}(L_{IHC}) = \frac{16}{8^2 4 N^4} \sum_{S_1 \geq r_1} \sum_{S_2 \geq r_2} p^{S_1+S_2} \sum_{k_1=0}^{S_1} \sum_{k_2=0}^{S_2} p^{k_1+k_2} \delta_{S_1-r_1}^{S_2-r_2} \quad (\text{F.41})$$

$$= \frac{p^{r_1+r_2}}{16N^4} \sum_{S \geq 0} p^{2S} \frac{(1-p^{S+r_1+1})(1-p^{S+r_2+1})}{(1-p)^2} \quad (\text{F.42})$$

$$= \frac{p^{r_1+r_2}}{16N} \left(\frac{1}{1+p} - \frac{p(p^{r_1} + r^{r_2})}{1+p+p^2} + \frac{p^{r_1+r_2+2}}{(1+p)(1+p^2)} \right). \quad (\text{F.43})$$

Its contribution to the variance of the Sobolev norm is

$$\frac{1}{16N^3} \left(\frac{L_\gamma(p)^2}{1+p} - \frac{2pL_\gamma(p)L_\gamma(p^2)}{1+p+p^2} + \frac{p^2L_\gamma(p^2)^2}{(1+p)(1+p^2)} \right) \quad (\text{F.44})$$

$$\stackrel{=}{p \rightarrow 1} \frac{N^{2\gamma-1}}{32} (\gamma!)^2 \left(1 - \frac{1}{2^{\gamma-1}3} + \frac{1}{2^{2\gamma+3}} \right) + o(N^{2\gamma-1}). \quad (\text{F.45})$$

For the dominant amplitudes of $L_{IIB/IHC}$ we compute

$$\mathcal{A}_{r_1, r_2}(L_{IIB/IHC}) = \frac{16}{8^2 4 N^4} \sum_{S_1 \geq r_1} \sum_{S_2 \geq r_2} p^{S_1+S_2} \sum_{k_1=0}^{S_1} \sum_{k_2=0}^{S_2} p^{k_1+k_2} \delta_{k_1}^{S_2-r_2} \quad (\text{F.46})$$

$$= \frac{p^{r_1+r_2}}{16N^4} \sum_{S_1 \geq 0} \sum_{S_2 \geq 0} p^{S_1+2S_2} \sum_{k_2=0}^{S_2+r_2} p^{k_2} \theta(S_1 + r_1 - S_2) \quad (\text{F.47})$$

$$= \frac{p^{r_1+r_2}}{16N^4} \sum_{S_1 \geq 0} p^{S_1} \sum_{S_2=0}^{S_1+r_1} p^{2S_2} \frac{1-p^{S_2+r_2+1}}{1-p} \quad (\text{F.48})$$

$$= \frac{p^{r_1+r_2}}{16N} \left(\frac{1}{1+p} - \frac{p^{r_2+1}}{1+p+p^2} - \frac{p^{2r_1+2}}{(1+p)(1+p+p^2)} - \frac{p^{3r_1+r_2+4}}{(1+p)(1+p^2)(1+p+p^2)} \right). \quad (\text{F.49})$$

Its contribution to the variance of the Sobolev norm is

$$\frac{1}{16N^3} \left(\frac{L_\gamma(p)^2}{1+p} - \frac{pL_\gamma(p)L_\gamma(p^2)}{1+p+p^2} - \frac{p^2L_\gamma(p)L_\gamma(p^3)}{(1+p)(1+p+p^2)} - \frac{p^4L_\gamma(p^2)L_\gamma(p^4)}{(1+p)(1+p^2)(1+p+p^2)} \right) \quad (\text{F.50})$$

$$\stackrel{=}{p \rightarrow 1} \frac{N^{2\gamma-1}}{32} (\gamma!)^2 \left(1 - \frac{1}{2^{\gamma}3} - \frac{1}{3^{\gamma+2}} - \frac{1}{2^{3\gamma+4}} \right) + o(N^{2\gamma-1}). \quad (\text{F.51})$$

The dominant amplitudes of $L_{IIB/IHC}$ is

$$\mathcal{A}_{r_1, r_2}(L_{IIB/IHC}) = -\frac{32}{8^2 4 N^4} \sum_{S_1 \geq r_1} \sum_{S_2 \geq r_2} p^{S_1+r_1+S_2} \sum_{k_1=0}^{S_1} \sum_{k_2=0}^{S_2} p^{k_2} \delta_{k_1}^{S_2-r_2} \quad (\text{F.52})$$

$$= -\frac{p^{2r_1+r_2}}{8N^4} \sum_{S_1 \geq 0} p^{S_1} \sum_{S_2=0}^{S_1+r_1} p^{S_2} \frac{1-p^{S_2+r_2+1}}{1-p} \quad (\text{F.53})$$

$$= -\frac{p^{2r_1+r_2}}{8N} \left(1 - \frac{p}{1+p} (p^{r_1} + p^{r_2}) + \frac{p^{2r_1+r_2+3}}{(1+p)(1+p+p^2)} \right). \quad (\text{F.54})$$

Its contribution to the variance of the Sobolev norm is

$$- \frac{1}{8N^3} \left(L_\gamma(p) L_\gamma(p^2) - \frac{p}{1+p} (L_\gamma(p) L_\gamma(p^3) + L_\gamma(p^2)^2) + \frac{p^3 L_\gamma(p^2) L_\gamma(p^3)}{(1+p)(1+p+p^2)} \right) \quad (\text{F.55})$$

$$\stackrel{p \rightarrow 1}{=} -\frac{N^{2\gamma-1}}{16} (\gamma!)^2 \left(\frac{1}{2^\gamma} - \frac{1}{2^{2\gamma+2}} - \frac{1}{3^{\gamma+1}} + \frac{1}{2^{\gamma+1} 3^{\gamma+2}} \right) + o(N^{2\gamma-1}). \quad (\text{F.56})$$

The dominant amplitudes of $L_{IA/IIIC}$ gives

$$\mathcal{A}_{r_1, r_2}(L_{IA/IIIC}) = -\frac{64}{8^2 4N^4} \sum_{S_1 \geq r_1} \sum_{S_2 \geq r_2} p^{2S_1-r_1+S_2} \sum_{k_1=0}^{S_1} \sum_{k_2=0}^{S_2} p^{k_2} \delta_{k_1}^{S_2-r_2} \quad (\text{F.57})$$

$$= -\frac{p^{r_1+r_2}}{4N^4} \sum_{S_1 \geq 0} p^{2S_1} \sum_{S_2=0}^{S_1+r_1} p^{S_2} \frac{1-p^{S_2+r_2+1}}{1-p} \quad (\text{F.58})$$

$$= -\frac{p^{r_1+r_2}}{4N} \left(1 - \frac{p^{r_2+1}}{(1+p)^2} - \frac{p^{r_1+1}}{1+p+p^2} + \frac{p^{2r_1+r_2+3}}{(1+p)^2(1+p^2)} \right). \quad (\text{F.59})$$

Its contribution to the variance of the Sobolev norm is

$$- \frac{1}{4N^3} \left(L_\gamma(p)^2 - \frac{3p^2 + 2p(1+p^2)}{(1+p)^2(1+p+p^2)} L_\gamma(p) L_\gamma(p^2) + \frac{p^3 L_\gamma(p^2) L_\gamma(p^3)}{(1+p)^2(1+p^2)} \right) \quad (\text{F.60})$$

$$\stackrel{p \rightarrow 1}{=} -\frac{N^{2\gamma-1}}{4} (\gamma!)^2 \left(1 - \frac{1}{2^{\gamma+1} 3} - \frac{1}{2^{\gamma+3}} + \frac{1}{2^{\gamma+4} 3^{\gamma+1}} \right) + o(N^{2\gamma-1}). \quad (\text{F.61})$$

Finally, the dominant amplitudes of $L_{IB/IIIC}$ writes

$$\mathcal{A}_{r_1, r_2}(L_{IB/IIIC}) = -\frac{32}{8^2 4N^4} \sum_{S_1 \geq r_1} \sum_{S_2 \geq r_2} p^{2S_1-r_1+S_2} \sum_{k_1=0}^{S_1} \sum_{k_2=0}^{S_2} p^{k_2} \delta_{S_1-r_1}^{S_2-r_2} \quad (\text{F.62})$$

$$= -\frac{p^{r_1+r_2}}{8N^4} \sum_{S \geq 0} p^{3S} (S+r_1+1) \frac{1-p^{S+r_2+1}}{1-p} \quad (\text{F.63})$$

$$= -\frac{p^{r_1+r_2}}{8N^4(1-p)} \left(\frac{1+r_1(1-p^3)}{(1-p^3)^2} - \frac{p^{r_2+1}}{(1-p^4)^2} (1+r_1(1-p^4)) \right) \quad (\text{F.64})$$

$$= -\frac{p^{r_1+r_2}}{8N} \left(\frac{1}{(1+p+p^2)^2} + \frac{r_1}{N(1+p+p^2)} - \frac{p^{r_2+1}}{(1+p)(1+p^2)} \left(\frac{1}{(1+p)(1+p^2)} + \frac{r_1}{N} \right) \right). \quad (\text{F.65})$$

Its contribution to the variance of the Sobolev norm is

$$- \frac{1}{8N^3} \left(\frac{L_\gamma(p)^2}{(1+p+p^2)^2} + \frac{L_\gamma(p) L_{\gamma+1}(p)}{N(1+p+p^2)} - \frac{p}{(1+p)^2(1+p^2)^2} L_\gamma(p) L_\gamma(p^2) \right)$$

$$- \frac{p}{N(1+p)(1+p^2)} L_\gamma(p^2) L_{\gamma+1}(p) \quad (\text{F.66})$$

$$\stackrel{p \rightarrow 1}{=} - \frac{N^{2\gamma-1}}{8} (\gamma!)^2 \left(\frac{1}{9} + \frac{\gamma+1}{3} - \frac{1}{2^{\gamma+5}} - \frac{1}{2^{\gamma+3}} \right) + o(N^{2\gamma-1}). \quad (\text{F.67})$$

Summing all the contributions we obtain $\bar{S}_{\gamma, L1}^{(4)}(t)$ in equation (4.2.34).

Then we need to compute the contribution of the second class of ladder diagrams whose dominant amplitudes are

$$\mathcal{A}_{r_1, r_2}(L_{IA}) = \frac{64}{8^2 4 N^4} \sum_{S_1 \geq r_1} \sum_{S_2 \geq r_2} p^{2(S_1+S_2)-r_1-r_2} \sum_{k_1=0}^{S_1} \sum_{k_2=0}^{S_2} \delta_{k_1}^{k_2}, \quad (\text{F.68})$$

$$\mathcal{A}_{r_1, r_2}(L_{IIB}) = \frac{16}{8^2 4 N^4} \sum_{S_1 \geq r_1} \sum_{S_2 \geq r_2} p^{S_1+S_2+r_1+r_2} \sum_{k_1=0}^{S_1} \sum_{k_2=0}^{S_2} \delta_{k_1}^{k_2}, \quad (\text{F.69})$$

$$\mathcal{A}_{r_1, r_2}(L_{IIIA}) = \frac{4}{8^2 4 N^4} \sum_{S_1 \geq r_1} \sum_{S_2 \geq r_2} p^{2(S_1+S_2)} \sum_{k_1=0}^{S_1} \sum_{k_2=0}^{S_2} p^{-k_1-k_2} \delta_{k_1}^{k_2}, \quad (\text{F.70})$$

$$\mathcal{A}_{r_1, r_2}(L_{IIIB}) = \frac{4}{8^2 4 N^4} \sum_{S_1 \geq r_1} \sum_{S_2 \geq r_2} p^{S_1+S_2} \sum_{k_1=0}^{S_1} \sum_{k_2=0}^{S_2} p^{k_1+k_2} \delta_{k_1}^{k_2}, \quad (\text{F.71})$$

$$\mathcal{A}_{r_1, r_2}(L_{IIB/IIIB}) = - \frac{16}{8^2 4 N^4} \sum_{S_1 \geq r_1} \sum_{S_2 \geq r_2} p^{S_1+S_2+r_1} \sum_{k_1=0}^{S_1} \sum_{k_2=0}^{S_2} p^{k_2} \delta_{k_1}^{k_2}, \quad (\text{F.72})$$

$$\mathcal{A}_{r_1, r_2}(L_{IA/IIIB}) = \frac{64}{8^2 4 N^4} p^{r_2-r_1} \sum_{S_1 \geq r_1} \sum_{S_2 \geq r_2} p^{2S_1+S_2} \sum_{k_1=0}^{S_1} \sum_{k_2=0}^{S_2} \delta_{k_1}^{k_2}, \quad (\text{F.73})$$

$$\mathcal{A}_{r_1, r_2}(L_{IA/IIIB}) = - \frac{32}{8^2 4 N^4} p^{-r_1} \sum_{S_1 \geq r_1} \sum_{S_2 \geq r_2} p^{2S_1+S_2} \sum_{k_1=0}^{S_1} \sum_{k_2=0}^{S_2} p^{k_2} \delta_{k_1}^{k_2}. \quad (\text{F.74})$$

Bibliography

- [1] Eugene P. Wigner. Characteristic vectors of bordered matrices with infinite dimensions. *Annals of Mathematics*, 62(3):548–564, 1955.
- [2] P. Di Francesco, Paul H. Ginsparg, and Jean Zinn-Justin. 2-D Gravity and random matrices. *Phys. Rept.*, 254:1–133, 1995.
- [3] Gerard 't Hooft. A Planar Diagram Theory for Strong Interactions. *Nucl. Phys. B*, 72:461, 1974.
- [4] B. Eynard. Topological expansion for the 1-Hermitian matrix model correlation functions. *JHEP*, 11:031, 2004.
- [5] B. Eynard. *Counting Surfaces*, volume 70. 70 of *Progress in Mathematical Physics*. Springer, 2016.
- [6] Harald Grosse and Raimar Wulkenhaar. Self-Dual Noncommutative φ^4 -Theory in Four Dimensions is a Non-Perturbatively Solvable and Non-Trivial Quantum Field Theory. *Commun. Math. Phys.*, 329:1069–1130, 2014.
- [7] R. Gurau, J. Magnen, V. Rivasseau, and A. Tanasa. A Translation-invariant renormalizable non-commutative scalar model. *Commun. Math. Phys.*, 287:275–290, 2009.
- [8] Jan Ambjorn, Bergfinnur Durhuus, and Thordur Jonsson. Three-dimensional simplicial quantum gravity and generalized matrix models. *Mod. Phys. Lett.*, A6:1133–1146, 1991.
- [9] Naoki Sasakura. Tensor model for gravity and orientability of manifold. *Mod. Phys. Lett.*, A6:2613–2624, 1991.
- [10] Mark Gross. Tensor models and simplicial quantum gravity in > 2 -D. *Nucl. Phys. Proc. Suppl.*, 25A:144–149, 1992.
- [11] Razvan Gurau. The $1/N$ expansion of colored tensor models. *Annales Henri Poincare*, 12:829–847, 2011.
- [12] Razvan Gurau. The complete $1/N$ expansion of colored tensor models in arbitrary dimension. *Annales Henri Poincare*, 13:399–423, 2012.
- [13] Razvan Gurau. Universality for Random Tensors. *Ann. Inst. H. Poincare Probab. Statist.*, 50(4):1474–1525, 2014.

- [14] Valentin Bonzom, Razvan Gurau, and Vincent Rivasseau. Random tensor models in the large N limit: Uncoloring the colored tensor models. *Phys. Rev.*, D85:084037, 2012.
- [15] Stephane Dartois, Vincent Rivasseau, and Adrian Tanasa. The $1/N$ expansion of multi-orientable random tensor models. *Annales Henri Poincare*, 15:965–984, 2014.
- [16] Joseph Ben Geloun and Vincent Rivasseau. A Renormalizable 4-Dimensional Tensor Field Theory. *Commun. Math. Phys.*, 318:69–109, 2013.
- [17] Sylvain Carrozza and Adrian Tanasa. $O(N)$ Random Tensor Models. *Lett. Math. Phys.*, 106(11):1531–1559, 2016.
- [18] Razvan Gurau and James P. Ryan. Colored Tensor Models - a review. *SIGMA*, 8:020, 2012.
- [19] Sylvain Carrozza. Flowing in Group Field Theory Space: a Review. *SIGMA*, 12:070, 2016.
- [20] Sylvain Carrozza. *Tensorial methods and renormalization in Group Field Theories*. PhD thesis, Orsay, LPT, 2014.
- [21] Joseph Ben Geloun and Vincent Rivasseau. A Renormalizable SYK-type Tensor Field Theory. *Annales Henri Poincare*, 19(11):3357–3395, 2018.
- [22] Astrid Eichhorn, Johannes Lumma, Tim Koslowski, and Antonio D Pereira. Towards background independent quantum gravity with tensor models. *Classical and Quantum Gravity*, 36(15):155007, jul 2019.
- [23] Astrid Eichhorn, Tim Koslowski, and Antonio D. Pereira. Status of background-independent coarse-graining in tensor models for quantum gravity. *Universe*, 5(2):53, 2019.
- [24] Thomas Krajewski and Reiko Toriumi. Exact Renormalisation Group Equations and Loop Equations for Tensor Models. *SIGMA*, 12:068, 2016.
- [25] S. Sachdev and J. Ye. Gapless spin fluid ground state in a random, quantum Heisenberg magnet. *Phys. Rev. Lett.*, 70:3339, 1993. arXiv:cond-mat/9212030.
- [26] A. Kitaev. A simple model of quantum holography, Talks at KITP, April 7, and May 27, 2015.
- [27] Juan Maldacena and Douglas Stanford. Remarks on the Sachdev-Ye-Kitaev model. *Phys. Rev.*, D94(10):106002, 2016.
- [28] Joseph Polchinski and Vladimir Rosenhaus. The spectrum in the Sachdev-Ye-Kitaev model. *Journal of High Energy Physics*, 2016. arxiv:1601.06768.
- [29] David J. Gross and Vladimir Rosenhaus. The Bulk Dual of SYK: Cubic Couplings. *JHEP*, 05:092, 2017.

- [30] David J. Gross and Vladimir Rosenhaus. All point correlation functions in SYK. *JHEP*, 12:148, 2017.
- [31] Alexandre Streicher. Syk correlators for all energies. *Journal of High Energy Physics*, 2020(2), Feb 2020.
- [32] Changha Choi, Márk Mezei, and Gábor Sárosi. Exact four point function for large q SYK from Regge theory. 11 2019.
- [33] David J. Gross and Vladimir Rosenhaus. A Generalization of Sachdev-Ye-Kitaev. *JHEP*, 1702:093, 2017.
- [34] David J. Gross and Vladimir Rosenhaus. A line of CFTs: from generalized free fields to SYK. *JHEP*, 07:086, 2017.
- [35] Ksenia Bulycheva. A note on the syk model with complex fermions. *Journal of High Energy Physics*, 2017(12), Dec 2017.
- [36] Wenbo Fu, Davide Gaiotto, Juan Maldacena, and Subir Sachdev. Supersymmetric Sachdev-Ye-Kitaev models. *Phys. Rev.*, D95(2):026009, 2017. [Addendum: *Phys. Rev.*D95,no.6,069904(2017)].
- [37] Micha Berkooz, Prithvi Narayan, Moshe Rozali, and Joan Simón. Higher Dimensional Generalizations of the SYK Model. *JHEP*, 01:138, 2017.
- [38] Gabor Sarosi. AdS₂ holography and the SYK model. *PoS*, Modave2017:001, 2018.
- [39] Vladimir Rosenhaus. An introduction to the syk model. *Journal of Physics A: Mathematical and Theoretical*, 52(32):323001, Jul 2019.
- [40] Edward Witten. An SYK-Like Model Without Disorder. *J. Phys. A*, 52(47):474002, 2019.
- [41] Igor R. Klebanov, Fedor Popov, and Grigory Tarnopolsky. TASI Lectures on Large N Tensor Models. *PoS*, TASI2017:004, 2018.
- [42] Razvan Gurau. Notes on Tensor Models and Tensor Field Theories. 7 2019.
- [43] Igor R. Klebanov and Grigory Tarnopolsky. Uncolored random tensors, melon diagrams, and the Sachdev-Ye-Kitaev models. *Phys. Rev.*, D95(4):046004, 2017.
- [44] Cheng Peng, Marcus Spradlin, and Anastasia Volovich. A Supersymmetric SYK-like Tensor Model. *JHEP*, 05:062, 2017.
- [45] Frank Ferrari. The large d limit of planar diagrams. *Annales de l'Institut Henri Poincaré D*, 6, 01 2017.
- [46] Frank Ferrari and Fidel I. Schaposnik Massolo. Phases Of Melonic Quantum Mechanics. *Phys. Rev. D*, 100(2):026007, 2019.
- [47] Valentin Bonzom, Luca Lionni, and Adrian Tanasa. Diagrammatics of a colored SYK model and of an SYK-like tensor model, leading and next-to-leading orders. *J. Math. Phys.*, 58(5):052301, 2017.

- [48] Dario Benedetti and Razvan Gurau. 2PI effective action for the SYK model and tensor field theories. *JHEP*, 05:156, 2018.
- [49] Igor R. Klebanov and Grigory Tarnopolsky. On Large N Limit of Symmetric Traceless Tensor Models. *JHEP*, 10:037, 2017.
- [50] Dario Benedetti, Sylvain Carrozza, Razvan Gurau, and Maciej Kolanowski. The $1/n$ expansion of the symmetric traceless and the antisymmetric tensor models in rank three. *Communications in Mathematical Physics*, 371(1):55–97, Aug 2019.
- [51] Dario Benedetti, Razvan Gurau, and Sabine Harribey. Line of fixed points in a bosonic tensor model. *JHEP*, 06:053, 2019.
- [52] Simone Giombi, Igor R. Klebanov, Fedor Popov, Shiroman Prakash, and Grigory Tarnopolsky. Prismatic Large N Models for Bosonic Tensors. *Phys. Rev. D*, 98(10):105005, 2018.
- [53] Dario Benedetti, Nicolas Delporte, Sabine Harribey, and Ritam Sinha. Sextic tensor field theories in rank 3 and 5. *JHEP*, 06:065, 2020.
- [54] Robert M. May. Will a large complex system be stable? *Nature*, 238:413–414, 1972.
- [55] Ben Craps and Oleg Evnin. Ads (in)stability: an analytic approach. *Fortschritte der Physik*, 64(4-5):336–344, Mar 2016.
- [56] Marine De Clerck and Oleg Evnin. Time-periodic quantum states of weakly interacting bosons in a harmonic trap, 2020.
- [57] Anxo F. Biasi, Javier Mas, and Angel Paredes. Delayed collapses of bose-einstein condensates in relation to anti-de sitter gravity. *Physical Review E*, 95(3), Mar 2017.
- [58] Oleg Evnin and Worapat Piensuk. Quantum resonant systems, integrable and chaotic. *J. Phys. A*, 52(2):025102, 2019.
- [59] V. K. B. Kota. *Embedded random matrix ensembles in quantum physics*. Springer, 2014.
- [60] Stéphane Dartois, Oleg Evnin, Luca Lionni, Vincent Rivasseau, and Guillaume Valette. Melonic Turbulence. *Commun. Math. Phys.*, 374(2):1179–1228, 2020.
- [61] Romain Pascalie, Carlos I. Pérez-Sánchez, and Raimar Wulkenhaar. Correlation functions of $U(N)$ -tensor models and their Schwinger-Dyson equations . 2017.
- [62] Carlos I. Pérez-Sánchez. The full Ward-Takahashi Identity for colored tensor models. *Commun. Math. Phys.*, 358(2):589–632, 2018.
- [63] Dine Ousmane Samary, Carlos I. Pérez-Sánchez, Fabien Vignes-Tourneret, and Raimar Wulkenhaar. Correlation functions of a just renormalizable tensorial group field theory: the melonic approximation. *Class. Quant. Grav.*, 32(17):175012, 2015.
- [64] Dine Ousmane Samary. Closed equations of the two-point functions for tensorial group field theory. *Class. Quant. Grav.*, 31:185005, 2014.

- [65] Razvan Gurau. A generalization of the Virasoro algebra to arbitrary dimensions. *Nucl. Phys.*, B852:592–614, 2011.
- [66] Thomas Krajewski and Reiko Toriumi. Exact Renormalisation Group Equations and Loop Equations for Tensor Models. *SIGMA*, 12:068, 2016.
- [67] Joseph Ben Geloun. Renormalizable Tensor Field Theories. In *18th International Congress on Mathematical Physics (ICMP2015) Santiago de Chile, Chile, July 27-August 1, 2015*, 2016.
- [68] Dine Ousmane Samary and Fabien Vignes-Tourneret. Just Renormalizable TGFT's on $U(1)^d$ with Gauge Invariance. *Commun. Math. Phys.*, 329:545–578, 2014.
- [69] Joseph Ben Geloun and Reiko Toriumi. Parametric representation of rank d tensorial group field theory: Abelian models with kinetic term $\sum_s |p_s| + \mu$. *J. Math. Phys.*, 56(9):093503, 2015.
- [70] Sylvain Carrozza, Daniele Oriti, and Vincent Rivasseau. Renormalization of Tensorial Group Field Theories: Abelian $U(1)$ Models in Four Dimensions. *Commun. Math. Phys.*, 327:603–641, 2014.
- [71] Valentin Bonzom and Stephane Dartois. Blobbed topological recursion for the quartic melonic tensor model. *J. Phys.*, A51(32):325201, 2018.
- [72] G. Borot. Blobbed topological recursion. *Theor. Math. Phys.*, 185(3):1729–1740, 2015.
- [73] Gaëtan Borot and Sergey Shadrin. Blobbed topological recursion: properties and applications. *Math. Proc. Cambridge Phil. Soc.*, 162(1):39–87, 2017.
- [74] Carlos I. Pérez-Sánchez. Graph calculus and the disconnected-boundary Schwinger-Dyson equations in tensor field theory. 2018.
- [75] Carlos I. Perez-Sanchez. Surgery in colored tensor models. *J. Geom. Phys.*, 120:262–289, 2017.
- [76] R. Pascalie, C. I. Pérez-Sánchez, A. Tanasa, and R. Wulkenhaar. On the large N limit of Schwinger-Dyson equations of a rank-3 tensor field theory. *Journal of Mathematical Physics*, 60(7):073502, July 2019.
- [77] Romain Pascalie. A solvable tensor field theory. *Letters in Mathematical Physics*, 110(5):925–943, May 2020.
- [78] M. Disertori, R. Gurau, J. Magnen, and V. Rivasseau. Vanishing of Beta Function of Non Commutative $\Phi^{4(4)}$ Theory to all orders. *Phys. Lett.*, B649:95–102, 2007.
- [79] Erik Panzer and Raimar Wulkenhaar. Lambert-W Solves the Noncommutative Φ^4 -Model. *Commun. Math. Phys.*, 374(3):1935–1961, 2019.
- [80] Razvan Gurau and Gilles Schaeffer. Regular colored graphs of positive degree. *Annales IHP D Comb. Phys. Interactions*, 3:257–320, 2016.

- [81] Razvan Gurau. *Random Tensors*. Oxford University Press, 2017.
- [82] J. L. Lagrange. Nouvelle méthode pour résoudre des équations littérales par le moyen de séries. *Mém. Acad. Roy. des Sci. et Belles-Lettres de Berlin*, 24, 1770.
- [83] H. Bürmann. Essai de calcul fonctionnaire aux constantes ad-libitum. *Mem.Inst. Nat. Sci Arts. Sci. Math. Phys.*, 2:316–347, 1799.
- [84] R. M. Corless, G. H. Gonnet, D. E. G. Hare, D. J. Jeffrey, and D. E. Knuth. On the lambertw function. *Advances in Computational Mathematics*, 5(1):329–359, Dec 1996.
- [85] T. Krajewski, M. Laudonio, R. Pascalie, and A. Tanasa. Non-Gaussian disorder average in the Sachdev-Ye-Kitaev model. *Phys. Rev. D*, 99(12):126014, 2019.
- [86] R. Gurau. *Random Tensor Models*. Oxford University Press, 2017.
- [87] Razvan Gurau. The complete $1/N$ expansion of a SYK-like tensor model. *Nucl. Phys.*, B916:386–401, 2017.
- [88] Razvan Gurau. Quenched equals annealed at leading order in the colored SYK model. *EPL*, 119(3):30003, 2017.
- [89] Stéphane Dartois, Harold Erbin, and Swapnamay Mondal. Conformality of $1/N$ corrections in Sachdev-Ye-Kitaev-like models. *Phys. Rev. D*, 100(12):125005, 2019.
- [90] É. Fusy, L. Lionni, and A. Tanasa. Combinatorial study of graphs arising from the sachdev-ye-kitaev model. *European Journal of Combinatorics*, 86:103066, 2020.
- [91] Thomas Krajewski and Reiko Toriumi. Polchinski’s exact renormalisation group for tensorial theories: Gaussian universality and power counting. *J. Phys.*, A49(38):385401, 2016.
- [92] Thomas Krajewski and Reiko Toriumi. Polchinski’s equation for group field theory. *Fortsch. Phys.*, 62:855–862, 2014.
- [93] Thomas Krajewski and Reiko Toriumi. Power counting and scaling for tensor models. *PoS*, CORFU2015:116, 2016.
- [94] Valentin Bonzom, Razvan Gurau, and Matteo Smerlak. Universality in p-spin glasses with correlated disorder. *Journal of Statistical Mechanics: Theory and Experiment*, 2013(02):L02003, Feb 2013.
- [95] Igor R. Klebanov and Grigory Tarnopolsky. Uncolored random tensors, melon diagrams, and the Sachdev-Ye-Kitaev models. *Phys. Rev.*, D95(4):046004, 2017.
- [96] Micha Berkooz, Mikhail Isachenkov, Vladimir Narovlansky, and Genis Torrents. Towards a full solution of the large N double-scaled SYK model. *JHEP*, 03:079, 2019.
- [97] Viet Anh Nguyen, Stéphane Dartois, and Bertrand Eynard. An analysis of the intermediate field theory of T^4 tensor model. *JHEP*, 01:013, 2015.

- [98] J. Zinn-Justin. *Quantum Field Theory and Critical Phenomena*. Oxford Science Publications, 2002. International Series of Monographs on Physics.
- [99] Joseph Polchinski. Renormalization and Effective Lagrangians. *Nucl. Phys.*, B231:269–295, 1984.
- [100] Valentin Bonzom. Revisiting random tensor models at large N via the Schwinger-Dyson equations. *JHEP*, 03:160, 2013.
- [101] Stéphane Dartois, Razvan Gurau, and Vincent Rivasseau. Double Scaling in Tensor Models with a Quartic Interaction. *JHEP*, 09:088, 2013.
- [102] Douglas Bowman and David M. Bradley. Multiple polylogarithms: A brief survey, 2003.
- [103] D. C. M. Wood. The computation of polylogarithms. 1992.
- [104] Valentin Bonzom, Victor Nador, and Adrian Tanasa. Diagrammatic proof of the large N melonic dominance in the SYK model. *Lett. Math. Phys.*, 109(12):2611–2624, 2019.
- [105] Luca Lionni and Johannes Thürigen. Multi-critical behaviour of 4-dimensional tensor models up to order 6. *Nucl. Phys.*, B941:600–635, 2019.
- [106] Ronald L. Graham, Donald E. Knuth, and Oren Patashnik. *Concrete Mathematics: A Foundation for Computer Science*. Addison-Wesley Longman Publishing Co., Inc., Boston, MA, USA, 2nd edition, 1994.